

TALLINN UNIVERSITY OF TECHNOLOGY  
DOCTORAL THESIS  
58/2018

**Origin and Geochemical Evolution of  
Palaeogroundwater in the Northern Part  
of the Baltic Artesian Basin**

JOONAS PÄRN



TALLINN UNIVERSITY OF TECHNOLOGY

School of Science

Department of Geology

This dissertation was accepted for the defence of the degree 03/09/2018

**Supervisor:**

Prof. Emerit. Rein Vaikmäe  
School of Science  
Tallinn University of Technology  
Tallinn, Estonia

**Co-supervisor:**

Dr. Valle Raidla  
School of Science  
Tallinn University of Technology  
Tallinn, Estonia

**Opponents:**

Prof. Dr. hab Kazimierz Rozanski  
Faculty of Physics and Applied Computer Science  
AGH University of Science and Technology  
Krakow, Poland

Dr. George Darling  
Principal Hydrogeochemist  
British Geological Survey  
Wallingford, UK

**Defence of the thesis:** 04/10/2018, Tallinn

**Declaration:**

Hereby I declare that this doctoral thesis, my original investigation and achievement, submitted for the doctoral degree at Tallinn University of Technology, has not been previously submitted for doctoral or equivalent academic degree.

Joonas Pärn

-----  
signature



European Union  
European Social Fund



Investing in your future

Copyright: Joonas Pärn, 2018

ISSN 2585-6898 (publication)

ISBN 978-9949-83-325-2 (publication)

ISSN 2585-6901 (PDF)

ISBN 978-9949-83-326-9 (PDF)

TALLINNA TEHNIKAÜLIKOOL  
DOKTORITÖÖ  
58/2018

# **Paleopõhjavete päritolu ja geokeemiline areng Balti arteesiabasseini põhjaosas**

JOONAS PÄRN



# Contents

List of Publications .....	6
Author's Contribution to the Publications .....	7
1 Introduction .....	8
Abbreviations .....	10
2 Theoretical background .....	11
2.1 Palaeogroundwater: definition, delineation and global distribution.....	11
2.2 Palaeogroundwater in the BAB and surrounding areas.....	16
3 Material and methods.....	22
3.1 Geological and hydrogeological setting of the study area.....	22
3.2 Sample collection and analysis.....	27
3.3 Geochemical modelling.....	29
4 Results and discussion.....	31
4.1 Isotopic composition of modern precipitation and shallow groundwater in the BAB area .....	31
4.2 Occurrence of palaeogroundwater in Estonian aquifer systems .....	34
4.3 Palaeogroundwater in the Ordovician-Cambrian (O-Cm) aquifer system .....	43
4.3.1 Origin of groundwater.....	43
4.3.2 Geochemical evolution of groundwater .....	44
4.3.3 Dating of groundwater.....	48
4.4 Important aspects concerning the management of glacial palaeogroundwater in Estonia.....	51
4.4.1 The occurrence of glacial palaeogroundwater in the light of previous understanding of groundwater flow and budget in Estonia .....	51
4.4.2 Differentiation of glacial palaeogroundwater during groundwater monitoring in Estonia.....	53
5 Conclusions .....	58
6 References .....	60
7 Acknowledgements.....	75
Abstract.....	76
Lühikokkuvõte.....	78
Appendix .....	81
Curriculum vitae.....	225
Elulookirjeldus.....	226

## List of Publications

The list of author's publications, on the basis of which the thesis has been prepared:

- I Raidla, Valle; Kern, Zoltan; Pärn, Joonas; Babre, Alise; Erg, Katrin; Ivask, Jüri; Kalvans, Andis, Kohán, Balázs; Lelgus, Mati; Martma, Tõnu; Mokrik, Robert; Popovs, Konrads; Vaikmäe, Rein (2016). A  $\delta^{18}\text{O}$  isoscape for the shallow groundwater in the Baltic Artesian Basin. *Journal of Hydrology*, 542, 254–267.
- II Pärn, Joonas; Raidla, Valle; Vaikmäe, Rein; Martma, Tõnu; Ivask, Jüri; Mokrik, Robert; Erg, Katrin (2016). The recharge of glacial meltwater and its influence on the geochemical evolution of groundwater in the Ordovician-Cambrian aquifer system, northern part of the Baltic Artesian Basin. *Applied Geochemistry*, 72, 125–135.
- III Pärn, Joonas; Affolter, Stéphane; Ivask, Jüri; Johnson, Sean, Kirsimäe, Kalle; Leuenberger, Markus; Martma, Tõnu; Raidla, Valle; Schloemer, Stefan; Sepp, Holar; Vaikmäe, Rein; Walraevens, Kristine (2018). Redox zonation and organic matter oxidation in palaeogroundwater of glacial origin from the Baltic Artesian Basin. *Chemical Geology*, 488, 149–161.
- IV Pärn, Joonas; Walraevens, Kristine; van Camp, Marc; Raidla, Valle; Aeschbach, Werner; Friedrich, Ronny; Ivask, Jüri; Kaup, Enn; Martma, Tõnu; Mažeika, Jonas; Mokrik, Robert; Weissbach, Therese; Vaikmäe, Rein. Dating of glacial palaeogroundwater in the Ordovician-Cambrian aquifer system, northern part of Baltic Artesian Basin. *Manuscript*.
- V Raidla, Valle; Pärn, Joonas; Czuppon, György; Ivask, Jüri; Marandi, Andres; Schloemer, Stefan; Sepp, Holar; Vaikmäe, Rein; Kirsimäe, Kalle. Origin and formation of methane in groundwater of glacial origin from the Cambrian-Vendian aquifer system in Estonia. *Manuscript*.

## **Author's Contribution to the Publications**

Contribution to the papers in this thesis are:

- I The author participated in fieldwork, data interpretation, and the writing of the manuscript.
- II The author was responsible for fieldwork, data interpretation, and the writing of the manuscript.
- III The author was responsible for fieldwork, sample preparation, data interpretation, and the writing of the manuscript.
- IV The author was responsible for fieldwork, sample preparation, data interpretation, and the writing of the manuscript.
- V The author participated in fieldwork, data interpretation and the writing of the manuscript.

# 1 Introduction

Groundwater is the most important global source of freshwater. It forms a second largest global freshwater reservoir with an estimated volume of  $11 \times 10^6 \text{ km}^3$  (~30% of global freshwater reserves) that is only inferior to freshwater stored in glaciers and ice sheets ( $24 \times 10^6 \text{ km}^3$ ; Gleick, 1996). Recent analyses suggest that the share of groundwater renewable in human timescales is small compared to total groundwater volumes stored in the upper portion of the Earth's crust. A compilation of globally available datasets together with numerical simulations and tritium age analysis showed that only about 6% of the groundwater in the uppermost portion of the crust is modern, i.e. less than 50 years old (Gleeson et al., 2016). Furthermore, it has been suggested that groundwater recharged prior to the beginning of the Holocene (11700 years ago) makes up 42-85% of total aquifer storage in the upper 1 km portion of the crust and is dominant below depths of 250 m (Jasechko et al., 2017). These findings illustrate the actual low groundwater renewal rates that make an important portion of globally stored groundwater essentially non-renewable in comparison to human life-span. Thus, the first step towards a responsible and sustainable management of groundwater resources in any given region should be the determination of their origin, age and renewal rates.

Baltic Artesian Basin (BAB) is a groundwater reservoir in north-eastern Europe. Here groundwater recharged prior to the beginning of the Holocene has been observed in various depths and locations. Brines in the deep central parts of the basin (Latvia and Lithuania) have ages  $>1.3 \text{ Ma}$  based on noble gas age tracers  $^{81}\text{Kr}$ ,  $^4\text{He}$  and  $^{40}\text{Ar}$  (Gerber et al., 2017). In the northern part of the BAB (northern Estonia) the distribution of groundwater originating from subglacial recharge during the Pleistocene glaciations has been shown to be wide in the deepest sedimentary bedrock aquifer of Cambrian-Vendian (Vaikmäe et al., 2001; Marandi, 2007; Raidla et al., 2009, 2012, 2014). However, despite evidence suggesting that the spread of the pre-Holocene groundwater could also be wide in more shallow aquifer systems in the northern BAB (e.g. Savitskaja et al., 1995, 1996a, 1997; Vaikmäe et al., 2001), their spatial distribution, origin and age were not extensively studied until recently.

This study assesses the spatial distribution, origin, geochemical evolution and age of groundwater originating from the Pleistocene in the northern part of the BAB. More specifically, the objective of the author was to study the extent to which groundwater originating from the Pleistocene is spread in the northern BAB. Since the Cambrian-Vendian aquifer system has been extensively studied in that respect, the focus of the study was on the aquifer systems overlying it, that had received less attention.

Based on previous evidence, the working hypothesis of the study was that groundwater originating from the Pleistocene could also be found in shallow aquifers of the northern BAB. It could be suspected that confined aquifers in the study area have not reached an equilibrium with modern topographically driven groundwater flow conditions and still exhibit groundwater flow patterns and composition established in the Pleistocene. It was supposed, however, that the greater influence of processes induced by modern recharge would be evident with decreasing depth from the surface. In addition, the study of Pleistocene groundwater in the northern BAB as a part of this thesis also involved the special characteristics of groundwater in the Cambrian-Vendian aquifer system (high concentrations of noble gases and methane). Those characteristics shed light to palaeoenvironmental conditions during the recharge of groundwater in the Pleistocene.

The groundwater samples were studied using a multi-tracer approach involving the hydrochemical composition of groundwater, a suite of stable ( $\delta^2\text{H}_{\text{H}_2\text{O}}$ ,  $\delta^{18}\text{O}_{\text{H}_2\text{O}}$ ,  $\delta^{13}\text{C}_{\text{DIC}}$ ,  $\delta^{34}\text{S}_{\text{SO}_4}$ ,  $\delta^{18}\text{O}_{\text{SO}_4}$ ,  $\delta^{13}\text{C}_{\text{CH}_4}$ ,  $\delta^2\text{H}_{\text{CH}_4}$ ) and radioactive isotope tracers ( $^3\text{H}$ ,  $^{14}\text{C}$  and  $^4\text{He}$ ) and the study of dissolved gas compositions in groundwater ( $\text{CH}_4$ ,  $\text{CO}_2$ ,  $\text{He}$ ,  $\text{Ne}$ ,  $\text{Ar}$ ,  $\text{Kr}$ ,  $\text{Xe}$ ). In addition, the geochemical evolution and groundwater age were studied with geochemical modelling using the software programs GWB (Bethke and Yeakle, 2015), PHREEQC (Parkhurst and Appelo, 2013) and NETPATH (Plummer et al., 1994; El-Kadi et al., 2011).

The thesis is written with an aim to provide a first synthesis on the occurrence and evolution of groundwater originating from Pleistocene glaciations in the northern part of the BAB. Such synthesis would enable one to acknowledge gaps in the current understanding of the groundwater system that need to be addressed to sustainably manage these special groundwater resources. More specifically, the results of this study are relevant in at least three important aspects:

- 1) Groundwater is the most important source of public water supply in Estonia making up ~60% of all consumed water from public water supply networks (Estonian Health Board, 2016). Understanding the processes influencing recharge and geochemical evolution of groundwater is crucial for predicting the effects of groundwater abstraction on its composition and availability;
- 2) In several aquifer systems in the study area, the rocks associated with the aquifer strata contain mineral resources that could have potential economic significance in the future. As an example, the upper portion of sandstones in the Ordovician-Cambrian aquifer system contain shell detritus of phosphatic brachiopods which form the biggest phosphorite deposit in Europe (Raudsep, 1997). Also, the Lower Ordovician organic-rich black shale known as graptolite argillite which is an important aquitard that separates the Ordovician-Cambrian aquifer system from the overlying shallow carbonate aquifers contains high concentrations of trace metals (e.g. U, Mo, V, Zn, Pb, Cu, Ni, As; Voolma et al., 2013; Hade and Soesoo, 2014). Any future plans for mining these mineral resources need to take into account the renewability of groundwater in the associated aquifer systems;
- 3) The results presented in the thesis illustrate the multi-faceted nature of information about pre-Holocene environmental conditions recorded in palaeogroundwater reservoirs. More specifically, they provide an example on how groundwater can serve as an important paleoenvironmental archive enabling the study of variations in climatic and environmental conditions during glacial-interglacial cycles in the Pleistocene (cf. Darling, 2011).

The main inferences presented in the thesis have been published in peer-reviewed scientific journals (Papers I-III) or are manuscripts (Papers IV-V). The thesis also uses data in the unpublished database of the Division of Isotope Geology in the Institute of Geology at Tallinn University of Technology (Martma, T., Ivask, J., Kaup, E., Pärn, J., Raidla, V., Vaikmäe, R., unpublished data, 2018).

The results in the thesis have also been presented in various international workshops and conferences such as the International Symposium on Isotope Hydrology: Revisiting Foundations and Exploring Frontiers: 11-15 May 2015 in Vienna, Austria; annual meeting of G@GPS IGCP 618 Project: Palaeogroundwater from past and present glaciated areas, 5-9 July 2015 in Tallinn, Estonia; 43rd IAH Congress: Groundwater and society, 60 years of IAH, 25-29 September 2016 in Montpellier, France and 25<sup>th</sup> Salt Water Intrusion Meeting, 18-22 June 2018 in Gdansk, Poland.

## Abbreviations

BAB	Baltic Artesian Basin
Cm-V	Cambrian-Vendian aquifer system
V <sub>2vr</sub>	Voronka aquifer in the Cambrian-Vendian aquifer system
V <sub>2gd</sub>	Gdov aquifer in the Cambrian-Vendian aquifer system
O-Cm	Ordovician-Cambrian aquifer system
S-O	Silurian-Ordovician aquifer system
D <sub>2-1</sub>	Lower-Middle-Devonian aquifer system
D <sub>2nr</sub>	Middle-Devonian Narva regional aquitard
GMWL	global meteoric water line
LMWL	local meteoric water line
LGM	Last Glacial Maximum (Late Weichselian Glaciation – MIS 2)
MIS	marine isotope stage
NGT	noble gas recharge temperature
a <sup>14</sup> C	radiocarbon activity in pmC (per cent modern carbon)
DIC	dissolved inorganic carbon

## 2 Theoretical background

### 2.1 Palaeogroundwater: definition, delineation and global distribution

Groundwater resources can be categorized as *modern groundwater* (recharged in the past ~50 years) or *sub-modern groundwater* (recharged more than 50 years ago) based on whether groundwater contains detectable amounts of tritium (e.g. Clark and Fritz, 1997; Gleeson et al., 2016). When *sub-modern groundwater* has residence times significantly exceeding 50 years, the terms *palaeogroundwater* (also *palaeowater*) and *fossil groundwater* can be used for it. *Palaeogroundwater* stands for groundwater that has originated from water cycles under environmental conditions which were different from the present ones (Fontes, 1981). The recharge to aquifers containing *palaeogroundwater* could have been both continuous or intermittent in the past (Edmunds, 2001).

Most of the authors use the term *fossil groundwater* almost as a synonym to the term *palaeogroundwater*, referring to it as groundwater recharged in the past by meteorological processes that no longer prevail that has been stored underground since the time of recharge (e.g. Clark and Fritz, 1997: 198; WMO, 2012). In a recent work Jasechko et al., (2017: 425) define *fossil groundwater* as groundwater recharged by precipitation more than ~12000 years ago, i.e. prior to the beginning of the Holocene.

It is important to note that, while the term *fossil groundwater* can be taken to have a more specific meaning designating groundwater in aquifers receiving negligible amount of modern recharge whose storage is almost entirely made up of groundwater recharged in past climatic conditions (e.g. Taylor et al., 2013), the absence of modern recharge is not a defining characteristic of *fossil groundwater* (Margat et al., 2006). More specific age-based definitions of *palaeogroundwater* have been put forward by Rozanski (1985) and Edmunds (2001). They state that the term *palaeowater* strictly refers to groundwater recharged in colder climate conditions in Late Pleistocene that can be identified in terms of radiocarbon age or another isotopic or noble gas signature.

In this thesis, the term *palaeogroundwater* is used for groundwater recharged prior to the Holocene (Fig. 1). Groundwater recharged in the Holocene is referred to as *recent* and groundwater in shallow aquifers having isotopic composition similar to modern recharge and containing tritium is referred to as *modern*. One must not forget that the definitions above work for groundwater of meteoric origin. Many sedimentary basins contain saline formation water mostly originating from ancient sea-water that is either *connate* (i.e. chemically and isotopically modified water out of contact with the atmosphere since deposition, e.g. groundwater originating from seawater intrusion in the past) or *syngenetic* (i.e. waters deposited together with sediments forming the aquifer matrix) in origin (Kharaka and Hanor, 2007).

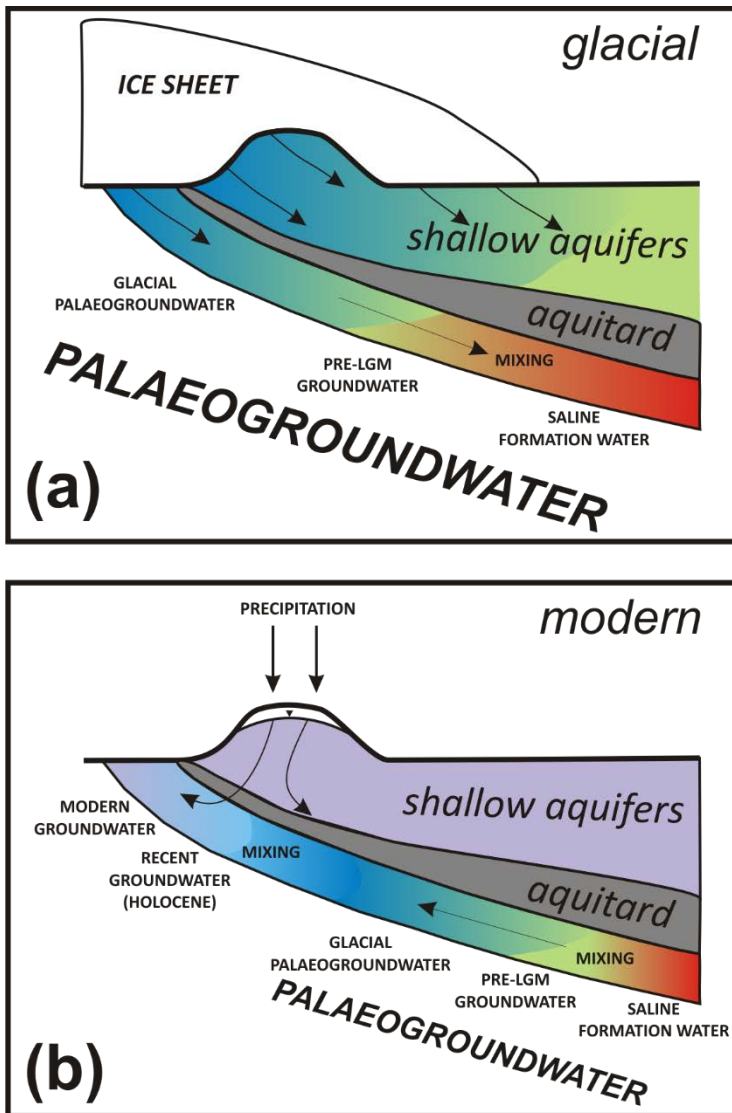


**Figure 1.** A simplified conceptual model of the formation, location and hydrogeologic history of palaeogroundwater in a groundwater system similar to the one in the northern part of the Baltic Artesian Basin. (after Edmunds, 2001)

The preservation of palaeogroundwater can be enhanced by several types of conditions or their combinations. These include the presence of strong confining layers, dry climate conditions with negligible amount modern recharge where ancient pluvial periods have provided enough water for groundwater recharge, great lengths of groundwater flow paths and a decrease of hydraulic conductivity with depth that results in low actual velocity of groundwater (Clark and Fritz, 1997; Edmunds et al., 2003; Sturchio et al., 2004; McIntosh et al., 2012; Sterckx et al., 2018). The presence of palaeogroundwater in an aquifer can be identified using a host of hydrochemical and isotopic tracers of which the isotopic composition of groundwater, the activity of

radioactive isotopes in groundwater constituents (e.g.  $^{14}\text{C}$  in dissolved inorganic carbon;  $^{36}\text{Cl}$  in  $\text{Cl}^-$ ) and noble gas concentrations are the most frequently used.

One of the main tools for identifying the presence of palaeogroundwater in a given area is the study of its isotopic composition ( $\delta^{18}\text{O}_{\text{H}_2\text{O}}$ ,  $\delta^2\text{H}_{\text{H}_2\text{O}}$ ). The stable isotopic composition of groundwater with meteoric origin depends on isotopic composition of precipitation which in turn depends upon a variety of climatic factors such as origin of water vapour, temperature of condensation, humidity and local distribution of rainfall with respect to evapotranspiration (Fontes, 1981; Clark and Fritz, 1997; Ingraham, 1998).

Any change in those factors which is long enough compared to aquifer turnover times will affect the isotopic composition of groundwater (Fontes, 1981). In addition, the *d*-excess parameter which assesses the differences between  $\delta^{18}\text{O}_{\text{H}_2\text{O}}$  and  $\delta^2\text{H}_{\text{H}_2\text{O}}$  in a water sample, is an important indicator for moisture provenance (Dansgaard, 1964; Darling, 2011):

$$d = \delta^2\text{H} - 8\delta^{18}\text{O} \quad (1)$$

The differences in isotopic composition and *d*-excess in palaeogroundwater with respect to modern groundwater constitute a “palaeoclimatic effect” which is one of the most important tools for identifying palaeogroundwater (Clark and Fritz, 1997).

The changes in isotopic composition and *d*-excess usually result in different positions of modern groundwater and palaeogroundwater on the local meteoric water line (LMWL) of the study area. For temperate regions the occurrence of palaeogroundwater is usually exemplified with a shift in its isotopic composition on the LMWL with respect to modern groundwater while in semi-arid and arid regions palaeogroundwater tends to plot away from the modern LMWL (Clark and Fritz, 1997). The stable isotopic composition of meteoric water also has a strong dependence on temperature which can be quantified into a  $\delta$ -T relationship for a local study area (e.g. Dansgaard, 1964; Rozanski et al., 1992, 1993).

Further evidence for palaeogroundwater occurrence is provided by various age tracers of which radiocarbon ( $^{14}\text{C}$ ; half-life  $t_{1/2}=5730$  a) activity of dissolved inorganic carbon (DIC) has been historically most extensively used. Alternatives are provided by radioactive age tracers with longer half-lives such as  $^{81}\text{Kr}$  ( $t_{1/2}=229$  ka),  $^{36}\text{Cl}$  ( $t_{1/2} \sim 300$  ka) and accumulation of radiogenic stable isotopes in groundwater (e.g.  $^4\text{He}$ ) (IAEA, 2013; Cartwright et al., 2017).

Each mentioned method has its advantages and limitations that need to be considered when interpreting the given tracer concentration or activity in terms of age. Successful radiocarbon dating requires that uncertainties of initial  $^{14}\text{C}$  activity ( $a^{14}\text{C}$ ) in recharge waters and the dilution of this initial  $^{14}\text{C}$  activity by chemical processes are overcome (Kalin, 2000; Plummer and Glynn, 2013). In addition, a critical issue in  $^{14}\text{C}$  dating concerns possible contamination of the original  $^{14}\text{C}$  signal with atmospheric  $^{14}\text{C}$  during sampling and sample preparation (Aggarwal et al., 2014). Also, physical processes related to groundwater flow such as dispersion, diffusion and mixing with water from adjacent aquitards or stagnant zones can modify the initial activity of  $^{14}\text{C}$  (Sanford, 1997; Bethke and Johnson, 2002).

$^{81}\text{Kr}$  has many advantages for dating palaeogroundwater with an age range of  $10^5$ – $10^6$  years due to its chemical inertness, constant atmospheric concentrations and the absence of subsurface sources and sinks other than radioactive decay (Jiang et al., 2012; Gerber et al., 2017).  $^{81}\text{Kr}$  dating is hampered by low activity of this isotope tracer

in natural waters and considerable cost of analysis for both of which significant advances have been made in the recent decade (Purtschert et al., 2013).

$^{36}\text{Cl}$  dating utilizes the fact that  $\text{Cl}^-$  acts as a conservative element in the subsurface. However, variations in chloride concentrations of groundwater caused by changes in evapotranspirative concentration, addition of  $\text{Cl}^-$  from the aquifer (e.g. through mixing) to atmospheric  $\text{Cl}^-$  in recharge waters and underground production of  $^{36}\text{Cl}$  need to be understood and quantified for successful groundwater dating (Phillips, 2013).

$^4\text{He}$  dating can provide a qualitative estimate of groundwater age as the concentration of radiogenic He increases with groundwater residence time (Kipfer et al., 2002). However, uncertainties in mixing with older water can make the studied waters seem older and uncertainties in  $^4\text{He}$  accumulation rates together with a possible variety of external sources (e.g. flux of  $^4\text{He}$  from the underlying crust or adjacent aquitards) makes the quantification of  $^4\text{He}$  model age a difficult task (e.g. Torgersen and Stute, 2013). Despite these potential shortcomings, several studies have shown how  $^4\text{He}$  dating can be successfully used to arrive at more quantitative groundwater age estimates and to quantify the contribution of external sources to the measured  $^4\text{He}$  concentrations (e.g. Torgersen and Ivey, 1985; Castro et al., 2000; Carey et al., 2004; Aggarwal et al., 2015).

Noble gases dissolved in groundwater (He, Ne, Ar, Kr, Xe) can provide important insight into paleoenvironmental conditions during groundwater recharge such as recharge temperatures and unsaturated zone conditions through the study of the excess-air component (Kipfer et al., 2002). The equilibrium concentration of noble gases in groundwater is a function of temperature, salinity and atmospheric pressure (i.e. recharge elevation, Aeschbach-Hertig et al., 2008). Noble gas concentrations in groundwater are in excess to atmospheric equilibrium (called "excess air") which can be either unfractionated or fractionated relative to pure air in composition (Kipfer et al., 2002). The composition and abundance of the excess air can be related to recharge conditions, e.g. the change in hydrostatic pressure and water table fluctuations during groundwater recharge (Aeschbach-Hertig et al., 2000; Kipfer et al., 2002).

Using different models to account for the excess air (Heaton and Vogel, 1981; Stute et al., 1995; Aeschbach-Hertig et al., 2000), noble gas concentrations in groundwater can be corrected to derive noble gas recharge temperatures (NGT) based on their solubilities in water. The calculated NGTs have been successfully used to study the Pleistocene glacial-interglacial palaeotemperature record in groundwater (e.g. Andrews and Lee, 1979; Stute et al., 1995; Clark et al., 1997; Aeschbach-Hertig et al., 2000; Grundl et al., 2013). In addition, NGTs have helped to identify palaeogroundwater in cases when their isotopic composition has not been distinguishable from modern counterparts or radiocarbon age records have been deemed unreliable (e.g. Beyerle et al., 1998; Aeschbach-Hertig et al., 2002; Zuber et al., 2004).

In terms of general hydrochemical quality, palaeogroundwater is frequently characterized by bacterial purity (with respect to bacteria of anthropogenic origin), and the absence of anthropogenic chemicals (e.g. Edmunds, 2001). In addition, long residence times of palaeogroundwater can lead to distinct changes in their hydrochemical composition. This is manifested in the ingrowth of specific trace elements not limited by solubility constraints (e.g. Li, Mn, Mo) and by an increase in the concentrations of redox-sensitive dissolved substances that accumulate in groundwater in strongly reducing conditions (e.g.  $\text{Fe}^{2+}$  and  $\text{CH}_4$ , Edmunds and Smedley, 2000; Edmunds, 2001). Differences in salinity between waters of different origin may lead to manifestation of cation exchange processes in the hydrochemical composition of

palaeogroundwater (e.g. Chappelle and Knoble, 1983; Walraevens et al., 2001; Ferguson et al., 2007).

Groundwater has been considered a low-resolution archive of past environmental signals compared to ice cores from polar regions due to dispersion and mixing of various flow paths with a different origin in aquifers (Darling, 2011). Despite this limitation, groundwater can retain signals of regional climatic and environmental events with long duration (e.g. changes in palaeotemperature, precipitation sources and recharge regimes during glacial-interglacial cycles) and complement proxy evidence found from higher resolution archives (e.g. ice cores, tree rings and speleothems; Edmunds, 2001). The relations between palaeogroundwater composition and hydrologic conditions during recharge makes them the only other direct archive, except for ice-cores, based on which reconstructions of hydrological history can be achieved (Edmunds, 2001).

Historically, the first type of palaeogroundwater thoroughly studied were the groundwater resources beneath the Sahara Desert (e.g. Nubian Sandstone aquifer, Continental Intercalaire aquifer). The isotopic composition and *d*-excess of these waters revealed that the water originates from older pluvial periods in the Holocene and the Pleistocene (e.g. Fontes, 1981; Edmunds et al., 2003). Palaeogroundwater resources in these aquifers frequently predate the last glacial-interglacial cycle having residence times >1 Ma (e.g. Sturchio et al., 2004; Guendouz and Michelot, 2006; Petersen et al., 2018). Later, similar palaeogroundwater resources have been identified from other regional aquifer systems such as the Great Artesian Basin in Australia (Lehmann et al., 2003) and Guarani aquifer in South America (Aggarwal et al., 2015).

Whereas variability in amounts of precipitation has had a dominant effect on the isotopic composition of palaeogroundwater in arid regions, the isotopic composition of palaeogroundwater in subtropical and temperate regions is more related to changes in vapour source, air mass trajectories and temperature (Fritz and Clark, 1997). Here, the differences in isotopic composition between palaeogroundwater and their modern counterparts can be manifested in both the depletion and enrichment depending on the location and past trajectories of air masses (e.g. Clark et al., 1997; Plummer and Sprinkle, 2001; Edmunds et al., 2006). In areas influenced by Pleistocene glaciations, the formation of palaeogroundwater resources is related to cyclic recharge events during glacial-interglacial cycles of Quaternary glaciations (Edmunds, 2001). Palaeogroundwater records in these areas show that groundwater recharge has often been intermittent in the past which is best exemplified by a widely reported recharge gap during the last glacial maximum (LGM) for palaeogroundwater in Europe (e.g. Rozanski, 1985; Beyerle et al., 1998; Edmunds, 2001; Darling, 2004; Blaser et al., 2010). This phenomenon has been explained by inhibition of groundwater recharge by permafrost conditions or general aridity and low moisture supply near the continental ice sheets (Darling, 2011).

In areas covered by continental ice sheets in the Pleistocene, a special type of palaeogroundwater is related to subglacial recharge of meltwater from the continental ice sheets into the subsurface. This type of palaeogroundwater is referred to as *glacial palaeogroundwater* in this thesis. Hydrodynamic modelling has shown that aquifers in sedimentary basins once covered by continental ice sheets had sufficient transmissivity to discharge subglacial meltwater (Boulton et al., 1995; Piotrowski, 1997; Person et al., 2007; Bense and Person, 2008; Lemieux et al., 2008; McIntosh et al., 2011; Sterckx et al., 2017, 2018). High hydraulic gradients imposed by continental ice sheets modified groundwater flow patterns which led in many cases to the reversal of regional groundwater flow with respect to previous topographically-driven flow systems (Person

et al., 2007; McIntosh et al., 2011; Sterckx et al., 2018). The intrusion of glacial meltwater into the subsurface is exemplified by distinct isotopic and chemical composition of glacial palaeogroundwater with respect to modern meteoric water and older formation water. The presence of groundwater originating from Pleistocene glaciations has been widely reported from North-America from areas overridden by the Laurentian Ice Sheet (e.g. Clayton et al., 1966; Siegel and Mandel, 1984; Siegel, 1991; Stueber and Walter 1991, 1994; Grasby et al., 2000; McIntosh and Walter, 2005, 2006; Grasby and Chen, 2005; Ferguson et al., 2007; Grundl et al., 2013). In Europe, the occurrence of glacial palaeogroundwater has been observed in the Fennoscandian Shield and the adjacent Baltic Artesian Basin (BAB) which were covered by the Scandinavian Ice Sheet in the Pleistocene (e.g. Blomqvist, 1999; Vaikmäe et al., 2001; Frape et al., 2003; Raidla et al., 2009, 2012).

## 2.2 Palaeogroundwater in the BAB and surrounding areas

Several palaeogroundwater resources with different origin have been found in the BAB and in the surrounding areas of Scandinavia, Denmark, Poland and Russia that were influenced by Scandinavian Ice Sheet in the Pleistocene (Fig. 2). The isotopic composition of these waters is generally ~1–5‰ depleted in  $\delta^{18}\text{O}$  values with respect to modern recharge. The glacial palaeogroundwater from the northern BAB is unique in this context having an extremely light isotopic composition that is up to ~12‰ depleted in  $^{18}\text{O}$  with respect to values found in modern groundwater (Vaikmäe et al., 2001; Raidla et al., 2009).

In the Fennoscandian Shield to the north and west from the BAB, where the extent and the temporal preservation of the Scandinavian Ice Sheet was the most extensive in the Pleistocene, the evidence on the existence of glacial palaeowater is related to brackish groundwater in fractures of crystalline rocks. The Palaeozoic sedimentary rocks are missing in large parts of Scandinavia in which case only a thin sequence of Quaternary sediments covers the Precambrian crystalline and metamorphic rocks (Lehtinen, 2012). High salinity Ca-Na-Cl brine is present in deep fractures of the crystalline bedrock below the active flow system, but due to heterogeneous nature of the mineralogic composition of the rocks, the composition of this brine is highly variable (Negrel et al., 2005). The geochemical evolution of the fluids in the crystalline bedrock of the Fennoscandian Shield has been influenced by water-rock interaction, chemical evolution of seawater, glacial meltwater intrusion and freezing processes (Negrel et al., 2005; Stotler et al., 2012). Groundwater influenced by glacial meltwater intrusion can be distinguished from other fluids by lower mineralisation and lighter isotopic composition. The most negative stable isotope signatures in deep groundwater from the Fennoscandian Shield are found at depths of 200-400 meters (Stotler et al., 2012).

The negative values of  $\delta^{18}\text{O}$  as low as ~-19‰ have been reported in Na-Cl and Na-SO<sub>4</sub> type waters from Palmottu deep borehole in Southern Finland in the U-Th mineralization hosted by Proterozoic crystalline bedrock at depths of ~400 m (Ahonen et al., 2004; Kietäväinen, 2017). The water in Palmottu is brackish with TDS concentrations reaching up to 1600 mg·L<sup>-1</sup> (Ahonen et al., 2004). Elsewhere in southern Finland, influence of glacial meltwater intrusion is also suspected in deep groundwaters from Hästhölm (rapakivi granite; 985 m) and Olkiluoto (gneisses; 960 m) sites, with  $\delta^{18}\text{O}$  values of ~-14‰ and ~-12.7‰, respectively (Pitkänen et al., 2001, 2004; Kietäväinen, 2017). Traces of glacial palaeogroundwater have also been found from the more northern parts of the Fennoscandian Shield. Blomqvist (1999) and Frape et al. (2003) report waters with

depleted  $\delta^{18}\text{O}$  and  $\delta^2\text{H}$  values from central Finland with  $\delta^{18}\text{O}$  values as low as  $-20.6\text{‰}$ . Brackish Na-Cl groundwater in the Outokumpu deep borehole in eastern Finland at depths of 427 m has  $\delta^{18}\text{O}$  values of  $-16.7\text{‰}$  (Ivanovich et al., 1992). Interestingly, the deep brines (1060 m) in Outokumpu have  $\delta^{18}\text{O}$  values only of  $\sim -11\text{‰}$  with residence time being up to 50 Ma (Kietäväinen et al., 2014). This shows that glacial meltwater was probably not able to penetrate to depths  $>1000$  m in the Fennoscandian Shield. Influence of glacial meltwater intrusion to waters in crystalline rocks of the Fennoscandian Shield has been also reported from its western part in Sweden. Waters from Äspö HRL (Hard Rock Laboratory) on an island off the south-eastern coast of Sweden are brackish at depths between 250 to 600 meters and have  $\delta^{18}\text{O}$  values as negative as  $\sim -16\text{‰}$  (Laaksoharju et al., 1999; Negrel et al., 2005). Groundwater with  $\delta^{18}\text{O}$  values of  $\sim -13\text{‰}$  have been reported from the Stripa granite in central Sweden at depths from  $\sim 400$  to 800 m (Moser et al., 1989).

Further to the south in the south-western margin of the Scandinavian Ice Sheet during the LGM, traces of groundwater originating from the Pleistocene have been reported by Hinsby et al. (2001) from Ribe Formation in Denmark. Groundwater with  $^{14}\text{C}$  model ages up to 14 ka BP has been found from the Rømø island off the Denmark's western coast. The inferred NGTs of those waters are about  $5^\circ\text{C}$  lower compared to modern temperatures with  $\delta^{18}\text{O}$  values  $\sim 1$  to  $2\text{‰}$  depleted with respect to groundwaters with modern ages. These waters have formed in low base-level conditions in the Late Pleistocene and have been isolated from present-day flow systems by rising sea levels in the Holocene (Hinsby et al., 2001).

Palaeogroundwater from the Pleistocene has also been found to the south of the BAB from Poland (Rozanski, 1985; Zuber et al., 2000, 2004). This area lay near the southern border of the Scandinavian Ice Sheet during its maximum extent in the LGM  $\sim 22$  ka BP (Lasberg and Kalm, 2013; Fig. 2). Glacial palaeogroundwater found in Poland is thought to have recharged in the final stages of the LGM. Their corresponding  $\delta^{18}\text{O}$  values are only slightly depleted ( $\sim 1$ – $2.5\text{‰}$ ) with respect to modern recharge. However, their Late Pleistocene origin is suggested by low  $^{14}\text{C}$  activities and NGTs  $\sim 4$  to  $5^\circ\text{C}$  lower compared to the present. In addition, Halas et al. (1993) report waters with  $\delta^{18}\text{O}$  values from  $-11$  to  $-14\text{‰}$  depleted with respect to modern groundwaters from the Upper Cretaceous aquifer in Hel peninsula at Gdansk area, Northern Poland, that the authors argue to have infiltrated during the glacial period.

To the east of the BAB, glacial palaeogroundwater can be found in the Cambrian-Vendian and Ordovician-Cambrian aquifer systems in north-western Russia. These aquifer systems are essentially the extensions of their counterparts in the northern BAB to eastern and north-eastern directions. The Scandinavian Ice Sheet advanced to these areas  $\sim 18$  ka BP (Lunkka et al., 2001). Voroniuk et al., (2016) report the occurrence of isotopically light fresh groundwater from the Karelian isthmus north from St. Petersburg from the Ediacaran sedimentary rocks and underlying metamorphosed crystalline basement. The  $\delta^{18}\text{O}$  values of these waters are  $\sim 4\text{‰}$  depleted with respect to modern precipitation in the area ranging from  $-11.3$  to  $-16.6\text{‰}$ . The authors relate the formation of these waters to groundwater recharge from the Baltic Ice Lake, a large proglacial lake that developed during the retreat of the Scandinavian Ice Sheet in the Late Pleistocene (Rosentau et al., 2009). The waters with similarly depleted isotopic composition ( $\delta^{18}\text{O}$  values from  $-15$  to  $-17\text{‰}$ ) also reside in the Voronka aquifer of the Cambrian-Vendian aquifer system south of St. Petersburg in Ivangorod area bordering the north-eastern parts of the BAB (Voroniuk et al., 2016).

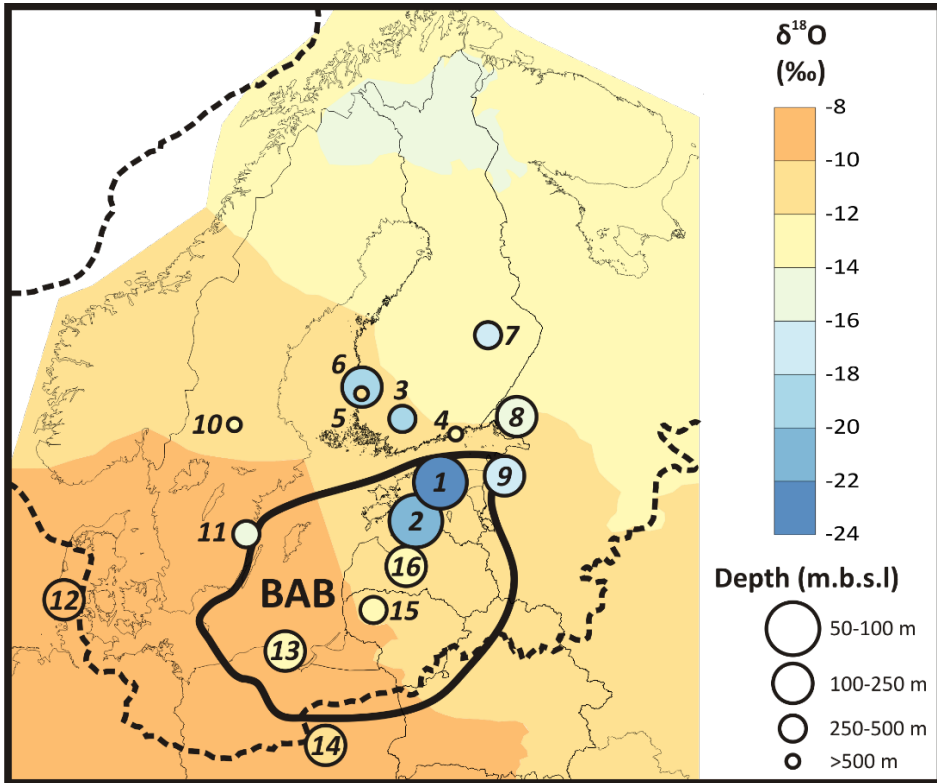


**Figure 2.** Isotopic composition of palaeogroundwater and their depth from the surface in the area covered by the Scandinavian Ice Sheet in the LGM. The maximum extent of the Scandinavian Ice Sheet in the LGM is shown by the dotted line (after Lasberg and Kalm, 2013). The coloured area shows the modelled annual mean  $\delta^{18}\text{O}$  values of precipitation in the study area (after Terzer et al., 2013). The solid line denotes the location of the Baltic Artesian Basin (BAB). Numbers denote aquifers from which glacial palaeogroundwater has been found: 1 – Cambrian-Vendian aquifer system/Ordovician-Cambrian aquifer system, Estonia (Savitski et al., 1993; Savitskaja and Viigand, 1994; Savitskaja et al., 1995; Vaikmäe et al., 2001; Raidla et al., 2009; Papers II-V); 2 – Lower-Middle-Devonian aquifer system, SW Estonia (Savitskaja et al., 1996a; T. Martma, J. Ivask, E. Kaup, J. Pärn, V. Raidla, R. Vaikmäe, unpublished data, 2018); 3 – Palmottu site, Finland (Ahonen et al., 2004); 4 – Hästholmen site, Finland (Pitkänen et al., 2001); 5 – Olkilouto site, Finland (Pitkänen et al., 2004); 6 – Pori/Pinomäki, Finland (Blomqvist, 1999; Frapé et al., 2003); 7 – Outokumpu site, Finland (Ivanovich et al., 1992); 8 – Cambrian-Vendian aquifer system, Karelian Isthmus, NW Russia (Voroniuk et al., 2016); 9 – Cambrian-Vendian aquifer system, Ivangorod, NW Russia (Voroniuk et al., 2016); 10 – Stripa granite, Sweden (Moser et al., 1989); 11 – Äspö HRL site, Sweden (Laaksoharju et al., 1999; Negrel et al., 2005); 12 – Ribe Formation, Rømø island, Denmark (Hinsby et al., 2001); 13 – Upper Cretaceous aquifer system, Hel peninsula, Poland (Halas et al., 1993); 14 – Oligocene aquifer, Mazovian basin, Poland (Zuber et al., 2000); 15 – Upper-Middle Devonian aquifer system, Lithuania (Mokrik & Mažeika, 2002; Mokrik et al., 2009); 16 – Lower-Middle Devonian aquifer system, Riga area, Latvia (Mokrik & Mažeika, 2002; Babre et al., 2016).

In the southern part of the BAB, the occurrence of groundwater of glacial origin with ages similar to the ones reported from central Poland (Zuber et al., 2000) has been observed by Mokrik et al., (2009) from the Upper-Middle Devonian aquifer system in Lithuania. The authors derive  $^{14}\text{C}$  model ages that range from 10 to 15 ka BP increasing up to 20 ka BP in the western margin of the aquifer system farther down the groundwater flow path. The  $\delta^{18}\text{O}$  values of those waters range from  $-10.9$  to  $-13\text{‰}$  being similar or slightly depleted with respect to modern recharge. Authors argue that these waters represent either a mixture glacial palaeogroundwater with sub-modern and modern meteoric water or originate from precipitation from the Late Weichselian Period. In an earlier work, Mokrik and Mažeika (2002) report the upwelling of palaeogroundwater in the mounts of larger river basins of Nemunas, Nevežis-Lielupe and Visla with  $\delta^{18}\text{O}$  values ranging from  $-12$  to  $-13.9\text{‰}$ . Similar upwelling of palaeogroundwater near the mouth of the Daugava river is suspected in the central parts of the BAB in Latvia, where Babre et al., (2016) report the most depleted values of  $\delta^{18}\text{O}$  in Latvia ( $-13.4\text{‰}$ ) from brackish groundwater in the Middle-Devonian aquifer. This value is some 3‰ depleted with respect to modern groundwater. The authors suggest that this groundwater could have formed in recharge conditions colder than present or through mixing between modern groundwater and periglacial meteoric water from the Late Pleistocene.

In the northern part of the BAB, the isotopic composition of groundwater is much more depleted with respect to modern precipitation than in the surrounding areas. Groundwater in the deepest sedimentary aquifer, the Cm-V aquifer system, has a very light isotopic composition ( $\delta^{18}\text{O}$  values from  $\sim -18.5$  to  $-23\text{‰}$ ) and low radiocarbon activities (Juodkakis and Zuzevičius, 1977; Punning et al., 1987; Mokrik and Vaikmäe, 1988; Vaikmäe and Vallner, 1989; Savitski et al., 1993; Savitskaja et al., 1994; Vaikmäe et al., 2001; Mokrik & Mažeika, 2002; Raidla et al., 2009, 2012). These are the lightest values for isotopic composition found in Europe which are  $\sim 6$  to  $12\text{‰}$  depleted with respect to modern groundwater in the area. The Cm-V aquifer system has been the most extensively studied groundwater system in Estonia.

The first hypothesis that were put forward to explain the formation of waters with such abnormal isotopic composition, related their origin to recharge from the pro-glacial Baltic Ice Lake in the Late Pleistocene (Yezhova et al., 1996) or to formation due to cryogenic metamorphism of glacial meltwater from the Scandinavian Ice Sheet during the LGM (Mokrik, 1997; Mokrik & Mažeika, 2002). The latter theory states that prior to the advance of the Scandinavian Ice Sheet in the LGM, the northern BAB was strongly influenced by permafrost that reached down to 450 m below ground surface (Mokrik & Mažeika, 2002). In these cold climate conditions similar to modern Siberia, the surface waters and shallow groundwater would have been significantly depleted with respect to modern precipitation in terms of their isotopic composition. The permafrost would have led to the freezing of discharge areas of shallow aquifers which would in turn have forced the infiltration of shallow groundwater with light isotopic composition down to the Cm-V aquifer system. According to the proposed model, this water was subsequently influenced by freezing and later by mixing with glacial meltwater originating from the Scandinavian Ice Sheet.

Vaikmäe et al., (2001) put forward the most widely accepted view on the origin of palaeogroundwater in the Cm-V aquifer system based on a multi-proxy study ( $\delta^{18}\text{O}_{\text{H}_2\text{O}}$ ,  $\delta^{13}\text{C}_{\text{DIC}}$ ,  $^3\text{H}$ ,  $^{14}\text{C}$ , noble gases, total gas content and composition). This states that waters in the Cm-V aquifer system originate directly from recharge of subglacial meltwater from the Scandinavian Ice Sheet during the LGM. The configuration of glacial land-forms and

end-moraines in the study area indicate that the advance of Scandinavian Ice Sheet to its maximum extent in LGM occurred predominantly from the north-western direction (Kalm et al., 2011) which would make this part of the aquifer system the recharge area during glacial meltwater intrusion. The recharge of glacial meltwater to the proglacial sedimentary aquifer systems in the northern BAB was made possible by the changes in the distribution of regional hydraulic heads during the advance of the continental ice sheet (Raidla et al., 2009). Jõelet (1998) has shown that molten conditions existed under the Scandinavian Ice Sheet in Estonian territory during the LGM with the imposed hydraulic gradient increasing to 0.0031 (compared to modern topographically induced hydraulic gradient of 0.0001-0.0004; Vallner, 1997) making the groundwater flow reversal possible in the northern part of the BAB. Subsequent studies have revealed that the groundwater in the Cm–V aquifer system is a mixture of three end-members (glacial meltwater, relict saline formation water and recent meteoric water; Marandi, 2007; Raidla et al., 2009). Calculated  $^{14}\text{C}$  model ages of glacial palaeogroundwater in the Cm-V aquifer system suggest that the glacial meltwater recharge was coeval with the advance and maximum extent of the Scandinavian Ice Sheet in the LGM (~14 to 27 ka BP; Raidla et al., 2012).

Scarce isotopic data in previous research suggests that glacial palaeogroundwater originating from glacial meltwater recharge could also be present in the aquifer systems overlying the Cm-V (Savitski et al., 1993; Savitskaja et al., 1995, 1996a, 1997; Vaikmäe et al., 2001; Mokrik & Mažeika, 2002; Raidla et al., 2009). The limited amount of previously published  $\delta^{18}\text{O}$  data from the Ordovician-Cambrian aquifer system (O-Cm) show that in the northern part of the aquifer system groundwater with depleted isotopic composition with respect to modern precipitation can be found. Previously reported  $\delta^{18}\text{O}$  values range from  $-15\text{‰}$  to  $-19\text{‰}$  (Savitski et al., 1993; Savitskaja et al., 1995; Vaikmäe et al., 2001; Raidla et al., 2009). Groundwater with  $\delta^{18}\text{O}$  values down to  $-17\text{‰}$  and  $-20\text{‰}$  has been found from shallower aquifer systems of Silurian-Ordovician (S-O) and Lower-Middle Devonian ( $\text{D}_{2-1}$ ), respectively (Savitskaja et al., 1996a, 1997; T. Martma, J. Ivask, E. Kaup, J. Pärn, V. Raidla, R. Vaikmäe, unpublished data, 2018).

The hypothesis of direct subglacial recharge of glacial meltwater into the bedrock aquifers in the northern BAB and the possibility of subsequent groundwater flow reversal was recently studied by numerical modelling (Sterckx et al. 2018). In the study glacial groundwater flow and transport of groundwater  $\delta^{18}\text{O}$  were simulated in two cross-sections in NW-SE direction. Several simulations using different subglacial boundary conditions (duration of the glacial maximum, maximal subglacial hydraulic head, initial  $\delta^{18}\text{O}$  in meltwater) confirmed that subglacial recharge under the Scandinavian Ice Sheet is able to explain currently observed  $\delta^{18}\text{O}$  distribution in the northern BAB under wide range of assumptions. Furthermore, the authors argue that the preservation of glacial palaeogroundwater in Estonia is mainly controlled by confining layers, proximity of the outcrop areas of the aquifers and the Baltic Sea. The general pattern emerging from the simulations was that shallow aquifers were more recharged by glacial meltwater in the Pleistocene compared to the deeper confined aquifers (e.g. the Cm-V and O-Cm). After the retreat of the ice sheet, the glacial meltwater was flushed out of the shallow aquifers, but it was preserved in deeper confined aquifers because meteoric recharge in the Holocene has not been sufficient to replace it entirely. The numerical modelling results of Sterckx et al. (2018) are largely in agreement with the empirical data discussed in Section 4 in this thesis.

Saline groundwater and brine in the Cambrian aquifer system from central deeper parts of the basin are probably of considerable age pre-dating the glacial palaeogroundwater in northern shallow parts of the basin. The origin of these deep formation waters has been related to relict seawater (Mokrik, 1997; Gerber et al., 2017). The  $^{81}\text{Kr}$  and  $^4\text{He}$  ages point to the origin of the brine from pre-Quaternary times (Gerber et al., 2017). In brines from Latvia and Lithuania  $^{81}\text{Kr}$  concentrations are below detection limit ( $R/R_{\text{air}} = 0.02$ ) indicating water that is older than 1.3 Ma.  $^4\text{He}$  and  $^{40}\text{Ar}$  measurements suggest even older ages ( $\sim 5$  Ma) for these waters. For brackish groundwater further north in Southern Estonia  $^{81}\text{Kr}$  ages are younger ranging from  $\sim 400$  to 600 ka (Gerber et al., 2017). The composition of the latter is influenced by mixing with fresh groundwater from the northern part of the BAB as manifested in changes in their chemical and isotopic composition (Raidla et al., 2009; Gerber et al., 2017). The  $\delta^{18}\text{O}$  and  $\delta^2\text{H}$  values in brackish water plot close to the GMWL while the brine in the central part of the BAB plot below the GMWL (Paper II). This indicates that these brines do not originate from meteoric recharge. The origin of chloride, which is one of the most important constituents of the TDS in brines from the central BAB, can be associated with various diagenetic processes in formation waters such as the dissolution of the late stage evaporates (e.g. halite), the entrapment and/or infiltration of evaporated seawater or membrane filtration (Kharaka and Hanor, 2007). There is no evidence for the occurrence of halite in the Lower Ordovician and Cambrian sedimentary rocks in the BAB. In the absence of evaporates, the high chloride concentrations found in brines suggest that they have most likely evolved from evaporated seawater later modified by water-rock interaction. In several sedimentary basins in North America evidence of brines originating from remnant evaporated seawater has been found (e.g. Stueber and Walter, 1991; Lampen and Rostron, 2000). The heavy mean  $\delta^{18}\text{O}$  value of  $-4.5\text{‰}$  with respect to modern precipitation in Na-Cl brines (Babre et al., 2016; Gerber et al., 2017) is close to the value of  $0 \pm 2\text{‰}$  reported by Muehlenbachs (1998) for the ice-free Palaeozoic ocean water. In addition, values for both the  $\text{Na}^+/\text{Cl}^-$  and  $\text{Br}^-/\text{Cl}^-$  ratios in brine are similar to seawater (Gerber et al., 2017; Paper II). The specific origin of these brines requires further studies. Mokrik (1997) has suggested that meteoric waters replaced the original connate seawater within the Cambrian sedimentary rocks during the Middle-Late Cambrian uplift of the BAB area and the seawater again intruded the sediments during a period from Ordovician to Devonian when the basin was considerably subsided.

## 3 Material and methods

### 3.1 Geological and hydrogeological setting of the study area

Baltic Sedimentary Basin is a Phanerozoic sedimentary basin that covers the territories of Estonia, Latvia, Lithuania and parts of Russia, Poland and Belarus (Fig. 3, Mokrik, 1997; 2003; Virbulis et al., 2013). Approximately half of the Baltic Sedimentary Basin is covered by the Baltic Sea. The total surface area of the basin is about 480000 km<sup>2</sup> (Virbulis et al., 2013). The hydrogeological equivalent of the Baltic Sedimentary Basin is the Baltic Artesian Basin (BAB) which is a complex multi-layered hydrogeological system. The thickness of the sedimentary cover reaches up to 5000 meters in the south-western part of the basin, while the crystalline basement reaches to the surface at its northern and south-eastern parts (Fig. 3). The northern part of the basin is situated on the southern slope of the Fennoscandian Shield while the southern part is situated on the north-western slope of the Belarusian-Masurian Anticline (Zuzevičius, 2010). In the northern part of the BAB (Estonia and Latvia), the sedimentary cover contains rocks of Ediacaran to Devonian age which overlie the Paleoproterozoic crystalline basement (Fig. 3). The crystalline basement gradually slopes towards the south by 2-4 m·km<sup>-1</sup>.

Previous studies have divided the vertical sequence of groundwater bearing formations in the BAB into three main hydrodynamic zones based on the groundwater flow velocity and residence times (Vallner, 1997; Mokrik, 2003). The uppermost part of the sequence forms an active water exchange zone in which the infiltration of recent meteoric water predominates. It has been thought previously that this zone can reach down to the depths of about 400 m. The zone of delayed (moderate) groundwater exchange is located at depths from 400 to ~1000 m. Below depths of 1000 m, one can find the stagnant Ca-Na-Cl type brine (Mokrik, 2003). The Baltic Sea is the main discharge area for the deep artesian groundwater associated with moderate water exchange zone. The general flow direction of the deep groundwater in the BAB is directed from the deeper southwestern part of the basin towards the periphery monoclines (Mokrik, 2003).

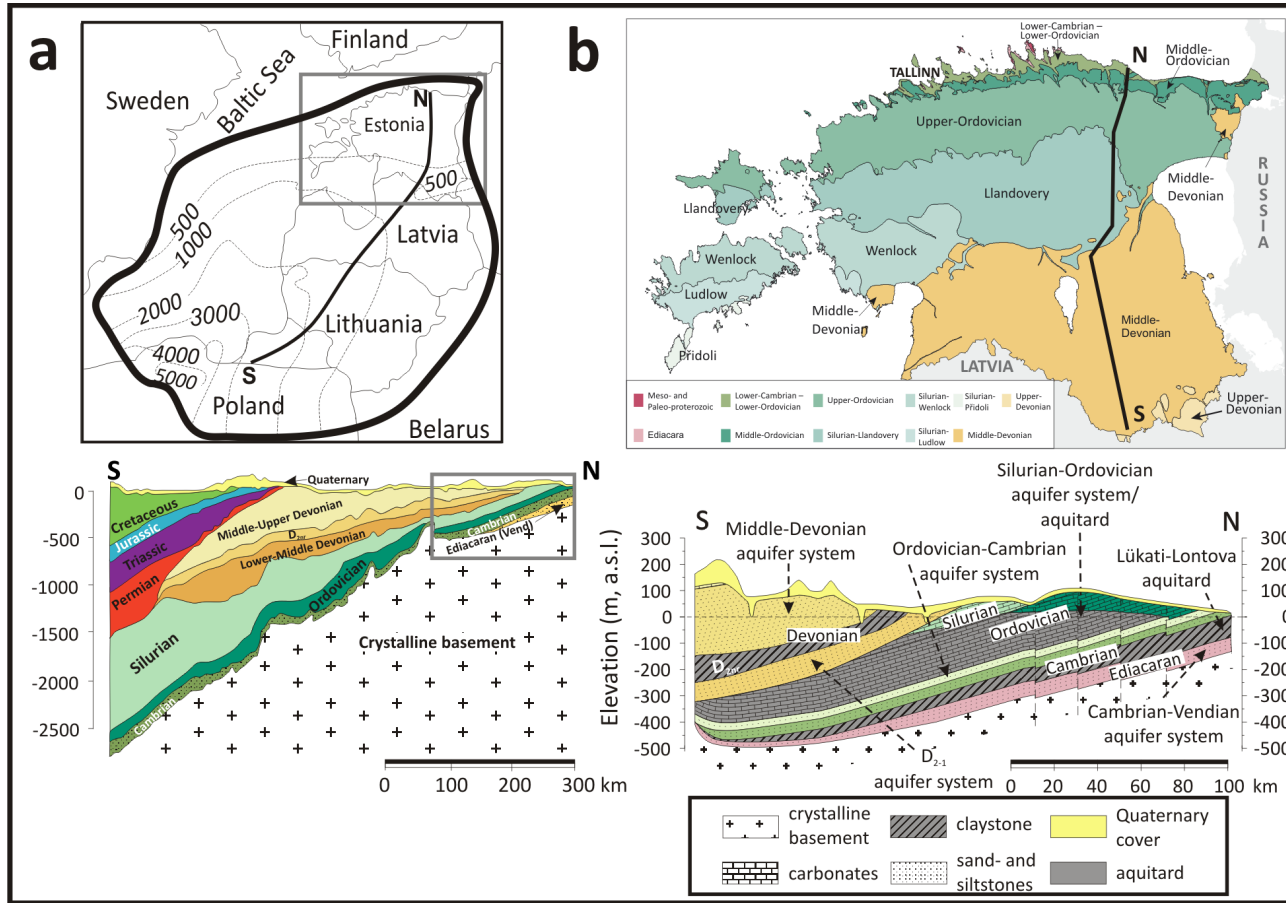


**Figure 3.** (a) The location and boundaries of the Baltic Artesian Basin (BAB). Contour lines mark the depth of the crystalline basement in meters b.s.l. The geologic cross-section of the BAB along the line N-S is also shown. Abbreviations:  $D_{2-1}$  aquifer system – Lower-Middle Devonian aquifer system,  $D_{2nr}$  – Middle-Devonian Narva regional aquitard, (b) the close up (grey square) depicting the geological and hydrogeological setting in the northern part of the BAB (Estonia). (modified from: Juodkazis, 1980; Virbulis et al., 2013; Paper II, IV)

Perens and Vallner (1997) divide the groundwater system in the northern part of the BAB (Estonia) into three principal hydrostratigraphical units:

1. *The Quaternary deposits*, which contain local aquifers influenced by meteorological conditions where a lot of water circulates by the agency of capillary force or evaporates, in addition to the filtration flow. The main aquifers are found in glaciofluvial sand and gravel which are the most exploited Quaternary aquifers in the study area (e.g. Vasavere water intake in East-Estonia) and glaciogenous sediments of loamy-sandy till which cover almost 2/3 of the Estonian territory;
2. *The bedrock*, which consists of terrigenous and carbonate Palaeozoic and Proterozoic (Ediacaran) rocks. These rocks form porous, fissured and occasionally karstified mostly confined aquifers, which are isolated from each other with aquitards of different isolation capacity. The confined aquifers are generally part of intermediate and regional flow systems. In the deeper strata the groundwater is high in TDS (values up to 20 g·L<sup>-1</sup>; Viigisaar, 1978; EELIS, 2018) and moves very slowly under natural conditions;
3. *The crystalline basement*, where the water resides in the weathered portion of the Meso- and Palaeoproterozoic igneous and metamorphic rocks. The water is high in TDS with values up to 22 g·L<sup>-1</sup> (Viigisaar, 1978; Karise, 1997) that is sporadically almost stagnant in natural conditions. The lower portion of the crystalline basement serves as an aquiclude for the whole overlying water-bearing formation.

The geology of the northern part of the BAB together with the distribution of main aquifer systems and regional aquitards is shown in Figure 3b. Taking into account the topic of the thesis, we next concentrate on hydrogeological characteristics of the major bedrock aquifers from where the occurrence of glacial palaeogroundwater has been reported. More detailed overviews of the hydrogeologic characteristics of aquifers and aquitards in the northern part of the BAB can be found in Perens and Vallner (1997) and Perens et al. (2012).

In Devonian formation, which is the uppermost Paleozoic sedimentary sequence of the northern BAB, the glacial palaeogroundwater can be first encountered in aquifers underlying the Narva regional aquitard (see Section 4). The Narva aquitard consists of siltstone, dolomite, marl and clay of the Middle Devonian Eifelian Stage with a total thickness reaching up to 90 meters (Perens and Vallner, 1997). In southern Estonia and Latvia, this sequence can be viewed as an uppermost effective bedrock aquitard. The transmissivity in the aquitard varies from 10<sup>-5</sup> to 10<sup>-4</sup> m·d<sup>-1</sup> and in places can have values as low as 10<sup>-6</sup> m·d<sup>-1</sup> (Perens and Vallner, 1997). The rocks in the uppermost portion of the Narva aquitard have water supplying qualities and have been used in water supply in central Estonia.

The underlying Middle–Lower Devonian aquifer system (D<sub>2-1</sub>) consists of the water-bearing layers of Middle and Lower Devonian rocks (Lochovian, Pragian and Emsian Stages) underlying the Narva regional aquitard. It consists of fine-grained weakly cemented sand- and siltstones with interlayers of clay and dolomitized sandstone (Perens and Vallner, 1997). The D<sub>2-1</sub> aquifer system has a thickness reaching up to 100 m (Perens and Vallner, 1997). The water in the aquifer system is predominantly confined. The lateral conductivity of sandstones is mostly 2-6 m·d<sup>-1</sup> (on average 3 m·d<sup>-1</sup>) and transmissivity of the aquifer system is 50-500 m<sup>2</sup>·d<sup>-1</sup> (Perens and Vallner, 1997; Perens et al., 2012). The dominant water type of the aquifer system is Ca-Mg-HCO<sub>3</sub> water which

changes gradually to Na-Ca-HCO<sub>3</sub> type with depth and has TDS concentrations varying between 300 to 500 mg·L<sup>-1</sup> (Perens et al., 2001). In the southern deeper parts of the aquifer system brackish Ca-Na- SO<sub>4</sub>-Cl water is found having the TDS concentrations up to 4600 mg·L<sup>-1</sup> (Perens et al., 2001).

The Silurian–Ordovician aquifer system (S-O) consists of limestone, dolomite and marls with clayey interlayers of Silurian and Ordovician Systems. These rocks underlie the Quaternary sediments in northern Estonia and the Devonian sedimentary rocks in southern Estonia (Fig. 3). The total thickness of the water-bearing rocks can reach up to 400 m. The upper 30 m of the rock matrix is karstified and is extremely cavernous, with numerous cracks and fissures (Perens and Vallner, 1997). In deeper parts of the rock matrix, the cracks and fissures are rare, and the S-O aquifer system gradually turns into an aquitard. The whole Silurian-Ordovician sequence can be viewed as a regional aquitard at increasing depths (>75 m, Perens and Vallner, 1997). The lateral and transversal conductivity of the aquifer system is very variable, and the arrangement of local aquifers and aquitards is often complex. The lateral conductivity ranges from 10-50 m·d<sup>-1</sup> in the topmost 20 m, 5-8 m·d<sup>-1</sup> at a depth down to 50 m and is only 1-2 m·d<sup>-1</sup> at the depth of 50 to 100 m (Perens and Vallner, 1997). The transmissivity is on average 400 m<sup>2</sup>·d<sup>-1</sup> (Perens and Vallner, 1997). Groundwater in the topmost 50 m of the S-O aquifer system is mainly of Ca-Mg-HCO<sub>3</sub> type with TDS concentrations between 300 and 500 mg·L<sup>-1</sup> (Perens et al., 2001). In Western Estonian Archipelago which has been subject higher rates of isostatic uplift in the Holocene, the groundwater is characterized by higher concentrations of Na<sup>+</sup> and Cl<sup>-</sup> (Mg-Ca-Na-HCO<sub>3</sub>-SO<sub>4</sub> and Na-HCO<sub>3</sub>-Cl water types) and by higher TDS concentrations (up to 2000 mg·L<sup>-1</sup>) as a result of the influence of the Baltic Sea (Perens et al., 2001). The Na<sup>+</sup> and Cl<sup>-</sup> concentrations also increase with depth in the S-O aquifer system.

The lower portion of the Silurian and Ordovician sedimentary rocks form a Silurian-Ordovician regional aquitard. In the northernmost part of the BAB in northern Estonia, this aquitard consists of Lower Ordovician (Tremadocian and Floian Stage) limestones, marls, siltstones, clays and black shale (graptolite argillite), extending ~100 km southward from Estonia's northern coast. The Lower Ordovician black shale is characterized by high abundance of pyrite (on average 2.4–6% of mineral phases) and is rich in the sedimentary organic matter (total organic content of 15–20%; Petersell, 1997; Voolma et al., 2013). The whole Silurian-Ordovician sedimentary sequence forms a regional aquitard at increasing depths >75 m and has a transversal hydraulic conductivity ranging from 10<sup>-9</sup> to 10<sup>-4</sup> m·d<sup>-1</sup> (Perens and Vallner, 1997; Perens et al., 2012).

The S-O regional aquitard is underlain by the Ordovician-Cambrian aquifer system which consists of Cambrian and Early Ordovician age sand- and siltstones (Fig. 3). The thickness of the aquifer system increases from 20-60 m in northern Estonia to ~120 m in Latvia (Juodkazis, 1980; Savitskaja et al., 1995; Perens and Vallner, 1997). The depth of the aquifer system strata is 10-20 m below ground surface in northern Estonia and increases southward to over 1000 meters in Latvia. O-Cm aquifer system merges with the underlying Cm-V aquifer system in south-western Estonia to form a single Cambrian aquifer system in the deeper parts of the BAB (Perens and Vallner, 1997). Cambrian and Lower Ordovician sandstones forming the aquifer matrix are mainly quartz arenites or subarkoses, with quartz content up to 90% (Raidla et al., 2006). In addition, they contain accessory phosphorite (authigenic apatite) and are cemented with carbonate minerals (mainly Fe-dolomite), whose abundance varies from 0 to 29 wt% with an average value of 3% (Raidla et al., 2006). The average content of pyrite and hematite is close to 1% or

less (Raidla et al., 2006). Hematite is the most abundant Fe(III)-oxide in the aquifer matrix, but the occurrence of secondary goethite has also been reported (Mens and Pirrus, 1997; Raidla et al., 2006). Also, dispersed sedimentary organic matter of sapropelitic type can be found from the Cambrian sandstones and in the underlying Lontova clays (total organic matter content of 0.8–2.6%; Raidla et al., 2006). The lateral hydraulic conductivity of Cambrian and Lower Ordovician sandstones ranges from 0.5 to 3 m·d<sup>-1</sup> (Perens and Vallner, 1997; Perens et al., 2012). Transmissivity increases from 25 to 50 m<sup>2</sup>·d<sup>-1</sup> in northern Estonia to a range from 80 to 130 m<sup>2</sup>·d<sup>-1</sup> in southern Estonia due to the increased thickness of the water-bearing rocks (Savitskaja et al., 1995; Perens and Vallner, 1997). In northern Estonia several chemical types of water such as Ca-Mg-HCO<sub>3</sub>, and Na-HCO<sub>3</sub> with the TDS concentrations of 200-500 mg·L<sup>-1</sup> have been reported (Savitskaja et al., 1995; Perens et al., 2001; Paper II). The TDS concentrations increase in southern and south-western directions where Na-Cl-HCO<sub>3</sub> and Na-Cl groundwater with TDS values >2000 mg·L<sup>-1</sup> has been found (Perens et al., 2001). The highest TDS values from the O-Cm aquifer system are reported from a deep borehole in Ruhnu, southern Estonia, where TDS values are as high as 20 g·L<sup>-1</sup> (EELIS, 2018).

The O-Cm aquifer system is separated from the underlying Cm-V aquifer system by the Lükati-Lontova regional aquitard which consists of siltstones and clays of the Lower Cambrian Lükati and Lontova Formations (Terraneuvian Series) that have a transversal hydraulic conductivity from 10<sup>-5</sup> to 10<sup>-10</sup> m·d<sup>-1</sup> (Perens and Vallner, 1997; Perens et al., 2012). In western Estonia, this aquitard is laterally replaced by siltstones and sandstones of the Voosi Formation (Fig. 3b). Here, the aquitard becomes sandier and thinner and its transversal hydraulic conductivity increases to ≥10<sup>-5</sup> m·d<sup>-1</sup> (Perens and Vallner, 1997).

The Cm–V aquifer system consists mostly of Ediacaran (Vendian) sand- and siltstones of the Kotlin Stage with interlayers of clay that lie directly on the Palaeoproterozoic crystalline basement. The thickness of the aquifer system decreases from 80–90 m in its north-eastern part to only a few metres in its north-western part (Perens and Vallner, 1997). In eastern Estonia up-to-50m-thick clays of Kotlin Formation with the transversal conductivity of 10<sup>-8</sup> to 10<sup>-5</sup> m·d<sup>-1</sup> divide the aquifer system into two aquifers: the upper, Voronka aquifer (V<sub>2vr</sub>), and the lower, Gdov aquifer (V<sub>2gd</sub>; Perens and Vallner, 1997). The former consists of quartzose sand- and siltstone with a thickness of up to 45 m. The latter is formed of up-to-68m-thick complex of mixed-grained sand- and siltstone (Perens and Vallner, 1997). The lateral hydraulic conductivities of the Voronka and Gdov aquifers are on average 2-6 m·d<sup>-1</sup> and 5-6 m·d<sup>-1</sup>, respectively, and decrease in southern parts of the aquifer system (Perens et al., 2012). Transmissivity of the Voronka aquifer decreases from 100-150 m<sup>2</sup>·d<sup>-1</sup> in northern Estonia to 50 m<sup>2</sup>·d<sup>-1</sup> and less in southern Estonia (Perens and Vallner, 1997). The transmissivity of the Gdov aquifer decreases from north-eastern Estonia (300-350 m<sup>2</sup>·d<sup>-1</sup>) in a southerly and westerly direction to 100 m<sup>2</sup>·d<sup>-1</sup> and less (Perens and Vallner, 1997). In northern part of the Cm-V aquifer system the groundwater is fresh or brackish with a Ca-Na-HCO<sub>3</sub>-Cl water type and TDS concentrations from 300 to ~2000 mg·L<sup>-1</sup> (Marandi, 2007). In north-eastern and southern part of the aquifer system brackish water of Na-Cl type with TDS from ~1000 to ~18000 mg·L<sup>-1</sup> can be found. These waters are a mixture between fresh groundwater in the northern part of the aquifer system and relict saline formation water (Marandi, 2007). In north Estonian coastal areas groundwater with Ca-HCO<sub>3</sub> type is found in the vicinity of the ancient buried valleys filled with Quaternary sediments that cut through the aquifer matrix. Here fresh groundwater from the overlying aquifers and modern precipitation can reach the aquifer system. This process has been accelerated by extensive water

abstraction from the aquifer system starting in the 1970s, that formed large depression cones in northern Estonia. The TDS concentration of groundwater filling the buried valleys varies between 200-500 mg·L<sup>-1</sup> (Marandi, 2007).

There is lithostratigraphic, biostratigraphic and geochronological evidence for the occurrence of at least three Pleistocene glaciations in the northern part of the BAB – Elsterian (480–420 ka BP; MIS 12), Saalian (300–130 ka BP; MIS 6–10) and Weichselian (110–11.7 ka BP; MIS 2–4) – separated by two major interglacial periods – Holsteinian (420–300 ka BP; MIS 11) and Eemian (130–110 ka BP; MIS 5, Kalm et al., 2011). Sedimentary records from older glaciations or from the pre-Quaternary times have not been preserved in Estonia (Raukas et al., 2004; Kalm et al., 2011). During the Late Pleistocene, Estonia was ice-free at least between 115 – 68 and 44 – 27 ka BP (Kalm et al., 2011). The beginning of the Late Weichselian glaciation in Estonia has not been directly dated, but the available data from areas located more centrally in relation to the Scandinavian Ice Sheet (e.g. Finland) suggest that the onset may have occurred around 22 ka BP (Ukkonen et al., 2011). The configuration of glacier bedforms and end moraines in south-eastern Lithuania, northern Belarus and on the Valdai Heights in north-western Russia indicate that the earliest advance to the most accepted Last Glacial Maximum (LGM) position was predominantly from the north-west direction (Kalm, 2013). Maximum thickness of the Scandinavian Ice Sheet during the Late Weichselian ice age over northern BAB (i.e. Estonian and Latvian territory) reached ~2000 meters (Siegert and Dowdeswell, 2004). Five major ice-marginal zones (in order of decreasing age: Haanja, Otepää, Sakala, Pandivere and Palivere) are usually distinguished in Estonia that mark the retreat of the ice sheet from the area (Kalm et al., 2011). They were formed either as a result of still-stands of the ice margin or in some cases, as a result of re-advances. At a larger scale, the ice-marginal zones in Estonia are sinuous compared to the next, more northerly, relatively linear Salpausselkä end moraines in southern Finland. This suggests a gentler slope of the ice sheet during the deglaciation of Estonia when large ice-stream complexes drained the ice sheet (Kalm et al., 2011). The deglaciation of the Estonian territory from the Haanja ice-marginal zone to the recession of ice from the Palivere zone took place in approximately 2000 years from 15 to 13 cal. ka BP (Kalm, 2006; Saarse et al., 2012). In contrast to the older oscillatory phases (Haanja, Otepää, Sakala, Pandivere), the Palivere ice-marginal zone is clearly of a re-advance character, as reflected by the distribution of push moraines and by the fact that the older glaciolacustrine sediments are overlain by glaciofluvial material (Kalm et al., 2011).

### 3.2 Sample collection and analysis

The fieldwork campaigns for groundwater sampling were conducted in the period from 2013–2016 during which a total number of 227 samples were collected. In 2013 samples were collected for hydrochemistry, stable isotope composition ( $\delta^2\text{H}_{\text{H}_2\text{O}}$ ,  $\delta^{18}\text{O}_{\text{H}_2\text{O}}$ ,  $\delta^{13}\text{C}_{\text{DIC}}$ ) and noble gases in the north-western part of the O-Cm aquifer system (Weissbach, 2014; Papers II and IV). In 2014 two separate fieldwork campaigns were undertaken. During the first campaign samples for hydrochemistry and stable isotopes ( $\delta^2\text{H}_{\text{H}_2\text{O}}$ ,  $\delta^{18}\text{O}_{\text{H}_2\text{O}}$ ) were collected from wells tapping shallow aquifers and from springs (Paper I). During the second campaign groundwater in the O-Cm aquifer system was sampled in its northern and north-eastern parts. Samples were taken to study the hydrochemistry and stable isotope composition of groundwater ( $\delta^2\text{H}_{\text{H}_2\text{O}}$ ,  $\delta^{18}\text{O}_{\text{H}_2\text{O}}$ ,  $\delta^{13}\text{C}_{\text{DIC}}$ ; Paper II). During the third fieldwork campaign in 2015 groundwater from both the O-Cm and Cm-V aquifer systems

was sampled for hydrochemistry, noble gases,  $^3\text{H}$ ,  $^{14}\text{C}$  (for dating with the conventional method) and for a suite of stable isotopes in water and dissolved species ( $\delta^2\text{H}_{\text{H}_2\text{O}}$ ,  $\delta^{18}\text{O}_{\text{H}_2\text{O}}$ ,  $\delta^{13}\text{C}_{\text{DIC}}$ ,  $\delta^{34}\text{S}_{\text{SO}_4}$ ,  $\delta^{18}\text{O}_{\text{SO}_4}$ ; Papers III-V). In 2016 two fieldwork campaigns were carried out. The first concerned the D<sub>2-1</sub> and S-O aquifer systems in southern Estonia. Groundwater samples were taken for the analyses of hydrochemistry,  $^{14}\text{C}$  (for dating with the AMS method) and a suite of stable isotopes in water and dissolved species ( $\delta^2\text{H}_{\text{H}_2\text{O}}$ ,  $\delta^{18}\text{O}_{\text{H}_2\text{O}}$ ,  $\delta^{13}\text{C}_{\text{DIC}}$ ,  $\delta^{34}\text{S}_{\text{SO}_4}$ ,  $\delta^{18}\text{O}_{\text{SO}_4}$ ). The second fieldwork campaign in 2016 was carried out for sampling many of the same wells as in 2015 from the O-Cm and Cm-V aquifer systems to be analysed for hydrochemistry,  $^{14}\text{C}$  dating with AMS method, stable isotopes ( $\delta^2\text{H}_{\text{H}_2\text{O}}$ ,  $\delta^{18}\text{O}_{\text{H}_2\text{O}}$ ,  $\delta^{13}\text{C}_{\text{DIC}}$ ) together with the abundance and the stable isotopic composition of methane and  $\text{CO}_2$  ( $\delta^{13}\text{C}_{\text{CH}_4}$ ,  $\delta^2\text{H}_{\text{CH}_4}$ ,  $\delta^{13}\text{C}_{\text{CO}_2}$ ; Papers III-V). In addition, several samples measured for the isotopic composition of groundwater discussed in the thesis and the related papers were collected by the Geological Survey of Estonia during the national groundwater monitoring programme (Papers I and II).

For further details about sample collection and analysis, the reader is referred to papers cited above. The general features of both sample collection and analysis for samples discussed in the thesis are the following. Water samples were collected into HDPE bottles once pH, electric conductivity values and dissolved  $\text{O}_2$  levels had stabilised. The pH, temperature, electric conductivity and dissolved oxygen were measured in the field using a Hach HQ40d<sup>TM</sup> multi-parameter digital meter.  $\text{HCO}_3^-$  and  $\text{CO}_3^{2-}$  concentrations were measured in the Laboratory of Geological Survey of Estonia using the titration method (ISO 9963-1) within 48 hours of the sample collection or in the field using a Millipore MColorTest<sup>TM</sup> titration kit. Major and minor ion concentrations were measured in the Department of Geology at Tallinn University of Technology using DIONEX ICS-1100 ion chromatograph.  $\text{Fe}^{2+}$  and  $\text{Mn}^{2+}$  concentrations for samples collected in 2016 were determined in the Laboratory for Applied Geology and Hydrogeology at Ghent University using atomic absorption spectrometry (AAS).

Stable isotope ratios of hydrogen ( $\delta^2\text{H}$ ) and oxygen ( $\delta^{18}\text{O}$ ) in water were analysed in the Laboratory of mass spectrometry at the Department of Geology, Tallinn University of Technology using the Picarro L2120-i Isotopic Water Analyzer (Papers I-IV). The  $\delta^{18}\text{O}_{\text{H}_2\text{O}}$  and  $\delta^2\text{H}_{\text{H}_2\text{O}}$  values for samples with  $\text{TDS} > 1500 \text{ mg}\cdot\text{L}^{-1}$  were measured at the Department of Climate and Environmental Physics at the University of Bern with Picarro L2140-i Isotopic Water Analyzer using the online method presented in Affolter et al. (2014; Papers II and III). For Paper V the stable hydrogen and oxygen isotope measurements of groundwater were performed at the Institute for Geological and Geochemical Research in Budapest using the Los Gatos Research LWIA-24d liquid water isotope analyser.

The carbon isotope composition of DIC ( $\delta^{13}\text{C}_{\text{DIC}}$ ) was determined using a Thermo Fisher Scientific Delta V Advantage mass spectrometer at the Department of Geology, Tallinn University of Technology from DIC precipitated as  $\text{BaCO}_3$  in the field using  $\text{BaCl}_2\cdot 2\text{H}_2\text{O}$  and  $\text{NaOH}$  (Clark and Fritz, 1997; Papers III and IV). The dissolved sulphate for  $\delta^{34}\text{S}_{\text{SO}_4}$  and  $\delta^{18}\text{O}_{\text{SO}_4}$  analysis was precipitated as  $\text{BaSO}_4$  and measured using a Thermo Scientific Delta V Plus with Flash HT Plus mass-spectrometer in the Department of Geology at the University of Tartu (Paper III). Methane concentration and stable isotope data of  $\text{CH}_4$  and  $\text{CO}_2$  ( $\delta^{13}\text{C}_{\text{CH}_4}$ ,  $\delta^2\text{H}_{\text{CH}_4}$ ,  $\delta^{13}\text{C}_{\text{CO}_2}$ ) were determined at BGR (Federal Institute for Geosciences and Natural Resources) in Hannover, Germany using a CF-IRMS (Trace GC coupled to a MAT 253; Paper V).

The samples for the measurement of radiocarbon activities were collected during two fieldwork campaigns in 2015 and 2016. In 2015 radiocarbon activities were measured by

a conventional method in the Radiocarbon Laboratory in Department of Geology at Tallinn University of Technology. The samples were collected into several vessels with the total volumes from 150 to 250 L from which DIC was precipitated as BaCO<sub>3</sub>. The samples for <sup>14</sup>C dating with AMS method were collected into 1 L glass bottles that were submerged into an overflowing container to minimize the connection to the atmosphere. These samples were prepared in the University of Heidelberg and measured by AMS (MICADAS system) at the Curt-Engelhorn-Center Archaeometry in Mannheim (Paper IV). Tritium samples were measured in the Laboratory of Nuclear Geophysics and Radioecology at Nature Research Centre at Vilnius, Lithuania (Paper IV). The samples were counted with electrolytic enrichment using Quantulus 1220 liquid scintillation spectrometer.

Noble gas samples were collected into copper tubes fixed on the aluminium racks (Torgersen and Stute, 2013; Paper IV). These copper tubes contained about 20 g of water and were closed vacuum tight by stainless steel clamps. Noble gas contents (He, Ne) were determined in at the Institute of Environmental Physics at Heidelberg University with a GV Instruments MM 5400 mass spectrometer.

### 3.3 Geochemical modelling

To study the geochemical evolution of groundwater, geochemical modelling was utilized for calculating saturation states of groundwater with respect to carbonate minerals (Papers II and IV) and for constructing both forward and inverse models to calculate the <sup>14</sup>C model age (Paper IV). Three geochemical modelling software programs were used: GWB (Bethke and Yeakle, 2015), PHREEQC (Parkhurst & Appelo, 2013) and NETPATH (Plummer et al., 1994; El-Kadi et al., 2011). The specific details about geochemical modelling can be found in Papers II and IV. To arrive at <sup>14</sup>C model ages the isotopic and chemical composition of recharge waters formed in three hypothetical recharge conditions (modern, interstadial and glacial; Paper IV) were calculated. The applied multi-step geochemical modelling concept in PHREEQC was based on the framework developed by Van Der Kemp et al. (2000) and Blaser et al. (2010). Firstly, the concentrations of total dissolved inorganic carbon (TDIC), DIC speciation, Ca<sup>2+</sup> and pH were calculated for calcite dissolution in different pCO<sub>2</sub>, temperature and system conditions (open, closed). Secondly, this speciation of DIC was used to calculate the δ<sup>13</sup>C compositions and initial <sup>14</sup>C activities of the recharge waters considering equations proposed by van der Kemp et al., (2000) and isotopic exchange during dissolution of carbonate minerals (Mook, 1968; Vogel et al., 1970; Mook et al., 1974; Friedman & O'Neill, 1977; Paper IV). The value for soil δ<sup>13</sup>C<sub>CO2</sub> was calculated from equation (van der Kemp et al., 2000; Blaser et al., 2010):

$$\delta^{13}C_{soil} = \frac{c_{atm}(\delta^{13}C_{atm}) + (c_{soil} - c_{atm}) \cdot (\delta^{13}C_{prod} + 1000 \ln \alpha)}{c_{soil}} \quad (2)$$

The explanation of the variables in Eq. 2 and their values are given in Table 1.

**Table 1.** Variables used to calculate the value for soil  $\delta^{13}\text{C}_{\text{CO}_2}$  in geochemical modelling exercise with the PHREEQC in Paper IV.

Variable	Explanation	Values	Reference
$C_{\text{atm}}$	CO <sub>2</sub> concentrations in the atmosphere (ppmV)	<i>glacial/interstadial conditions:</i> 10 <sup>-3.70</sup> <i>Holocene conditions:</i> 10 <sup>-3.55</sup>	Leuenberger et al., 1992
$C_{\text{soil}}$	CO <sub>2</sub> concentrations in the soil (ppmV)	from 10 <sup>-3.70</sup> to 10 <sup>-1.8</sup>	Paper IV
$\delta^{13}\text{C}_{\text{atm}}$	$\delta^{13}\text{C}$ value (‰) of CO <sub>2</sub> in the atmosphere	glacial conditions: -6.9 interstadial conditions: -6.6‰ Holocene conditions: -6.5‰	Leuenberger et al., 1992
$\delta^{13}\text{C}_{\text{prod}}$	$\delta^{13}\text{C}$ value (‰) of biogenically produced CO <sub>2</sub> in the soil	-27‰	Vogel, 1993
$\alpha$	fractionation factor determined by the relation of the diffusion coefficients for <sup>12</sup> CO <sub>2</sub> and <sup>13</sup> CO <sub>2</sub>	1.0044	Cerling et al., 1991

To arrive at <sup>14</sup>C model ages, series of inverse models were developed using inverse modelling software NETPATH and its interactive user version NETPATH-WIN (Paper IV). As initial waters, the composition of hypothetical recharge waters calculated with PHREEQC was used. For each sample, ~20-30 different models were run in NETPATH with different recharge waters representing modern, glacial and interstadial conditions. Models which did not take into account the characteristic processes observed in the aquifer system (e.g. oxidation of organic matter) were rejected. The models were evaluated on the basis of consistency with  $\delta^{13}\text{C}_{\text{DIC}}$  value and the total dissolved carbon concentration in the end well. Initial waters from recharge conditions that best reproduced the measured  $\delta^{13}\text{C}_{\text{DIC}}$  value were considered the most plausible for calculating <sup>14</sup>C model ages (Paper IV). For age calculations, the <sup>14</sup>C half-life of 5730 years was used.

## 4 Results and discussion

### 4.1 Isotopic composition of modern precipitation and shallow groundwater in the BAB area

The isotopic composition of precipitation in the BAB and surrounding areas ranges from  $-70\text{‰}$  to  $-90\text{‰}$  for mean annual  $\delta^2\text{H}$  values and from  $-10\text{‰}$  to  $-12\text{‰}$  for mean annual  $\delta^{18}\text{O}$  values (Fig. 2; Punning et al., 1987; Kortelainen and Karhu, 2004; Terzer et al., 2013; Skuratovič et al., 2015, IAEA/WMO, 2018; Paper I). The oxygen isotope composition of precipitation in the northern part of the BAB (Estonia) was first studied during 1982-1985 by Punning et al. (1987) in Tiirikoja, eastern Estonia (Fig. 4). The monthly weighted mean value of  $\delta^{18}\text{O}$  in precipitation for the period was  $-10.4\text{‰}$ . The difference between the highest and lowest monthly  $\delta^{18}\text{O}$  values was  $9.1\text{‰}$  on average. The weighted mean  $\delta^{18}\text{O}$  values of precipitation in winter and summer months during the observation period were  $-13.8\text{‰}$  and  $-8.4\text{‰}$ , respectively.



**Figure 4.** Locations of the Tiirikoja, Tartu/Tõravere and Vilsandi meteorological stations in Estonia where the isotopic composition of precipitation has been studied (Punning et al., 1987; IAEA/WMO, 2018) together with the location of the Pandivere Upland discussed in Papers I-IV. (modified from Estonian Land Board, 2018)

In July 2013 two new GNIP stations were established in the Estonian territory on Vilsandi Island, western Estonia and in Tartu/Tõravere meteorological station in southern Estonia (Fig. 4). The precipitation samples have been collected up to present time and measured in the Department of Geology at Tallinn University of Technology. The Vilsandi station represents maritime climate in western Estonia close to the central parts of the Baltic Sea, while Tartu/Tõravere station is located  $\sim 120$  km inland from the Baltic Sea coast and exhibits more continental conditions. The monthly weighted mean values for  $\delta^{18}\text{O}$  in precipitation for the period 2013-2015 were  $-10.06 \pm 0.38\text{‰}$  and  $-10.60 \pm 0.48\text{‰}$  for Vilsandi and Tartu/Tõravere stations, respectively (IAEA/WMO, 2018). In Vilsandi, the weighted mean  $\delta^{18}\text{O}$  values of winter and summer months during the observation period

were  $-11.9\text{‰}$  and  $-8.4\text{‰}$ , respectively (IAEA/WMO, 2018). In Tartu/Tõravere, the same values were  $-13.1\text{‰}$  and  $-8.6\text{‰}$ , respectively (IAEA/WMO, 2018). These values agree well with results reported from Tiirikoja by Punning et al. (1987). The consistency with Tiirikoja measurements is better for Tartu/Tõravere station which can be explained by the similar inland location of the two stations (Fig. 4).

The local meteoric water lines (LMWLs) from Vilsandi and Tartu/Tõravere stations is close to the global meteoric water line (GMWL, Craig, 1961; Rozanski et al., 1993). The LMWL for Vilsandi station based on the reduced major axis regression (RMA; Crawford et al., 2014) is (IAEA/WMO, 2018):

$$\delta^2H = 8.3\delta^{18}O + 11.5 \quad (3)$$

For Tartu/Tõravere station the LMWL based on RMA is (IAEA/WMO, 2018):

$$\delta^2H = 8.0\delta^{18}O + 8.6 \quad (4)$$

The  $\delta^{18}O_{H_2O}$  and  $\delta^2H_{H_2O}$  values in shallow groundwater (depths from 4 to 70 m) of the northern BAB (Estonia) is in the same range as the variations in modern precipitation varying from  $-10.9$  to  $-12.7\text{‰}$  and from  $-78$  to  $-91\text{‰}$ , respectively (Paper I). The isotopic ratios of oxygen and hydrogen in shallow groundwater and springs in Estonia yield the following regression line using RMA:

$$\delta^2H = 7.7\delta^{18}O + 6.0 \quad (5)$$

In Paper I, it is shown that in Estonia, the  $\delta^{18}O$  values of shallow groundwater are depleted with respect to annual weighted mean values of local precipitation (Punning et al., 1987; IAEA/WMO, 2018; Fig. 5). Several factors influence the formation of groundwater isotopic composition, such as climate, local vegetation type, soil type (moisture storage) and local geological conditions (Gehrels et al., 1998; Gray et al., 2001; Song et al., 2009; Gleeson et al., 2009; Hayashi and Farrow, 2014) which can explain this deviation.

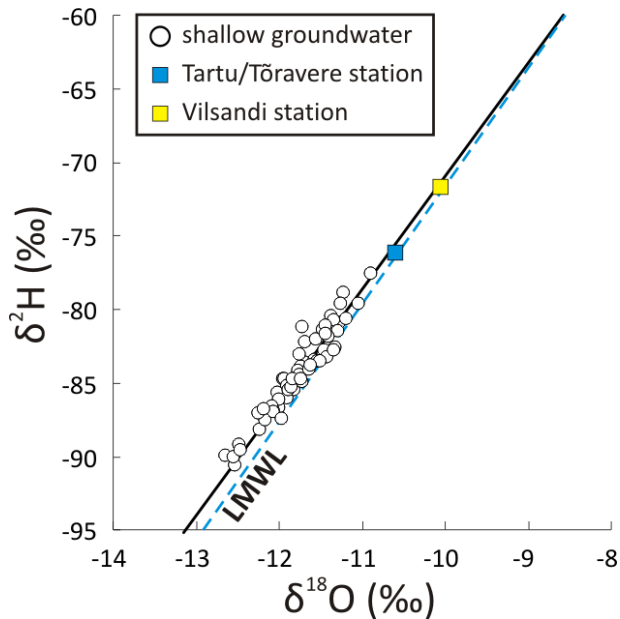


**Figure 5.** The co-variance of  $\delta^{18}\text{O}$  versus  $\delta^2\text{H}$  in groundwater from shallow wells (depths from 4 to 70 m) and springs together with the annual weighted mean isotopic composition of precipitation (Tartu/Tõravere and Vilsandi stations) in the northern BAB (Estonia, IAEA/WMO, 2018; Paper I). The dotted blue line depicts the LMWL in the Tartu/Tõravere station (Eq. 4). The solid black line depicts the co-variance of  $\delta^{18}\text{O}$  and  $\delta^2\text{H}$  in shallow groundwater (Eq. 5).

It has been shown that vegetative transpiration and evaporation in the Great Lakes area in North America are capable of transferring 45–70% of the annual precipitation back to the atmosphere, making it unavailable for recharge (Saxton and McGuinness, 1982; Telmer and Veizer, 2000). Due to the more northern position of Estonia (60°N) with respect to the Great Lakes area (50°N), the duration of daylight during the vegetative period is longer here. That is why the proportion of evapotranspiration in the BAB area should be close to or even higher than 70%. Additionally, it has been shown by numerous studies (e.g., Maulé et al., 1994; DeWalle et al., 1997; Clark and Fritz, 1997; O’Driscoll et al., 2005; Earman et al., 2006; Jasechko et al., 2014) that in areas, where snow forms the essential part of annual precipitation, recharge is seasonally biased towards spring snowmelt and  $\delta^{18}\text{O}$  values in groundwater may be depleted with respect to annual weighted mean values in precipitation. In Estonia, a significant proportion of precipitation accumulates as snow in winter (10–40%; Tooming and Kadaja, 2006) and the snowmelt in spring together with the enhanced influence of evapotranspiration in the summer could impact the observed depleted isotopic composition of shallow groundwater.

In addition to the general depletion with respect to modern precipitation observed in shallow groundwater, smaller scale spatial variations in the isotopic composition of shallow groundwater are observed in Estonia reaching up to 1‰ per 50 km for the  $\delta^{18}\text{O}$  values. These changes are much more abrupt than the spatial changes in  $\delta^{18}\text{O}$  values of precipitation with distance reported from other flatland areas (e.g., Darling et al., 2003; Kortelainen and Karhu, 2004). It is observed that in well-drained areas like river valleys, where surface runoff of floodwater is prevalent, positive anomalies of  $\delta^{18}\text{O}$  values

prevail, while in karstified areas the opposite is the case (Paper I). Several negative anomalies in  $\delta^{18}\text{O}$  values of shallow groundwater occur in karst areas (Paper I). The phenomenon is especially evident in the Pandivere upland in northeastern Estonia (Fig. 4), where there are no river or stream networks, and most rain and meltwater can percolate directly into karst interstices. In spring, rapid snowmelt is often associated with extensive floods over the frozen soil which enhances surface runoff and inhibits groundwater recharge. In karst areas, where uncovered deep crevice systems or depressions occur, the infiltration conditions are better and large amounts of isotopically depleted floodwater can infiltrate into the subsurface (Paper I).

Several general conclusions can be drawn from the results presented in Paper I. Firstly, during palaeoclimate and palaeoenvironmental research, one should not assume that the average  $\delta^{18}\text{O}$  values of shallow groundwater in temperate climates correspond to the annual mean values in precipitation. The bias between the two values is greater in areas where important portion of precipitation falls as snow in winter. In addition, the negligence of the local factors influencing groundwater recharge which cause the isotopic composition of groundwater to deviate from the isotopic composition of local precipitation can lead to misinterpretations in palaeoclimatic studies.

## **4.2 Occurrence of palaeogroundwater in Estonian aquifer systems**

In several aquifer systems in the northern BAB, the isotopic composition of groundwater differs markedly from the values found in modern precipitation and in shallow groundwater. Several reports from the Geological Survey of Estonia (Savitskaja et al., 1995, 1996a, 1997) and unpublished data (T. Martma, J. Ivask, E. Kaup, J. Pärn, V. Raidla, R. Vaikmäe, 2018) show that in areas farther down the groundwater flow paths  $\delta^{18}\text{O}$  values as light as  $\sim -20\text{‰}$  can be found even in the shallow D<sub>2-1</sub> and S-O aquifer systems (Figs. 6 and 7). Such light values are already observed at depths as shallow as  $\sim 50$  m (Savitskaja et al., 1997). In deeper aquifers of O-Cm and Cm-V underlying the regional aquitards of S-O and Lükati-Lontova, respectively (Section 2.1), the  $\delta^{18}\text{O}$  values decrease to values  $< -20\text{‰}$  (Vaikmäe et al., 2001; Raidla et al., 2009; Paper II; Figs. 8 and 9).

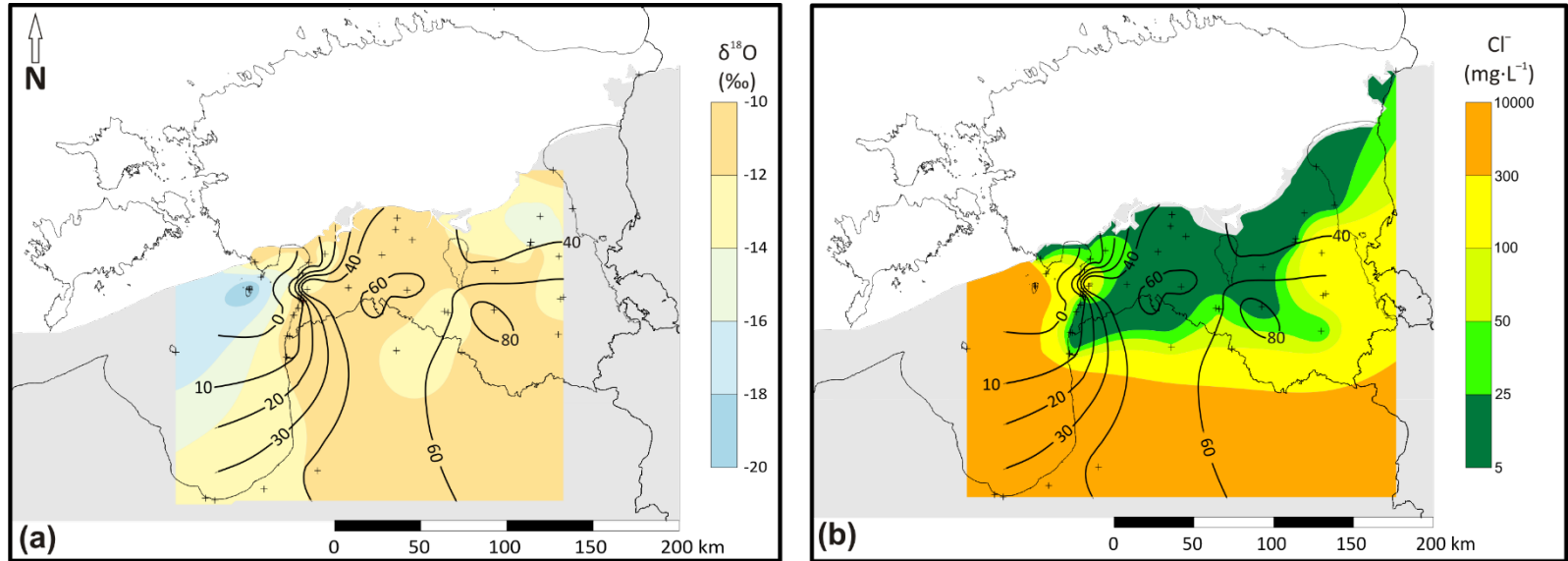


**Figure 6.** Spatial distribution of (a) the isotopic composition of groundwater ( $\delta^{18}\text{O}$  values) and (b) salinity ( $\text{Cl}^-$  concentrations) in the Lower-Middle Devonian aquifer system ( $D_{2-1}$ ) in the northern BAB. The lines denote pre-development freshwater head (m.a.s.l.) calculated based on hydraulic head data reported in Tšeban (1966) and acquired from Konrads Popovs (personal communication, 2016). The hydrochemical and stable isotope data is from Savitskaja et al. (1996a) and unpublished data (T. Martma, J. Ivask, E. Kaup, J. Pärn, V. Raidla, R. Vaikmäe, 2018).

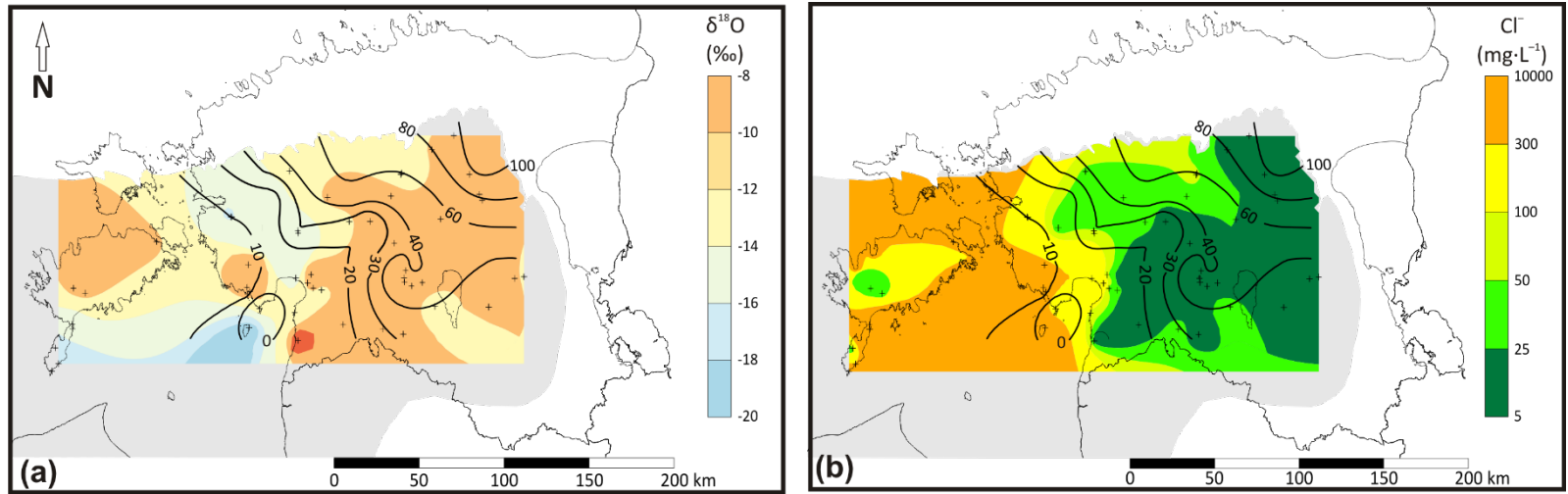


**Figure 7.** Spatial distribution of (a) the isotopic composition of groundwater ( $\delta^{18}\text{O}$  values) and (b) salinity ( $\text{Cl}^-$  concentrations) in the Silurian part of the Silurian-Ordovician aquifer system (S-O) in the northern BAB. The lines denote pre-development freshwater head (m.a.s.l.) calculated based on hydraulic head data reported in Tšeban (1966). The hydrochemical and stable isotope data is from Savitskaja et al. (1996a, 1997, 1998), Vaikmäe et al. (2001) and unpublished data (T. Martma, J. Ivask, E. Kaup, J. Pärn, V. Raidla, R. Vaikmäe, 2018).

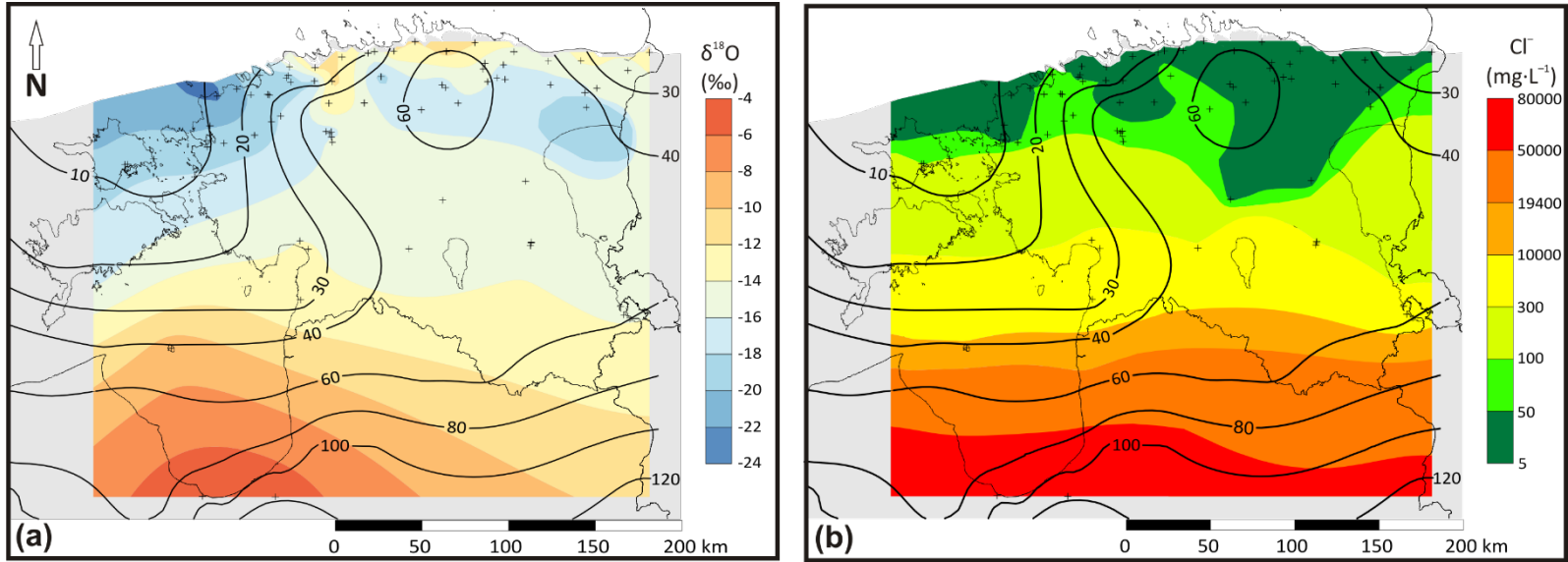


**Figure 8.** Spatial distribution of (a) the isotopic composition of groundwater ( $\delta^{18}\text{O}$  values) and (b) salinity ( $\text{Cl}^-$  concentrations) in the Cambrian and Ordovician-Cambrian aquifer systems (O-Cm) in the northern BAB. The lines denote pre-development freshwater head (m.a.s.l.) calculated based on hydraulic head data reported in Tšeban (1966) and Takcidi (1999). The hydrochemical and stable isotope data is from Raudsep et al., (1989), Savitski et al. (1993); Savitskaja et al. (1995); Takcidi (1999); Vaikmäe et al. (2001); Raidla et al. (2009); Babre et al. (2016); Gerber et al. (2017), Paper II-IV.

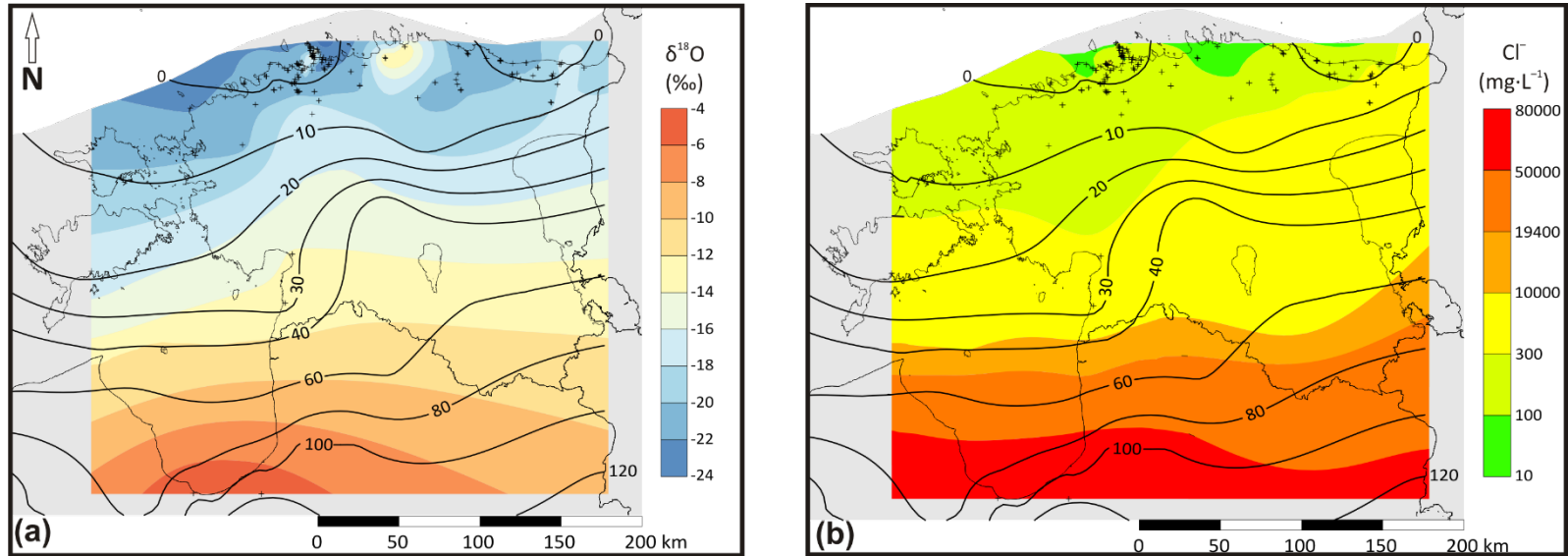


**Figure 9.** Spatial distribution of (a) isotopic composition of groundwater ( $\delta^{18}\text{O}$  values) and (b) salinity ( $\text{Cl}^-$  concentrations) in the Cambrian and Cm-V aquifer systems in the northern BAB. The lines denote pre-development freshwater head (m.a.s.l.) calculated based on hydraulic head data reported in Tšeban (1966) and Takcidi (1999). The hydrochemical and stable isotope data is from Savitski et al. (1993); Savitskaja and Viigand (1994); Takcidi (1999); Vaikmäe et al. (2001); Karro et al. (2004); Raidla et al. (2009, 2012, 2014); Babre et al. (2016); Gerber et al. (2017), Suursoo et al. (2017), Paper V.

Groundwater with such a light isotopic composition described above cannot originate from modern precipitation. The annual weighted mean  $\delta^{18}\text{O}$  and  $\delta^2\text{H}$  values for winter precipitation in Estonia, the accumulation of which provides the main input for groundwater recharge in spring, range from  $-11.9$  to  $-13.8\text{‰}$  and from  $-85$  to  $-97\text{‰}$ , respectively (Punning et al., 1987; IAEA/WMO, 2018). In southern Finland, north of the study area,  $\delta^{18}\text{O}$  values for months where precipitation has fallen solely as snow range from  $-10.2$  to  $-21.6\text{‰}$  and are on average  $\sim -16\text{‰}$  (IAEA/WMO, 2018). These values are heavier than the ones observed in the deeper aquifer systems in the northern BAB. Furthermore, the isotopic composition of the snowpack does not represent the isotopic composition of spring snowmelt. The isotopic composition of snow is modified during melting by evaporation during the sublimation of snow and isotope exchange between meltwater and the snow (Clark and Fritz, 1997). Both processes lead to enrichment in the isotopic composition of average snowmelt with respect to the initial isotopic composition of snow. The isotopic enrichment between the snowpack and the snowmelt at the point of snowpack exhaustion have been estimated to be in the range from 4 to 5.6‰ for  $\delta^{18}\text{O}$  values (e.g. Taylor et al., 2001; Ala-aho et al., 2017). Thus, the actual isotopic composition of snowmelt is probably considerably heavier compared to the weighted mean monthly values of snow given above. This is supported by isotopic composition of shallow groundwater shown to be strongly affected by recharge of snowmelt in spring (Paper I) as its  $\delta^{18}\text{O}$  and  $\delta^2\text{H}$  values (from  $-11.7$  to  $-12.7\text{‰}$  and from  $-78$  to  $-91\text{‰}$ , respectively) are heavier with respect to snow samples collected in GNIP stations in the area. One must also keep in mind that the shallow groundwater samples in Paper I have not been dated with tracers providing absolute age estimates and thus may contain groundwater that does not originate from modern recharge.

The previous discussion suggests that groundwater with isotopic composition strongly depleted with respect to values found in shallow aquifers is palaeogroundwater that has recharged in different climatic conditions compared to the present. The most plausible source for this isotopically light water is the subglacial meltwater recharge from ice sheets that covered the northern part of the BAB in the Pleistocene (Savitskaja and Viigand, 1994; Savitskaja et al., 1995, 1996a, 1997; Vaikmäe et al., 2001; Raidla et al., 2009; Sterckx et al., 2018; Paper II).

The evolution of glacial palaeogroundwater in northern BAB (Estonia) has been influenced by mixing between groundwater originating from several end-members with different origin. These include shallow groundwater recharged by modern precipitation, glacial meltwater, saline formation water from the deeper parts of the aquifer systems and possibly also from the Baltic Sea (Raidla et al., 2009; Paper II; III; Fig. 10). A similar multi-component mixing trend has previously been observed in groundwater from the Canadian Shield also influenced by glacial meltwater recharge (e.g. Clark et al., 2000; Douglas et al., 2000; Stotler et al., 2012). The described mixing processes can be disclosed using chloride concentrations and  $\delta^{18}\text{O}$  values that serve as conservative geochemical tracers in low-temperature systems (Hem, 1985; Geyh, 2000). Based on recurring advances and retreats of continental ice sheets in the study area during the Pleistocene (Section 2.1), one can expect that the mixing between groundwater originating from those end-members has not been simultaneous. The mixing has rather occurred in at least two separate stages. Firstly, the pre-glacial formation waters were displaced by fresh groundwater originating from glacial meltwater recharge due to the reversal of groundwater flow under high hydraulic gradient imposed by the Scandinavian Ice Sheet. During this stage, the mixing occurred between intruding glacial meltwater and saline

formation waters in deeper parts of the aquifer systems. Relations between concentrations of radiogenic  $^4\text{He}$  and  $\text{Cl}^-$  shown in Paper IV suggest that at least for the O-Cm aquifer system the mixing end-member for glacial palaeogroundwater has not been the brine in the central parts of the BAB (cf. Paper II). Rather it seems that glacial palaeogroundwater has mixed with a brackish groundwater end-member located in central or southern Estonia that has probably evolved through a long period of mixing between infiltrating glacial meltwater from previous glaciations and subsequent inflow of more saline water after the hydraulic pressure exerted by the ice sheets had dissipated.

The second stage of mixing occurred after the retreat of the Scandinavian Ice Sheet in the Lateglacial period and the Holocene when the topographically driven flow system was activated. This initiated the recharge of meteoric waters in the modern recharge areas. These meteoric waters then mixed with both glacial palaeogroundwater originating from glacial meltwater recharge but probably also with brackish groundwater in the southern parts of the basin (Paper II; Fig. 10).

Sterckx et al. (2018) observed that the best fit between the measured and simulated  $\delta^{18}\text{O}$  values of groundwater in the northern BAB during numerical modelling were achieved by using less negative estimates for  $\delta^{18}\text{O}$  values ( $-22.5\text{‰}$ ) for the subglacial meltwater from the Scandinavian Ice Sheet. Although the authors were not able to perform a proper inverse modelling study, this suggests that groundwater with the lightest isotopic composition in the northern BAB could have experienced little mixing after its infiltration.

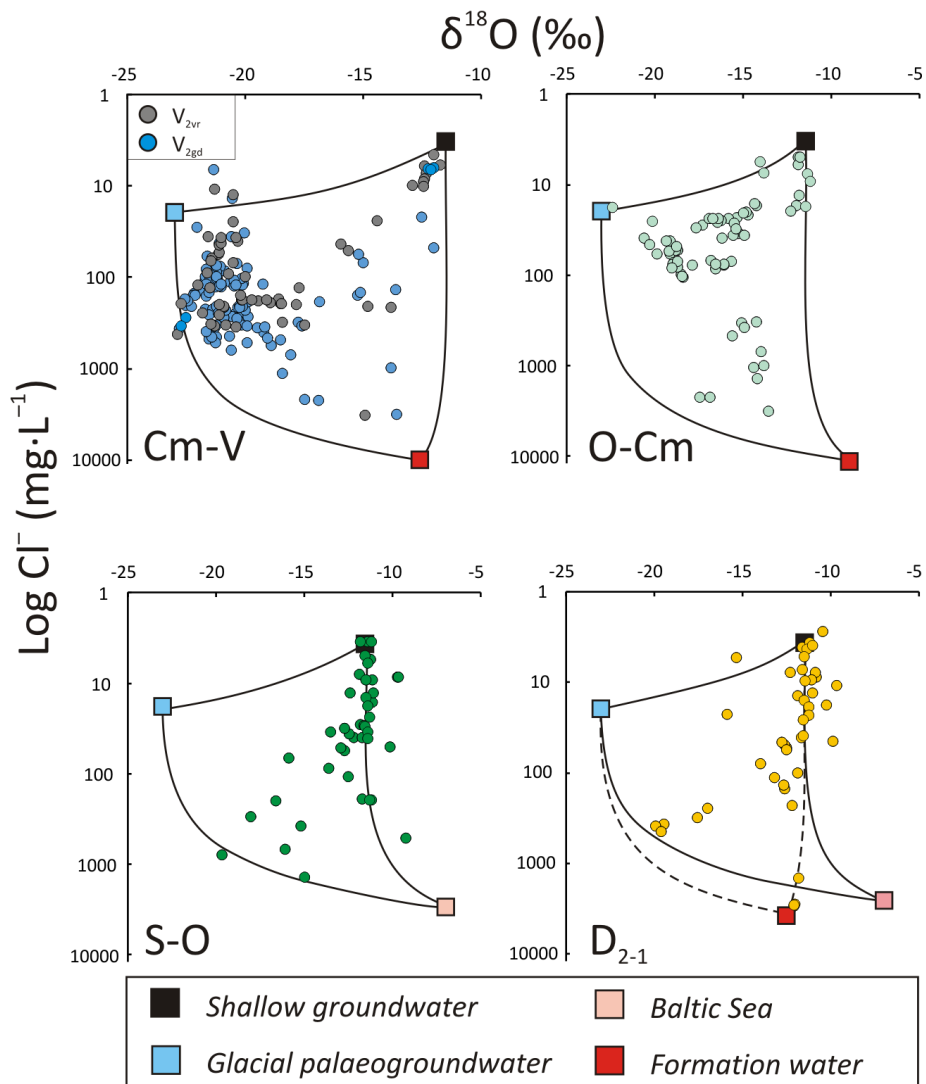


**Figure 10.** Mixing relationships in the northern BAB depicted using conservative tracers  $\delta^{18}\text{O}$  and chloride. Data is from Raudsep et al. (1989), Savitski et al. (1993); Savitskaja and Viigand (1994); Savitskaja et al. (1995, 1996a, 1997, 1998); Vaikmäe et al. (2001); Karro et al., (2004); Raidla et al., (2009, 2012, 2014); Babre et al., (2016); Gerber et al., (2017), Suursoo et al. (2017), Papers I-V and unpublished data (T. Martma, J. Ivask, E. Kaup, J. Pärn, V. Raidla, R. Vaikmäe, 2018). **The end-member values for  $\delta^{18}\text{O}$  and chloride are the following:** shallow groundwater ( $-11.7\text{‰}$ ,  $4\text{ mg}\cdot\text{L}^{-1}$ ; Paper I), glacial palaeogroundwater ( $-23\text{‰}$ ,  $20\text{ mg}\cdot\text{L}^{-1}$ ; Raidla et al., 2009; Sterckx et al., 2018; Paper II); the Baltic Sea in the Gulf of Riga ( $-7.0\text{‰}$ ,  $3735\text{ mg}\cdot\text{L}^{-1}$ ; Fröhlich et al., 1988; Feistel et al., 2010), formation water (Cm-V:  $-12.6\text{‰}$ ,  $9800\text{ mg}\cdot\text{L}^{-1}$ ; Raidla et al., 2009; O-Cm:  $-9\text{‰}$ ,  $11438\text{ mg}\cdot\text{L}^{-1}$ ; EELIS, 2018; T. Martma, J. Ivask, E. Kaup, J. Pärn, V. Raidla, R. Vaikmäe, unpublished data, 2018;  $D_{2-1}$ :  $-12.5\text{‰}$ ,  $3740\text{ mg}\cdot\text{L}^{-1}$ ; Babre et al., 2016). Abbreviations: Cm-V – Cambrian-Vendian aquifer system;  $V_{2vr}$  – Voronka aquifer;  $V_{2gd}$  – Gdov aquifer; O-Cm – Ordovician-Cambrian aquifer system; S-O – Silurian-Ordovician aquifer system;  $D_{2-1}$  – Lower-Middle-Devonian aquifer system.

The occurrence of glacial palaeogroundwater in the S-O and D<sub>2-1</sub> aquifer systems has not been studied extensively. As a part of this thesis, new data on the hydrochemical and isotopic composition of groundwater ( $\delta^2\text{H}_{\text{H}_2\text{O}}$ ,  $\delta^{18}\text{O}_{\text{H}_2\text{O}}$ ,  $\delta^{13}\text{C}_{\text{DIC}}$ ,  $\delta^{34}\text{S}_{\text{SO}_4}$ ,  $\delta^{18}\text{O}_{\text{SO}_4}$ ,  $\delta^{14}\text{C}$ ) were collected from these aquifer systems to study the spatial distribution of palaeogroundwater and processes that have affected its hydrochemical evolution (T. Martma, J. Ivask, E. Kaup, J. Pärn, V. Raidla, R. Vaikmäe, unpublished data, 2018). This data is, however, still to be published. Below a short summary of the preliminary results of these studies is given.

Several factors have probably helped to preserve glacial palaeogroundwater in the S-O and D<sub>2-1</sub> aquifer systems. D<sub>2-1</sub> aquifer system is covered by a regional aquitard (Narva aquitard; Section 2.1) with a thickness of up to 90 m (Perens and Vallner, 1997). The presence of that aquitard could potentially help to preserve glacial palaeogroundwater in the underlying aquifer system especially in areas farther down the groundwater flow path (cf. Sterckx et al., 2018). While groundwater in large parts of the aquifer system has an isotopic composition similar to modern groundwater in the BAB area (Paper I), the isotopic composition of groundwater farther down the groundwater flow path in its north-eastern and north-western part is significantly depleted with respect to it (Fig. 6). Furthermore, the <sup>14</sup>C activities in these waters are also very low being <7 pmC. The glacial palaeogroundwater in the D<sub>2-1</sub> aquifer system is mainly of Na-Cl type and occasionally brackish. This could be related to the fact that most of the glacial palaeogroundwater can be found in the peripheral parts of the aquifer system where it can mix with saline formation water (see also Section 2.1; Fig. 6). The higher salinity of glacial palaeogroundwater located on islands in the Gulf of Riga (Fig. 6) and on the Baltic Sea coast could also be related to mixing between glacial palaeogroundwater with seawater during groundwater abstraction (Fig. 10). The role of the Baltic Sea could, however, be pivotal in preserving the glacial palaeogroundwater in the aquifer system (Sterckx et al., 2018). The presence of the Baltic Sea and its predecessors in the Holocene considerably decreased the SE-NW hydraulic gradient and thus decreased the rate of flushing of the glacial palaeogroundwater from the confined aquifers below it. During the formation of the Baltic Sea in the Holocene, the discharge area of the aquifer system was relocated landwards which led to the formation of much steeper hydraulic gradient in the inland part of the aquifer system. Thus, the glacial palaeogroundwater under the Baltic Sea became essentially isolated from the modern topographically driven flow system and could be preserved for over 10 ka in natural conditions without groundwater abstraction (cf. Hinsby et al., 2001).

Similarly to the D<sub>2-1</sub> aquifer system, the majority of waters in the S-O aquifer system have isotopic composition characteristic to the shallow groundwater in the study area (Fig. 7). However, in areas farther down the groundwater flow path in the Silurian carbonate rocks, the isotopic composition of groundwater is depleted with respect to shallow groundwater decreasing to values characteristic to glacial palaeogroundwater ( $\delta^{18}\text{O}$  values from -14 to -20‰; Savitskaja et al., 1997; T. Martma, J. Ivask, E. Kaup, J. Pärn, V. Raidla, R. Vaikmäe, unpublished data, 2018). The lightest values have been observed in western Estonia and especially on the islands in the Gulf of Riga (Fig. 7). The preservation of glacial palaeogroundwater in these areas could be related to the Baltic Sea, similar to the D<sub>2-1</sub> aquifer system. As in the latter, the presence of glacial palaeogroundwater in the S-O aquifer system is supported by the observations of low <sup>14</sup>C activities <12 pmC. A further similarity with the D<sub>2-1</sub> aquifer system is that also in the S-O aquifer system, the groundwater with the lightest isotopic composition has a Na-Cl water

type and is occasionally brackish indicating possible mixing with seawater during groundwater abstraction (Fig. 10).

### 4.3 Palaeogroundwater in the Ordovician-Cambrian (O-Cm) aquifer system

The Cm-V aquifer system has been the most extensively studied hydrogeological unit in Estonia due to its significantly depleted isotopic composition and limited mixing with modern groundwater (see Section 2). Glacial palaeogroundwater also forms a significant portion of groundwater in the O-Cm aquifer system that overlies the Cm-V aquifer system. Although groundwater in the O-Cm aquifer system is more influenced by mixing with post-glacial meteoric recharge, the wider spatial distribution of wells in the O-Cm aquifer system with respect to the Cm-V aquifer system offers more possibilities to study the geochemical trends in glacial palaeogroundwater. The studies on the O-Cm aquifer system form the most important part of this thesis and are covered in Papers II-IV.

#### 4.3.1 Origin of groundwater

Groundwater in the northern part of the O-Cm aquifer system is fresh and characterized by a wide variety in  $\text{Cl}^-$  concentrations (from 4 to  $105 \text{ mg}\cdot\text{L}^{-1}$ ) and in isotopic composition ( $\delta^{18}\text{O}$  values from  $-11.2\text{‰}$  to  $-22.4\text{‰}$ , Paper II; Fig. 8). Fresh groundwater in the O-Cm aquifer system is of meteoric origin as illustrated by the  $\delta^{18}\text{O}$ - $\delta^2\text{H}$  co-variance that defines a line close to the GMWL (Paper II):

$$\delta^2\text{H} = 7.9\delta^{18}\text{O} + 7.7 \quad (6)$$

Groundwater with  $\delta^{18}\text{O}$  values in the same range as the observed variation in shallow groundwater (from  $-11.7$  to  $-12.7\text{‰}$ , Paper I) are found in the northern Estonian coastal regions close to the outcrop area of the aquifer system (Paper II; Fig. 8). In these areas the thickness of the overlying formations is small ( $<20 \text{ m}$ ) leading to a more active exchange with modern meteoric water.

Further south from the outcrop area, the aquifer system is occupied by fresh groundwater with significantly depleted isotopic composition compared to modern precipitation ( $\delta^{18}\text{O}$  and  $\delta^2\text{H}$  values from  $-14.3\text{‰}$  to  $-22.4\text{‰}$  and from  $-104\text{‰}$  to  $-169\text{‰}$ , respectively, Paper II; Fig. 8). The  $\delta^{18}\text{O}$  values of these waters are similar to values that have been proposed for glacial meltwater of the Scandinavian Ice Sheet during the LGM (from  $-19\text{‰}$  to  $-25\text{‰}$ , Olausson, 1982; Pitkänen et al., 1999). Furthermore, the values are also very similar to groundwater from the underlying Cm-V aquifer system (from  $-18\text{‰}$  to  $-23.5\text{‰}$ ) where the occurrence of glacial palaeogroundwater has been well documented (e.g. Savitskaja and Viigand, 1994; Vaikmäe et al., 2001; Raidla et al., 2009). This suggests that the isotopically light groundwater in the O-Cm aquifer system is glacial palaeogroundwater originating from glacial meltwater recharge in the Pleistocene (Paper II). Waters with the light isotopic composition also occur near the Pandivere Upland, where the highest hydraulic heads of the aquifer system are observed (Tšeban, 1966; Figs. 4, 8). This observation indicates that the modern hydraulic heads do not characterize the flow system during the glacial meltwater recharge in the Pleistocene (Fig. 8, Papers II and III).

About 400 km southward from the northern coastal areas of Estonia Na-Cl type brine is found in the Cambrian aquifer system (merged Cm-V and O-Cm aquifer system, see

Section 2.1) in Latvia with  $\text{Cl}^-$  concentrations and  $\delta^{18}\text{O}$  values up to  $\sim 80000$  mg/L and  $\sim -4.5\text{‰}$ , respectively (Takcidi, 1999; Babre et al., 2016; Gerber et al., 2017). The salinity of groundwater decreases in northerly directions and brackish Na-Cl waters appear in the O-Cm aquifer system in southern Estonia (Fig. 8, Papers II and III). The  $\delta^{18}\text{O}$  values also decrease from a mean value of  $-4.5\text{‰}$  in brine to minimum values of  $-17.6\text{‰}$  in brackish waters (Fig. 8, Papers II and III).  $^{81}\text{Kr}$  ages calculated by Gerber et al. (2017) show that the brackish Na-Cl waters have long residence times ( $\sim 500$  ka) but are much younger compared to brines in the central parts of the basin (with ages  $>1.3$  Ma). Thus, these brackish waters have probably evolved through mixing between intruding glacial palaeogroundwater and the saline formation water that occupied the aquifer system prior to the glacial meltwater intrusion (Paper II).

#### 4.3.2 Geochemical evolution of groundwater

##### *Carbonate mineral dissolution*

In addition to simple mixing between waters of different origin (see Section 4.2), several types of water-rock interaction have influenced the geochemical evolution of groundwater in the O-Cm aquifer system. The most important of these are the dissolution of carbonate minerals (calcite, Fe-dolomite), cation exchange, and oxidation of organic matter.

The  $\text{Ca}^{2+}$  and  $\text{Mg}^{2+}$  activities suggest that groundwater in the O-Cm aquifer system is mainly in equilibrium with respect to calcite and slightly undersaturated with respect to dolomite (Papers II, IV). This shows that the groundwater is buffered by dissolution of carbonate minerals through the incongruent dissolution of dolomite where calcite is precipitated as dolomite is dissolved (Paper IV). Cambrian and Lower Ordovician sandstones are weakly cemented with authigenic carbonate minerals such as Fe-rich dolomite and calcite with an average content of 3 wt.% and 1 wt.%, respectively (Raidla et al., 2006). Additionally, the intruding glacial meltwaters could have been in contact with the overlying Ordovician and Silurian carbonate rocks dominated by calcite (Paper IV). It has been argued that carbonate rocks could have acted as important pathways for transmission of glacial meltwater into the subsurface (e.g. Grasby and Chen, 2005; McIntosh et al., 2006, 2011).

It is evident that in waters with different origin the carbonate mineral dissolution has commenced under different conditions. In glacial palaeogroundwater higher  $\text{Ca}^{2+}$  and  $\text{HCO}_3^-$  concentrations coincide with lower pH values, which is in contradiction to the expected pattern where pH rises together with progressing dissolution of carbonates (e.g. Garrels and Christ, 1965; Langmuir, 1971; Deines et al., 1974). This phenomenon can be related to recharge conditions for waters originating from glacial meltwater recharge. The initial dissolution of carbonate minerals would have depended on the concentration of  $\text{CO}_2$  that was acquired by the recharging glacial meltwater. The high partial pressures of  $\text{CO}_2$  in modern groundwater are mostly derived from the soil zone where bacterial oxidation of vegetation can raise the  $\text{pCO}_2$  value from the modern atmospheric value of  $10^{-3.4}$  to  $10^{-1}$  atm (Clark and Fritz, 1997). Groundwater originating from glacial meltwater recharge would have carried less carbon dioxide than modern waters due to the fact that the  $\text{pCO}_2$  in soils overlain by a continental ice sheet would have been lower (Paper II). However, the  $\text{pCO}_2$  values in these soils were probably higher than in the atmosphere as  $\text{pCO}_2$  in glacial meltwater in the margins of modern ice sheets and glaciers in Greenland and Svalbard ranges from  $10^{-2.4}$  to  $10^{-3.2}$  atm (Souchez et al. 1993; Wadham et al., 2004; Ryu and Jacobson 2012). These elevated  $\text{pCO}_2$  pressures with

respect to atmospheric pCO<sub>2</sub> in glacial meltwaters have been related to subglacial microbial metabolism and organic matter originating from vegetation and soils overridden by ice sheets (Sharp et al. 1999; Tranter et al. 2002, 2005; Bhatia et al. 2010; Boyd et al. 2010; Wadham et al. 2008; Montross et al. 2013).

Paper II shows that a clear relation exists between HCO<sub>3</sub><sup>-</sup> and δ<sup>18</sup>O values in the O-Cm aquifer system with waters having the lightest isotopic composition also having the lowest HCO<sub>3</sub><sup>-</sup> concentrations. Geochemical modelling has shown that the evolution of glacial palaeogroundwater with the lightest isotopic composition is most consistent with carbonate mineral dissolution in closed system conditions, which is the most plausible scenario for subglacial recharge conditions under a continental ice sheet (Paper IV). The geochemical evolution of groundwater with modern isotopic composition and glacial palaeogroundwater influenced by mixing with a recent meteoric end-member is more consistent with calcite dissolution in open system conditions which is a plausible scenario for periods when the continental ice sheets had retreated from the study area (Paper IV). In closed system conditions, the saturation with respect to carbonate minerals is reached at lower HCO<sub>3</sub><sup>-</sup> concentrations and higher pH values compared to carbonate mineral dissolution in open system conditions (Langmuir, 1971). This can explain the observed inverse relationship between HCO<sub>3</sub><sup>-</sup> and δ<sup>18</sup>O values in the O-Cm aquifer system.

#### *Cation exchange reactions*

The Na<sup>+</sup> and Cl<sup>-</sup> relations show that the brackish Na-Cl waters from the southern part of the aquifer system plot close to the seawater dilution line (SDL), while fresh groundwater from the northern part of the aquifer system deviates from this relation having Na<sup>+</sup>/Cl<sup>-</sup> values which exceed the marine values (Paper II). The surplus of Na<sup>+</sup> over marine concentrations can be associated with the silicate mineral dissolution (e.g. albite) or cation exchange reactions (e.g. Toran and Saunders, 1999; Appelo and Postma, 2005). Albite is present as an accessory mineral (<5 wt.%) in the Cambrian and Lower-Ordovician sandstones (Raidla et al., 2006). However, due to very slow kinetics of albite dissolution in the low-temperature conditions (from 7.5°C to 15°C) and at low pH from 7.0 to 8.5 encountered in the O-Cm aquifer system, the silicate mineral dissolution is extremely slow and can be considered a negligible source of Na<sup>+</sup> in the aquifer system (Appelo and Postma, 2005; Zhu 2005; Paper II).

The Na<sup>+</sup> surplus and a characteristic Na-HCO<sub>3</sub> water type of glacial palaeogroundwater is rather related to cation exchange reactions. The Cambrian and Lower Ordovician sandstones forming the aquifer matrix together with the over- and underlying formations contain various minerals with notable cation exchange capacity (Appelo and Postma, 2005) such as illite, illite-smectite, chlorite, glauconite and kaolinite (Kirsimäe and Jørgensen, 2000; Raidla et al., 2006; Voolma et al., 2013). The cation exchange reactions in the O-Cm aquifer system are of the freshening type, where fresh groundwater containing Ca<sup>2+</sup> as the dominant cation enters the pore water solution with higher salinity and Na<sup>+</sup> as the dominant cation (Appelo and Postma, 2005). In the exchange sites, Na<sup>+</sup> is replaced by Ca<sup>2+</sup> that has a greater affinity for sorption. Na<sup>+</sup> is subsequently released to the pore water solution and the Na-HCO<sub>3</sub> water type develops. The freshening of aquifers due to recharge of glacial meltwater and the emergence of a related Na-HCO<sub>3</sub> water type has previously been reported from various sedimentary basins in North America (e.g. Siegel, 1989; McIntosh and Walter, 2006; Ferguson et al., 2007).

### *Oxidation of organic matter and the redox zonation in the aquifer system*

Groundwater in the O-Cm aquifer system is anoxic as both  $O_2$  and  $NO_3^-$  concentrations are below the detection limit ( $<0.2 \text{ mg}\cdot\text{L}^{-1}$  and  $<1.8 \text{ mg}\cdot\text{L}^{-1}$ , Paper III). In terms of concentration  $Fe^{2+}$  and  $SO_4^{2-}$  are the most important redox-sensitive dissolved substances in the aquifer system (Paper III).  $CH_4$  is also present in large areas at the northern part of the aquifer system. Higher  $CH_4$  concentrations are found in areas with low  $SO_4^{2-}$  concentrations and also in the deeper southern parts of the aquifer system.

The distribution of redox-sensitive dissolved substances in the aquifer system is unusual with respect to the modern groundwater flow patterns, as the conditions in the modern recharge area (the Pandivere Upland) are more strongly reducing than in areas farther down the groundwater flow path (Paper III). In the modern recharge area, low concentrations for both  $SO_4^{2-}$  ( $<5 \text{ mg}\cdot\text{L}^{-1}$ ) and  $Fe^{2+}$  ( $<0.5 \text{ mg}\cdot\text{L}^{-1}$ ) are observed together with the presence of  $CH_4$  suggesting that the sulphate reduction has run close to completion. This inference is supported by the fact that the concentrations of  $Fe^{2+}$  tend to decrease in a sulphate reducing zone due to precipitation of iron-sulphides (e.g. Jakobsen and Postma, 1999; Hansen et al., 2001; Appelo and Postma, 2005; Park et al., 2006; Jakobsen and Cold, 2007). The sulphate concentrations increase ( $>5 \text{ mg}\cdot\text{L}^{-1}$ ) and  $CH_4$  concentrations decrease farther down the groundwater flow path (Paper III). The relations between  $SO_4^{2-}$  and  $Cl^-$  together with the isotopic composition of sulphate ( $\Delta^{18}O_{SO_4-H_2O}$  from +20.5 to +31.1‰ and  $\Delta^{34}S_{SO_4-H_2S}$  value of 47.9‰) point to the fact that in these waters farther down the groundwater flow path, elevated sulphate concentrations do not originate from mixing with saline waters having high concentrations of  $SO_4^{2-}$  (Paper III). Rather, sulphate in the glacial palaeogroundwater originates from pyrite oxidation by  $O_2$  in infiltrating glacial meltwater (Raidla et al., 2012, 2014) that has been subsequently reduced during bacterial sulphate reduction (Paper III). Brackish groundwater in the southern deeper parts of the aquifer system has sulphur and oxygen isotope systematics of sulphate that suggests an origin from mixing with saline formation waters from the deeper parts of the BAB.

Higher  $CH_4$  concentrations in the modern recharge area where  $SO_4^{2-}$  reduced zone is established suggest, that this part of the aquifer system has already evolved to methanogenic conditions (Paper III). Lower  $CH_4$  concentrations farther down the groundwater flow path where  $SO_4^{2-}$  concentrations are higher, may rather be related to transport processes than to active  $CH_4$  production. The available stable isotopic data of  $CH_4$  support the ongoing methanogenesis in the aquifer system (Paper III). Methane near the  $SO_4^{2-}$  reduced zone with  $\delta^{13}C_{CH_4}$  values lower than  $-60\%$  can be attributed to a bacterial origin (Whiticar, 1999) and the comparison between  $\delta^{13}C_{CO_2}$  and  $\delta^{13}C_{CH_4}$  values indicates carbonate reduction as the main methanogenic pathway (Paper III). Methane with a heavier isotopic composition is found farther down the groundwater flow path in areas where the  $SO_4$ -reduction is still ongoing (Voitov et al., 1983; Pihlak et al., 2001; Paper III) and seems to represent methane transported from more reducing conditions that has been subsequently oxidized.

The observed redox zonation where more strongly reducing conditions are encountered near the modern recharge area, suggests that this zonation has not developed as a response to the modern hydraulic head gradient. Rather, it can be suspected that the observed redox zonation largely follows groundwater flow patterns established in the Pleistocene (Paper III). However, the isotopic and chemical composition of groundwater suggests that glacial palaeogroundwater has still been influenced by mixing with a more recent meteoric end-member (Papers II, III). Thus, the

influence of post-glacial recharge conditions cannot be ruled out in explaining the strongly reducing conditions surrounding the modern recharge area. Indeed, the groundwater in the overlying S-O aquifer system becomes progressively depleted in higher free energy electron acceptors ( $\text{NO}_3^-$ ;  $\text{Fe}^{3+}$ ) with depth during the vertical movement of groundwater through the Silurian and Ordovician carbonates that contain various types of sedimentary organic matter (Paper III). When these higher free energy electron acceptors become unavailable,  $\text{SO}_4^{2-}$  is left for bacteria to be utilized for oxidation of organic matter. Consequently, recharging groundwater has the potential to evolve towards low  $\text{SO}_4^{2-}$  concentrations and the dissolved sulphate can become enriched in  $^{34}\text{S}$ . As the redox potential decreases, methanogenesis is initiated as all higher free energy electron acceptors have already been consumed during the vertical movement of groundwater into the aquifer system.

The areas farther down the groundwater flow path are less influenced by post-glacial groundwater recharge. Here, the ongoing  $\text{SO}_4^{2-}$  reduction could be sustained by the diffusive transport of both the fermentation products of organic matter as well as  $\text{SO}_4^{2-}$  from the adjacent aquitards into the aquifer system (Paper III). According to the interpretation provided above, the extent of a  $\text{SO}_4^{2-}$ -reduced zone near the modern recharge area could represent the extent to which the post-glacial topographically driven recharge has influenced the O-Cm aquifer system. The spatial extent of this zone is in general agreement with the proposal by Vallner (1997) which states that under the modern hydraulic gradient groundwater could have flowed only 30–40 km along the groundwater flow path during the last 10000 years in the O-Cm aquifer system. Overall, the unusual distribution of redox zones with respect to modern recharge area shows the presence of two different flow systems in the O-Cm aquifer system: 1) modern flow system which is manifested in recharge of modern meteoric water through the overlying carbonate formation in the outcrop area and the modern recharge area, and 2) flow system established in the Pleistocene where the recharge of glacial meltwaters occurred at the northern/north-western margin of the aquifer system under a high hydraulic gradient imposed by an advancing ice sheet. The study of the redox zonation has shown that the time elapsed since the termination of Late Weichselian glaciation has been too short for the O-Cm aquifer system to reach an equilibrium with post-glacial flow conditions. As an aquifer system containing glacial palaeogroundwater, it is still in a transient state after the ice sheet retreated more than 10 ka ago (cf. Bense and Person, 2008; Rousseau-Guentin et al., 2013; Paper III).

The  $\delta^{13}\text{C}_{\text{DIC}}$  values of glacial palaeogroundwater in the O-Cm aquifer system (from  $-7.0\text{‰}$  to  $-15.5\text{‰}$ ; Paper III, IV) are enriched in  $^{13}\text{C}$  with respect to values found in organic matter from adjacent aquitards and the aquifer matrix ( $\delta^{13}\text{C}_{\text{org}}$  from  $-20\text{‰}$  to  $-32\text{‰}$ ; Bityukova et al., 2000; Mastalerz et al., 2003; Kosakowski et al., 2017; Johnson et al., 2017; Paper III), showing that the occurrence of organic matter oxidation has not been the dominant process in its hydrochemical evolution. The  $\delta^{13}\text{C}_{\text{DIC}}$  values in glacial palaeogroundwater from the underlying Cm-V aquifer system are much lighter ( $\delta^{13}\text{C}$  from  $-11.5\text{‰}$  to  $-22\text{‰}$ , Raidla et al., 2012, 2014). It has been suggested that these light carbon isotope signatures reflect that an important portion of DIC is derived from oxidation of organic matter (Raidla et al., 2012). If we suppose that the light  $\delta^{13}\text{C}_{\text{DIC}}$  was characteristic to pristine glacial palaeogroundwater in the BAB, the enriched  $\delta^{13}\text{C}_{\text{DIC}}$  values in the O-Cm aquifer system suggest that this glacial palaeogroundwater has gone through significant geochemical changes after its infiltration through processes such as carbonate mineral dissolution and cation exchange (Paper III).

### 4.3.3 Dating of groundwater

Activities of age tracers ( $^{14}\text{C}$  and  $^3\text{H}$ ) suggest that groundwater in the O-Cm aquifer system is of considerable age (Paper IV). Only waters with a chemical and isotopic composition similar to modern groundwater in shallow aquifers have tritium activities above detection limit ( $>0.2$  TU) reaching 1 TU (Paper IV). In glacial palaeogroundwater where the isotopic composition of groundwater is depleted with respect to modern groundwater, the tritium activities remain below the detection limit indicating that modern groundwater component recharged during the last 50 years is missing in these waters (Paper IV).  $^{14}\text{C}$  activities ( $a^{14}\text{C}$ ) of glacial palaeogroundwater are also very low being generally  $<5$  pmC and yielding conventional ages  $>25000$   $^{14}\text{C}$  years (Paper IV). The  $^{14}\text{C}$  model ages of groundwater in the O-Cm aquifer system were calculated using geochemical modelling (Section 3.3, Paper IV). The plausibility of these age estimates was evaluated by using a multi-tracer approach that looked at radiogenic  $^4\text{He}$  concentrations and hydrochemical and isotopic composition of groundwater in conjunction with  $^3\text{H}$  and  $^{14}\text{C}$  activities (Paper IV).

The composition of initial waters ( $a^{14}\text{C}_{\text{recharge}}$ ,  $\delta^{13}\text{C}_{\text{recharge}}$ , pH, DIC concentrations) used in the inverse modelling exercise was modelled with PHREEQC (Parkhurst and Appelo, 2013) in three hypothetical recharge conditions: modern, glacial and interstadial (Paper IV). The three hypothetical groups of initial waters characterize recharging groundwater at the point when they arrive in the saturated zone. The composition of these initial waters was calculated by considering the dissolution of calcite (the most abundant mineral in the strata overlying the aquifer system) in different system conditions (isotopically and chemically open, chemically open and isotopically closed and chemically and isotopically closed),  $p\text{CO}_2$  values and temperature. The values of the abovementioned parameters for all considered recharge conditions are summarized in Table 2 and the results are reported in Paper IV. In the following inverse modelling exercise with NETPATH, the phases and chemical reactions were chosen based on the hydrochemical evolution of groundwater in the O-Cm aquifer system outlined in Papers II–IV.

**Table 2.** The system conditions (open - isotopically and chemically open; open/closed - chemically open and isotopically closed; closed - isotopically and chemically closed),  $p\text{CO}_2$  values and temperature range considered in calculating initial water compositions with the PHREEQC.

<b>Recharge conditions</b>	<b>Temperature (<math>^{\circ}\text{C}</math>)</b>	<b><math>p\text{CO}_2</math> (atm)</b>	<b>System conditions</b>
Glacial	2	$10^{-3.2}$ – $10^{-2.4}$	closed
Interstadial/Early Holocene	2–4	$10^{-3.7}$ – $10^{-2.6}$	open; open/closed; closed
Modern	6	$10^{-2.5}$ – $10^{-1.8}$	open; open/closed; closed

Besides the uncertainties of initial  $a^{14}\text{C}$  activities in recharge waters and in the dilution of this initial  $^{14}\text{C}$  activity by physical and chemical processes, a critical issue in  $^{14}\text{C}$  dating concerns possible contamination of the original  $^{14}\text{C}$  signal with atmospheric  $^{14}\text{C}$  during sampling and sample preparation. To check for this possible contamination in samples

collected from the O-Cm aquifer system, the initial set of activities collected in volumes up to 250 L to be measured with the conventional method were complemented by parallel  $^{14}\text{C}$  samples measured by AMS. For waters with the modern isotopic composition the activities measured by AMS were in the same range compared to samples collected with the conventional method (Paper IV). For glacial palaeogroundwater the  $^{14}\text{C}$  activities in samples measured by AMS were in many cases  $\sim 1$  to 3 pmC lower (Paper IV) suggesting that some samples collected with conventional method were subject to contamination with atmospheric  $\text{CO}_2$ . The differences between the two measurements were greater for brackish groundwater with higher TDS. However, for several samples of glacial palaeogroundwater the  $a^{14}\text{C}$  measured with the two methods were very similar ( $\pm 0.3$  pmC; Paper IV) showing that some influence of contamination during sampling or sample preparation is also possible for samples measured by AMS (cf. Aggarwal et al., 2014). Thus, the  $a^{14}\text{C}$  ages calculated in this study should be considered minimum age estimates for the studied waters as the largest effects of contamination on the  $^{14}\text{C}$  model age calculations occur in the low activity range of  $^{14}\text{C}$  ( $< 5$  pmC) characteristic for waters considered in this study.

The calculated  $^{14}\text{C}$  model ages of groundwater in the O-Cm aquifer system were on average  $\sim 20$  ka BP younger than conventional ages (Paper IV) showing the significance of geochemical reactions in diluting the original  $^{14}\text{C}$  activity in the O-Cm aquifer system. Groundwater with an isotopic composition similar to modern groundwater end-member ( $\delta^{18}\text{O}$  from  $-11.3\text{‰}$  to  $-11.9\text{‰}$ ) containing tritium can be considered modern in age as it was characterized by negative average model ages within modern recharge conditions. Negative ages can reflect the fact that the  $a^{14}\text{C}$  of the last 60 years has been considerably higher than the value of 100 pmC used for atmospheric  $a^{14}\text{C}$  in this study (cf. Toth and Katz, 2006).

Geochemical evolution of glacial palaeogroundwater with the lightest isotopic composition ( $\delta^{18}\text{O}$  from  $-17.7\text{‰}$  to  $-22.4\text{‰}$ ) from the north-western part of the aquifer system was consistent with closed system evolution of recharge waters in glacial conditions. The average  $^{14}\text{C}$  model ages of these waters ranged from  $\sim 10$  ka BP to 14 ka BP (Paper IV). These estimates roughly coincide with the deglaciation of the study area in the Lateglacial period (Kalm, 2006; Saarse et al., 2012). Although it is generally assumed that the recharge of glacial meltwater should occur during the advance of an ice sheet (e.g. Lemiaux et al., 2008; McIntosh et al., 2011), favorable conditions for glacial meltwater recharge are also encountered during its retreat as the most active glacial meltwater production and its transport to the bed occurs near the ice sheet margin (Vidstrand et al., 2013). In addition, during deglaciation of the northern part of the BAB re-advances of the Scandinavian Ice Sheet occurred the most famous of which was the re-advance during the Palivere stage from  $\sim 14.7$  to 12.7 ka BP ago (Kalm, 2006). Palivere end-moraines related to the ice sheet re-advance are situated in north-western part of the study area and their age agrees with the  $^{14}\text{C}$  model ages of glacial palaeogroundwater in these parts of the O-Cm aquifer system (Kalm, 2006; Lasberg and Kalm, 2013; Paper IV). In addition, there is evidence of palaeogroundwater originating from the end of the LGM from various locations in the BAB and adjacent areas (Section 2.2; Fig. 2).

Glacial palaeogroundwater from the north-eastern parts of the aquifer system was previously interpreted to be a mixture between groundwater originating from glacial meltwater and modern precipitation end-members (Paper II). However, these waters have calculated  $^{14}\text{C}$  model ages ranging from  $\sim 14$  to 22 ka BP. These ages lie closer to the period of maximum extent of the Scandinavian Ice Sheet in the Late Weichselian rather

than to the Holocene when the mixing with more recent meteoric waters could have occurred. Moreover, inverse modelling for these waters gave the most consistent results with initial waters evolved in chemically open and open/closed system conditions under interstadial recharge conditions (Paper IV). This together with the calculated  $^{14}\text{C}$  model ages make these waters potentially older than glacial palaeogroundwater farther down the groundwater flow path with more depleted isotopic composition. It suggests that even if glacial palaeogroundwater from the north-eastern parts of the aquifer system is influenced by mixing with recent meteoric water, it still contains an important component of water recharged in interstadial conditions prior to the LGM.

Brackish groundwater in deeper parts of the aquifer system (Type IV) has been shown to have  $^{81}\text{Kr}$  ages significantly older (~500 ka; Gerber et al., 2017) compared to the average calculated  $^{14}\text{C}$  model ages of ~22 ka BP (Paper IV). Three of the five brackish water samples dated in this study have a  $^{14}\text{C}$  model age >25 ka BP and can be considered to lie beyond the  $^{14}\text{C}$  dating range in agreement with the old  $^{81}\text{Kr}$  ages (Paper IV). The geochemical evolution of brackish waters is also most consistent with recharge waters evolved in interstadial recharge conditions. Due to their considerable  $^{81}\text{Kr}$  age, they have probably been influenced by groundwater flow reversals during several advance and retreat cycles of the Scandinavian Ice Sheet and could also contain a meteoric component from previous interglacials (Gerber et al., 2017).

The proposed pattern of  $^{14}\text{C}$  model ages for glacial palaeogroundwater in the O-Cm aquifer system is in general agreement with the accumulation of radiogenic  $^4\text{He}$  in the studied waters (Paper IV). The dissolved  $^4\text{He}$  in the O-Cm aquifer system is dominantly of radiogenic origin as its  $^3\text{He}/^4\text{He}$  and  $\text{He}/\text{Ne}$  ratios plot very close to the crustal end-member (Paper IV). In situ  $^4\text{He}$  accumulation rates in Cambrian sandstones are up to 5 magnitudes lower compared to the accumulation of  $^4\text{He}$  through the crustal flux of  $3.4 \cdot 10^{-6} \text{ cm}^3\text{STPcm}^{-2}\text{a}^{-1}$  (Oxburgh and O'Nions 1987). However, very high  $^4\text{He}$  concentrations in brackish groundwater seem to originate from mixing with deep saline formation water (Paper IV). Thus, due to mixing effects, the groundwater in the O-Cm aquifer system cannot be viewed to have a single well-defined age. Rather, the studied samples seem to contain fractions of differing ages. One must take into account, that while the  $^{14}\text{C}$  model ages date the meteoric component (precipitation, glacial meltwater) of groundwater, the radiogenic  $^4\text{He}$  component mostly depends on mixing with older saline groundwater (cf. Gerber et al. 2017; Paper IV). In the future an attempt should be made to date the groundwater in the aquifer system with more reliable age tracers (e.g.  $^{81}\text{Kr}$ ) to better constrain the groundwater age and  $^4\text{He}$  accumulation. However, despite the difficulties described above, the dating of groundwater in the O-Cm aquifer system allowed to identify groundwater originating from three different climatic periods: (1) the Holocene (0–10 ka BP); (2) the LGM (~10–22 ka BP) and (3) the pre-LGM period (>22 ka BP).

## 4.4 Important aspects concerning the management of glacial palaeogroundwater in Estonia

### 4.4.1 The occurrence of glacial palaeogroundwater in the light of previous understanding of groundwater flow and budget in Estonia

A wide occurrence of glacial palaeogroundwater in Estonia has important implications for groundwater abstraction and management in the area. Glacial palaeogroundwater is essentially a non-renewable resource within the time-frame of human activities. *Non-renewable groundwater* can be defined as groundwater resource available for abstraction which has a low current rate of annual renewal but a large storage capacity (Margat et al., 2006). Generally, there is a lack of awareness by policy makers in Estonia about the occurrence of glacial palaeogroundwater and its spatial extent. The presence of palaeogroundwater has only received slight attention in groundwater management and related legislation (e.g. Vee erikasutusõiguse..., 2014; Andresson et al., 2018). There is a considerable risk that groundwater balances in Estonia are not properly understood, and that groundwater withdrawals could exceed the actual replenishment of aquifers containing glacial palaeogroundwater. This could lead to overexploitation of groundwater. Essentially, glacial palaeogroundwater resources are being mined similarly to mineral resources (Clark and Fritz, 1997; Edmunds, 2001). Mining of non-renewable groundwater could lead to depletion of aquifer reserves to a degree that they will not be available for the future strategic use (Margat et al., 2006; WMO 2012).

A widespread view in the literature concerning groundwater flow and groundwater budget in Estonia holds that all aquifer systems receive some degree of modern recharge (e.g. Vallner, 1997, 2003; Karise et al., 2004; Perens et al., 2012). For example, Vallner (1997) suggests that about  $150000 \text{ m}^3 \cdot \text{d}^{-1}$  or ~4% of groundwater reaching the bedrock aquifers from the overlying Quaternary cover recharges the O-Cm aquifer system. About 1/3 of this volume is deemed to reach the underlying Cm-V aquifer system as leakage through the Lükati-Lontova regional aquitard. It cannot be disputed that in all aquifer systems except the Cm-V, the modern hydraulic heads are controlled by topographically-driven groundwater flow and are in equilibrium with present day conditions (Tšeban, 1966; Perens and Vallner, 1997; Vallner, 2003; Perens et al., 2012; Sterckx et al., 2018, Figs. 6–9). This is further supported by the fact that there are no abnormal pressures observed in aquifers from the the northern BAB today (Sterckx et al., 2018).

However, this does not mean a priori, that the groundwater in the confined aquifer systems in Estonia has reached an equilibrium with modern flow conditions with respect to its composition. On the contrary, the hydrochemical and isotopic composition of groundwater in the O-Cm, D<sub>2-1</sub> and S-O aquifer systems show that parts of these aquifer systems are still dominated by flow conditions induced upon them by the Pleistocene glaciations. Previous studies have shown that the time after the end of the LGM has been too short for aquifer systems in previously glaciated areas to attain equilibrium with modern recharge conditions. Gerber et al. (2017) have estimated that a time of ~50 ka is needed for the deep Cambrian aquifer system to reach a new steady state with respect to post-glacial hydraulic conditions while Bense and Person (2008) show that the aquifers influenced by glaciations in sedimentary basins of North America have probably never reached a steady state during the advance and retreat cycles of ice sheets in the Pleistocene.

The chemical and isotopic composition of groundwater in the O-Cm, D<sub>2-1</sub> and S-O aquifer systems suggests that the vertical extent of the active water exchange zone in

Estonia can be less extensive than previously thought. Based on hydrodynamic modelling, Vallner (1997) states that the active water exchange zone reaches down to 250 meters below sea level in Estonia. According to this estimate, all aquifer systems overlying the Lükati-Lontova regional aquitard in northern Estonia and all aquifer systems overlying the S-O regional aquitard in southern Estonia belong to the active water exchange zone. While the influence of modern recharge is clear near the recharge areas of D<sub>2-1</sub> and S-O aquifer systems and near the outcrop area of the O-Cm aquifer system, the composition of groundwater suggests that the depth of active water exchange zone in these aquifer systems is highly variable. For example, isotopic composition and dating of groundwater in the O-Cm aquifer system suggest that the active water exchange zone in its northern margin is confined to depths <30 m (Papers II and IV). In the D<sub>2-1</sub> and S-O aquifer systems groundwater with isotopic composition significantly different from modern precipitation and shallow groundwater can be found in areas farther down the groundwater flow path at depths of ~50 and ~60 m, respectively (Savitskaja et al., 1996a, 1997, 1998; Vaikmäe et al., 2001; T. Martma, J. Ivask, E. Kaup, J. Pärn, V. Raidla, R. Vaikmäe, unpublished data, 2018). These depths suggest that the extent of the active water exchange zone can be confined to very shallow depths in certain areas. The parts of O-Cm, D<sub>2-1</sub> and S-O aquifer systems containing glacial palaeogroundwater rather belong to a zone of passive water exchange together with the Cm-V aquifer system according to the classification of Vallner (1997).

Currently, the estimations of groundwater budget and the rate of modern infiltration into the aquifer systems in Estonia rely on the results of hydrodynamic modelling that have only been calibrated against observed hydraulic heads or base flow but not against solute transport or age estimations (e.g. Vallner, 2003). The results of this thesis suggest that the zone where active exchange with modern infiltration takes place and renewable groundwater is formed does not reach as deep as previously thought. Quantitative dating of groundwater with absolute age tracers has only been attempted in the Cm-V and O-Cm aquifer systems (Raidla et al., 2012; Paper IV). In the light of the isotopic and chemical composition of groundwater in the shallower D<sub>2-1</sub> and S-O aquifer systems, it is critical that quantitative dating of groundwater is also carried out in these aquifer systems and that the results of hydrodynamic modelling and groundwater budget calculations are critically evaluated with respect to these estimates.

In addition to traces of glacial palaeogroundwater discovered in the D<sub>2-1</sub> aquifer system and the Silurian part of the S-O aquifer system, there are other aquifers in the northern part of the BAB that could host glacial palaeogroundwater. There is hydrochemical evidence which points to a slow recharge through the Pandivere Upland in north-eastern Estonia (Papers II-IV). This suggests that groundwater in the deeper aquifers in the Ordovician carbonate rocks (below the fractured zones at depths >75 m; Perens and Vallner, 1997) could not be of modern origin but recharged at earlier periods in the Holocene or in the Pleistocene.

The study of the age and origin of these waters is critical for the understanding of the hydrological system in Estonia. Currently, the Pandivere Upland is seen as a major recharge area in northern Estonia that drives modern infiltration waters down to at least the O-Cm aquifer system (e.g. Perens and Vallner, 1997; Vallner, 2003; Perens et al., 2012; Figs. 3, 4). The fact that glacial palaeogroundwater containing a fraction of palaeogroundwater originating from pre-LGM recharge has been found in the O-Cm aquifer system below the Pandivere Upland challenges this assumption. If it were to be the case that the active water exchange zone in the Pandivere area would be constrained

to the shallow depths in the Ordovician carbonate rocks, this would dramatically decrease the volume of groundwater in north Estonian aquifers that could be deemed renewable in human timescales.

Several problems encountered in groundwater management in Estonia in recent decades can be related to the fact that groundwater budgets are not properly understood and the occurrence of glacial palaeogroundwater has not been accounted for. These problems are related to salinization of groundwater in the coastal parts of the Cm-V aquifer system in the Tallinn area (Karro et al., 2004; Suursoo et al., 2017). In the last 60 years, this aquifer system has been extensively used for public water supply. Groundwater exploitation has led to the drawdown of hydraulic heads down to about 30 meters below the pre-development levels (Perens et al. 2012; Erg et al. 2017).

In the Kopli peninsula the Cl<sup>-</sup> concentrations reached up to ~700 mg·L<sup>-1</sup> from the natural baseline levels of ~150 mg·L<sup>-1</sup> in the period from 1950–1995 (Karro et al., 2004). Based on the isotopic composition of groundwater and ratios between major cations and Cl<sup>-</sup> the authors concluded that the increased salinity probably originated from the underlying weathered portion of the crystalline basement. Although during the last 25 years the groundwater consumption has decreased and hydraulic heads in most areas have slowly recovered, there are areas in Estonia, where recent increase in population has led to a larger groundwater consumption and groundwater salinization (Suursoo et al., 2017; Pärn et al., 2018). For example, in Viimsi peninsula near Tallinn the chloride concentration in the deeper portion of the Cm-V aquifer system has risen from the natural baseline level of 150 mg·L<sup>-1</sup> to ~400 mg·L<sup>-1</sup> (Suursoo et al., 2017; Pärn et al., 2018). In the case of Viimsi, the actual source of salinity (seawater intrusion versus the upconing of saline water from the underlying crystalline basement) is currently unknown. The preliminary results point to the underlying crystalline basement as the main source of salinity, although the effects of seawater intrusion could become an issue in the future when the depression cone grows wider (Pärn et al., 2018). This case study provides a cautionary example of how the failure to take into account the presence of glacial palaeogroundwater in groundwater management has led to overexploitation of groundwater and deterioration in groundwater quality.

#### **4.4.2 Differentiation of glacial palaeogroundwater during groundwater monitoring in Estonia**

The major reason that has led to ignorance on the wide existence of glacial palaeogroundwater in the Estonian bedrock has been the lack of specific tracers characteristic to palaeogroundwater measured during national groundwater monitoring in Estonia. The most important of such characteristics not monitored for is the stable isotopic composition of groundwater.

In the following section, several simple diagnostic features are proposed that can help to identify glacial palaeogroundwater. The features are based on the results discussed in this thesis (Papers I-V) together with the synthesis of data from previous studies (Raudsep et al., 1989; Savitski et al., 1993; Savitskaja and Viigand 1994; Savitskaja et al., 1995, 1996a, 1996b, 1997, 1998; Vaikmäe et al., 2001; Raidla et al., 2009, 2012, 2014; Weissbach, 2014; Gerber et al., 2017). They are chosen such that they could be implemented in the national groundwater monitoring programme and in other hydrogeological studies at a local level. The selected suite of features enables the detection of the occurrence of glacial palaeogroundwater based on hydrochemical and isotopic analysis ( $\delta^{18}\text{O}_{\text{H}_2\text{O}}$ ,  $\delta^2\text{H}_{\text{H}_2\text{O}}$ ). The diagnostic features that can help to identify glacial

palaeogroundwater in Estonia are (1) the light isotopic composition, (2) high volumes of dissolved gases, (3) Na<sup>+</sup>-excess over Ca<sup>2+</sup> in hydrochemical composition and the (4) absence of high free energy electron acceptors (O<sub>2</sub>, NO<sub>3</sub><sup>-</sup> and Fe<sup>2+</sup>) among the dissolved constituents.

*(1) Isotopic composition of groundwater*

Fresh groundwater containing an important glacial component is significantly depleted in isotopic composition with respect to values found in modern precipitation and shallow aquifers. Based on isotopic data of modern precipitation (Punning et al., 1987; IAEA/WMO, 2018) and of shallow groundwater (Paper I) in the study area, the proposed diagnostic threshold values for glacial palaeogroundwater are <-14‰ for the δ<sup>18</sup>O and <-102‰ for the δ<sup>2</sup>H (see also discussion in Sections 4.1 and 4.2). The absolute dating of groundwater with age tracers (<sup>3</sup>H, <sup>14</sup>C and <sup>4</sup>He) has shown that waters with such isotopic composition are ≥10 ka old (Raidla et al., 2012; Paper IV).

*(2) High concentration of dissolved gases*

An additional feature that indicates the presence of glacial palaeogroundwater is distinctly visible degassing in a sampling vessel (e.g. flow-through cell, bucket; Fig. 11) during groundwater sampling. The reason for intensive degassing and bubble formation in a sampling vessel is the reduction of pressure in glacial palaeogroundwater as it is exposed to the atmospheric conditions (Weissbach, 2014). Although this characteristic is qualitative, it is directly linked to the enormous amounts of excess air and dissolved gases (e.g. N<sub>2</sub>, CH<sub>4</sub>, noble gases) characteristic to glacial palaeogroundwater (Vaikmäe et al., 2001; Paper V).

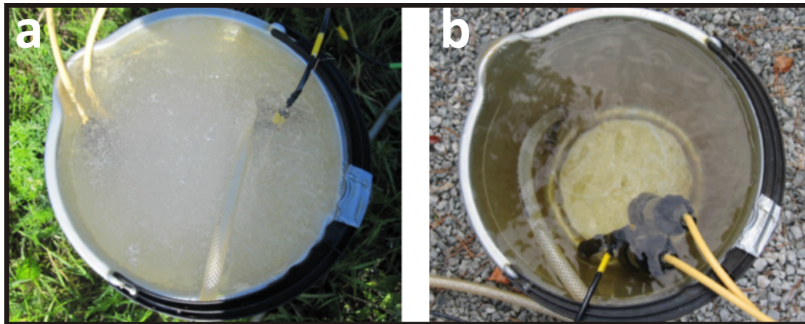


**Figure 11.** (a) Characteristic degassing of glacial palaeogroundwater in a bucket during sampling compared to (b) modern groundwater with no visible bubble formation during sampling. (modified from Weissbach, 2014)

Recent studies into the dissolved gas composition of glacial palaeogroundwater in the Cm-V aquifer system have helped to explain the formation of these anomalously high dissolved gas concentrations. Vaikmäe et al. (2001) hypothesized that dissolved gases in the Cm-V groundwater are related to ablation processes in the ice sheet. Indeed, the relation between Ar and Kr in the groundwater follows the trend expected for addition of air to the air-equilibrated water (Raidla et al., 2017) which supports this hypothesis because noble gas composition in ice generally correspond to atmospheric composition (Severinghaus et al., 1998). However, the amounts of excess Ar in the sampled wells reach up to anomalously high values of 240% (Weissbach, 2014; Raidla et al., 2017). The cause for the formation of such anomalously high excess air could have been the daily

and seasonal fluctuations of the water level in the englacial channel systems depending on the intensity of ablation which led to an entrapment of large volumes of air with an atmospheric origin in the system (Raidla et al., 2017). This entrapped air would have been later pressed into the subglacial meltwater (Raidla et al., 2017). The observation that the relation between Ar and Kr in glacial palaeogroundwater of the Cm-V aquifer system corresponds to atmospheric composition, points to the possibility that they can be used to quantify concentrations of other atmospheric gases in pristine subglacial meltwater. For instance, by knowing the concentration of Ar in groundwater, one can also calculate the initial oxygen concentration in glacial meltwater. This would give valuable background information for studying the alternation of redox conditions in aquifers affected by glacial meltwater recharge and explain the precipitation of redox sensitive dissolved substances (e.g. Fe-oxides, Fe-hydroxides and U).

Additionally, very high dissolved methane content (up to 50% of the total gas volume) in the Cm-V aquifer system has been observed (Paper V). The methane concentrations are lower (0.01 to 1%) in the north-western part of the aquifer system, but considerably higher (1 to 50%) in the north-eastern part of the aquifer system (Paper V). In addition, the  $\delta^{13}\text{C}_{\text{CH}_4}$  values vary widely (from  $-6$  to  $-105\text{‰}$ ). The  $\delta^{13}\text{C}_{\text{CH}_4}$  values of the methane in the north-western part of the aquifer system range from  $-6$  to  $-80\text{‰}$  whereas the isotopic composition of methane is more depleted in  $^{13}\text{C}$  in the north-eastern part of the aquifer system ( $\delta^{13}\text{C}_{\text{CH}_4}$  values from  $-80$  to  $-105\text{‰}$ , Paper V). Isotopic composition of methane in the Cm-V aquifer system ( $\delta^{13}\text{C}_{\text{CH}_4}$  and  $\delta^2\text{H}_{\text{CH}_4}$  values) suggest that it is of biogenic origin as it lies in  $\delta^{13}\text{C}_{\text{CH}_4}$  range comparable to the methane produced via  $\text{CO}_2$  reduction pathway on the  $\delta^2\text{H}_{\text{CH}_4}$  versus  $\delta^{13}\text{C}_{\text{CH}_4}$  diagram (Paper V).

Several lines of evidence show that the  $\text{CH}_4$  in the aquifer system is not produced *in situ* but is rather of allochthonous origin (Paper V). It is proposed that the methane could originate from pre-LGM terrestrial systems that were overridden by the Scandinavian Ice Sheet during its advance in the LGM (Paper V). This fact is significant as it shows that subglacial environments have played an important part in the global carbon cycle due to accumulation of the pre-glacial organic matter under the ice sheets. It also confirms previous findings from the Greenland Ice Sheet (Souchez et al., 2006), which showed that the Pleistocene ice sheets did not advance over polar deserts but rather over terrestrial environments (e.g. wetlands) that had recently been biologically active. The origin of methane in palaeogroundwater from the BAB supports these findings and provides a strong supporting evidence that significant amounts of organic matter were stored under the continental ice sheets in the Pleistocene (Sharp et al., 1999; Wadham et al., 2008).

As hydrogen bound in methane during  $\text{CO}_2$  reduction is ultimately derived from the water in which it has formed (Waldron et al., 1999; Chanton et al., 2006), its isotopic composition could be used to estimate the isotopic composition of the formation water. Assuming the GMWL relationship (Craig, 1961) for the formation water, the corresponding  $\delta^{18}\text{O}$  values for water where the  $\text{CH}_4$  was formed would be  $-17.0 \pm 1.25\text{‰}$  (Paper V). Today such isotopic composition of precipitation is characteristic to areas where taiga and tundra biomes dominate. According to the  $\delta^{18}\text{O}$ -temperature relationship presented in Rozanski et al. (1992, p. 984), the annual average air temperature during the period of methane formation in the pre-LGM period could have ranged from  $-2$  to  $-8$  °C (Paper V).

### (3) The $\text{Na}^+/\text{Ca}^{2+}$ ratio

Hydrochemically, a characteristic feature of glacial palaeogroundwater in the majority of aquifer systems in Estonia is the excess of  $\text{Na}^+$  concentrations over other main cations ( $\text{Ca}^{2+}$ ,  $\text{Mg}^{2+}$ ). This is related to the fact that isotopically light groundwater is characterized by  $\text{Na-HCO}_3$  and  $\text{Na-Cl}$  water types (Paper II, Sections 4.2 and 4.3). The cause for such composition is either the cation exchange reactions or mixing with more saline water (saline formation water or seawater; Paper II, Section 4.2). Strong connection between excess  $\text{Na}^+$  concentrations and glacial palaeogroundwater is exemplified by relation between the  $\text{Na}^+/\text{Ca}^{2+}$  ratio and  $\delta^{18}\text{O}$  values (Fig. 12). Whereas values for the  $\text{Na}^+/\text{Ca}^{2+}$  ratio are  $<1$  in groundwater with  $\delta^{18}\text{O}$  values  $>-14\text{‰}$ , the values increase to  $>2$  in glacial palaeogroundwater with lighter isotopic composition. The values for  $\text{Na}^+/\text{Ca}^{2+}$  ratio are somewhat lower in the Cm-V aquifer system (1.5 on average) compared to glacial palaeogroundwater from other aquifer systems, although these values still exceed the ones found in groundwater with modern isotopic composition (Fig. 12). This is probably related to mixing between glacial palaeogroundwater with brackish and saline Na-Ca-Cl type groundwater in the fracture zones in the underlying weathered portion of the crystalline basement where waters are enriched in  $\text{Ca}^{2+}$  (Karro et al., 2004; Marandi, 2007; Raidla et al., 2009, 2012). Today, many wells that are opened in the O-Cm and Cm-V aquifer systems in central and southern Estonia have been dismantled and cannot be measured for  $\delta^{18}\text{O}$  and dissolved gases. Because from many of such wells, the hydrochemical data has been collected, the values for the  $\text{Na}^+/\text{Ca}^{2+}$  ratio can give an indication whether these wells pumped glacial palaeogroundwater.

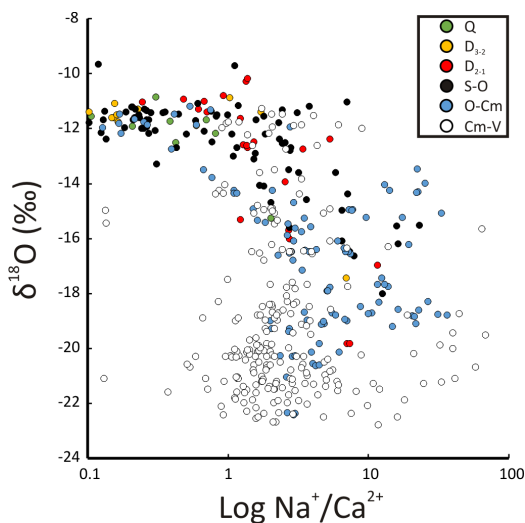


**Figure 12.** Relation between the log of  $\text{Na}^+/\text{Ca}^{2+}$  ratio and  $\delta^{18}\text{O}$  values in groundwater from the northern part of the Baltic Artesian Basin (Cm-V – Cambrian-Vendian aquifer system; O-Cm – Ordovician-Cambrian aquifer system; S-O – Silurian-Ordovician aquifer system; D<sub>2-1</sub> – Lower-Middle-Devonian aquifer system; D<sub>3-2</sub> – Middle-Devonian and Upper Devonian aquifer systems; Q – Quaternary aquifer systems). Data from Raudsep et al., (1989), Savitski et al., (1993); Savitskaja and Viigand (1994); Savitskaja et al., (1995, 1996a, 1996b, 1997, 1998); Vaikmäe et al., (2001); Karro et al., (2004); Raidla et al., (2009, 2012, 2014); Suursoo et al., (2017); Papers I-V, unpublished data (T. Martma, J. Ivask, E. Kaup, J. Pärn, V. Raidla, R. Vaikmäe, 2018).

#### *(4) Redox-sensitive dissolved substances*

Due to long residence times of glacial palaeogroundwater (Vaikmäe et al., 2001; Raidla et al., 2012; Gerber et al., 2017; Paper IV) and accumulation of interstadial organic matter below the advancing Scandinavian Ice Sheet (Raidla et al., 2012, 2014; Papers IV, V), the waters originating from glacial meltwater intrusion are characterized by absence of higher free energy electron acceptors ( $O_2$ ,  $NO_3^-$ ) and by ongoing sulphate reduction that has occasionally evolved into methanogenesis. All studied waters with  $\delta^{18}O_{H_2O}$  values  $<-14\text{‰}$  are devoid of  $O_2$  and  $NO_3^-$  and if the latter has been detected its presence is related to mixing with modern groundwater or analytical errors (Paper III; T. Martma, J. Ivask, E. Kaup, J. Pärn, V. Raidla, R. Vaikmäe, 2018). Furthermore, in more regional scales the redox zonation of aquifers containing glacial palaeogroundwater have been shown to be opposite to those inferred from modern hydraulic head patterns because they follow hydrologic gradients established in the Pleistocene (Paper III).

#### *The relative importance of the proposed diagnostic features*

The most important diagnostic feature for identifying glacial palaeogroundwater is its distinctive light isotopic composition (feature no. 1). All other features related to the amount of dissolved gases (feature no. 2) and the hydrochemical composition of groundwater (features no. 3 and 4) are complementary or characterise secondary qualities of glacial palaeogroundwater. Thus, the identification of glacial palaeogroundwater cannot be made solely based on features no. 2-4. However, the identification of threshold values characteristic to glacial palaeogroundwater with respect to those features can point to the necessity to conduct stable isotope analysis on the given sample which can then confirm the presence of glacial palaeogroundwater.

One important field of study, where the proposed diagnostic features could be implemented, is the estimation of the volume of non-renewable palaeogroundwater in the Estonian aquifers. This could then be compared to the volume of groundwater originating from modern recharge that belongs to the active water exchange zone and is replenished during human lifespan. Such analysis could be further extended to quantify the volumes of non-renewable palaeogroundwater that are currently extracted for water supply. The abstracted volumes could then be compared with estimations of glacial palaeogroundwater volumes present in the Estonian bedrock to evaluate whether there is a risk of overexploitation of this unique groundwater resource.

## 5 Conclusions

1. The results presented above have confirmed the proposed hypothesis that glacial palaeogroundwater has been preserved in a number of aquifer systems in the northern BAB. Their presence is revealed mainly by very light isotopic composition that differs markedly from values found in modern precipitation and shallow groundwater in the study area. The spatial and vertical distribution of glacial palaeogroundwater in the aquifer systems overlying the Lükati-Lontova regional aquitard has been shown to be wider than previously thought. The results of this thesis suggest that the zone where active exchange with modern infiltration takes place and renewable groundwater is formed, does not reach as deep as previously thought. In the aquifer systems overlying the Lükati-Lontova regional aquitard, glacial palaeogroundwater can be found at depths as shallow as 30 m (Papers II-IV). Such a wide distribution of glacial palaeogroundwater in Estonian bedrock makes it a special location in the world and a unique one in Europe. The closest region where such a wide distribution of glacial palaeogroundwater can be found is in North America (McIntosh et al., 2012);
2. The occurrence of glacial palaeogroundwater is particularly wide in the O-Cm aquifer system where it occupies most of the aquifer system similarly to the underlying Cm-V aquifer system. In shallower aquifer systems of S-O and D<sub>2-1</sub> the presence of glacial palaeogroundwater is confined to areas farther down the groundwater flow path. They are best preserved on the Baltic Sea islands. The development of the Baltic Sea in the Holocene could be an important factor that has helped to preserve these waters until the present day;
3. Glacial palaeogroundwater in the northern BAB has gone through a significant geochemical evolution after its infiltration. The most important processes that have influenced its chemical composition are the dissolution of carbonate minerals, cation exchange reactions, oxidation of organic matter and mixing with groundwater originating from modern precipitation, saline formation water and the Baltic Sea. More specifically, the dating of glacial palaeogroundwater in the O-Cm aquifer system allowed to identify groundwater originating from three different climatic periods: (1) the Holocene (0–10 ka BP); (2) the LGM (~10–22 ka BP) and (3) the pre-LGM period (>22 ka BP);
4. Aquifers containing glacial palaeogroundwater in the study area are in a transient state with respect to modern topographically-driven groundwater flow conditions. Both the <sup>14</sup>C model ages and redox zonation in the O-Cm aquifer system suggest that glacial palaeogroundwater under the modern recharge area (Pandivere Upland) has a long residence times which can be explained by the prevalence of groundwater flow patterns established under the influence of continental ice sheets in the Pleistocene. This indicates that under natural conditions a significant time period is needed for the deeper confined aquifer systems in northern BAB to gain hydrochemical and isotopic equilibrium with groundwater originating from modern recharge;
5. Glacial palaeogroundwater in the northern BAB can be used as a proxy to study paleoenvironmental conditions in the study area prior to the advance of the Scandinavian Ice Sheet in the LGM. The study of the isotopic composition of

methane in the Cm-V aquifer system suggests that Pleistocene ice sheets advanced over areas where terrestrial vegetation had been only recently active. During the advance of continental ice sheet, large volumes of this organic matter accumulated beneath it. Subsequently, both the organic matter and its oxidation products were carried into the subsurface by infiltrating glacial meltwaters;

6. Wide occurrence of glacial palaeogroundwater in Estonia has important implications for groundwater abstraction and management. A weak connection of glacial palaeogroundwater reservoirs with modern groundwater recharge and isolation from potential anthropogenic contamination makes them a high-quality resource which should be treated as a strategic reserve and not be wasted, but rather used for specific purposes (e.g. for potable water, not for agriculture and dewatering of mines). Their sustainable use should be protected by appropriate legislation (Edmunds, 2001). It is critical to sustainably manage palaeogroundwater resources, as their withdrawals will be compensated by modern recharge very slowly if at all. Several case studies in northern Estonia show that if palaeogroundwater is overexploited, water yields and quality may greatly deteriorate;
7. The results of the thesis show that areas which have experienced drastic environmental changes during their recent geological history (e.g. the Pleistocene glaciations), steady-state conditions with respect to modern groundwater flow conditions cannot be assumed a priori. This also implies that a simple equilibrium model of topographically driven groundwater flow where groundwater abstraction is balanced by recharge of meteoric waters is not adequate for aquifers in previously glaciated areas. As recent global overviews (e.g. Gleeson et al., 2016; Jasechko et al., 2017) have shown, the occurrence of palaeogroundwater weakly connected to modern groundwater flow system should be considered a norm, not an exception.

## 6 References

- Aeschbach-Hertig, W., Peeters, F., Beyerle, U. & Kipfer, R. (2000). Palaeotemperature reconstruction from noble gases in ground water taking into account equilibration with entrapped air. *Nature*, *205*, 1040–1044.
- Aeschbach-Hertig, W., Stute, M., Clark, J. F., Reuter, R.F. & Schlosser, P. (2002). A paleotemperature record derived from dissolved noble gases in groundwater of the Aquia Aquifer (Maryland, USA). *Geochim. Cosmochim. Acta*, *66*, 797–817.
- Aeschbach-Hertig, W., Peeters, F., Beyerle, U. & Kipfer, R. (2008). Interpretation of dissolved atmospheric noble gases in natural waters. *Water Resour. Res.*, *35*, 2779–2792.
- Affolter, S., Fleitmann, D. & Leuenberger, M., 2014. New online method for water isotope analysis of speleothem fluid inclusions using laser absorption spectroscopy (WS-CRDS). *Clim. Past*, *10*, 1291–1304.
- Aggarwal, P.K., Araguas-Araguas, L., Choudhry, M., van Duren, M. & Froehlich, K. (2014). Lower groundwater <sup>14</sup>C age by atmospheric CO<sub>2</sub> uptake during sampling and analysis. *Groundwater*, *52*, 20–24.
- Aggarwal, P.K., Matsumoto, T., Sturchio, N.C., Chang, H.K., Gastmans, D., Araguas-Araguas, L.J., Jiang, W., Lu, Z.T., Mueller, P., Yokochi, R., Purtschert, R. & Torgersen, T. (2015). Continental degassing of <sup>4</sup>He by surficial discharge of deep groundwater. *Nat. Geosci.*, *8*, 35–39.
- Ahonen, L., Kaija, J., Paananen, M., Hakkarainen, V. & Ruskeeniemi, T. (2004). *Palmottu natural analogue: A summary of the studies*. Espoo: Geological Survey of Finland.
- Ala-aho, P., Tetzlaff, D., McNamara, J.P., Laudon, H., Kormos, P. & Soulsby, C. (2017). Modeling the isotopic evolution of snowpack and snowmelt: Testing a spatially distributed parsimonious approach. *Water Resour. Res.*, *53*, 5813–5830, doi:10.1002/2017WR020650.
- Andresson, A., Viss, V. & Lääne, M. (2018). *Activities of the state upon protecting groundwater*. Tallinn: National Audit Office of Estonia.
- Andrews, J.N. & Lee, D.J. (1979). Inert gases in groundwater from the Bunter Sandstone of England as indicators of age and palaeoclimatic trends. *J. Hydrol.*, *41*, 233–252.
- Appelo, C.A.J. & Postma, D. (2005). *Geochemistry, Groundwater and Pollution, 2nd Edition*. Leiden: Balkema, Leiden.
- Babre, A., Kalvāns, A., Popovs, K., Retiķe, I., Dēliņa, A., Vaikmäe, R. & Martma, T. (2016). Pleistocene age paleo-groundwater inferred from water-stable isotope values in the central part of the Baltic Artesian Basin. *Isotopes Environ. Health Stud.*, *52*, 706–725.
- Bense, V.F. & Person, M.A. (2008). Transient hydrodynamics within intercratonic sedimentary basins during glacial cycles. *J. Geophys. Res.*, *113*, F04005, doi:10.1029/2007JF000969.
- Bethke, C.M. & Johnson, T.M. (2002). Ground water age. *Ground water*, *40*, 337–339.
- Bethke, C.M. & Yeakel, S. (2015). *The Geochemist's Workbench. Release 10.0. GWB Essentials guide*. Illinois: Aqueous Solutions.
- Beyerle, U., Purtschert, R., Aeschbach-Hertig, W., Imboden, D.M., Loosli, H.H., Wieler, R. & Kipfer, R. (1998). Climate and groundwater recharge during the last glaciation in an ice-covered region. *Science*, *282*, 731–734.

- Bhatia, M.P., Das, S.B., Longnecker, K., Charette, M.A. & Kujawinski, E.B. (2010). Molecular characterization of dissolved organic matter associated with the Greenland ice sheet. *Geochim. Cosmochim. Acta*, *74*, 3768–3784.
- Bityukova, L., Bityukov, M., Shogenova, A., Rasteniene, V., Šliaupa, S., Zabele, A., Lashkova, L., Eihmanis, E., Kirsimäe, K., Jöeleht, A. & Huegens, E. (2000). Organic matter distribution and variations of isotopic composition of organic carbon in Cambrian siliciclastic rocks in Baltic Region. Sediment 2000, Leoben, Austria, 20–23 June, 2000. Mitteilungen der Gesellschaft der Geologie und Bergbauaustudenten in Österreich. Sediment 2000. Kurzfassungen/Abstracts, pp. 27–28.
- Blaser, P.C., Coetsiers, M., Aeschbach-Hertig, W., Kipfer, R., Van Camp, M., Loosli, H.H. & Walraevens, K. (2010). A new groundwater radiocarbon correction approach accounting for palaeoclimate conditions during recharge and hydrochemical evolution: The Ledo-Paniselian Aquifer, Belgium. *Appl. Geochem.*, *25*, 437–455.
- Blomqvist, R. 1999. *Hydrogeochemistry of deep groundwaters in the central part of the Fennoscandian Shield*. Academic dissertation. Espoo: Geological Survey of Finland.
- Boulton, G.S., Caban, P. & van Gijssel, K. (1995). Groundwater flow beneath ice sheets: Part I – Large scale patterns. *Quaternary Sci. Rev.*, *14*, 545–562.
- Boyd, E.S., Skidmore, M., Mitchell, A.C., Bakermans, C. & Peters, J.W. (2010). Methanogenesis in subglacial sediments. *Environ. Microbiol. Rep.*, *2*, 685–692.
- Cadieux, S.B., White, J.R., Sauer, P.E, Peng, Y., Goldman, A.E. & Pratt, L.M. (2016). Large fractionations of C and H isotopes related to methane oxidation in Arctic lakes. *Geochim. Cosmochim. Acta*, *187*, 141–155.
- Carey, A.E., Dowling, C.B. & Poreda, R.J., (2004). Alabama Gulf Coast groundwaters:  $^4\text{He}$  and  $^{14}\text{C}$  as groundwater-dating tools. *Geology*, *32*, 289–292.
- Cartwright, I., Cendón, D., Currell, M. & Meredith, K. (2017). A review of radioactive isotopes and other residence time tracers in understanding groundwater recharge: Possibilities, challenges, and limitations. *J. Hydrol.*, *555*, 797–811.
- Castro, M.C., Stute, M. & Schlosser, P., 2000. Comparison of  $^4\text{He}$  ages and  $^{14}\text{C}$  ages in simple aquifer systems: Implications for groundwater flow and chronologies. *Appl. Geochem.*, *15*, 1137–1167.
- Cerling, T.E., Solomon, D.K., Quade, J. & Bowman, J.R. (1991). On the isotopic composition of carbon in soil carbon dioxide. *Geochim. Cosmochim. Acta*, *55*, 3403–3405.
- Chanton, J.P., Fields, D., Hines, M.E., 2006. Controls on the hydrogen isotopic composition of biogenic methane from high-latitude terrestrial wetlands. *J. Geophys. Res.*, *111*, G04004, doi:10.1029/2005JG000134.
- Chapelle, F.H. & Knobel, L.L. (1983). Aqueous geochemistry and the exchangeable cation composition of glauconite in the Aquia aquifer, Maryland. *Ground Water*, *21*, 343–352.
- Clark, I.D. & Fritz, P. (1997). *Environmental Isotopes in Hydrogeology*. New York: CRC Press.
- Clark, I.D., Douglas, M., Raven, K. & Bottomley, D. (2000). Recharge and preservation of Laurentide glacial melt water in the Canadian Shield. *Ground Water*, *38*, 735–742.

- Clark, J.F., Stute, M., Schlosser, P. & Drenkard, S. (1997). A tracer study of the Floridan aquifer in southeastern Georgia: Implications for groundwater flow and paleoclimate. *Water Resour. Res.*, *33*, 281–289.
- Clayton, R.N., Friedman, I., Graf, D.L., Mayeda, T.K., Meents, W.F. & Shimp, N.F. (1966). The origin of saline formation waters. 1. Isotopic composition. *J. Geophys. Res.*, *71*, 3869–3882.
- Craig, H. (1961). Isotopic variations in meteoric waters. *Science*, *133*, 1702–1703.
- Crawford, J., Hughes, C.E. & Lykoudis, S. (2014). Alternative least squares methods for determining the meteoric water line, demonstrated using GNIP data. *J. Hydrol.*, *519*, 2331–2340.
- Dansgaard, W. (1964). Stable isotopes in precipitation. *Tellus*, *16*, 436–468.
- Darling, W.G., Bath, A.H. & Talbot, J.C. (2003). The O and H stable isotopic composition of fresh waters in the British Isles. Surface waters and groundwater. *Hydrol. Earth Syst. Sci.*, *7*, 183–195.
- Darling, W.G. (2004). Hydrological factors in the interpretation of stable isotopic proxy data present and past: a European perspective. *Quaternary Sci. Rev.*, *23*, 743–770.
- Darling, W.G. (2011). The isotope hydrology of quaternary climate change. *J. Hum. Evol.*, *60*, 417–427.
- Deines, P., Langmuir, D. & Harmon, R. (1974). Stable carbon isotope ratios and the existence of a gas phase in the evolution of carbonate ground waters. *Geochim. Cosmochim. Acta*, *38*, 1147–1164.
- DeWalle, D.R., Edwards, P.J., Swistock, B.R., Aravena, R. & Drimmie, R.J. (1997). Seasonal isotope hydrology of three Appalachian forest catchments. *Hydrol. Process.*, *11*, 1895–1906.
- Douglas, M., Clark, I.D., Raven, K. & Bottomley, D. (2000). Groundwater mixing dynamics at a Canadian Shield mine. *J. Hydrol.*, *235*, 88–103.
- Earman, S., Campbell, A.R., Phillips, F.M. & Newman, B.D. (2006). Isotopic exchange between snow and atmospheric water vapor: estimation of the snowmelt component of groundwater recharge in the southwestern United States. *J. Geophys. Res.*, *111*, D09302. <http://dx.doi.org/10.1029/2005JD006470>.
- Edmunds, W.M. (2001). Palaeowaters in European coastal aquifers – the goals and main conclusions of the PALAEAUX project. In: Edmunds, W.M. & Milne, C.J. (Eds.), *Palaeowaters of Coastal Europe: Evolution of Groundwater since the late Pleistocene* (pp. 1–16). London: Geological Society, Special Publications, vol. 189.
- Edmunds, W.M., Guendouz, A.H., Mamou, A., Moulla, A., Shand, P. & Zouari, K. (2003). Groundwater evolution in the Continental Intercalaire aquifer of southern Algeria and Tunisia: trace element and isotopic indicators. *Appl. Geochem.*, *18*, 805–822.
- Edmunds, W.M., Ma, J., Aeschbach-Hertig, W., Kipfer, R. & Darbyshire, D.P.F. (2006). Groundwater recharge history and hydrogeochemical evolution in the Minqin Basin, North West China. *Appl. Geochem.*, *21*, 2148–2170.
- Edmunds, W.M. & Smedly, P.L. (2000). Residence time indicators in groundwater: the East Midlands Triassic sandstone aquifer. *Appl. Geochem*, *15*, 737–752.
- EELIS, 2018. Estonian Environmental Agency - Estonian Nature Information System. VEKA database. Retrieval (2018, June 7). Retrieved from: <http://loodus.keskkonnainfo.ee/WebEelis/veka.aspx?type=artikkel&id=757660072>.

- El-Kadi, A.I., Plummer, L.N. & Aggarwal, P. (2011). NETPATH-WIN: An interactive user version of the mass-balance model, NETPATH. *Ground Water*, 49, 593–599.
- Erg, K., Truu, M., Kebbinau, K., Lelgus, M. & Tarros, S. (2017). *Report of Estonian environmental monitoring “Monitoring of groundwater bodies in 2016” of state environmental programme*. Tallinn: Geological Survey of Estonia. (in Estonian)
- Estonian Health Board (2016). Joogivesi tarbijale. Retrieval (2018, June 25). Retrieved from: <http://www.terviseamet.ee/keskkonnatervis/vesi.html>. (in Estonian)
- Estonian Land Board (2018). Topographic data. Retrieval (2018, June 21). Retrieved from: <https://geoportaal.maaamet.ee/eng/Maps-and-Data/Topographic-Data-p59.html>.
- Feistel, R., Weinreben, S., Wolf, H., Seitz, S., Spitzer, P., Adel, B., Nausch, G., Schneider, B. & Wright, D.G. (2010). Density and Absolute Salinity of the Baltic Sea 2006 – 2009. *Ocean Science*, 6, 3–24.
- Ferguson, G.A.G., Betcher, R.N. & Grasby, S.E. (2007). Hydrogeology of the Winnipeg formation in Manitoba, Canada. *Hydrogeol. J.*, 15, 573–587.
- Fisher, R.E., Sriskantharajah, S., Lowry, D., Lanoiselle, M., Fowler, C., James, R., Hermansen, O., Lund, M.C., Stohl, A., Greinert, J., Nisbet-Jones, P.B.R., Mienert, J. & Nisbet, E.G. (2011). Arctic methane sources: isotopic evidence for atmospheric inputs. *Geophys. Res. Lett.*, 38, L21803. <https://doi.org/10.1029/2011GL049319>.
- Fontes, J.-C., 1981. Palaeowaters. In: Gat, J.R., Gonfiantini, R. (Eds.), *Stable Isotope Hydrology. Deuterium and Oxygen-18 in the Water Cycle* (pp. 273–298). Vienna: IAEA.
- Frape, S.K., Blyth, A., Blomqvist, R., McNutt, R.H. & Gascoyne, M. (2003). Deep fluids in the continents: II. Crystalline rocks. In: Drever, J.I. (Ed.), *Surface and Ground Water, Weathering, and Soils. Treatise on Geochemistry, Volume 5* (pp. 541–580). Oxford: Elsevier.
- Friedman, I. & O’Neil, J.R. (1977). *Compilation of stable isotope fractionation factors of geochemical interest*. In: Fleischer, M. (Ed.), *Data of Geochemistry*. US Geol. Survey Prof. Paper 440-KK, 6th ed.
- Fröhlich, K., Grabczak, J. & Rozanski, K. (1988). Deuterium and oxygen-18 in the Baltic Sea. *Chem. Geol.*, 72, 77–83.
- Garrels, R.M. & Christ, C. (1965). *Solutions, Minerals and Equilibria*. San Fransisco: Freeman.
- Gehrels, J.C., Peeters, J.E., de Vries, J.J. & Dekkers, M. (1998). The mechanism of soil water movement as inferred from O-18 stable isotope studies. *Hydrol. Sci. J.–J. Des Sci. Hydrol.*, 43, 579–594.
- Gerber, C., Vaikmäe, R., Aeschbach, W., Babre, A., Jiang, W., Leuenberger, M., Lu, Z.T., Mokrik, R., Müller, P., Raidla, V., Saks, T., Waber, H.N., Weissbach, T., Zappala, J.C. & Purtschert, R. (2017). Using <sup>81</sup>Kr and noble gases to characterize and date groundwater and brines in the Baltic Artesian Basin on the one-million-year timescale. *Geochim. Cosmochim. Acta*, 205, 187–210.
- Geyh, M. (2000). *Groundwater. Saturated and Unsaturated Zone*. Technical Documents in Hydrology No. 39, Vol. IV. Paris: UNESCO.
- Gleeson, T., Novakowski, K. & Kyser, T.K. (2009). Extremely rapid and localized recharge to a fractured rock aquifer. *J. Hydrol.*, 376, 496–509. <http://dx.doi.org/10.1016/j.jhydrol.2009.07.056>.

- Gleeson, T., Befus, K.M., Jasechko, S., Luijendijk, E., & Cardenas, M.B. (2016). The global volume and distribution of modern groundwater. *Nat. Geosci.*, *9*, 161–167.
- Gleick, P.H. (1996). Water resources. In: S. Schneider (Ed.), *Encyclopedia of Climate and Weather*, vol. 2 (pp. 817–823). New York: Oxford University Press.
- Grasby, S.E. & Chen, Z. (2005). Subglacial recharge into the Western Canada Sedimentary Basin: impact of Pleistocene glaciation on basin hydrodynamics. *Geol. Soc. Am. Bull.*, *117*, 500–514.
- Grasby, S.E., Osadetz, K., Betcher, R. & Render, F. (2000). Reversal of the regional-scale flow system of the Williston Basin in response to Pleistocene glaciation. *Geology*, *29*, 635–638.
- Gray, D.M., Toth, B., Zhao, L., Pomeroy, J.W. & Granger, R.J., (2001). Estimating areal snowmelt infiltration into frozen soils. *Hydrol. Process.*, *15*, 3095–3111.
- Grundl, T., Magnusson, N., Brennwald, M.S. & Kipfer, R. (2013). Mechanisms of subglacial groundwater recharge as derived from noble gas, <sup>14</sup>C, and stable isotopic data. *Earth Planet. Sci. Lett.*, *369–370*, 78–85.
- Guendouz, A. & Michelot, J.L. (2006). Chlorine-36 dating of deep groundwater from northern Sahara. *J. Hydrol.*, *328*, 572–580.
- Hade, S. & Soesoo, A. (2014). Estonian graptolite argillites revisited: A future resource? *Oil Shale*, *31*, 4–18.
- Halas, S., Trembacowski, A., Soltyk, W. & Valenziak, J. (1993). Sulphur and oxygen in natural waters: (2) deep-waters from horizons below Baltic Sea floor. *Isotopenpraxis*, *28*, 229–235.
- Hansen, L.K., Jakobsen, R. & Postma, D. (2001). Methanogenesis in a shallow sandy aquifer, Romo, Denmark. *Geochim. Cosmochim. Acta*, *65*, 2925–2935.
- Hayashi, M. & Farrow, C.R., 2014. Watershed-scale response of groundwater recharge to inter-annual and inter-decadal variability in precipitation (Alberta, Canada). *Hydrogeol. J.*, *22*, 1825–1839.
- Heaton, T.H.E., & Vogel, J.C. (1981). "Excess air" in groundwater. *J. Hydrol.*, *50*, 201–216.
- Hem, J.D. (1985). *Study and Interpretation of the Chemical Characteristics of Natural Water*. U.S. Geological Survey, Water Supply Paper 2254, USGS Publishing Service Centre, <http://pubs.usgs.gov/wsp/wsp2254>.
- Hinsby, K., Harrar, W.G., Nyegaard, P., Konradi, P.B., Rasmussen, E.S., Bidstrup, T., Gregersen, U. & Boaretto, E. (2001). The Ribe Formation in western Denmark - Holocene and Pleistocene groundwaters in a coastal Miocene sand aquifer. In: Edmunds, W.M. & Milne, C.J. (Eds.), *Palaeowaters of Coastal Europe: Evolution of Groundwater since the late Pleistocene* (pp. 29–48). London: Geological Society, Special Publications, vol. 189.
- Iampen, H.T. & Rostron, B.J. (2000). Hydrogeochemistry of pre-Mississippian brines, Williston Basin, Canada–USA. *J. Geochem. Explor.*, *69–70*, 29–35.
- IAEA, (2013). *Isotope Methods for Dating Old Groundwater*. Vienna: IAEA.
- IAEA/WMO, (2018). WISER – Water Isotope System for data analysis, visualization and Electronic Retrieval (2018, April 29). Retrieved from <https://nucleus.iaea.org/wiser/index.aspx>.
- Ingraham, N.L., 1998. Isotopic variations in precipitation. In: Kendall, C. & McDonnell J.J. (Eds.), *Isotope Tracers in Catchment Hydrology* (pp. 87–117). Amsterdam: Elsevier Science B.V.

- Ivanovich, M., Blomqvist, R. & Frøpe, S.K. 1992. Rock/water interaction study in deep crystalline rocks using isotopic and uranium series radionuclide techniques. *Radiochimica Acta*, 58–59, 401–408.
- Jakobsen, R. & Cold, L. (2007). Geochemistry at the sulfate reduction-methanogenesis transition zone in an anoxic aquifer—A partial equilibrium interpretation using 2D reactive transport modeling. *Geochim. Cosmochim. Acta*, 71, 1949–1966.
- Jakobsen, R. & Postma, D. (1999). Redox zoning, rates of sulfate reduction and interactions with Fe-reduction and methanogenesis in a shallow sandy aquifer, Romo, Denmark. *Geochim. Cosmochim. Acta*, 63, 137–151.
- Jasechko, S., Birks, S.J., Gleeson, T., Wada, Y., Fawcett, P.J., Sharp, Z.D., McDonnell, J.J. & Welker, J.M. (2014). The pronounced seasonality of global groundwater recharge. *Water Resour. Res.*, 50, 8845–8867.
- Jasechko, S., Perrone, D., Befus, K.M., Bayani Cardenas, M., Ferguson, G., Gleeson, T., Luijendijk, E., McDonnell, J.J., Taylor, R.G., Wada, Y. & Kirchner, J.W. (2017). Global aquifers dominated by fossil groundwaters but wells vulnerable to modern contamination. *Nat. Geosci.*, 10, 425–429.
- Jiang, W., Bailey, K., Lu, Z.-T., Mueller, P., O'Connor, T.P., Cheng, C.-F., Hu, S.-M., Purtschert, R., Sturchio, N.C., Sun, Y.R., Williams, W. D. & Yang, G.-M. (2012). An atom counter for measuring <sup>81</sup>Kr and <sup>85</sup>Kr in environmental samples. *Geochim. Cosmochim. Acta*, 91, 1–6.
- Johnson, S.C., Large, R.R., Coveney, R.M., Kelley, K.D., Slack, J.F., Steadman, J.A., Gregory, D.D., Sack, P.J. & Meffre, S. (2017). Secular distribution of highly metalliferous black shales corresponds with peaks in past atmosphere oxygenation. *Mineral. Deposita*, 52, 791–798.
- Jõelett, A. (1998). *Geothermal studies of the Precambrian Basement and Phanerozoic Sedimentary Cover in Estonia and in Finland*. Dissertationes Geologicae Universitatis Tartuensis 7. Tartu: Tartu University Press.
- Juodkaziš, I. & Zuzevičius, A. (1977). *Estimation of the Fresh Groundwater Storage in the Baltic Artesian Basin*. Vilnius: LGF. (in Russian)
- Juodkaziš, V. (Ed.) (1980). *Hydrogeological Map of the Pre-Quaternary Deposits of the Soviet Baltic Republics*. Ministry of Geology of the USSR.
- Kalin, R.M. (2000). Radiocarbon Dating of Groundwater Systems. In: Cook P.G. & Herczeg A.L. (Eds), *Environmental Tracers in Subsurface Hydrology* (pp. 111–143). Boston, MA: Springer.
- Kalm, V. (2006). Pleistocene chronostratigraphy in Estonia, southeastern sector of the Scandinavian glaciation. *Quat. Sci. Rev.*, 25, 960–975.
- Kalm, V., Raukas, A., Rattas, M. & Lasberg, K. (2011). Pleistocene glaciations in Estonia. In Ehlers, J., Gibbard, P.L. & Hughes, P.D. (Eds), *Quaternary Glaciations – Extent and Chronology – A Closer Look* (pp. 95–104). Amsterdam: Elsevier.
- Kalm, V. (2013). Ice-flow pattern and extent of the last Scandinavian Ice Sheet southeast of the Baltic Sea. *Quaternary Sci. Rev.*, 44, 51–59.
- Karise, V. (1997). Composition and properties of groundwater under natural conditions. In: Raukas, A. & Teedumäe, A. (Eds.), *Geology and Mineral Resources of Estonia* (pp. 152–155). Tallinn: Estonian Academy Publishers.
- Karise, V., Metsur, M., Perens, R., Savitskaja, L. & Tamm, I. (2004). *Eesti põhjavee kasutamise ja kaitse*. Tallinn: Eesti Põhjaveekomisjon. (in Estonian)

- Karro, E., Marandi, A. & Vaikmäe, R. (2004). The origin of increased salinity in the Cambrian-Vendian aquifer system on the Kopli Peninsula, northern Estonia. *Hydrogeol. J.*, *12*, 424–435.
- Kharaka, Y.K. & Hanor, J.S. (2007). Deep fluids in the continents: I. Sedimentary basins. In: Drever, J.I. (Ed.), *Surface and Ground Water, Weathering and Soils. Treatise on Geochemistry, Volume 5* (pp. 1–48). Oxford: Elsevier.
- Kietäväinen, R., Ahonen, L., Kukkonen, I. T., Niedermann, S. & Wiersberg, T. (2014). Noble gas residence times of saline waters within crystalline bedrock, Outokumpu Deep Drill Hole, Finland. *Geochim. Cosmochim. Acta*, *32*, 159–174.
- Kietäväinen, R. (2017). *Deep Groundwater Evolution at Outokumpu, Eastern Finland: From Meteoric Water to Saline Gas-Rich Fluid*. Academic dissertation. Espoo: Geological Survey of Finland.
- Kipfer, R., Aeschbach-Hertig, W., Peeters, F. & Stute, M. (2002). Noble gases in lakes and ground waters. *Rev. Mineral. Geochemistry*, *47*, 615–700.
- Kirsimäe, K. & Jørgensen, R. (2000). Mineralogical and Rb-Sr isotope studies of low-temperature diagenesis of Lower Cambrian clays of the Baltic paleobasin of Northern Estonia. *Clays Clay Min.*, *48*, 95–105.
- Kortelainen, N.M. & Karhu, J.A. (2004). Regional and seasonal trends in the oxygen and hydrogen isotope ratios of Finnish groundwaters: a key for mean annual precipitation. *J. Hydrol.*, *285*, 143–157.
- Kosakowski, P., Kotarba, M.J., Piestrzyński, A., Shogenova, A. & Więclaw, D. (2017). Petroleum source rock evaluation of the Alum and Dictyonema Shales (Upper Cambrian–Lower Ordovician) in the Baltic Basin and Podlasie Depression (eastern Poland). *Int. J. Earth Sci.*, *106*, 743–761.
- Laaksoharju, M., Tullborg, E.-L., Wikberg, P., Wallin, B. & Smellie, J. (1999). Hydrogeochemical conditions and evolution at the Äspö HRL, Sweden. *Appl. Geochem.*, *14*, 835–859.
- Lasberg, K. & Kalm, V. (2013). Chronology of Late Weichselian glaciation in the western part of the East European Plain. *Boreas*, *42*, 995–1007.
- Lehmann, B.E. *et al.* (2003). A comparison of groundwater dating with  $^{81}\text{Kr}$ ,  $^{36}\text{Cl}$  and  $^4\text{He}$  in four wells of the Great Artesian Basin, Australia. *Earth. Planet. Sc. Lett.*, *211*, 237–250.
- Lehtinen, R. (2012). Main geological features of Fennoscandia. In: Eilu, P. (Ed.), *Mineral Deposits and Metallogeny of Fennoscandia* (pp. 13–18). Espoo: Geological Survey of Finland, Special Paper 53.
- Langmuir, D. (1971). The geochemistry of some carbonate ground waters in central Pennsylvania. *Geochim. Cosmochim. Acta*, *35*, 1023–1045.
- Lemieux, J.M., Sudicky, E.A., Peltier, W.R. & Tarasov, L. (2008). Dynamics of groundwater recharge and seepage over the Canadian landscape during Wisconsinian glaciation. *J. Geophys. Res.*, *113*. <http://dx.doi.org/10.1029/2007JF000838>.
- Leuenberger, M., Siegenthaler, U. & Langway, C., (1992). Carbon isotope composition of atmospheric CO<sub>2</sub> during the last ice age from an Antarctic ice core. *Nature*, *357*, 488–490.
- Lunkka, J.P., Saarnisto, M., Gey, V. & Demidov, I. 2001: Extent and age of the Last Glacial Maximum in the southeastern sector of Scandinavian Ice Sheet. *Glob. Planet. Change*, *31*, 407–425.

- Margat, J., Foster, S. & Droubi, A. (2012). Concept and importance of non-renewable resources. In: Foster, S. & Loucks, D.P. (Eds.), *Non-renewable groundwater resources — A guidebook on socially sustainable management for water policy makers* (pp. 13–24). Paris: UNESCO IHP.
- Marandi, A., 2007. *Natural Chemical Composition of Groundwater as a Basis for Groundwater Management in the Cambrian-Vendian Aquifer System in Estonia*. Dissertationes Geologicae Universitatis Tartuensis 21. Tartu: Tartu University Press.
- Mastalerz, M., Schimmelmann, A., Hower, J.C., Lis, G., Hatch, J. & Jacobson, S.R. (2003). Chemical and isotopic properties of kukersites from Iowa and Estonia. *Org. Geochem.*, 34, 1419–1427.
- Maulé, C.P., Chanasyk, D.S. & Muehlenbachs, K. (1994). Isotopic determination of snow-water contribution to soil water and groundwater. *J. Hydrol.*, 155, 73–91.
- McIntosh, J.C. & Walter, L.M. (2005). Volumetrically significant recharge of Pleistocene glacial meltwaters into epicratonic basins: constraints imposed by solute mass balances. *Chem. Geol.*, 222, 292–309.
- McIntosh, J.C. & Walter, L.M. (2006). Paleowaters in Silurian–Devonian carbonate aquifers: geochemical evolution of groundwater in the Great Lakes region since the Late Pleistocene. *Geochim. Cosmochim. Acta*, 70, 2454–2479.
- McIntosh, J.C., Garven, G. & Hanor, J.S. (2011). Impacts of Pleistocene glaciation on large-scale groundwater flow and salinity in the Michigan Basin. *Geofluids*, 11, 18–33.
- McIntosh, J.C., Schlegel, M.E. & Person, M. (2012). Glacial impacts on hydrologic processes in sedimentary basins: evidence from natural tracer studies. *Geofluids*, 12, 7–21.
- Mens, K. & Pirrus, E. (1997). Cambrian. In: Raukas, A. & Teedumäe, A. (Eds.), *Geology and Mineral Resources of Estonia* (pp. 39–48.). Tallinn: Estonian Academy Publishers.
- Mokrik, R., 1997. *The Palaeohydrogeology of the Baltic Basin. Vendian and Cambrian*. Tartu: Tartu University Press.
- Mokrik, R., 2003. *The Paleohydrogeology of the Baltic Basin. Neoproterozoic and Phanerozoic*. Vilnius: Vilnius University Publishing House.
- Mokrik, R. & Vaikmäe, R., 1988. Palaeohydrogeological aspects of formation of isotope composition of groundwater in the Cambrian-Vendian aquifer system in Baltic area. In: Punning, J.M. (Ed.), *Isotope-geochemical investigations in the Baltic area and in Belorussia* (pp. 133–143). Tallinn: Estonian Academy of Sciences.
- Mokrik, R. & Mažeika, J. (2002). Palaeohydrogeological reconstruction of groundwater recharge during Late Weichselian in the Baltic basin. *Geologija* 39, 49–57.
- Mokrik, R., Mažeika, J., Baublyte, A. & Martma, T. (2009). The groundwater age in the Middle-Upper Devonian aquifer system, Lithuania. *Hydrogeol. J.*, 17, 871–889.
- Montross, S.N., Skidmore, M., Tranter, M., Kivimäki, A.L. & Parkes, R.J. (2013). A microbial driver of chemical weathering in glaciated systems. *Geology*, 41, 215–218.
- Mook, W.G. (1968). *Geochemistry of the Stable Carbon and Oxygen Isotopes of Natural Waters in the Netherlands*. PhD thesis, Groningen.
- Mook, W.G., Bommerson, J.C. & Staverman, W.H. (1974). Carbon isotope fractionation between dissolved bicarbonate and gaseous carbon dioxide. *Earth Planet. Sci. Lett.*, 22, 169–176.

- Moser, H., Wolf, M., Fritz, P., Fontes, J.-C., Florkowski, T. & Payne, B.R. (1989). Deuterium, oxygen-18, and tritium in Stripa groundwater. *Geochim. Cosmochim. Acta*, *53*, 1757–1763.
- Muehlenbachs, K., 1998. The oxygen isotopic composition of the oceans, sediments and the seafloor. *Chem. Geol.*, *145*, 263–273.
- Negrel, P., Casanova, J. & Blomqvist R. (2005).  $^{87}\text{Sr}/^{86}\text{Sr}$  of brines from the Fennoscandian Shield: a synthesis of groundwater isotopic data from the Baltic Sea region. *Can. J. Earth Sci.*, *42*, 273–285.
- O'Driscoll, M.A., DeWalle, D.R., McGuirec, K.J. & Gburek, W.J. (2005). Seasonal  $^{18}\text{O}$  variations and groundwater recharge for three landscape types in central Pennsylvania, USA. *J. Hydrol.*, *303*, 108–124.
- Olausson, E. (1982). Stable isotopes. In: Olausson, E. (Ed.), *The Pleistocene/Holocene Boundary in South-Western Sweden (pp. 82–92)*. Uppsala: Sveriges geologiska undersökning 794E.
- Oxburgh, E. R. & O'Nions, R. K. (1987). Helium loss, tectonics, and the terrestrial heat budget. *Science*, *237*, 1583–1588.
- Park, J., Sanford, R.A. & Bethke, C.M. (2006). Geochemical and microbiological zonation of the Middendorf aquifer, South Carolina. *Chem. Geol.*, *230*, 88–104.
- Parkhurst, D.L. & Appelo, C.A.J. (2013). *Description of Input and Examples for PHREEQC Version 3 — A Computer Program for Speciation, Batch-Reaction, One-Dimensional Transport, and Inverse Geochemical Calculations*. U.S. Geological Survey Techniques and Methods, book 6, chapter A43, 497 p. U.S. Geol. Surv. Tech. Methods, B. 6, chapter A43 6–43A.
- Perens, R. & Vallner, L. (1997). Water-bearing formation. In: Raukas, A. & Teedumäe, A. (Eds.), *Geology and Mineral Resources of Estonia (pp. 137–145)*. Tallinn: Estonian Academy Publishers.
- Perens, R., Savva, V., Lelgus, M. & Parm, T. (2001). *The Hydrogeochemical Atlas of Estonia*. Tallinn: Geological Survey of Estonia. (in Estonian)
- Perens, R., Savitski, L., Savva, V., Jashtshuk, S. & Häelm, M. (2012). *Delineation of groundwater bodies and description of their boundaries and hydrogeological conceptual models*. Tallinn: Geological Survey of Estonia.
- Person, M., McIntosh, J.C., Remenda, V. & Bense, V. (2007). Pleistocene hydrology of North America: the role of ice sheets in reorganizing groundwater systems. *Rev. Geophys.* *45*, <http://dx.doi.org/10.1029/2006RG000206>.
- Petersell, V. (1997). Dictyonema argillite. In: Raukas, A. & Teedumäe, A. (Eds.), *Geology and Mineral Resources of Estonia (pp. 313–326)*. Tallinn: Estonian Academy Publishers.
- Petersen, J.O., Deschamps, P., Hamelin, B., Fourré, E., Gonçalves, J., Zouari, K., Guendouz, A., Michelot, J. L., Massault, M., Dapoigny, A. & Team, A. (2018). Groundwater flowpaths and residence times inferred by  $^{14}\text{C}$ ,  $^{36}\text{Cl}$  and  $^4\text{He}$  isotopes in the Continental Intercalaire aquifer (North-Western Africa). *J. Hydrol.*, *560*, 11–23.
- Phillips, F.M. (2013). Chlorine-36 dating of old groundwater. In: Suckow, A., Aggarwal, P.K. & Araguas-Araguas, L. (Eds.), *Isotope Methods for Dating Old Groundwater (pp. 125–152)*. Vienna: IAEA.
- Pihlak, A.T., Matvienko, N. & Bogdanov, R. (2003). Natural gases in Estonian wells. *Ekologicheskaya khimia*, *12*, 141–159. (in Russian)

- Piotrowski, J. (1997). Subglacial hydrology in north-western Germany during the last glaciations: groundwater flow, tunnel valleys and hydrological cycles. *Quaternary Sci. Rev.*, *16*, 169–185.
- Pitkänen, P., Luukkonen, A., Ruotsalainen, P., Leino-Forsman, H. & Vuorinen, U. (1999). *Geochemical modelling of groundwater evolution and residence time at the Olkiluoto site*. Posiva OY, Helsinki. POSIVA 98-10.
- Pitkänen, P., Luukkonen, A., Ruotsalainen, P., Leino-Forsman, H. & Vuorinen, U. (2001). *Geochemical modelling of groundwater evolution and residence time at the Hästholmen site*. Eurajoki: Posiva OY.
- Pitkänen, P., Partamies S. & Luukkonen, A. (2004). *Hydrogeochemical interpretation of baseline groundwater conditions at the Olkiluoto site*. Eurajoki: Posiva OY.
- Plummer, L.N. & Glynn, P.D. (2013). Radiocarbon dating in groundwater systems. In: Suckow, A., Aggarwal, P.K. & Araguas-Araguas, L. (Eds.), *Isotope Methods for Dating Old Groundwater* (pp. 33–89). Vienna: IAEA.
- Plummer, L.N., Prestemon, E.C. & Parkhurst, D.L. (1994). *An interactive code (NETPATH) for modeling net geochemical reactions along a flow path, version 2.0*. Water-Resources Investig. Rep. 94–4169.
- Plummer, L.N. & Sprinkle, C.L. (2001). Radiocarbon dating of dissolved inorganic carbon in groundwater from confined parts of the Upper Floridan aquifer, Florida, USA. *Hydrogeol. J.*, *9*, 127–150.
- Punning, J.M., Toots, M. & Vaikmäe, R. (1987). Oxygen-18 in Estonian natural waters. *Isotopenpraxis*, *23*, 232–234.
- Purtschert, R., Yokoschi R. & Sturchio, N.C. (2013). Krypton-81 dating of old groundwater. In: Suckow, A., Aggarwal, P.K. & Araguas-Araguas, L. (Eds.), *Isotope Methods for Dating Old Groundwater* (pp. 91–124). Vienna: IAEA.
- Pärn, J., Polikarpus, M., Raidla, V., Tarros, S., Jõelet, A., Paat, R. & Marandi, A. (2018). The intrusion of saline water into a coastal aquifer containing palaeogroundwater in northern Estonia. Proceedings of the 25th Salt Water Intrusion Meeting, Gdansk, Poland, pp. 206–207.
- Raidla, V., Aeschbach, W. & Weissbach, T. (2017). Noble gases in the Cambrian-Vendian aquifer system in Estonia. PAGES Global Challenges for our Common Future: a paleoscience perspective, Zaragoza, Spain, 9-13 May 2017.
- Raidla, V., Kirsimäe, K., Bitjukova, L., Jõelet, A., Shogenova, A. & Šliaupa, S. (2006). Lithology and diagenesis of the poorly consolidated Cambrian siliciclastic sediments in the northern Baltic Sedimentary Basin. *Geol. Q.*, *50*, 11–22.
- Raidla, V., Kirsimäe, K., Ivask, J., Kaup, E., Knöller, K., Marandi, A., Martma, T. & Vaikmäe, R. (2014). Sulphur isotope composition of dissolved sulphate in the Cambrian-Vendian aquifer system in the northern part of the Baltic Artesian Basin. *Chem. Geol.*, *383*, 147–154.
- Raidla, V., Kirsimäe, K., Vaikmäe, R., Jõelet, A., Karro, E., Marandi, A. & Savitskaja, L. (2009). Geochemical evolution of groundwater in the Cambrian-Vendian aquifer system of the Baltic Basin. *Chem. Geol.*, *258*, 219–231.
- Raidla, V., Kirsimäe, K., Vaikmäe, R., Kaup, E. & Martma, T. (2012). Carbon isotope systematics of the Cambrian – Vendian aquifer system in the northern Baltic Basin: Implications to the age and evolution of groundwater. *Appl. Geochem.*, *27*, 2042–2052.

- Raudsep, R., Liivrand, H., Belkin, V., Mardiste, A., Rass, V., Meriküll, V., Madalik, J., Pajupuu, A., Maltseva, I., Semjonova, N., Kelder, N. & Kuptsov, A. (1989). *Detailed Research Results from Rakvere Phosphorite Deposit in Kabala Area*. Tallinn: Estonian Geology. (in Russian)
- Raudsep, R. (1997). Phosphorite. In: Raukas, A. & Teedumäe, A. (Eds), *Geology and mineral resources of Estonia* (pp. 331–337). Tallinn: Estonian Academy Publishers.
- Raukas, A., Kalm, V., Karukäpp, R. & Rattas, M. (2004). Pleistocene glaciations in Estonia. In: Ehlers, J. & Gibbard, P.L. (Eds), *Quaternary Glaciations – Extent and Chronology. Part I: Europe* (pp. 83–91). Amsterdam: Elsevier.
- Rosentau, A., Vassiljev, J., Hang, T., Saarse, L. & Kalm, V. (2009). Development of the Baltic Ice Lake in eastern Baltic. *Quatern. Int.*, 206, 16–23.
- Rousseau-Gueutin P., Love A.J., Vasseur G., Robinson N.I., Simmons C.T. & de Marsily G. (2013). Time to reach near steady state in large aquifers. *Water Resour. Res.*, 49, 6893–6908.
- Rozanski, K. (1985). Deuterium and oxygen-18 in European groundwaters—links to atmospheric circulation in the past. *Chem. Geol.*, 52, 349–363.
- Rozanski, K., Araguás-Araguás, L. & Gonfiantini, R. (1992). Relation between long-term trends of oxygen-18 isotope composition of precipitation and climate. *Science*, 258, 981–985.
- Rozanski, K., Araguas-Araguas, L. & Gonfiantini, R. (1993). Isotopic patterns in modern global precipitation. *Climate Change in Continental Isotopic Records. Am. Geophys. Union Geophys. Monogr.*, 78, 1–36.
- Ryu, J.S. & Jacobson, A.D. (2012). CO<sub>2</sub> evasion from the Greenland Ice Sheet: A new carbon-climate feedback. *Chem. Geol.*, 320–321, 80–95.
- Saarse, L., Heinsalu, A. & Veski, S. (2012). Deglaciation chronology of the Pandivere and Palivere ice-marginal zones in Estonia. *Geol. Q.*, 56, 353–362.
- Sanford, W.E. (1997). Correcting for diffusion in carbon-14 dating of groundwater. *Groundwater*, 35, 357–361.
- Savitski, L., Viigand, A., Belkina, V. & Jashtshuk, S. (1993). *Hydrogeological investigations of the Tallinn area and safe yield calculations of Tallinn water intakes*. Tallinn: Geological Survey of Estonia. (in Estonian)
- Savitskaja, L. & Viigand A. (1994). *Report on microcomponent and isotopic composition of groundwater in the Cambrian-Vendian aquifer system for estimating drinking water quality in North Estonia*. Tallinn: Geological Survey of Estonia. (in Estonian)
- Savitskaja, L., Viigand, A. & Jashtshuk, S. (1995). *Report on microcomponent and isotopic composition of groundwater in the Ordovician-Cambrian aquifer system for estimating drinking water quality in North Estonia*. Tallinn: Geological Survey of Estonia. (in Estonian)
- Savitskaja, L., Viigand, A. & Jashtshuk, S. (1996a). *Report on water quality in the Middle-Devonian-Silurian aquifer system*. Tallinn: Geological Survey of Estonia. (in Estonian)
- Savitskaja, L., Viigand, A. & Jashtshuk, S. (1996b). *Report on water quality in the Middle-Devonian aquifer system*. Tallinn: Geological Survey of Estonia. (in Estonian)
- Savitskaja, L., Viigand, A. & Jashtshuk, S. (1997). *Report on microcomponent and radionuclide composition of groundwater in the Silurian-Ordovician aquifer system*. Tallinn: Geological Survey of Estonia. (in Estonian)

- Savitskaja, L., Viigand, A. & Jashtshuk, S. (1998). *Report on microcomponent and radionuclide composition of groundwater in the Silurian-Ordovician aquifer system. VI phase*. Tallinn: Geological Survey of Estonia. (in Estonian)
- Saxton, K.E. & McGuinness, J.L. (1982). Evapotranspiration. In: Haan, C.T., Johnson, H.P. & Brakensiek, D.L. (Eds.), *Hydrologic Modeling of Small Watersheds. ASAE Monograph no. 5* (pp. 229–273). Michigan: American Society of Agricultural Engineers.
- Severinghaus, J.P., Sowers, T., Brook, E., Alley, R. & Bender, M. (1998). Timing of abrupt climate change at the end of the Younger Dryas interval from thermally fractionated gases in polar ice. *Nature*, *391*, 141–146.
- Sharp, M., Parkes, J., Cragg, B., Fairchild, I. J., Lamb, H. & Tranter, M. (1999). Widespread bacterial populations at glacier beds and their relationship to rock weathering and carbon cycling. *Geology*, *27*, 107–110.
- Siegel, D.I. (1989). *Geochemistry of the Cambrian-Ordovician aquifer system in the northern Midwest, United States*. In: Regional Aquifer-System Analysis—Northern Midwest Aquifer System (pp. D1–D76). US Geological Survey.
- Siegel, D.I. (1991). Evidence for dilution of deep, confined ground water by vertical recharge of isotopically heavy Pleistocene water. *Geology*, *19*, 433–436.
- Siegel, D.I. & Mandle, R.J. (1984). Isotopic evidence for glacial meltwater recharge to the Cambrian Ordovician aquifer, north-central United States. *Quaternary Res.*, *22*, 328–335.
- Siegert, M.J. & Dowdeswell, J.A. (2004). Numerical reconstructions of the Eurasian Ice Sheet and climate during the Late Weichselian. *Quaternary Sci. Rev.*, *23*, 1273–1283.
- Skuratovič, Ž., Mažeika, J., Petrošius, R. & Martma, T. (2015). Investigations of the unsaturated zone at two radioactive waste disposal sites in Lithuania. *Isot. Environ. Health Stud.*, *1–9*. <http://dx.doi.org/10.1080/10256016.2015.1092968>.
- Song, X., Wang, S., Xiao, G., Wang, Z., Liu, X. & Wang, P. (2009). A study of soil water movement combining soil water potential with stable isotopes at two sites of shallow groundwater areas in the North China Plain. *Hydrol. Process.*, *23*, 1376–1388.
- Souchez, R., Lemmens, M., Tison, J.L., Lorrain, R. & Janssens, L. (1993). Reconstruction of basal boundary conditions at the Greenland Ice Sheet margin from gas composition in the ice. *Earth Planet. Sci. Lett.*, *118*, 327–333.
- Souchez, R., Jouzel, J., Landais, A., Chappellaz, J., Lorrain, R. & Tison, J.-L. (2006). Gas isotopes in ice reveal a vegetated central Greenland during ice sheet invasion. *Geophys. Res. Lett.*, *33*. L24503, doi:10.1029/2006GL028424.
- Sterckx, A., Lemieux, J.M. & Vaikmäe, R. (2017). Representing glaciations and subglacial processes in hydrogeological models: a numerical investigation. *Geofluids*, <https://doi.org/10.1155/2017/4598902>.
- Sterckx, A., Lemieux, J.M. & Vaikmäe, R. (2018). Assessment of paleo-recharge under the Fennoscandian Ice Sheet and its impact on regional groundwater flow in the northern Baltic Artesian Basin using a numerical model. *J. Hydrol.*, <https://doi.org/10.1007/s10040-018-1838-7>.
- Stotler, R.L., Frappe, S.K., Ruskeeniemi, T., Pitkänen, P. & Blowes, D.W. (2012). The interglacial–glacial cycle and geochemical evolution of Canadian and Fennoscandian Shield groundwaters. *Geochim. Cosmochim. Acta*, *76*, 45–67.

- Stueber, A.M. & Walter, L.M. (1991). Origin and chemical evolution of formation waters from Silurian–Devonian strata in the Illinois Basin, USA. *Geochim. Cosmochim. Acta*, *55*, 309–325.
- Stueber, A.M. & Walter, L.M. (1994). Glacial recharge and paleohydrologic flow systems in the Illinois Basin: evidence from chemistry of Ordovician carbonate (Galena) formation waters. *Geol. Soc. Am. Bull.*, *106*, 1430–1439.
- Sturchio N.C *et al.* (2004). One-million-year-old groundwater in the Sahara revealed by krypton-81 and chlorine-36. *Geophys. Res. Lett.*, *31*, L05503, doi:10.1029/2003GL019234.
- Stute, M., Forster, M., Frischkorn, H., Serejo, A., Clark, J.F., Schlosser, P., Broecker, W.S. & Bonani, G. (1995). Cooling of tropical Brazil (5°C) during the Last Glacial Maximum. *Science*, *69*, 379–383.
- Suursoo, S., Hill, L., Raidla, V., Kiisk, M., Jantsikene, A., Nilb, N., Czuppon, G., Putk, K., Munter, R., Koch, R. & Isakar, K. (2017). Temporal changes in radiological and chemical composition of Cm-V groundwater in conditions of intensive water consumption. *Sci. Total Environ.*, *601-602*, 679–690.
- Takcidi, E. (1999). *Documentation of the Database "Boreholes"*. Valsts ģeoloģijas dienests, Riga. (in Latvian)
- Taylor, R.G *et al.* (2013). Ground water and climate change. *Nat. Clim. Change*, *3*, 322–329.
- Taylor, S., Feng, X., Kirchner, J.W., Osterhuber, R., Klaue, B. & Renshaw, C.E. (2001). Isotopic evolution of a seasonal snowpack and its melt. *Water Resour. Res.*, *37*, 759–769.
- Telmer, K. & Veizer, J. (2000). Isotopic constraints on the transpiration, evaporation, energy, and gross primary production budgets of a large boreal watershed: Ottawa River basin, Canada. *Global Biogeochem. Cycles*, *14*, 149–165.
- Terzer, S., Wassenaar, L.I., Araguás-Araguás, L.J. & Aggarwal, P.K. (2013). Global isoscapes for  $\delta^{18}\text{O}$  and  $\delta^2\text{H}$  in precipitation: improved prediction using regionalized climatic regression models. *Hydrol. Earth Syst. Sci. Discuss.*, *10*, 7351–7393.
- Tooming, H. & Kadaja, J. (2006). *Handbook of Estonian Snow Cover*. Tallinn: Estonian Meteorology and Hydrology Institute, Estonian Research Institute of Agriculture.
- Toran, L.E. & Saunders, J.A. (1999). Modeling alternative paths of chemical evolution of Na-HCO<sub>3</sub>-type groundwater near Oak Ridge, Tennessee, USA. *Hydrogeol. J.*, *7*, 355–364.
- Torgersen, T. & Ivey, G.N. (1985). Helium accumulation in groundwater. II: A model for the accumulation of the crustal <sup>4</sup>He degassing flux. *Geochim. Cosmochim. Acta.*, *49*, 2445–2452.
- Torgersen, T. & Stute, M., 2013. Helium (and other noble gases) as a tool for understanding long timescale groundwater transport, In: In Suckow, A., Aggarwal, P.K. & Araguas-Araguas, L. (Eds.), *Isotope Methods for Dating Old Groundwater (pp. 179–216)*. Vienna: IAEA.
- Toth, D.-J. & Katz, B.-G. (2006). Mixing of shallow and deep groundwater as indicated by the chemistry and age of karstic springs. *Hydrogeol. J.*, *14*, 827–847.
- Tranter, M., Sharp, M.J., Lamb, H.R., Brown, G.H., Hubbard, B.P. & Willis, I.C. (2002). Geochemical weathering at the bed of Haut glacier d’Arolla, Switzerland - A new model. *Hydrol. Process.*, *16*, 959–993.

- Tranter, M., Skidmore, M. & Wadham, J. (2005). Hydrological controls on microbial communities in subglacial environments. *Hydrol. Process.*, 19, 995–998.
- Tšeban, E., 1966. *Hydrogeology of the USSR XXX (Estonian SSR)*. Moskow: VSEGINGEO. (in Russian)
- Ukkonen, P., Aaris-Sørensen, K., Arppe, L., Clark, P.U., Daugnora, L., Lister, A.M., Lõugas, L., Seppä, H., Sommer, R.S., Stuart, A.J., Wojtal, P. & Zupinš, I. (2011). Woolly mammoth (*Mammuthus primigenius* Blum.) and its environment in northern Europe during the last glaciation. *Quat. Sci. Rev.*, 30, 693–712.
- Vaikmäe, R. & Vallner, L. (1989). Oxygen-18 in Estonian groundwaters. Fifth Working Meeting of Isotopes in Nature, Leipzig, 25–29 September, pp. 161–162.
- Vaikmäe, R., Vallner, L., Loosli, H.H., Blaser, P.C. & Juillard-Tardent, M. (2001). Palaeogroundwater of glacial origin in the Cambrian-Vendian aquifer of northern Estonia. In: Edmunds, W.M. & Milne, C.J. (Eds.), *Palaeowaters of Coastal Europe: Evolution of Groundwater since the late Pleistocene* (pp. 17–27). London: Geological Society, Special Publications, vol. 189.
- Vallner, L. (1997). Groundwater flow. In Raukas, A. & Teedumäe, A. (Eds), *Geology and Mineral Resources of Estonia* (pp. 137–152). Tallinn: Estonian Academy Publishers.
- Vallner, L. (2003). Hydrogeological model of Estonia and its applications. *P. Est. Acad. Sci. Geology*, 52, 179–192.
- Van Der Kemp, W.J.M., Appelo, C.A.J. & Walraevens, K. (2000). Inverse chemical modeling and radiocarbon dating of palaeogroundwaters: The Tertiary Ledo-Paniselian aquifer in Flanders, Belgium. *Water Resour. Res.*, 36, 1277–1287.
- Vee erikasutusõiguse tasumäärad veevõtu eest veekogust või põhjaveekihist (21.11.2014). *Riigi teataja I*, 21.11.2014, 11. Retrieval (2018, 18<sup>th</sup> June). Retrieved from <https://www.riigiteataja.ee/akt/121112014011>. (in Estonian)
- Vidstrand, P., Follin, S., Selroos, J.-O., Näslund, J.-O. & Rhén, I. (2011). Modeling of groundwater flow at depth in crystalline rock beneath a moving ice-sheet margin, exemplified by the Fennoscandian Shield, Sweden. *Hydrogeol. J.*, 21, 239–255.
- Viigisaar, P. (1978). Estonian mineral waters and their exploitation. In: Heinsalu, Ü. (Ed.), *Exploitation and Protection of Estonian Ground Water Reserves* (pp. 54–71). Tallinn: Estonian Academy Publishers. (in Estonian)
- Virbulis, J., Bethers, U., Saks, T., Sennikovs, J. & Timuhins, A. (2013). Hydrogeological model of the Baltic Artesian Basin. *Hydrogeol. J.*, 21, 845–862.
- Voitov, G., Karpov, I., Tibar, K. & Sozinova, T. (1982). The natural anomalies in methane's carbon isotope composition in Estonia. *Doklady Akademii Nauk USSR*, 264, 1217–1221. (in Russian)
- Vogel, J.C. (1970). Carbon-14 dating of groundwater. In Isotope Hydrology 1970, IAEA Symposium 129, March 1970, Vienna. IAEA, Vienna, pp. 225–239.
- Vogel, J.C. (1993). Variability of carbon isotope fractionation during photosynthesis. In: Ehleringer, J.R., Hall, A.E. & Farquhar, G.D. (Eds.), *Stable Isotopes and Plant Carbon-Water Relations* (pp. 29–46). London: Academic Press.
- Voolma, M., Soesoo, A., Hade, S., Hints, R. & Kallaste, T. (2013). Geochemical heterogeneity of Estonian graptolite argillite. *Oil Shale*, 30, 377–401.
- Voroniuk, G.Y., Borodulina, G.S., Krainyukova, I.A. & Tokarev, I.V. (2016). Groundwater exchange in the Baltic Shield marginal areas and adjacent artesian basins based on isotope and hydrochemistry data. Scientific problems and practical applications, Karelian isthmus. *Transactions of the Karelian Research Centre of the Russian Academy of Sciences*, 9, 46–56. (in Russian)

- Väikmann, S., Savva, V., Otsmaa, M., Boldõreva, N. & Simm, D. (1992). *Evaluation of groundwater resources in Tartu area*. Tallinn: Geological Survey of Estonia. (in Estonian)
- Wadham, J.L., Bottrell, S., Tranter, M. & Raiswell, R. (2004). Stable isotope evidence for microbial sulphate reduction at the bed of a polythermal high Arctic glacier. *Earth Planet. Sci. Lett.*, *219*, 341–355.
- Wadham, J.L., Tranter, Tulaczyk, S. & Sharp, M. (2008). Subglacial methanogenesis: A potential climatic amplifier. *Global Biogeochem. Cycles*, *22*, doi:10.1029/2007GB002951.
- Waldron, S., Lansdown, J.M., Scott, E.M., Fallick, A.E. & Hall, A.J. (1999). The global influence of H isotopic composition of water on that of bacteriogenic methane from shallow freshwater environments. *Geochim. Cosmochim. Acta*, *63*, 2237–2245.
- Walraevens, K., Van Camp, M., Lermytte, J., van der Kemp, W.J.M. & Loosli, H.H., (2001). Pleistocene and Holocene groundwaters in the freshening Ledo-Paniselian aquifer in Flanders, Belgium. In: Edmunds, W.M. & Milne, C.J. (Eds.), *Palaeowaters in Coastal Europe: Evolution of Groundwater Since the Late Pleistocene* (pp. 49–70). London: Geological Society, Special Publications, vol. 189.
- Weissbach, T. (2014). *Noble Gases in Palaeogroundwater of Glacial Origin in the Cambrian-Vendian Aquifer System, Estonia*. Master Thesis, Heidelberg: University of Heidelberg.
- Whiticar, M. J. (1999). Carbon and hydrogen isotope systematics of bacterial formation and oxidation of methane. *Chem. Geol.*, *161*, 291–314.
- WMO (2012). *International glossary of hydrogeology*. Retrieval (2018, April 29). Retrieved from [http://www.wmo.int/pages/prog/hwrrp/publications/international\\_glossary/385\\_IGH\\_2012.pdf](http://www.wmo.int/pages/prog/hwrrp/publications/international_glossary/385_IGH_2012.pdf).
- Yezhova, M., Polyakov, V., Tkachenko, A., Savitski, L. & Belkina, V. (1996). Palaeowaters of North Estonia and their influence on changes of resources and the quality of fresh groundwaters of large coastal water supplies. *Geologija*, *19*, 37–40.
- Zhu, C. (2005). In situ feldspar dissolution rates in an aquifer. *Geochim. Cosmochim. Acta*, *69*, 1435–1453.
- Zuber, A., Weise, S.M., Osenbrück, K., Pajnowska, H. & Grabczak, J. (2000). Age and recharge pattern of water in the Oligocene of the Mazovian basin (Poland) as indicated by environmental tracers. *J. Hydrol.*, *233*, 174–188
- Zuber, A., Weise, S.M., Motyka, J., Osenbrück, K. & Rozanski, K. (2004). Age and flow pattern of groundwater in a Jurassic limestone aquifer and related Tertiary sands derived from combined isotope, noble gas and chemical data. *J. Hydrol.*, *286*, 87–112.
- Zuzevičius, A. (2010). The groundwater dynamics in the southern part of the Baltic artesian Basin during the Late Pleistocene. *Baltica*, *23*, 1–12.

## 7 Acknowledgements

I would like to thank my supervisors Prof. Emeritus Rein Vaikmäe and Valle Raidla for their help, support and dedication during my PhD project. I am extremely grateful to Rein Vaikmäe for providing me with a work environment where I could really concentrate on my PhD project. I am also grateful to him for providing me with an opportunity to participate in international workshops and to spend a year studying in Ghent University. I am especially grateful to Valle Raidla for all the discussions, assistance and guidance during fieldworks. In addition, his thoroughness in correcting the manuscripts has been invaluable. I would like to thank my co-workers Jüri Ivask, Tõnu Martma, Enn Kaup and Heivi Rajamäe from the Division of Isotope Geology for preparing and analyzing the samples, assistance during fieldwork, help in writing the papers and general discussions on hydrogeology. My thanks also go to Helle Pohl-Raidla and Gennadi Baranov whose help with administrative issues and good company made my time in the Institute of Geology all the more enjoyable.

I am most grateful to Prof. Kristine Walraevens, Marc van Camp and their co-workers in the Laboratory of Hydrogeology and Applied Geology at Ghent University. The year I spent in Ghent allowed me to learn and gain experience in working as a hydrogeologist. I was also introduced to a wonderfully complex world of geochemical modelling. Some of the advice from Prof. Kristine will surely stay with me until the end of my career.

I am also grateful to many of the colleagues from other institutions and universities for discussions that have influenced the ideas developed in this work. More specifically, I would like to thank Robert Mokrik, Arnaud Sterckx, Oliver Koit, Kalle Kirsimäe, Christoph Gerber and Jüri Nemliher. It has been a joy to discuss geology and hydrogeology with you.

The thesis would have been very hard to complete without the support of my current employer Geological Survey of Estonia. I am particularly grateful to my head of department Andres Marandi who enabled me to take time off for completing this thesis. His comments on the draft version of the thesis also helped to improve it significantly.

I would like to acknowledge the institutions that have funded the research presented in this thesis. At different stages of the PhD project the work together with participation in conferences and workshops was funded by Estonian Science Foundation Grant ETF8948, the Estonian Research Council Projects IUT19-22 and PUTJD127, European Regional Development Fund's Doctoral Studies and Internationalization Program DoRa Plus, Archimedes Foundation Kristjan Jaak Scholarship, INQUA/UNESCO supported G@GPS Project and IAEA CRP Project F33019 (Contract No. 17850). I would also like to thank all well owners, who have provided access to their wells for sampling, some of them even multiple times.

Lastly and most importantly I would like to thank my wife Reeli and my family without whose support and patience you would not have this thesis before you today.

## Abstract

### Origin and Geochemical Evolution of Palaeogroundwater in the Northern Part of the Baltic Artesian Basin

The PhD thesis was designed to study the spatial distribution, origin, geochemical evolution and age of glacial palaeogroundwater in the northern part of the Baltic Artesian Basin (BAB). In this area, groundwater recharged prior to the beginning of the Holocene has been previously observed in various depths and locations. The brine in the deep central parts of the basin (Latvia) has ages >1.3 Ma based on noble gas age tracers  $^{81}\text{Kr}$ ,  $^4\text{He}$  and  $^{40}\text{Ar}$  (Gerber et al., 2017). In the northern part of the basin (northern Estonia) the distribution of glacial palaeogroundwater originating from subglacial meltwater recharge during the Pleistocene glaciations has been shown to be wide in the deepest Cambrian-Vendian aquifer system (Vaikmäe et al., 2001; Raidla et al., 2009). Despite previous evidence suggesting that the spatial distribution of glacial palaeogroundwater could also be wide in the aquifer systems overlying the Cambrian-Vendian (e.g. Savitskaja et al., 1995, 1996b, 1997), their occurrence, origin and age were not extensively studied until recently.

The main objective of the author was to study the extent to which groundwater originating from the Pleistocene glaciations is spread in the aquifer systems overlying the Cambrian-Vendian aquifer system. Based on previous evidence, the working hypothesis was that groundwater originating from the Pleistocene is far more widely distributed in the northern BAB than previously thought. It could be suspected that confined aquifers in the study area have not reached an equilibrium with modern topographically-driven groundwater flow conditions and still exhibit groundwater flow patterns and composition established in the Pleistocene.

The study of Pleistocene groundwater in the thesis also involved the study of the special characteristics of groundwater in the Cambrian-Vendian aquifer system (high concentrations of noble gases and methane). Those characteristics shed light to palaeoenvironmental conditions during the recharge of glacial palaeogroundwater that provide a starting point for the geochemical evolution of the Pleistocene groundwater in shallower aquifer systems. Understanding the spatial distribution and processes influencing the geochemical evolution of this non-renewable groundwater resource is crucial for predicting the effects of groundwater abstraction on its composition and availability. The results presented in the thesis illustrate the multi-faceted nature of information about pre-Holocene palaeoenvironmental conditions that can be recorded in palaeogroundwater reservoirs.

Glacial palaeogroundwater was studied using a multi-tracer approach utilizing the hydrochemical composition of groundwater, a suite of stable ( $\delta^2\text{H}_{\text{H}_2\text{O}}$ ,  $\delta^{18}\text{O}_{\text{H}_2\text{O}}$ ,  $\delta^{13}\text{C}_{\text{DIC}}$ ,  $\delta^{34}\text{S}_{\text{SO}_4}$ ,  $\delta^{18}\text{O}_{\text{SO}_4}$ ,  $\delta^{13}\text{C}_{\text{CH}_4}$ ,  $\delta^{13}\text{C}_{\text{CO}_2}$ ) and radioactive isotope tracers ( $^3\text{H}$ ,  $^{14}\text{C}$  and  $^4\text{He}$ ) together with the study of dissolved gas compositions in groundwater ( $\text{CH}_4$ ,  $\text{CO}_2$ , He, Ne, Ar, Kr, Xe). In addition, the geochemical evolution and groundwater age were studied with geochemical modelling using the software programs GWB, PHREEQC and NETPATH. Many of these methods were utilized for the first time in studying groundwater in aquifer systems overlying the Cambrian-Vendian.

The results of the thesis confirmed the proposed hypothesis that glacial palaeogroundwater has been preserved in a number of aquifer systems in the northern part of the BAB. Their presence is revealed mainly by a light isotopic composition that differs markedly from values found in modern precipitation and shallow groundwater in

the study area. In the Ordovician-Cambrian, Silurian-Ordovician and Lower-Middle-Devonian aquifer systems groundwater with  $\delta^{18}\text{O}$  values as light as  $\sim -22\text{‰}$  was found. These values are markedly depleted with respect to the mean value of  $-11.7\text{‰}$  found in shallow groundwater originating from modern recharge. Such a wide distribution of glacial palaeogroundwater in the northern BAB is unique in Europe as the closest analogues to this situation can be found in North America.

The occurrence of glacial palaeogroundwater is particularly wide in the Ordovician-Cambrian aquifer system where it has a similarly wide distribution compared to the underlying Cambrian-Vendian aquifer system. In shallower aquifer systems of Silurian-Ordovician and Lower-Middle-Devonian the presence of glacial palaeogroundwater is confined to areas farther down the groundwater flow path. The glacial palaeogroundwater in the northern part of the BAB has gone through significant geochemical evolution after its infiltration involving dissolution of carbonate minerals, cation exchange reactions, oxidation of organic matter and mixing with groundwater originating from modern precipitation, previous interstadials, saline formation water and the Baltic Sea. The dating of glacial palaeogroundwater in the Ordovician-Cambrian aquifer system allowed to identify groundwater originating from three different climatic periods: (1) the Holocene period (0–10 ka BP); (2) the Late Glacial Maximum ( $\sim 10\text{--}22$  ka BP) and (3) from earlier interstadials ( $>22$  ka BP).

Aquifers containing glacial palaeogroundwater have been shown in a transient state in the study area with respect to modern topographically-driven groundwater flow conditions. This indicates that under natural conditions a significant time period is needed for the deeper aquifer systems to gain equilibrium with groundwater originating from modern recharge in terms of their chemical and isotopic composition. The study of the isotopic composition of methane in the Cm-V aquifer system suggests that the Pleistocene ice sheets advanced over areas where terrestrial vegetation had been only recently active.

The wide spread of glacial palaeogroundwater in Estonia has important implications for groundwater abstraction and management. A weak connection of glacial palaeogroundwater reservoirs with modern groundwater recharge and with potential anthropogenic contamination makes them a high-quality resource which should be treated as a strategic reserve, to be used only for specific purposes (e.g. potable water). Furthermore, their sustainable use should be protected with appropriate legislation to avoid overexploitation of this non-renewable groundwater resource. In several aquifer systems containing palaeogroundwater, the rocks associated with the aquifer strata contain mineral resources that could have potential economic significance in the future (e.g. biogenic phosphorite in the upper portion of sandstones forming the Ordovician-Cambrian aquifer system). Any future plans for mining these mineral resources need to take into account the renewability of groundwater in the associated aquifer systems.

The results of the thesis show that in areas that have experienced drastic environmental changes during their recent geological history (e.g. the Pleistocene glaciations), steady-state conditions with respect to modern topographically-driven groundwater flow cannot be assumed a priori. As the recent global overviews have shown (Gleeson et al., 2016; Jasechko et al., 2017), the occurrence of palaeogroundwater weakly connected to modern groundwater flow system should be considered a norm, not an exception.

## Lühikokkuvõte

### Paleopõhjaveete päritolu ja geokeemiline areng Balti arteesiabasseini põhjaosas

Viimastel aastatel läbiviidud uuringud on näidanud, et tänapäevase (kuni 50 aastat vana) põhjavee kogus on globaalses mastaabis palju väiksem võrreldes vanemas minevikus tekkinud põhjaveega (Gleeson jt., 2016; Jasechko jt., 2017). Põhjaveett, mis moodustus minevikus valitsenu kliimas, mis erines oluliselt tänapäevasest kliimast, võib nimetada paleopõhjaveeks. Doktoritöös keskenduti liustikutekkelise paleopõhjavee uurimisele Balti Arteesiabasseini põhjaosas. Varasemad uuringud olid näidanud, et uuringuala sügavaimas Kambriumi-Vendi põhjaveekompleksis on laialt levinud põhjavesi, mis pärineb Pleistotseenis Eesti ala katnud mandriliustike sulavetest. Kuigi varasemad uuringud olid osutanud ka võimalusele, et taolist päritolu põhjavee levik Eesti alal ei piirdu vaid Kambriumi-Vendi põhjaveekompleksiga, ei olnud seda seni põhjalikumalt uuritud. Doktoritöös lähtuti eeldusest, et liustikutekkeline paleopõhjavesi on laialt levinud ka põhjaveekompleksides, mis lasuvad Kambriumi-Vendi põhjaveekompleksi katval Lükati-Lontova regionaalsel veepidemel. Töös keskenduti peamiselt Ordoviitsiumi-Kambriumi põhjaveekompleksi põhjaveele, aga uusi andmeid koguti ka Siluri-Ordoviitsiumi ja Alam-Kesk-Devoni põhjaveekompleksis esineva paleopõhjavee uurimiseks. Peamisteks töös püstitatud eesmärkideks oli: (1) uurida liustikutekkelise põhjavee ja teiste varasemates kliimatingimustes kujunenud põhjavee esinemist ja paiknemist Eesti aluspõhjas; (2) selgitada paleopõhjavee päritolu ning protsesse, mis on mõjutanud selle keemilise ja isotoopkoostise kujunemist; (3) uurida paleopõhjavee vanust ja (4) kasutada paleopõhjavee koostises salvestunud signaale viimasel jääajal ja selle eel Eesti alal valitsenu keskkonna- ja kliimatingimuste uurimiseks.

Dokoritöös ja sellega seotud artiklites uuriti Eesti põhjavett mitmekesise meetodikaga, et kirjeldada paleopõhjaveett ja selle koostist erinevatest vaatepunktidest. Töös püstitatud eesmärkide saavutamiseks uuriti põhjavee keemilist koostist, põhjavee ja selles lahustunud ainete isotoopkoostist ( $\delta^2\text{H}_{\text{H}_2\text{O}}$ ,  $\delta^{18}\text{O}_{\text{H}_2\text{O}}$ ,  $\delta^{13}\text{C}_{\text{DIC}}$ ,  $\delta^{34}\text{S}_{\text{SO}_4}$ ,  $\delta^{18}\text{O}_{\text{SO}_4}$ ,  $\delta^{13}\text{C}_{\text{CH}_4}$ ,  $\delta^{13}\text{C}_{\text{C}_2\text{H}_6}$ ), põhjavee vanust kirjeldavate radioaktiivsete isotoopide aktiivsust ( $^3\text{H}$ ,  $^{14}\text{C}$ ) ja põhjavees lahustunud gaaside sisaldust ( $\text{CH}_4$ ,  $\text{CO}_2$ ,  $\text{He}$ ,  $\text{Ne}$ ,  $\text{Ar}$ ,  $\text{Kr}$ ,  $\text{Xe}$ ). Andmete interpreteerimisel kasutati muuhulgas ka geokeemilise modelleerimise tarkvarasid GWB, PHREEQC ja NETPATH. Enamikku kirjeldatud meetoditest kasutati Ordoviitsiumi-Kambriumi, Siluri-Ordoviitsiumi, ja Alam-Kesk Devoni põhjaveekomplekside põhjavee uurimisel esmakordselt.

Töö tulemused kinnitasid liustikutekkelise paleopõhjavee laialdast levikut Kambriumi-Vendi põhjaveekompleksil lasuvates põhjaveekompleksides. See kajastub eelkõige põhjavee kerges isotoopkoostises. Kõigis kolmes eelpool nimetatud põhjaveekompleksis leidub kerge isotoopkoostisega vett, mille  $\delta^{18}\text{O}_{\text{H}_2\text{O}}$  väärtused on kuni  $\sim -20\%$  ja Ordoviitsiumi-Kambriumi põhjaveekompleksis kohati isegi kuni  $\sim -22,5\%$ . Need väärtused on oluliselt kergemad Eesti tänapäevaste sademete aasta keskmistest väärtustest ( $\delta^{18}\text{O}_{\text{H}_2\text{O}}$  vahemikus  $-10,1$  kuni  $-10,6\%$ ; Punning jt., 1997; IAEA/WMO, 2018) või selle infiltratsioonil kujunenud maapinnalähedastes põhjaveekihtides esinevatest väärtustest ( $\delta^{18}\text{O}_{\text{H}_2\text{O}}$  vahemikus  $-10,9$  kuni  $-12,7\%$ ). Isotoopkoostise erinevused on veenvaks tõendiks minevikus külmemates kliimatingimustes kujunenud põhjavee esinemisest Eesti aluspõhjas. Taolise kerge isotoopkoostisega vesi sai tõenäoliselt kujuneda vaid Pleistotseenis Eesti ala katnud mandriliustike sulavete infiltrerumisel aluspõhja settelistesse põhjaveekompleksidesse. Eriti lai on taolise liustikutekkelise

põhjavee levik Ordoviitsiumi-Kambriumi põhjaveekompleksis. Seal on tänapäevastele kliimatingimustele viitav signaal jälgitav vaid kitsal ribal veekompleksi põhjaosas, kus seda kattev karbonaatkivimite kompleks on õhuke või puudub hoopis. Paleopõhjavee lai levik Ordoviitsiumi-Kambriumi põhjaveekompleksis muudab selle palju sarnasemaks Kambriumi-Vendi põhjaveekompleksiga kui sellel lasuvate Siluri ja Ordoviitsiumi karbonaatkivimites esineva põhjaveega. Siluri-Ordoviitsiumi ja Alam-Kesk Devoni põhjaveekompleksides leidub paleopõhjaveet peamiselt nende põhjaveekomplekside tänapäevastest toitealadest (Haanja, Otepää, Sakala ja Pandivere kõrgustikud) kaugemal asuvatel aladel, põhjavee voolusüsteemi perifeersetes osades. Neis põhjaveekompleksides on paleopõhjavesi paremini säilinud Läänemere ja Liivi lahe saartel (nt. Sõrve poolsaar Saaremaal, Kihnu ja Ruhnu). Meri on sealjuures tõenäoliselt olnud jääajajärgsel ajal oluliseks paleopõhjavee säilimist soodustavaks teguriks.

Paleopõhjavee koostis on pärast selle infiltreerumist teinud läbi mitmeid olulisi muutusi. Peamiseks vete koostist mõjutanud protsessideks on olnud karbonaatsete mineraalide lahustumine, kationvahetus, orgaanilise aine oksüdatsioon ja segunemisprotsessid. Segunemine on toimunud liustikutekkelise paleopõhjavee, viimase jäätumise eelsetest kliimaperioodidest pärineva põhjavee, põhjaveekompleksides enne liustiku sulavete sissetungi olnud soolasema reliktsse põhjavee, tänapäeva sademetest pärineva põhjavee ja kohati ka merevee vahel. Paleopõhjavee dateerimine  $^3\text{H}$ ,  $^{14}\text{C}$  ja  $^4\text{He}$  meetoditega kinnitab, et tänapäevaste väärtustega võrreldes oluliselt kergema isotoopkoostisega vesi Ordoviitsiumi-Kambriumi põhjaveekompleksis on vähemalt 10000 aastat vana. Põhjavee modelleeritud vanused annavad alust kahtlustada, et vähemasti Ordoviitsiumi-Kambriumi põhjaveekompleksis leidub teatud ulatuses ka Hilis-Weichseli jäätumise eelsest ajast pärinevat põhjaveet. Paleopõhjavee keemilise ja isotoopkoostise võrdlus tänapäevaste põhjaveetasemetega viitab sellele, et need põhjaveed ei ole saavutanud tasakaalu pärast-jääaegsete põhjavee voolutingimustega ja nende koostises on endiselt esil Pleistotseenis väljakujunenud mustrid. See on kooskõlas varem Põhja-Ameerikas saadud modelleerimise tulemustega paleopõhjavee käitumisest aladel, kus jääajad ja jäävaheajad on Kvaternaari ajastul tsükliliselt vaheldunud.

Doktoritöö raames uuriti ka Kambriumi-Vendi põhjaveekompleksi paleopõhjavees lahustunud gaaside sisaldust ja päritolu. Seda põhjaveet iseloomustab erakordselt suur üleküllastus lahustunud gaaside suhtes (nt. 240% üleküllastus Ar suhtes). Valdav osa põhjavees lahustunud vääriskaasidest (Ar ja Kr) on atmosfäärset päritolu. Suur osa põhjaveekompleksis esinevast metaanist ei ole aga tekkinud põhjaveekompleksis endas, vaid on sinna sisse kantud koos infiltreerunud mandriliustike sulavetega. See on oluline tõend sellest, et Pleistotseeni mandriliustike ees paiknesid enne selle pealetungi bioloogiliselt aktiivsed alad, milles tekkinud orgaaniline aine mattus mandriliustiku alla. Lisaks sellele on suurte koguste bioloogilist päritolu metaani esinemine liustikutekkelistes põhjavetes viiteks selle kohta, et ka tänapäevaste suurte mandriliustike all Gröönimaal ja Antarktikas võib olla säilinud märkimisväärses kogustes orgaanilisi setteid, mis jää alt vabanedes võivad mõjutada tänapäevast süsinikuringet ja kliimat.

Liustikutekkelise paleopõhjavee lai levik Eesti aluspõhjas tähendab ka seda, et Eesti põhjavee kasutamist reguleerivad põhimõtted ja seadusandlus vajavad ülevaatamist. Paleopõhjavee lai levik viitab sellele, et aktiivse veevahetuse tsoonis paikneva põhjavee hulk, kust veevõttu kompenseerib tänapäevaste sademete infiltreerumine, võib olla palju väiksem kui varem arvatud. Eesti põhjaveekompleksid, kus paleopõhjavee esinemine on kindlaks tehtud, on tänapäeval olulisteks joogi- ja tarbevee allikateks. Suur

osa paleopõhjaveest on väikese soolsusega ja moodustab kvaliteetse põhjaveeressursi. Paleopõhjavee esinemine näitab, et veekompleksid või nende osad, kus selline vesi paikneb, on hästi kaitstud maapinnalt lähtuva reostuse eest. Oma olemuselt on aga tegemist vähemalt inimese eluea piires taastumatu loodusvaraga. Tulevikus tuleks seista hea selle eest, et seda kvaliteetset põhjaveeressursi majandataks vastutustundlikult ega toimuks selle tarbetut raiskamist (nt. kasutamine kastmisveena põllumajanduses, väljapumpamine kaevandustest jne.). Paleopõhjaveet tuleks ületarbimise eest kaitsta vastava seadusandlusega, mis Eestis praegu suuresti puudub. Mitmetes paleopõhjaveet sisaldavates kivimites esineb tuleviku perspektiivis ka potentsiaalselt olulisi maavarasid (nt. Kallavere kihistu biogeenne fosforiit Ordoviitsiumi-Kambriumi põhjaveekompleksis). Nende maavarade kaevandamise planeerimisel tuleb taastumatu paleopõhjavee levikuga kindlasti arvestada.

## Appendix

### Paper I

Raidla, Valle; Kern, Zoltan; Pärn, Joonas; Babre, Alise; Erg, Katrin; Ivask, Jüri; Kalvans, Andis, Kohán, Balázs; Lelgus, Mati; Martma, Tõnu; Mokrik, Robert; Popovs, Konrads; Vaikmäe, Rein (2016). A  $\delta^{18}\text{O}$  isoscape for the shallow groundwater in the Baltic Artesian Basin. *Journal of Hydrology*, 542, 254–267.





ELSEVIER

Contents lists available at ScienceDirect

## Journal of Hydrology

journal homepage: [www.elsevier.com/locate/jhydrol](http://www.elsevier.com/locate/jhydrol)

## Research papers

A  $\delta^{18}\text{O}$  isoscape for the shallow groundwater in the Baltic Artesian Basin

Valle Raidla<sup>a,g,\*</sup>, Zoltan Kern<sup>b</sup>, Joonas Pärn<sup>a</sup>, Alise Babre<sup>c</sup>, Katrin Erg<sup>d</sup>, Jüri Ivask<sup>a</sup>, Andis Kalvāns<sup>c</sup>, Balázs Kohán<sup>e</sup>, Mati Lelgus<sup>d</sup>, Tõnu Martma<sup>a</sup>, Robert Mokrik<sup>f</sup>, Konrāds Popovs<sup>c</sup>, Rein Vaikmäe<sup>a</sup>

<sup>a</sup>Institute of Geology at Tallinn University of Technology, Ehitajate tee 5, 19086 Tallinn, Estonia

<sup>b</sup>Institute for Geological and Geochemical Research, Research Centre for Astronomy and Earth Sciences, MTA, Budaörsi út 45., H-1112 Budapest, Hungary

<sup>c</sup>University of Latvia, 19 Raina Blvd., LV 1580 Riga, Latvia

<sup>d</sup>Geology Survey of Estonia, Kadaka tee 60/62, Tallinn, Estonia

<sup>e</sup>Department of Environmental and Landscape Geography, Eötvös Loránd University, 1/c Pázmány Péter sétány, H-1117 Budapest, Hungary

<sup>f</sup>Vilnius University, M.K. Čiurlionio str. 21/27, LT-03101 Vilnius, Lithuania

<sup>g</sup>Institute of Environmental Physics, University of Heidelberg, Neuenheimer Feld 229, Heidelberg, Germany

## ARTICLE INFO

## Article history:

Received 18 January 2016

Received in revised form 14 July 2016

Accepted 2 September 2016

Available online 8 September 2016

This manuscript was handled by A.

Bardossy, Editor-in-Chief, with the assistance of Dongmei Han, Associate Editor

## Keywords:

Shallow groundwater

Precipitation

Stable isotopes

Isoscape

The Baltic region

## ABSTRACT

The study presents a shallow groundwater isoscape for the Baltic region, which covers the major part of the Baltic Artesian Basin (BAB). BAB is an important palaeogroundwater reservoir, but prior to this study, little has been known about the spatial variability of  $\delta\text{D}$  and  $\delta^{18}\text{O}$  values in modern precipitation input across the region. To overcome this limitation, we hypothesized that the isotopic composition of shallow groundwater in the BAB could be used as a proxy for the mean weighted annual isotopic composition of local precipitation. However, the results of the study reveal many clear discrepancies between the isotopic composition of precipitation and shallow groundwater in the area. The isotopic composition of shallow groundwater is mostly biased towards isotopically depleted wintertime precipitation. We propose that the formation of shallow groundwater in the BAB area could be largely affected by variations in soil structure and land cover. The derived isoscape based on  $\delta^{18}\text{O}$  values of shallow groundwater in the BAB area is characterised by high spatial resolution and can therefore serve as a fairly reliable reference basis for further hydrogeological, ecological and forensic applications.

© 2016 Elsevier B.V. All rights reserved.

## 1. Introduction

Stable isotopes of oxygen and hydrogen are excellent tracers for studying the physical processes of the global hydrologic cycle. The spatial distribution of isotopic signals in precipitation is modified by several factors, such as latitude, altitude, continentality and the predominant moisture sources in the region (e.g., Dansgaard, 1964; Clark and Fritz, 1997). When studying water reservoirs, it is critical to describe the stable isotopic composition of modern precipitation, because it serves as an input signal to the isotopic composition of surface water bodies and aquifers. The network monitoring the isotopic composition of precipitation over space and time (Global Network of Isotopes in Precipitation or GNIP) covers the Earth unevenly (IAEA/WMO, 2015). The Baltic countries serve as an example of a region, where historically only one GNIP station (Riga) provided data for an area of over 175,000 km<sup>2</sup>, although a few other nearby stations (e.g., St. Petersburg, Russia; Espoo, Finland) also attributed to the local data. Now, the region

has two active GNIP stations established in 2013 and located in Estonia (Vilsandi and Tartu), but their sampling period is not long enough yet for a long-term description on the mean isotopic composition of precipitation in the area. Interpolation models need to be developed (e.g., Bowen and Revenaugh, 2003; Terzer et al., 2013; Kern et al., 2014), to establish a spatially contiguous reference database for the isotopic composition of precipitation in a specific location. Isoscapes based on isotopic composition of shallow groundwater offer a good alternative for amending and supplementing precipitation data in regions, where the spatial distribution of stations measuring the isotopic composition of precipitation is insufficient (e.g., Darling et al., 2003; Kortelainen and Karhu, 2004; Wassenaar et al., 2009; West et al., 2014; Pacheco and Van der Weijden, 2014).

The isoscape method is based on an assumption that the isotopic composition of shallow groundwater closely reflects the isotopic composition of the amount-weighted long-term mean of precipitation (e.g., Rozanski, 1985; Ingraham and Taylor, 1991). At the same time, some authors (e.g., Deines et al., 1990; Aquilina et al., 2006; Jasechko et al., 2014) show that annual variations of  $\delta^{18}\text{O}$  and  $\delta\text{D}$  values in groundwater also depend on the

\* Corresponding author.

E-mail address: [valle.raidla@ttu.ee](mailto:valle.raidla@ttu.ee) (V. Raidla).

heterogeneous characteristics of recharge areas. In the recharge areas studied thus far, spatial variability of the isotopic input signal is influenced by variations in precipitation type (rain or snow), vegetation cover, rock type and soil depth (e.g., O'Driscoll et al., 2005; Song et al., 2009; Gleeson et al., 2009).

It is very important for a region to have a well-supported isoscape, as it allows to develop a deeper understanding of the regional hydrological processes such as seasonal infiltration bias, precipitation/evapotranspiration ratios, or catchment hydrology (Bowen et al., 2011; Bowen and Good, 2015). Over the years, isotopic composition of groundwater in the Baltic Artesian Basin (BAB) has been intensively studied, but most of the research has focused on the palaeogroundwaters found in the basin (e.g., Vaikmäe et al., 2001; Mokrik et al., 2009; Raidla et al., 2009, 2012, 2014). The isotopic composition of surface waters and shallow groundwater in the BAB area has been poorly researched. Only a few studies have concentrated on shallow, modern groundwaters and their relations with precipitation (Punning et al., 1987; Mažeika et al., 2013; Mokrik et al., 2014; Skuratovič et al., 2015). The present study focuses on the isotopic composition of shallow groundwater in the BAB area, in the topmost layer of the saturated zone, reaching the depth of 70 m. The aims of the study are to clarify how well the isotopic composition of shallow groundwater reflects the isotopic composition of modern precipitation and to reveal how the seasonality of recharge and the characteristics of recharge areas (e.g., location and geological setting) influence the isotopic composition of shallow groundwater in the BAB area.

## 2. Site description

The BAB underlies the Baltic Sea and its eastern coast between the 50° and 60° northern latitudes. The basin covers the territories of Estonia, Latvia, Lithuania and parts of Russia, Poland, Sweden (Island of Gotland) and Belarus (Fig. 1). The study area is situated in a transitional zone between areas of maritime climate in north-western Europe and areas of continental climate in northeastern Europe. According to the Köppen–Geiger climate classification, BAB belongs to the Dfb zone (Kotttek et al., 2006). The climate is humid and moderately cool with an annual mean temperature

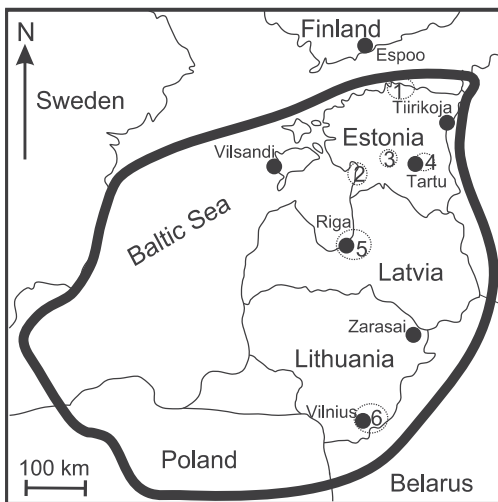


Fig. 1. The location of the Baltic Artesian Basin with the positions of the GNIP stations and vertical profiles of groundwater (see Table 1).

varying from 5 to 8 °C. The amount of mean annual precipitation ranges from 500 to 750 mm with lower values in the coastal areas and ca. 10–20% higher values in the uplands. The precipitation derives mainly from a sole vapour source in the North Atlantic Ocean (Alalampi, 1987). In early winter, evaporation from the Baltic Sea serves as an additional source of humidity that causes more precipitation in coastal areas (Remm et al., 2011).

BAB is a complex multi-layered hydrogeological system in the Neoproterozoic and Phanerozoic sedimentary rocks. The thickness of the sedimentary cover reaches up to 5000 m in the southwestern part, while the crystalline basement outcrops in northern and southeastern regions of the BAB (Fig. 2). Carbonate rocks prevail in northern and central parts of the basin's outcrop area, sandstones are present in its central and southern parts, while clays and claystones are less common (Nikishin et al., 1996).

The topography of the region is slightly dissected and mostly characterised by low altitudes without considerable natural barriers affecting air mass movement. The average absolute elevation of the area is about 50 m a.s.l., the maximum reaching 316 m a.s.l. The northern and central parts of the basin belong to the glacial erosion zone or to that of moderate accumulation, which is why the Quaternary cover is rather thin in those areas (usually less than 5 m, or, in some places lacking altogether). The thickness of Quaternary deposits increases generally towards the south and is at its thickest in the uplands (often more than 100 m) and also in the ancient buried valleys (up to 200–300 m) (Raukas and Kajak, 1997; Satkunus et al., 2009).

The annual infiltration rate of precipitation in the BAB has been estimated to vary from 2 to 50% (Vallner, 1997; Levins et al., 1998), depending on the permeability of the prevalent deposits in the area. The low-permeability glacial till and limnoglacial sediments form a significant portion of the topmost part of the Quaternary sediment cover in the basin. The areas with prevailing sandy deposits of late glacial origin are equally significant (Grigelis, 1978). Additionally, thin and in most parts highly permeable Quaternary cover has led to the development of karst in the carbonate rocks and gypsum in northern and central Baltic, respectively. Surface karst forms consist of pits, wells, kettles and sinkholes. Unevenly distributed underground forms include fissures, channels and cavities of various shape and size (Kink, 1997; Taminskas and Marcinkevicius, 2002).

The groundwater flows into the basin mainly from SE to NW, but this trend predominates only below the regional aquitards. Groundwater flow in local and intermediate flow systems in the shallow and intermediate depths is directed from recharge areas in the uplands towards discharge areas in river valleys, lake depressions and the Baltic Sea as indicated by groundwater piezometric levels (Fig. 2). In most shallow aquifers,  $\delta^{18}\text{O}$  values are close to those of the isotopic composition of the weighted mean annual values of local precipitation (around  $-10\text{‰}$ ). In deeper central and southern parts of the basin, groundwater salinity increases significantly (Raidla et al., 2009) and  $\delta^{18}\text{O}$  values range from  $-3.5$  to  $-12.6\text{‰}$  (Mokrik, 1997). In the shallower northern part of the BAB, the situation is reverse. Here, oxygen isotope values are depleted with respect to modern precipitation and have values as negative as  $-23\text{‰}$ . Such extremely negative  $\delta^{18}\text{O}$  values have been detected in relatively shallow depths, from 50 to 300 m (Vaikmäe et al., 2001; Raidla et al., 2009; Pärn et al., 2016). To explain this phenomenon, earlier studies have proposed that groundwater in these aquifer systems has originated from meltwater of the Scandinavian Ice Sheet covering the area during the Late Weichselian glaciation (e.g., Punning et al., 1987; Vaikmäe et al., 2001). In the central parts of the BAB, the  $\delta^{18}\text{O}$  values of groundwater are also depleted with respect to modern precipitation in depths of 125–200 m, with the most negative  $\delta^{18}\text{O}$  of  $-13.4\text{‰}$  (Mokrik, 2003; Babre et al., 2016).

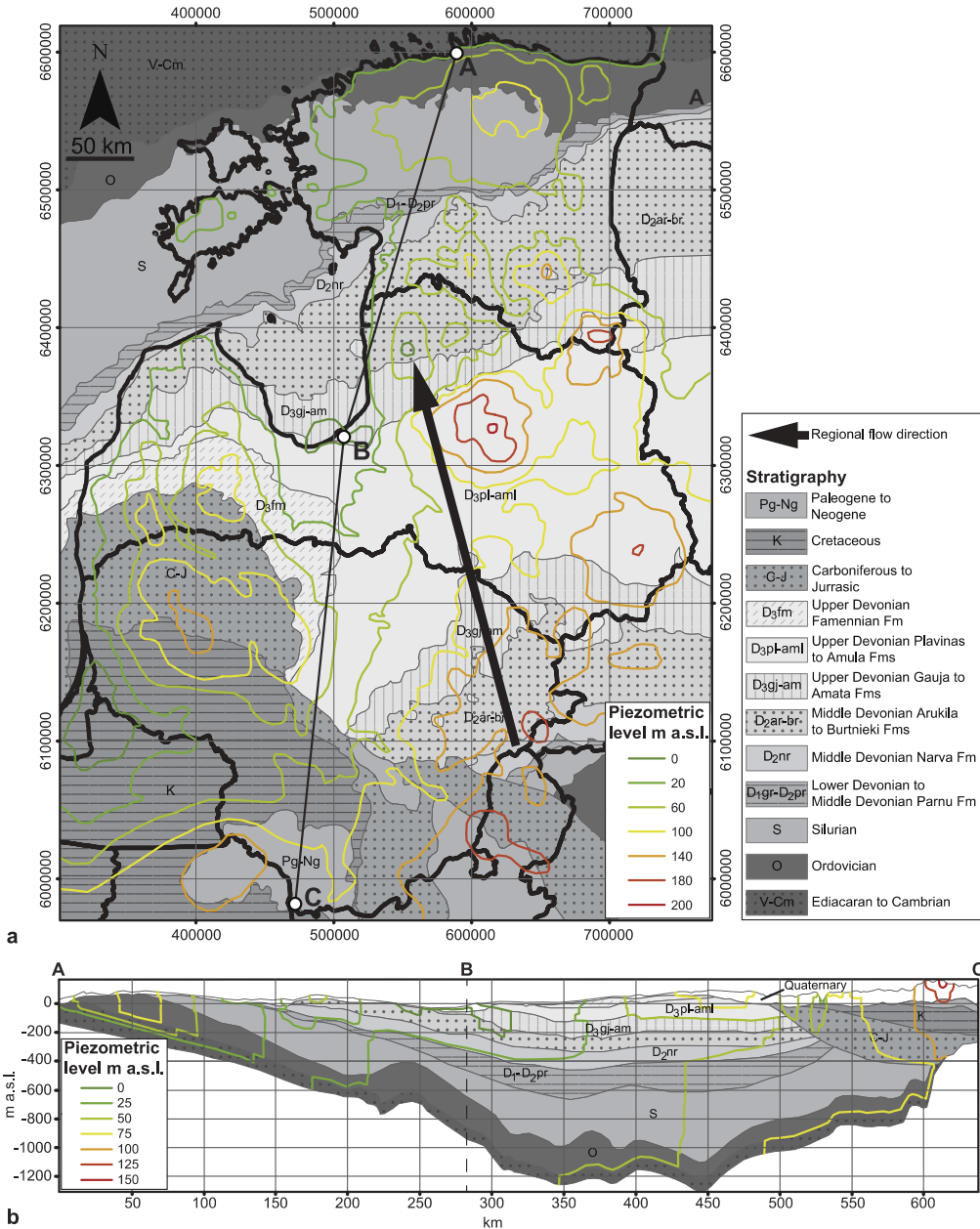


Fig. 2. Geological map (a) and geological cross-section of the study region (b), generated from the geological–hydrogeological model of the BAB. Coordinates given in TM Baltic 93 coordinate system. The black arrow marks the regional groundwater flow direction.

The main recharge period of shallow groundwater in temperate climates occurs usually in spring when, in addition to snowmelt, rainfall enhances surface runoff and increases groundwater recharge. In summer, the effect of the well-developed vegetation cover combined with higher temperatures increases evapotranspiration, which in turn lowers the level of groundwater table. Water

usually reaches its minimum depth at the end of summer. In autumn, groundwater levels tend to rise again because of more frequent rain events and decreased evapotranspiration. Due to low temperatures and frozen ground surface in winter, groundwater levels decline once more, reaching their minimum at the end of winter (Tolstovs et al., 1986). The water table in the region rises

approximately 0.7 m in spring and lowers about 1.8 m in summer (Vallner, 1997; Vitola et al., 2012; Skuratović et al., 2015). In the areas affected by karst phenomena, the depth of the water table can fluctuate annually from 4 to 6 m. Such relatively large fluctuations are caused by karst cavities in the carbonate bedrock, which collect a significant amount of water in spring, discharging it to streams in summer (Vallner, 1997; Taminskas and Marcinkevicius, 2002).

### 3. Material and methods

#### 3.1. Sampling

The study was based on 131 groundwater samples collected from wells and springs from Estonia, Latvia and Lithuania. Researchers from the Estonian Geological Survey, Tallinn University of Technology, University of Latvia and Vilnius University collected the samples from 2010 to 2014. In order to improve the spatial coverage of the study area in both vertically and laterally, the dataset was complemented by the results from earlier studies and by unpublished data from the period of 1996–2009 ( $n = 25$ ).

The majority of sampling sites were springs or consumption wells opened in aquifers belonging to part of local and intermediate flow systems and located above the regional aquitards, but some dug wells were also included. Groundwater from dug wells and springs was sampled with a clean plastic bucket. When sampling the drilled wells, water was directed into a clean bucket whence the sample was subsequently taken. In order to obtain a representative sample, wells were flushed until the field parameters of sampled water (oxygen concentration and electric conductivity) became stable. Then, the unfiltered samples for isotope analyses were poured into 15 mL HDPE bottles and stored in cold and dark.

#### 3.2. Chemical and stable isotope analysis

$\text{Cl}^-$  concentrations from Estonian and Lithuanian groundwaters were measured using Dionex ICS-1000 ion chromatograph at Tallinn University of Technology (TUT). Stable isotope ratios of hydrogen and oxygen in water were analysed in the Institute of Geology at TUT. For samples collected in 2010, both isotope ratios of hydrogen and oxygen were measured using the cavity ring-down laser spectroscopy (CRDS) method with a Picarro L2120-i Isotopic Water Analyzer (Brand et al., 2009). Hydrogen and oxygen isotope ratios were expressed in permil (‰) relative to Vienna Standard Mean Ocean Water (VSMOW) (Coplen, 1994). Reproducibility of stable isotope measurements was  $\pm 0.1\text{‰}$  for  $\delta^{18}\text{O}$  and  $\pm 1\text{‰}$  for  $\delta\text{D}$ , respectively.

To eliminate samples that had been influenced by evaporation, all samples were evaluated using their deuterium excess ( $d_{\text{excess}}$ ) value defined as (Dansgaard, 1964):

$$d_{\text{excess}} = \delta\text{D} - 8\delta^{18}\text{O} \quad (1)$$

An analogous study in Finland showed that the  $d_{\text{excess}}$  values in shallow groundwater fall in the range of 8.1–12‰ (Kortelainen and Karhu, 2004). We interpreted  $d_{\text{excess}}$  values under 8‰ as being influenced by evaporation and omitted these samples from the dataset.

For precipitation data, the study used the IAEA/WMO GNIP database (IAEA/WMO, 2015). A considerable amount of data on stable isotopic composition of precipitation was collected in Riga (1980–1983), and in Espoo (2000–2005). We also used the precipitation data published by Punning et al. (1987) from Tiirikoja station in Estonia and by Mažeika et al. (2013) from Eastern Lithuania (from Zarasai and Vilnius) (Fig. 1).

#### 3.3. Identification of the critical depth of groundwater with no seasonal variations in its isotopic composition

For our study, it was critical to find the depth, where annual variations in the isotopic composition would not exceed the analytical precision of  $\delta^{18}\text{O}$  measurements, often taken as the depth, where fluctuations reach 1‰ of surface  $\delta^{18}\text{O}$  value (e.g., Sellers, 1972; Clark and Fritz, 1997). The attenuation effect depends on climate and surface structure and can be found from 0.3 to 9 m from the ground surface (Eichinger et al., 1984; Darling and Bath, 1988; Deines et al., 1990; Wenner et al., 1991; Rank et al., 1992; DeWalle et al., 1997; O'Driscoll et al., 2005). Since similar research in the BAB area is lacking, we conservatively presumed that in their isotopic composition groundwater samples from the topmost 10 m of the surface layer had been influenced by the seasonal fluctuations. Still, we have used the data from three shallow wells in the areas where data from deeper wells or springs was lacking.

Table 1 and Fig. 3 show that  $\delta^{18}\text{O}$  values are rather stable within the depth of 10–70 m. In the northern part of the BAB, water of glacial origin ( $\delta^{18}\text{O}$  less than  $-18\text{‰}$ ) has been detected even below 70 m (Vaikmäe et al., 2001; Raidla et al., 2009, 2012; Pärn et al., 2016). However, the area where waters with a more negative isotopic composition reside is well researched and all the sampled wells included in the study represent modern groundwater. Therefore, it is unlikely that the studied samples contain any groundwater from the last glacial period.

However, this approach is not applicable in the Riga area, where isotopic composition throughout the hydrogeological units varies considerably (Fig. 3). Groundwater discharges into the Gulf of Riga from both the eastern lowlands and the western uplands (Fig. 2), and sometimes even from the vertical direction (Levins et al., 1998; Virbulis et al., 2013; Babre et al., 2016), which is why waters with long residence times could easily get mixed with waters having shorter residence times. Therefore, in the Riga area, we only used wells with their screens located at depths between 10 and 30 m.

#### 3.4. Isoscape derivation

Due to low altitudes in the BAB domain, the elevation-induced precipitation and any accompanied isotopic fractionation (the so-called altitude effect) are not expected to play a significant role in influencing the isotopic composition of precipitation and the related groundwater. Hence, latitude (LAT) and longitude (LON) expressed in the local TM Baltic 93 projection system were entered into the initial bilinear model as potential explanatory variables to account for the sequential rain-out events and the accompanied isotopic fractionation (the so-called continentality effect) during the time marine moisture travels inland.

The bilinear regression equation can be written in a general form

$$\delta^{18}\text{O}_{\text{model}} = b_0 + b_1\text{LAT} + b_2\text{LON} \quad (2)$$

where  $\delta^{18}\text{O}_{\text{model}}$  is the predicted dependent variable,  $b_0$  is the constant;  $b_1$  and  $b_2$  are partial regression coefficients (Brown, 1998). The  $t$ -tests were used for both coefficients to estimate whether the value of the coefficient was zero and if its  $p$ -value was less than 0.05. In that case, the calculated value was considered as statistically significant. Similarly, the  $F$ -statistic was used to test whether the values of the coefficients for the entire equation were equal to zero. If the  $p$ -value for the  $F$ -statistic was less than 0.05, the equation was statistically significant (e.g., Lachniet and Patterson, 2006). An initial grid with  $1 \times 1$  km resolution using the best-fit regression coefficients has been computed for the study area.

**Table 1**  
The isotopic data and Cl<sup>-</sup> composition in six sites in the BAB. The location of the sites is shown in Fig. 1. The  $\delta^{18}\text{O}$  values used in the preparation of the isoscape map are marked in bold. 1 - Pärn et al. (2016); 2 - Raidla et al. (2009); 3 - Raidla et al. (2014); 4 - Raidla et al. (2012); 5 - Savitskaja et al. (1996a); 6 - Vaikmäe et al. (2001); 7 - Savitskaja et al. (1996b); 8 - Savitskaja et al. (1995); 9 - Babre et al. (2016); 10 - Mokrik et al. (2009); 11 - Mokrik et al. (2014).

Region	Well ID	Well location	Sampling date	Coordinates		Well screen		$\delta^{18}\text{O}$ ‰	$\delta\text{D}$	Cl <sup>-</sup> mg L <sup>-1</sup>
				Long E (°)	Lat N	Upper m	Lower			
1		Palmse village	31-Aug-14	25.9567	59.5250	1	3	-12.5	-89.9	3.7
		Valgejõe village	21-Aug-13	25.7890	59.4675	5	20	-11.9	-84.7	9.9
		Kolgaküla village <sup>1</sup>	27-Aug-13	25.6915	59.5178	10	34	<b>-12.0</b>	-84.8	17.0
	22,386	Sõitme village <sup>1</sup>	7-Aug-14	25.4732	59.4669	21	36	<b>-11.7</b>	-84.0	4.8
	2509	Altja village <sup>2</sup>	29-Aug-02	26.1312	59.5832	57	76	-12.0		4.7
	4642	Tammispea village <sup>2</sup>	28-Aug-02	25.8295	59.5529	106	130	-12.2		6.6
	743	Kolga village <sup>2</sup>	19-Apr-05	25.6156	59.4885	107	150	-12.1		6.7
	680	Loksa city	27-Aug-13	25.7296	59.5866	106	145	-11.8	-84.1	11.7
	745	Kolga village	25-Sep-07	25.6120	59.4932	143	192	-12.0		6.4
	2775	Kunda city <sup>3</sup>	29-Nov-11	26.5046	59.5062	148	205	-21.4		316.0
	1096	Kehra city <sup>4</sup>	26-Nov-09	25.3301	59.3331	158	230	-20.7		421.7
2		Zabli village	3-Aug-14	24.4502	58.0189	3	7	-11.4	-81.9	4.1
	6578	Krundiküla village	20-Oct-14	24.7425	58.0311	26	37	<b>-11.5</b>	-81.4	12.0
	6687	Uulu village	11-Mar-03	24.5778	58.2872	39	55	<b>-11.5</b>		
	4299	Pärnu city	20-Oct-14	24.4703	58.3587	35	56	<b>-11.3</b>	-82.6	
	5057	Pärnu city <sup>5</sup>	6-Jun-96	24.6584	58.3328	46	80	-11.8		29.1
	13,688	Munalaiu port	11-Mar-03	24.1193	58.2349	46	80	-12.5		110.0
	7620	Võidu village	11-Mar-03	24.5608	58.1360	74	90	-13.2		110.0
3		Õnniste village	30-Jul-14	25.6418	58.5063	2	10	-12.3	-88.0	4.0
		Maimu spring	2-Aug-14	25.4846	58.1334			<b>-11.3</b>	-81.5	6.9
		Sinialliku spring	2-Aug-14	25.5606	58.3025			<b>-11.2</b>	-80.6	9.1
	7241	Viljandi city <sup>6</sup>	26-Sep-97	25.5977	58.3686	46	65	<b>-11.2</b>		
	7241	Viljandi city <sup>7</sup>	4-Jun-96	25.5977	58.3686	46	65	<b>-11.3</b>		52.8
	7213	Viljandi city <sup>7</sup>	4-Jun-96	25.5738	58.3743	113	190	-11.5		9.2
	7239	Viljandi city <sup>7</sup>	4-Jun-96	25.5774	58.3547	114	200	-11.3		16.3
	7239	Viljandi city <sup>6</sup>	26-Sep-97	25.5774	58.3547	114	200	-11.0		
7298	Viljandi city <sup>8</sup>	21-Jun-95	25.5760	58.3543	418	480	-15.6		473.8	
4		Vasula village	1-Aug-14	26.7348	58.4619	10	30	<b>-11.6</b>	-83.4	4.8
	4400	Tartu city	2-Oct-14	25.9225	58.3509	44	70	<b>-11.8</b>	-84.6	3.2
	2005	Tartu city <sup>7</sup>	3-Jun-96	26.7829	58.3710	42	80	-11.9		14.5
	1297	Tartu city	2-Oct-14	26.7730	58.3510	105	136	-12.3	-88.8	8.0
	1286	Tartu city <sup>7</sup>	3-Jun-96	26.7829	58.3710	115	132	-15.7		25.5
	1291	Tartu city <sup>7</sup>	3-Jun-96	26.7790	58.3604	138	220	-12.4		12.8
	1241	Tartu city <sup>7</sup>	3-Jun-96	26.6849	58.3540	168	220	-11.5		9.2
	1224	Tartu city	2-Oct-14	26.7732	58.3511	342	397	-14.3	-106.3	331.5
	1222	Tartu city <sup>8</sup>	21-Jun-95	26.7826	58.3710	359	406	-15.1		336.1
5	4	Piukas <sup>9</sup>	14-Nov-10	24.4591	57.0774	8	11	-11.1	-80.4	
	53,447	Jaunkemeri <sup>9</sup>	17-Sep-10	23.5606	56.9678	4	14	-10.0		
	13,754	Dole <sup>9</sup>	02-Sep-11	24.1546	56.8911	9	15	-11.3	-80.1	17.7
	1600	Tīrelī <sup>9</sup>	01-Sep-10	23.8010	56.8809	9	20	-9.6	-70.5	
	1484	Kalngale <sup>9</sup>	14-Sep-10	24.1738	57.0852	12	18	<b>-11.5</b>	-80.1	10.7
	3077	Zakumuiža <sup>9</sup>	02-Nov-10	24.4053	57.0213	22	27	<b>-11.1</b>	-79.7	7.3
	693	Jaundubulti <sup>9</sup>	14-Oct-10	23.7516	56.9586	25	29	<b>-11.4</b>	-80.4	25.3
	1243	Baltezers <sup>9</sup>	07-Oct-10	24.3198	57.0239	25	32	-9.8	-72.2	38.6
	1599	Tīrelī <sup>9</sup>	01-Oct-10	23.8010	56.8809	24	33	-10.1	-70.5	10.0
	1	Piukas <sup>9</sup>	14-Nov-10	24.4592	57.0775	36	43	-10.6	-77.4	
	3076	Zakumuiža <sup>9</sup>	02-Nov-10	24.4054	57.0213	48	50	-10.7	-77.5	8.7
	685	Imanta <sup>9</sup>	21-Nov-10	24.0375	56.9622	40	51	-10.9	-80.0	19.0
	1483	Kalngale <sup>9</sup>	14-Oct-10	24.1738	57.0851	50	60	-11.0	-77.7	8.0
	3075	Zakumuiža <sup>9</sup>	02-Nov-10	24.4054	57.0213	65	70	-10.8	-78.1	18.0
		Marupe <sup>10</sup>	15-Aug-86			71		-11.5		
683	Imanta <sup>9</sup>	21-Nov-10	24.0375	56.9623	68	89	-11.2	-81.4	21.0	
24,579	Rīga city <sup>9</sup>	07-Nov-10	23.9829	57.0167	82	90	-12.3	-90.2		
	Rīga city <sup>10</sup>	15-Aug-86			125		-13.1			
6	28,809	Vilnius city <sup>11</sup>	16-Jun-09	25.2379	54.6660	19	24	<b>-10.9</b>		60.1
	28,814	Vilnius city <sup>11</sup>	16-Jun-09	25.2363	54.6677	23	31	<b>-10.6</b>		
	196	Salininkai	15-Aug-14	25.2634	54.6012	43	50	<b>-10.7</b>	-76.3	17.6
	28,811	Vilnius city <sup>11</sup>	16-Jun-09	25.2357	54.6668	46	51	<b>-11.0</b>		51.9
	28,813	Vilnius city <sup>11</sup>	6-Oct-09	25.4342	54.6668	47	58	<b>-11.1</b>		
	4023	Vilnius city <sup>11</sup>	6-Oct-09	25.4541	54.6667	63	70	<b>-11.1</b>		
	198	Salininkai	15-Aug-14	25.2634	54.6012	142	150	-10.8	-76.4	

Values from the initial grids were subtracted from the corresponding raw data. Variogram analysis was carried out on  $\delta^{18}\text{O}$  data of the residual shallow groundwater to determine the characteristic spatial dependence structure. Variograms can be measured in many directions with a tolerance angle to characterise geometric

anisotropy and zonal anisotropy of the spatial variability (Pyrz and Deutsch, 2014). Variograms were constructed using the VBA-based script (Kohán and Szalai, 2014) for Surfer 13. Maximum lag distance was set to 220 km and the number of lags to 11. Empirical semivariograms were calculated by the Matheron algorithm

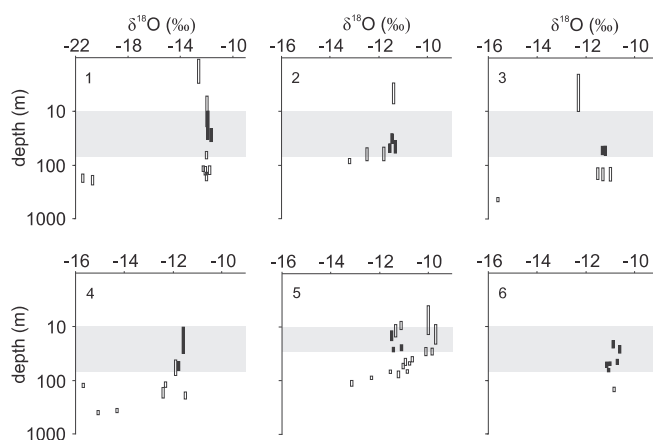


Fig. 3. The isotopic data profiles at six sites in the BAB. The rectangular mark shows the location of a well screen. The wells used in compiling the isoscape map are marked in black. The location of the sites is shown in Fig. 1. Data from Table 1 have been used to prepare the figure.

(Matheron, 1965) and semivariogram's surface was generated from directional empirical semivariograms. Directional semivariograms were extracted along the major perpendicular axis (SE–NW and NE–SW) with 45° tolerance to characterise the structure of the anisotropy and to define the range. Spherical models (theoretical semivariogram) were fitted to the empirical semivariograms to derive weighting function for kriging of the residual  $\delta^{18}\text{O}$  data. Residuals were interpolated to the same grid ( $1 \times 1$  km) using ordinary kriging (Cressie, 1993). At the final step, corresponding initial and residual grids were summed.

## 4. Results

### 4.1. Isotopes

The stable isotopic data of groundwater in the BAB region can be found in Table 2. The measured  $\delta^{18}\text{O}$  values varied from  $-9.9$  to  $-12.7\text{‰}$  and  $\delta\text{D}$  values from  $-69.8$  to  $-90.6\text{‰}$ . More depleted values were observed in the northern part and less depleted in the southern part of the BAB, respectively. The isotopic ratios of oxygen and hydrogen were highly correlated and yielded the following regression line (Fig. 4):

$$\delta\text{D} = 7.6 \delta^{18}\text{O} + 4.9 \quad (3)$$

( $n = 127$ ,  $R^2 = 0.93$ )

Strong linear relation between  $\delta\text{D}$  and  $\delta^{18}\text{O}$  values in precipitation and the mean annual temperature is well known (Dansgaard, 1964). Our data also showed the similar correspondence between isotopic composition of shallow groundwater and local air temperatures (Fig. 5).

### 4.2. $\delta^{18}\text{O}$ isoscape of shallow groundwater in the BAB

#### 4.2.1. A preliminary model based on geographical predictors

Based on the  $\delta^{18}\text{O}$  data from groundwaters and springs, an initial linear model of  $\delta^{18}\text{O}$  distribution was created. Relying upon the best-fit linear relationship between mean annual  $\delta^{18}\text{O}$  values of groundwater and the location of the sampling points, the following equation (based on Eq. (2)) was used to describe the spatial variation of  $\delta^{18}\text{O}$  values in the BAB area:

$$\delta^{18}\text{O}_{\text{model}} = 6.73484 - 0.00000223 \cdot X - 0.0000026304 \cdot Y \quad (4)$$

where

$$\begin{aligned} X &= \text{latitude in TM Baltic 93 system} \\ Y &= \text{longitude in TM Baltic 93 system} \end{aligned}$$

Using the linear model of  $\delta^{18}\text{O}$  distribution over the study area, residual  $\delta^{18}\text{O}$  values were calculated in the sampling points:

$$\delta^{18}\text{O}_{\text{residual}} = \delta^{18}\text{O}_{\text{measured}} - \delta^{18}\text{O}_{\text{model}} \quad (5)$$

#### 4.2.2. Variography of the residual $\delta^{18}\text{O}$ in groundwater

Variogram surface indicated a complex anisotropic structure with a well-defined zone of diminished variance trending along the ENE–WSW direction (Fig. 6). Directional variograms generally reflected a smaller variance along the SE–NW and a larger variance along the NE–SW line, indicative of a zonal anisotropy component. A weak first sill was discernible at  $\sim 40$  km (more pronounced in the SE–NW direction). Directional variograms indicated a second sill, which robustly existed in all directions on the variogram surface (Fig. 6), presenting a shorter range ( $\sim 75$  km) to the SE–NW and a slightly longer range ( $\sim 90$  km) to the NE–SW directions. Thus, the theoretical model was fitted to the second sill and the revealed anisotropic interdependence structure of the  $\delta^{18}\text{O}$  values in groundwater from the BAB was taken into account in the subsequent geospatial modelling.

#### 4.2.3. The final model

The final  $\delta^{18}\text{O}$  isoscape of shallow groundwater in the BAB has been derived by adding the gridded data at each corresponding point from the preliminary linear model and the geospatial modelling of the residuals. The map is presented in Fig. 7a. Almost in the entire study area, the standard deviation of the  $\delta^{18}\text{O}$  values was between 0.18 and 0.28‰ (Fig. 7c), which is close to the measurement accuracy of the  $\delta^{18}\text{O}$  analysis. It suggests that the isoscape map is fairly accurate and can serve as a basis for further applications. Due to low data density, the standard deviation is the highest in the southern parts of the BAB, which is why the isoscape map (Fig. 7c) is less accurate there. Kortelainen and Karhu (2004) conducted a similar long-term regional study on isotopic composition in surface waters and in shallow groundwater in Finland, north of the BAB area. Despite the different methods of sample collection, our extrapolated isoscape map matches well their

**Table 2**  
The isotopic composition of shallow groundwater in the BAB. 1 - Savitskaja et al. (1997); 2 - Pärn et al. (2016); 3 - Savitskaja et al. (1998); 4 - Vaikmäe et al. (2001); 5 - Savitskaja et al. (1996b); 6 - Babre et al. (2016); 7 - Mokrik et al. (2009); 8 - Zuzevičius et al. (2007); 9 - Mokrik et al. (2014).

No	Well ID	Location	Date	Coordinates				Well screen		$\delta^{18}\text{O}$	$\delta\text{D}$	$d_{\text{excess}}$	$\delta^{18}\text{O}_{\text{residual}}$
				Long E (°)	Lat N	TM Baltic X	TM Baltic Y	Upper m	Lower m				
<i>Estonian wells</i>													
1	9181	Hullo village <sup>1</sup>	2-Jul-97	23.2431	58.9912	456,487	6,539,375	10	13	-11.7			-0.22
2	8791	Kärda town <sup>1</sup>	1-Jul-97	22.7462	59.0015	427,946	6,540,961	11	20	-11.7			-0.28
3	12,521	Kärda village	29-Sep-14	22.2518	58.3220	397,570	6,465,929	23	40	-11.2	-78.9	10.9	-0.06
4	13,766	Roosta village	7-Oct-14	23.5217	59.1561	472,634	6,557,597	11	30	-11.7	-82.2	11.3	-0.12
5	11,596	Roobuka village <sup>1</sup>	17-Jun-97	24.6749	59.2243	538,535	6,565,295	11	36	-11.6			0.14
6	278	Tallinn city	26-Aug-13	24.5855	59.4396	533,222	6,589,234	30	35	-11.7	-83.6	9.9	0.10
7	1194	Vasalemma village <sup>1</sup>	11-Jun-97	24.2501	59.2316	514,277	6,565,936	34	69	-11.8			-0.12
8	50,476	Peeteristi village <sup>2</sup>	2-Sep-14	28.0696	59.4036	731,020	6,592,087	17	35	-11.8	-85.4	9.2	0.41
9	22,386	Sõitme village <sup>2</sup>	7-Aug-14	25.4726	59.4662	583,486	6,592,969	21	36	-11.7	-84.0	9.4	0.24
10	1037	Koigaküla village <sup>2</sup>	27-Aug-13	25.6907	59.5171	595,709	6,598,925	10	34	-12.0	-84.8	10.9	-0.01
11	20,265	Aegviidu village	10-Aug-14	25.6104	59.2843	591,784	6,572,885	18	23	-12.0	-86.7	9.3	-0.13
12	1947	Aegviidu village <sup>1</sup>	2-Jun-97	25.6068	59.2976	591,541	6,574,367	29	50	-12.2			-0.32
13	2816	Vinni village <sup>3</sup>	16-Jun-98	26.4304	59.2661	638,578	6,572,264	24	50	-12.2			-0.22
14	8610	Jõgeva town <sup>3</sup>	10-Jun-98	26.3844	58.7444	638,022	6,514,098	27	40	-11.7			0.12
15	11,848	Kuremaa village	21-Aug-13	26.5367	58.7346	646,874	6,513,326	18	45	-11.7	-83.9	10.0	0.10
16	4009	Nüri village	14-Aug-13	26.8518	59.3226	662,325	6,579,499	21	38	-12.1	-86.9	9.7	-0.03
17	7584	Liivoja village	22-Aug-13	26.3585	58.7737	636,409	6,517,302	12	70	-11.4	-80.5	10.5	0.45
18	1593	Laekvere village <sup>3</sup>	16-Jun-98	26.5664	59.0679	647,171	6,550,490	47	63	-12.4			-0.46
19	3516	Tamsalu town <sup>4</sup>	16-Oct-97	26.1258	59.1627	621,580	6,560,167	30	61	-11.7			0.21
20	3598	Raeküla village	21-Aug-13	26.3308	59.1658	633,287	6,560,899	19	60	-12.2	-87.5	9.8	-0.23
21	20,798	Väike-Maarja village	21-Aug-13	26.2298	59.1409	627,607	6,557,931	17	32	-12.0	-85.7	10.5	-0.10
22	8599	Põltsamaa town <sup>3</sup>	10-Jun-98	25.9568	58.6590	613,556	6,503,788	26	60	-11.6			0.14
23	7241	Viljandi town <sup>3</sup>	4-Jun-96	25.5972	58.3682	593,462	6,470,860	46	65	-11.3			0.31
24	7241	Viljandi town	26-Sep-97	25.5972	58.3682	593,462	6,470,860	46	65	-11.2			0.41
25	5247	Lõhavere village	2-Oct-13	25.4829	58.5464	586,338	6,490,545	43	61	-11.7	-81.2	12.5	-0.07
26	51,956	Särghaua farm	30-Jul-14	25.2404	58.6564	571,990	6,502,508	16	52	-11.4	-81.1	10.0	0.25
27	15,027	Järvakandi borough	2-Oct-13	24.8136	58.7779	547,057	6,515,659	10	24	-11.6	-82.1	10.4	0.06
28	7631	Kilingi-Nõmme town <sup>5</sup>	12-Jun-96	24.9837	58.1569	557,908	6,446,637	31	50	-11.3			0.17
29	50,432	Ruhnu island	17-Oct-13	23.2454	57.8048	455,138	6,407,245	35	51	-10.9	-77.6	9.5	0.24
30	6687	Uulu village	11-Mar-03	24.5776	58.2869	533,877	6,460,831	39	55	-11.5			-0.09
31	4299	Pärnu town	20-Oct-14	24.6019	58.3584	535,233	6,468,806	35	56	-11.3	-82.6	8.0	0.15
32	6578	Krundiküla village	20-Oct-14	24.4701	58.0309	527,772	6,432,270	26	37	-11.5	-81.4	10.4	-0.11
33	8664	Tõlli village <sup>1</sup>	9-Jun-97	22.3708	58.2993	404,482	6,463,229	17	40	-11.4			-0.23
34		Vasula village	1-Aug-14	26.7341	58.4615	659,535	6,483,386	10	30	-11.6	-83.4	9.2	0.22
35	4400	Tartu city	2-Oct-14	26.7723	58.3505	662,274	6,471,127	44	70	-11.8	-84.6	9.6	-0.01
36	13,376	Krabi village	22-Jul-14	26.8240	57.6037	668,799	6,388,153	10	19	-11.5	-83.5	8.8	0.02
37	14,338	Lüta border checkpoint	23-Jul-14	27.3780	57.6422	701,671	6,393,962	50	60	-11.3	-80.9	9.3	0.38
38	14,702	Kalatsova village	23-Jul-14	27.4166	57.7393	703,423	6,404,876	49	57	-11.5	-82.8	8.9	0.22
39	10,722	Misso village	23-Jul-14	27.2345	57.6011	693,334	6,388,971	44	70	-11.9	-86.0	9.2	-0.28
40	23,270	Varbola village	7-Oct-14	24.4514	59.0459	525,910	6,545,313	12	54	-12.0	-86.1	10.0	-0.36
41	1894	Välgejõe village	21-Aug-13	25.7883	59.4668	601,380	6,593,469	10	20	-11.9	-84.7	10.8	0.01
42		Taikse village	30-Jul-14	25.4594	58.7788	584,402	6,516,395	10	25	-11.4	-83.2	8.2	0.29
43		Kitsa village	30-Sep-14	22.4828	58.7865	412,275	6,517,331	10	30	-11.4	-80.7	10.1	-0.02
44		Pähu village	31-Jul-14	25.8861	59.0020	608,376	6,541,867	10	22	-11.9	-85.1	9.9	-0.04
45		Kärda town	30-Sep-14	22.7261	59.0002	426,789	6,540,828	10	25	-11.5	-83.5	8.6	-0.09
<i>Estonian springs</i>													
46		Oruveski	30-Aug-14	25.9567	59.5252	610,733	6,600,237			-12.7	-89.9	11.3	-0.66
47		Riigiküla	8-Aug-14	28.1261	59.4296	734,046	6,595,170			-12.5	-90.6	9.6	-0.28
48		Kuremäe	9-Aug-14	27.5269	59.2026	701,422	6,567,980			-12.6	-90.0	10.4	-0.44
49		Lavi	7-Aug-14	26.6320	59.2920	649,953	6,575,580			-12.5	-89.2	10.6	-0.47
50		Ohvriallikas, Helme	2-Aug-14	25.8793	58.0160	611,063	6,432,071			-11.9	-85.2	10.1	-0.36
51		Mäeotsa	7-Aug-14	26.3554	59.3459	633,989	6,580,998			-12.5	-89.6	10.2	-0.48
52		Siniallikas, Pirta	24-Nov-11	24.8497	59.4621	548,179	6,591,900			-12.1	-86.6	10.0	-0.25
53		Nõmmeveski	7-Aug-14	25.7886	59.5075	601,275	6,597,997			-12.3	-87.1	10.9	-0.29
54		Punane	1-Aug-14	27.1238	58.6079	681,503	6,500,669			-12.1	-87.0	9.6	-0.19
55		Purtse	8-Aug-14	27.0226	59.4092	671,605	6,589,571			-12.2	-88.2	9.6	-0.13
56		Prandi	31-Jul-14	25.7671	58.8440	602,008	6,524,087			-11.8	-84.2	10.0	-0.01
57		Eipre	31-Jul-14	25.7042	59.0224	597,871	6,543,859			-11.9	-85.5	9.6	-0.08
58		Merioone, Kanepi	24-Nov-11	26.9241	58.0256	672,732	6,435,356			-11.8	-83.1	11.0	-0.07
59		Kooli, Palamuse	31-Jul-14	26.5820	58.6831	649,717	6,507,702			-11.9	-85.3	9.6	-0.03
60		Katku, Simuna	9-Aug-14	26.4019	59.0418	637,845	6,547,244			-12.2	-86.8	10.7	-0.28
61		Norra	31-Jul-14	26.0713	58.8649	619,486	6,526,913			-11.7	-84.9	8.9	0.10
62		Sopa	31-Jul-14	26.0415	58.8701	617,751	6,527,433			-11.8	-84.5	9.5	0.06
63		Suurearu	30-Jul-14	24.7802	58.9849	544,857	6,538,692			-11.8	-84.7	10.0	-0.16
64		Emaläte, Otepea	2-Aug-14	27.0454	58.1099	679,464	6,445,052			-11.7	-84.7	9.2	-0.01
65		Silmaallikas, Salumäe	3-Aug-14	23.5901	58.6902	476,232	6,505,681			-11.5	-81.1	10.5	-0.01
66		Odalätsi	29-Sep-14	22.1269	58.3991	390,495	6,474,712			-11.3	-79.6	10.5	-0.09
67		Kaveläte	1-Aug-14	26.3616	58.3406	638,284	6,469,100			-11.6	-84.1	9.0	0.06
68		Siniallikas, Saula	31-Jul-14	25.0427	59.2139	559,554	6,564,408			-11.6	-83.8	9.2	0.16

Table 2 (continued)

No	Well ID	Location	Date	Coordinates				Well screen		$\delta^{18}\text{O}$ ‰	$\delta\text{D}$	$d_{\text{excess}}$	$\delta^{18}\text{O}_{\text{residual}}$
				Long E (°)	Lat N	TM Baltic X	TM Baltic Y	Upper m	Lower				
69		Ohvriallikas, Koila	8-Aug-14	26.7179	59.4597	654,090	6,594,446			-12.0	-87.4	8.4	0.10
70		Maimu	2-Aug-14	25.4841	58.1331	587,426	6,444,521			-11.3	-81.5	8.9	0.23
71		Sinialliku	2-Aug-14	25.5601	58.3021	591,459	6,463,449			-11.2	-80.6	9.0	0.39
72		Hinni	2-Aug-14	26.8767	57.7640	671,180	6,406,122			-11.4	-81.9	9.4	0.20
73		Rebaseallikas	1-Aug-14	27.4043	57.9412	701,553	6,427,306			-11.3	-82.8	7.9	0.40
74		Tori Põrgu	3-Aug-14	24.8171	58.4831	547,662	6,482,831			-11.1	-79.6	8.8	0.49
75		Lümandu	30-Jul-14	24.3961	58.9904	522,771	6,539,111			-11.5	-81.7	9.9	0.18
<i>Latvian wells</i>													
76	1484	Kalngale village <sup>6</sup>	14-Oct-10	24.1737	57.0854	510,536	6,326,878	12	19	-11.5	-80.1	11.5	-0.40
77	9648	Virane village <sup>6</sup>	10-Aug-11	26.3914	57.0600	645,111	6,326,616	13	17	-10.9	-78.3	9.1	0.43
78	693	Jurmala <sup>6</sup>	14-Oct-10	23.7518	56.9589	484,894	6,312,800	25	29	-11.4	-80.4	10.7	-0.44
79		Ruijenas town <sup>6</sup>	23-Aug-11	25.3423	57.8941	579,602	6,417,741	23	27	-11.5	-81.7	10.2	-0.05
80	[16,944	Liepupe village <sup>6</sup>	24-Aug-11	24.3969	57.4634	523,822	6,369,040	17	20	-10.8	-75.0	11.2	0.41
81	14,447	Griva village <sup>6</sup>	22-Sep-11	26.5030	55.8476	656,704	6,191,946	10	16	-10.6	-76.0	9.0	0.40
82	14,448	Griva village <sup>6</sup>	22-Sep-11	26.5157	55.8440	657,511	6,191,585	40	44	-10.7	-76.0	9.6	0.32
83	9600	Rimeikas village <sup>6</sup>	21-Oct-10	25.0255	57.8045	560,973	6,407,431	36	41	-10.7			0.63
84	13,754	Dole manor <sup>6</sup>	02-Oct-11	24.1545	56.8915	509,418	6,305,273	10	15	-11.3	-80.1	10.3	-0.31
85	2327	Sasmaka manor <sup>6</sup>	27-Oct-10	22.6586	57.3134	419,156	6,353,071	24	30	-11.0	-77.7	10.5	-0.11
86		Sasmaka manor <sup>7</sup>	2000	22.5905	57.3726	415,236	6,359,744	30	42	-10.8			0.12
87	25,662	Suitumi farm <sup>6</sup>	06-Dec-11	22.6148	57.1822	416,215	6,338,509	60	64	-11.2	-79.2	10.2	-0.30
88	26,036	Dridranks farm <sup>6</sup>	06-Dec-11	22.6056	57.1945	415,684	6,339,890	42	45	-10.9	-77.4	10.1	-0.07
89	9655	Trepe village <sup>6</sup>	10-Jan-12	26.0776	56.4441	628,074	6,257,446	49	56	-11.0	-77.2	10.6	0.15
90	9656	Trepe village <sup>6</sup>	10-Jan-12	26.0776	56.4441	628,075	6,257,448	12	41	-11.0	-78.1	10.1	0.10
91	9669	Stirmene <sup>6</sup>	28-Mar-12	26.6441	56.5615	662,487	6,271,707	35	55	-11.0	-79.5	8.6	0.23
92	[9680	Kapune village <sup>6</sup>	12-May-12	27.0547	56.9733	685,775	6,318,602	25	27	-11.2	-82.0	7.9	0.17
93	9687	Kaitra <sup>6</sup>	12-May-12	27.6469	56.0732	727,847	6,220,021	28	36	-11.3	-80.0	10.2	-0.02
94	9686	Kaitra <sup>6</sup>	12-May-12	27.6609	56.0710	727,845	6,220,024	45	61	-11.1	-79.6	9.4	0.13
95	3077	Zaķumuiža village <sup>6</sup>	02-Nov-10	24.4050	57.0216	524,609	6,319,832	22	27	-11.1	-79.7	8.8	0.00
96	22,605	Skaistkalne village <sup>6</sup>	06-Jun-12	24.6980	56.4157	543,065	6,252,568	16	20	-10.8	-77.6	8.4	0.17
97	22,609	Skaistkalne village <sup>6</sup>	07-Jun-12	24.6941	56.4083	542,832	6,251,739	20	25	-10.6	-77.0	8.1	0.28
99	1497	Murjani village <sup>6</sup>	05-May-11	24.6409	57.1369	538,814	6,332,790	25	29	-11.0	-77.8	10.1	0.13
98	9578	Tīnūži village <sup>6</sup>	12-Nov-10	24.5642	56.8717	534,422	6,303,200	20	25	-10.8	-75.7	10.4	0.28
100	2911	Pampali village <sup>6</sup>	18-May-11	22.2601	56.4993	392,898	6,263,004	35	40	-10.1	-70.1	10.5	0.55
101	2916	Evarži village <sup>6</sup>	18-May-11	22.4438	56.5794	404,403	6,271,652	24	30	-10.1	-71.9	8.5	0.61
102	2914	Evarži village <sup>6</sup>	18-May-11	22.4438	56.5795	404,402	6,271,661	44	53	-9.9	-69.8	9.7	0.72
103	9322	Skrunda town <sup>6</sup>	15-Jun-11	22.0275	56.6460	379,052	6,279,725	38	52	-10.2	-72.3	9.1	0.45
104	9323	Skrunda town <sup>6</sup>	13-Jun-11	22.0269	56.6461	379,011	6,279,729	15	25	-10.2	-72.2	9.7	0.39
105		Paulami village <sup>7</sup>	2000	27.1914	57.2206	692,682	6,346,453	28	39	-10.9			0.60
106		Dzerbene manor <sup>7</sup>	2000	25.6418	57.2212	599,137	6,343,206	40	65	-11.1			0.19
<i>Latvian springs</i>													
107	1605	Sloka <sup>6</sup>	08-Oct-10	23.5880	56.9340	474,921	6,310,086			-11.2	-81.3	8.3	-0.28
108	24,558	Mežmuiža <sup>6</sup>	08-Jul-11	24.7985	57.1022	548,404	6,329,024			-11.6	-81.3	11.8	-0.50
109		Svetavots Akņiste <sup>6</sup>	14-Jul-11	25.7384	56.1679	607,944	6,226,131			-10.6	-75.0	9.6	0.42
110	24,551	Briņķu <sup>6</sup>	08-Jul-11	25.2703	57.4510	576,272	6,368,304			-10.8	-78.5	8.2	0.46
111		Ulmale <sup>6</sup>	05-Aug-11	21.2637	56.9287	333,376	6,312,804			-10.5	-74.5	9.2	0.15
112		Kalnasmīdes <sup>6</sup>	22-Aug-11	25.2526	57.2138	575,702	6,341,876			-11.0	-77.7	10.3	0.23
113	24,567	Bārbele <sup>6</sup>	14-Jul-11	24.5920	56.4340	536,507	6,254,542			-10.7	-76.7	8.7	0.23
114	24,564	Saurieši <sup>6</sup>	21-Sep-11	24.4037	56.9024	524,607	6,306,550			-11.0	-77.3	10.3	0.07
115	24,576	Tukums <sup>6</sup>	20-Nov-10	23.2860	56.9739	456,594	6,314,708			-11.3	-80.6	9.4	-0.36
116		Līči <sup>6</sup>	21-Sep-11	24.3741	56.9441	522,779	6,311,190			-11.2	-79.8	9.7	-0.15
117		Līzēre <sup>6</sup>	14-Jul-11	24.4559	56.5244	528,049	6,264,542			-10.9	-78.7	8.3	0.04
118		Elkuzemes <sup>6</sup>	06-Aug-11	21.7341	56.4294	360,266	6,256,180			-10.7	-75.1	10.3	-0.15
119	24,560	Saltavots <sup>6</sup>	08-Jul-11	24.8504	57.1312	551,514	6,332,290			-11.2	-80.7	9.2	-0.09
120	24,552	Dāvida <sup>6</sup>	08-Jul-11	25.3872	57.2680	583,708	6,348,072			-11.3	-78.3	12.3	-0.07
121		Kandava <sup>6</sup>	20-Nov-10	22.7776	57.0308	425,755	6,321,454			-11.1	-79.5	9.1	-0.24
122		Dzērves-Bērziņu <sup>6</sup>	06-Aug-11	21.4692	56.7318	345,176	6,290,393			-10.8	-75.2	11.0	-0.20
123	24,550	Bānūžu <sup>6</sup>	08-Jul-11	25.5700	57.1581	595,025	6,336,069			-11.6	-82.3	10.3	-0.31
124		Kuldīga <sup>6</sup>	17-Nov-11	21.8974	56.9814	372,130	6,317,278			-11.1	-77.5	10.9	-0.34
125		Baldone <sup>6</sup>	21-Sep-11	21.4692	56.7318	524,707	6,288,806			-11.3	-80.5	9.5	-0.27
126		Raunas staburags <sup>6</sup>	22-Aug-11	25.5959	57.3259	596,147	6,354,801			-11.3	-80.0	10.6	-0.01
127	24,557	Elīte <sup>6</sup>	08-Jul-11	25.4262	57.3840	585,789	6,361,032			-11.2	-79.6	10.3	0.06
128		Ciecere <sup>6</sup>	19-Nov-11	22.0709	56.6801	381,816	6,283,438			-10.4	-72.2	11.1	0.23
129		Zušu <sup>6</sup>	22-Aug-11	24.9776	57.1004	559,266	6,328,971			-10.7	-75.8	9.9	0.45
130		Galtenes <sup>6</sup>	04-Aug-11	22.8378	57.1531	429,646	6,335,013			-11.0	-77.6	10.6	-0.13
131		Kaļļu <sup>6</sup>	22-Aug-11	25.3603	57.1875	582,266	6,339,065			-11.3	-78.5	11.7	-0.03
132		Mucenieku <sup>6</sup>	11-Aug-11	25.3392	56.8748	581,623	6,304,253			-11.3	-80.4	9.6	-0.11
133		Rutkaviņu <sup>6</sup>	22-Aug-11	26.1572	57.2510	630,221	6,347,400			-11.3	-80.9	9.7	0.05
157		Tirzas Svētavots <sup>6</sup>	22-Aug-11	25.5698	57.1244	647,490	6,335,656			-11.5	-81.1	10.7	-0.11
134		Aglonas <sup>6</sup>	11-Aug-11	27.0206	56.1288	687,725	6,224,529			-11.3	-81.2	8.9	-0.09
135	24,565	Serenes <sup>6</sup>	11-Aug-11	25.2210	56.5700	575,024	6,270,189			-11.2	-73.3	16.6	-0.20
136	24,563	Zīļu <sup>6</sup>	23-Aug-11	26.7079	57.5296	662,194	6,379,621			-11.9	-83.5	11.7	-0.38

(continued on next page)

Table 2 (continued)

No	Well ID	Location	Date	Coordinates				Well screen		$\delta^{18}\text{O}$	$\delta\text{D}$	$d_{\text{excess}}$	$\delta^{18}\text{O}_{\text{residual}}$
				Long E (°)	Lat N	TM Baltic X	TM Baltic Y	Upper m	Lower				
137	24,562	Vecsaunipu <sup>6</sup>	22-Aug-11	25.9480	57.3989	617,118	6,363,481			-11.7	-83.1	10.3	-0.30
138	14,354	Kõveles <sup>6</sup>	06-Aug-11	22.8210	56.4830	427,390	6,260,461			-10.2			0.53
139	24,561	Spigü <sup>6</sup>	23-Aug-11	25.5624	57.7833	592,941	6,405,687			-11.3	-79.8	10.5	0.15
140	24,554	Govs <sup>6</sup>	23-Aug-11	25.0016	57.8938	559,401	6,417,349			-11.5	-78.5	13.3	-0.08
<i>Lithuania wells</i>													
141	26,580	Aldona <sup>8</sup>	2006	24.0305	54.6039	501,970	6,051,929	40	46	-10.5			-0.20
142	517	Akvilė <sup>8</sup>	2006	23.9888	54.5838	499,278	6,049,686	46	53	-10.6			-0.31
143	43,515	Karmėlava town <sup>9</sup>		24.0612	54.9690	503,916	6,091,340	56	60	-10.7			-0.24
	42,169	Medininkai village <sup>9</sup>		25.6476	54.5379	606,600	6,044,615	62	70	-11.2			-0.65
	196	Salininkai city	15-Aug-14	25.2634	54.6012	581,633	6,052,361	43	50	-10.7	-76.3	9.1	-0.19
	28,809	Vilnius city <sup>9</sup>	16-Jun-09	25.2379	54.6660	583,140	6,060,650	19	24	-10.9			-0.39
147	28,814	Vilnius city <sup>9</sup>	16-Jun-09	25.2363	54.6677	583,140	6,060,650	23	31	-10.6			-0.09
148	28,811	Vilnius city <sup>9</sup>	16-Jun-09	25.2363	54.6677	583,140	6,060,650	46	51	-11.0			-0.49
149	28,813	Vilnius city <sup>9</sup>	6-Oct-09	25.4342	54.6668	583,156	6,060,668	47	58	-11.1			-0.59
150	4023	Vilnius city <sup>9</sup>	6-Oct-09	25.4541	54.6667	583,156	6,060,668	63	70	-11.1			-0.54
151		Mikenai town	23-Aug-14	24.4929	55.4921	531,146	6,149,668			-10.3	-73.7	8.7	0.33
152		Rinkunu	23-Aug-14	24.4109	55.9600	525,653	6,201,708			-10.8	-77.7	8.4	-0.01
153		Naiviu village	23-Aug-14	25.1383	55.8419	571,282	6,189,072			-10.6	-76.9	8.1	0.19
<i>Lithuanian springs</i>													
154		Aukštadvaris	20-Aug-14	24.5278	54.5757	534,115	6,047,708			-11.0	-77.9	9.9	-0.62
155		Gulbinai	1-Aug-14	25.3495	54.8085	586,731	6,074,312			-10.7	-76.9	8.9	-0.17
156		Punia	20-Aug-14	24.0866	54.5122	505,610	6,040,511			-10.2	-72.9	8.6	0.09

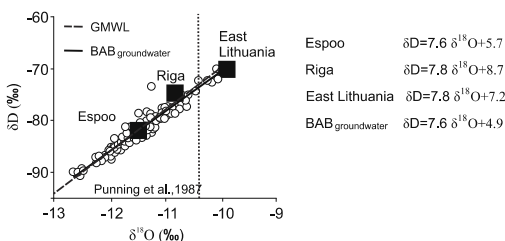


Fig. 4. Plot of  $\delta^{18}\text{O}$  versus  $\delta\text{D}$  for the shallow groundwater and for the IAEA/WMO GNIP stations in the BAB area. The vertical dotted line marks the annual weighted mean  $\delta^{18}\text{O}$  value for the local precipitation reported by Punning et al. (1987) from Estonia.

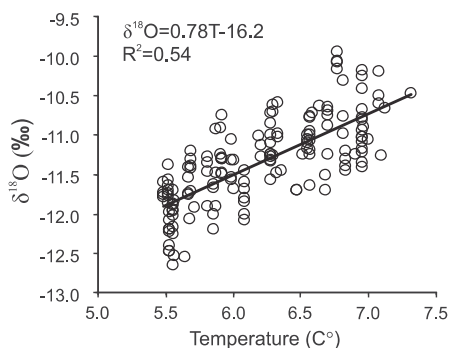


Fig. 5. The  $\delta^{18}\text{O}$  values in shallow groundwater as a function of the annual mean surface temperature in the BAB area. The average air temperatures are computed from the ERA-Interim database (Dee et al., 2011) for the period of 1981–2010.

results obtained from southern Finland (Fig. 7a), even though standard deviation in this region is 0.26‰, which is similar to the value in the southern part of the BAB (Fig. 7c).

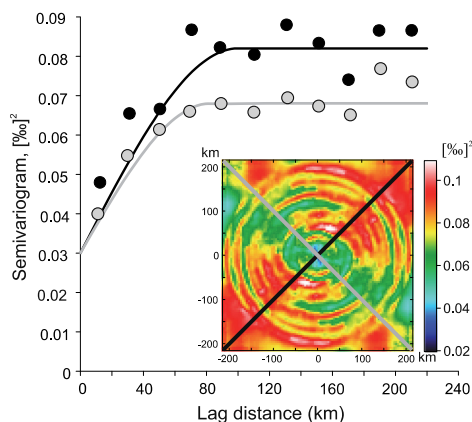
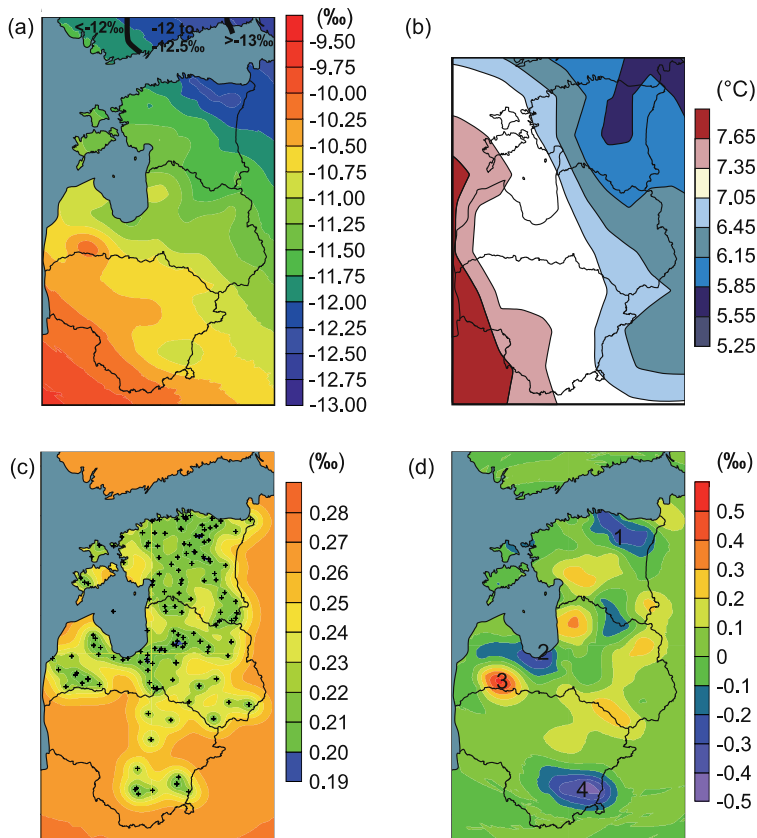


Fig. 6. The variogram analysis for  $\delta^{18}\text{O}$  values in groundwater of the BAB. The inset figure shows the variogram surface derived from the residual  $\delta^{18}\text{O}$  values of groundwater. Experimental directional semivariograms (dots) and fitted spherical models (line) are shown for the SE–NW (black) and NE–SW (gray) directions [tolerance: 45°, max lag distance: 220 km, number of (non-overlapping) lags: 11]. Centre lines of the represented sectors are drawn in the same color over the variogram surface.

## 5. Discussion

### 5.1. Seasonality of recharge

In the BAB area, most  $\delta^{18}\text{O}$  values of shallow groundwater are depleted with respect to mean weighted annual values of local precipitation measured in the Riga GNIP station (central part of the BAB) and in Tiirikoja, Estonia (in the northern part of the BAB; Punning et al., 1987) (Fig. 4). Many studies (e.g., Maule et al., 1994; DeWalle et al., 1997; O’Driscoll et al., 2005; Earman et al., 2006; Hayashi and Farrow, 2014; Jasechko et al., 2014) have shown that in the areas, where snow forms the essential part of annual precipitation, recharge is seasonally biased and  $\delta^{18}\text{O}$  values in groundwater can be more depleted with respect to mean weighted



**Fig. 7.** Isoscape of  $\delta^{18}\text{O}$  values of groundwater in the BAB (the thick isolines in South Finland show the results from Kortelainen and Karhu (2004)) (a); average air temperature computed from the ERA-Interim database (Dee et al., 2011) for the period 1981–2010 (b); standard deviation of the presented geospatial modelling (kriging) of  $\delta^{18}\text{O}$  values (c); residual values of  $\delta^{18}\text{O}$  calculated based on the Eqs. (4) and (5) (the numbers mark the anomalies of  $\delta^{18}\text{O}_{\text{residual}}$  in Pandivere Upland (1), the Riga region (2), western Latvia (3) and the Vilnius region (4), respectively) (d).

annual values in precipitation. Moreover, in the summertime, higher temperatures that enhance evaporation as well as more actively transpiring plants prevail, that do not allow much bypass flow of isotopically heavier rainfall, (Welker et al., 1991; Abbott et al., 2000; Chimner and Welker, 2005; Earman et al., 2006; Blumenthal et al., 2008; Hayashi and Farrow, 2014). In the BAB area, where a significant proportion of precipitation accumulates as snow in winter (10–40%; Tooming and Kadaja, 2006), the snow-melt in spring and the enhanced influence of vegetation and evapotranspiration in summer could impact the observed isotopic composition of shallow groundwater. Saxton and McGuinness (1982) and Telmer and Veizer (2000) have shown that vegetative transpiration and evaporation in the Great Lakes area in North America are capable of transferring 45–70% of the annual precipitation back to the atmosphere, thereby making it unavailable for recharge. During the vegetation period and due to the basin's more northern position, the duration of daylight in the BAB area is longer than that of the Great Lakes. That is why the proportion of evapotranspiration in the BAB area could be close to or even higher than 70%. In contrast to evaporation, transpiration loss does not result in isotopic fractionation in the remaining soil water (e.g., Wershaw et al., 1966; Dawson and Ehleringer, 1991). Therefore, this process is not reflected in  $d_{\text{excess}}$  values.

## 5.2. The influence of the recharge areas

Local changes of up to 1‰ per 50 km in the  $\delta^{18}\text{O}$  values of shallow groundwater are evident in the BAB area (Fig. 7a), which is much more abrupt than the spatial changes reported in earlier studies from other flatland areas (e.g., Darling et al., 2003; Kortelainen and Karhu, 2004). In our case, some isolated areas exist, where the isotopic composition of shallow groundwater is either depleted or enriched in contrast to the surrounding areas (Fig. 7a).

In the  $\delta^{18}\text{O}_{\text{residual}}$  map, the strongest anomalies can be seen in the northern part (Pandivere upland), in the central (Riga region and western Latvia) and southeastern parts (Vilnius region) of the BAB, respectively (Fig. 7d). The Vilnius anomaly is quite possibly caused by a low spatial density of sampling points towards East Lithuania as the shallow groundwater's isotopic composition becomes steadily more depleted eastwards. That means that this anomaly may not reflect the real-life conditions.

In other cases, it is possible that the anomalies are caused by variations in recharge conditions. The local vegetation type has a great influence on spatial variability of runoff and evapotranspiration (Gehrels et al., 1998; O'Driscoll et al., 2005; Song et al., 2009). Croplands usually generate the highest amount of runoff, and grass

pastures the lowest (Elliott and Efetha, 1999; van der Kamp et al., 2003), but the capacity of woody plants to limit recharge leads to large differences in recharge volumes in woodlands and in other vegetation types (Darling and Bath, 1988; Kim and Jackson, 2012). The Baltic States are characterised by a high variability of vegetational communities (CLC, 2012). In Lithuania, the agricultural areas cover about 61% of the territory (Vaitkus, 2004), but in Estonia and Latvia, forest is the predominant vegetation type covering about 50% of the territory (Hansen et al., 2013). It is very likely that different vegetation types have affected transpiration efficiency, which means that the amount of recharge in surface water over the area can be remarkably different. This could have an especially important effect in early spring when the vegetation activity of trees has started, but croplands are still bare (Kim and Jackson, 2012). However, to clarify or quantify the influence of this vegetation effect on groundwater recharge, a more detailed research is needed.

Alternatively, spatial variation in the isotopic composition of shallow groundwater would not be related not to vegetation but to surface conditions in the recharge areas. Several negative  $\delta^{18}\text{O}_{\text{residual}}$  values are tied to karst areas (Fig. 8). These phenomena are especially evident in the Pandivere upland (NE part of the BAB), where river or stream networks are entirely lacking and most rain- and meltwater can percolate directly into karst interstices.

Gleeson et al. (2009) have shown that the rate and amount of rapid recharge of meltwater in spring is controlled not only by vertical fracture aperture, but also by soil thickness and by hydraulic conductivity. The latter could be related to the moisture conditions of soil prior to its freezing in autumn. The period in autumn when temperatures are still beyond zero is typically the rainiest time in the BAB area (Tolstovs et al., 1986) and the surface is mostly over-saturated with water. With higher water contents in the soil, a

greater blockage of soil pores by ice can be expected when this water freezes in winter (Kane, 1980; Seyfried and Murdock, 1997; Gray et al., 2001; Hayashi and Farrow, 2014). In spring, rapid snowmelt is often associated with extensive floods over the frozen soil. In karst areas, where uncovered deep crevice systems or depressions occur, the infiltration conditions are better and large amounts of floodwater can infiltrate into the subsurface. In the unkarstified areas, most floodwaters are directed into rivers or wetlands. Fig. 8 shows that well-drained areas like river valleys, where surface runoff of floodwater is prevalent, are characterised by pronounced positive  $\delta^{18}\text{O}_{\text{residual}}$  values.

The described relationships are not as clear in the central part of the BAB as in the northern part of the basin. In flat regions, where most of the Latvian and Lithuanian karst areas are found, a single sinkhole could affect an area as large as 50–500 m in radius (Herczeg et al., 1997). Additionally, while karst areas and their spring systems in the northern part of the BAB serve as head-springs for rivers, karst areas in the central part of the BAB are often drained by rivers, which could have a good connection to the karstic crevice systems and could thus produce anomalies in the recharge balance (Fig. 8).

In the Riga region, the negative anomaly can be explained by the upward leakage of groundwaters with longer residence times. The Gulf of Riga is essentially a regional discharge area for multiple groundwater horizons, where isotopically depleted groundwater formed in Late Pleistocene can discharge. Moreover, the formation of the Riga depression cone by rapid increase of water extraction during the 1990s, caused water upflow from deeper water horizons and could also have enhanced the leakage of groundwater from the adjacent areas (Kalvans, 2012). Today, the piezometric levels of the affected horizons have recovered (Klints and Delija, 2012), but the composition of groundwater may still contain signals from deeper

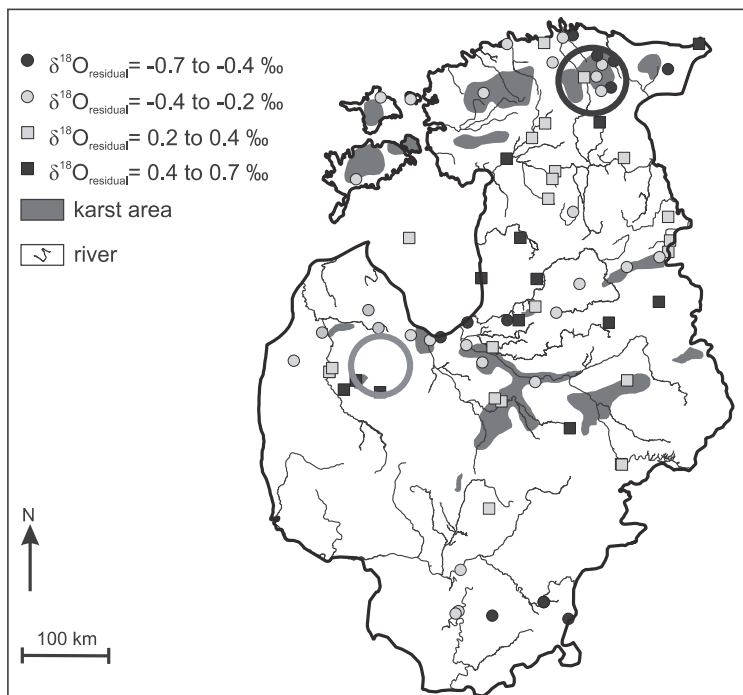


Fig. 8. The map characterising the high deviation of  $\delta^{18}\text{O}_{\text{residual}}$  values. The black circle marks the location of the Pandivere Upland and the Gray—the location of the Kurzeme Upland.

aquifers. In addition, three larger rivers discharge in this area and cause a decrease of heads in the upper aquifers. This causes an intrusion of deeper pressurized groundwater through the aquitards to upper aquifers. Together, these processes could be responsible for the anomaly observed in  $\delta^{18}\text{O}$  values. A similar phenomenon has also been described in the southern coast of the Baltic Sea (in Lithuania), near the discharge areas of large rivers (Mokrik and Mazeika, 2002).

In western Latvia, the reason for strongly positive  $\delta^{18}\text{O}_{\text{residual}}$  values (Fig. 7d) remains unclear. We assume that the anomalies are caused by modern recharge conditions in the area. In the upper part of the geological cross-section, the Kurzeme upland located in the vicinity is covered in permeable deposits. In the deeper part of the section, rocks of much lower porosity are found. In contrast to the fractured or epikarst sub-systems, which enhance groundwater storage and mixing (Aquilina et al., 2005; Mueller et al., 2013; Genty et al., 2014), the unfractured systems have a low water storage capacity, which could lead to shorter residence times and a higher variability in the chemical and isotopic compositions of groundwater. Compared to shallow groundwaters in other parts of Latvia ( $2\text{--}25\text{ mg L}^{-1}$ ), the relatively low  $\text{Cl}^{-}$  values ( $2\text{--}5\text{ mg L}^{-1}$ ) observed in this area could indicate freshly infiltrated waters and despite their relatively great depths, point to the influence of the seasonal effect. However, research is needed, in order to clarify details of the recharge balance in the BAB area.

### 5.3. Application of the presented isoscape

The obtained results show that the isotopic composition of shallow groundwater does not necessarily correspond to the annual mean of local precipitation. It suggests that when making palaeoclimatic interpretations in palaeoenvironmental research, we should not assume that  $\delta^{18}\text{O}$  values of shallow groundwater are identical to those of precipitation, even when the area under investigation has not been influenced by major changes in mean annual temperatures in the past. The negligence of the factors which can cause the isotopic composition of the studied tracer to deviate from the isotopic composition of local precipitation could lead to various misinterpretations. A similar problem can occur in hydrogeological studies, where variation between  $\delta^{18}\text{O}$  values does not reflect seasonal signals, but only differences in recharge conditions.

Moreover, the modelled global precipitation map (Terzer et al., 2013) shows that the modelled precipitation's  $\delta^{18}\text{O}$  in the BAB is only slightly depleted (less than 0.5‰) with respect to the isotopic composition of shallow groundwater in the region. At the same time, our results show the difference of up to 2‰. This raises a question of how well global precipitation models can be used as references for research on regional or local hydrology. A regional isoscape, such as the one presented in this study, can be more suitable for these purposes as it is able to reveal local anomalies in isotopic composition of shallow groundwater, where the isotopic composition of groundwater does not represent that of local annual mean of precipitation. The identification of such local anomalies gives an opportunity to trace other hydrogeological processes, for example, to determine in which proportions groundwater and precipitation are present in the out-pumped water from mines. It is a practical problem in mining areas in Northeast Estonia and so far the estimations have only been based on hydrodynamic models (Savitski, 2005; Perens et al., 2010), although isotopic mixing models could give a better result.

Hydrogen and oxygen isotopes in water are incorporated into plant and animal tissues in a predictable manner and could potentially be used for forensic tracing of wildlife in a region (e.g., Podlesak et al., 2008; Kahmen et al., 2011). Several studies have used  $\delta^{18}\text{O}$  isotope analyses for achieving a better resolution in tracing the migration of the people (e.g., Bentley and Knipper, 2005;

Ehleringer et al., 2008; Chenery et al., 2011). Thus, it could be that the observed differences in  $\delta^{18}\text{O}$  and  $\delta\text{D}$  values in bone or hair samples are not caused by migration (e.g., Price et al., 2012; Oras et al., 2016), but may point to different sources of drinking water—surface water (river, lake) or groundwater (spring).

## 6. Conclusions

The isotopic composition of shallow groundwater in the BAB area is depleted with respect to mean weighted annual values of local precipitation. We believe that the long daylight period in the BAB area during the summer growing season allows plants to transpire a substantial portion of the summer precipitation input, which causes the groundwater recharge to be strongly biased towards the spring snowmelt and autumn precipitation. The results of the study suggest that when making palaeoclimatic interpretations in palaeoenvironmental research, we should not assume that  $\delta^{18}\text{O}$  values of shallow groundwater are identical to those of precipitation, even when the area under investigation has not been influenced by major changes in mean annual temperature in the past. Soil texture, soil structure and land cover could strongly impact the water flow in the soil, its percolation to the water table and groundwater recharge.

Although our results show a difference between isotope composition of precipitation and shallow groundwater, the shallow groundwater isoscape for the BAB can be used as input in isotope-based hydrogeological models and the presented methodology can be adopted in other regions, where monitoring observed precipitation (GNIP or national network) is lacking, but shallow groundwater isotope data is available. The derived isoscape of  $\delta^{18}\text{O}$  values in the BAB shallow groundwater is characterised by a high spatial resolution ( $1 \times 1\text{ km}$ ) and its estimated error is comparable to the analytical precision of the  $\delta^{18}\text{O}$  measurements. Therefore, it can serve as a fairly accurate reference base for further hydrogeological modelling and also for ecological, or even forensic applications.

## Acknowledgements

We would like to thank Mrs. Helle Pohl-Raidla and Ms. Reeli Viikberg for the improvement of English. Financial support of the Hungarian Academy of Sciences (Lendület program, No LP2012-27/2012 to Z.K.), the Estonian Research Council (Grants PUTJD127 to V.R. and IUT19-22 to R.V.), National Research, Development and Innovation Office (SNN118205 to Z.K. and B.K.) and the Latvian NRP programme “The value and dynamic of Latvia's ecosystems under changing climate” are gratefully acknowledged. The manuscript was improved by the constructive and helpful comments of two anonymous reviewers and Fernando Pacheco.

## References

- Abbott, M.D., Lini, A., Bierm, P.R., 2000.  $\delta^{18}\text{O}$ ,  $\delta\text{D}$  and  $^3\text{H}$  measurements constrain groundwater recharge patterns in an upland fractured bedrock aquifer, Vermont, USA. *J. Hydrol.* 228, 101–112. [http://dx.doi.org/10.1016/S0022-1694\(00\)00149-9](http://dx.doi.org/10.1016/S0022-1694(00)00149-9).
- Alalamm, P. (Ed.), 1987. *Atlas of Finland, Fölio 131, Climate, vol. 31. National Board of Survey and Geographical Society of Finland, Helsinki.*
- Aquilina, L., Ladouche, B., Dörfli, N., 2005. Recharge processes in karstic systems investigated through the correlation of chemical and isotopic composition of rain and spring-waters. *Appl. Geochem.* 20, 2189–2206. <http://dx.doi.org/10.1016/j.apgeochem.2005.07.011>.
- Aquilina, L., Ladouche, B., Dörfli, N., 2006. Water storage and transfer in the epikarst of karstic systems during high flow periods. *J. Hydrol.* 327, 472–485. <http://dx.doi.org/10.1016/j.jhydrol.2005.11.054>.
- Babre, A., Kalvāns, A., Popovs, K., Retiķe, I., Dēliņa, A., Vaikmāe, R., Martma, T., 2016. Pleistocene age paleo-groundwater inferred from water-stable isotope values in the central part of the Baltic Artesian Basin. *Isot. Environ. Health Stud.* <http://dx.doi.org/10.1080/10256016.2016.1168411>.

- Bentley, R.A., Knipper, C., 2005. Geographical patterns in biologically available strontium, carbon and oxygen isotope signatures in prehistoric SW Germany. *Archaeometry* 47 (3), 629–644. <http://dx.doi.org/10.1111/j.1475-4754.2005.00223.x>.
- Blumenthal, D., Chimner, R., Welker, J.M., Morgan, J., 2008. Increased snow facillitates plant invasion in mixed grass prairie. *New Phytol.* 179, 440–448. <http://dx.doi.org/10.1111/j.1469-8137.2008.02475.x>.
- Bowen, G.J., Revenaugh, J., 2003. Interpolating the isotopic composition of modern meteoric precipitation. *Water Resour. Res.* 39, 1299. <http://dx.doi.org/10.1029/2003WR002086>.
- Bowen, G.J., Kennedy, C.D., Liu, Z.F., Stalker, J., 2011. Water balance model for mean annual hydrogen and oxygen isotope distributions in surface waters of the contiguous United States. *J. Geophys. Res.* 116, G04011. <http://dx.doi.org/10.1029/2010JG001581>.
- Bowen, G.J., Good, S.P., 2015. Incorporating water isoscapes in hydrological and water resource investigations. *WIREs Water* 2, 107–119. <http://dx.doi.org/10.1002/wat2.1069>.
- Brand, W.A., Geilmann, H., Crosson, E.R., Rella, C.W., 2009. Cavity ring-down spectroscopy versus high-temperature conversion isotope ratio mass spectrometry: a case study on  $\delta^2\text{H}$  and  $\delta^{18}\text{O}$  of pure water samples and alcohol/water mixtures. *Rapid Commun. Mass Spectrom.* 23, 1879–1884. <http://dx.doi.org/10.1002/rcm.4083>.
- Brown, C.E., 1998. *Applied Multivariate Statistics in Geohydrology and Related Sciences*. Springer-Verlag, Berlin, p. 248.
- Chenery, C., Eckardt, H., Müldner, G., 2011. Cosmopolitan Catterick? Isotopic evidence for population mobility on Rome's northern frontier. *J. Archaeol. Sci.* 38 (7), 1525–1536. <http://dx.doi.org/10.1016/j.jas.2011.02.018>.
- Chimner, R.A., Welker, J.M., 2005. Ecosystem respiration responses to experimental manipulations of winter and summer precipitation in a Mixed grass Prairie, WY, USA. *Biogeochemistry* 73, 257–270. <http://dx.doi.org/10.1007/s10533-004-1989-6>.
- Clark, I., Fritz, P., 1997. *Environmental Isotopes in Hydrogeology*. Lewis Publishers, New York.
- CLC, 2012. CORINE Land Cover Map <<http://land.copernicus.eu/pan-european/corine-land-cover/clc-2012>> (Cited 13th July 2016).
- Coplen, T.B., 1994. Reporting of stable hydrogen, carbon, and oxygen isotopic abundances. *Pure & Appl. Chem.* 66, 273–276. <http://dx.doi.org/10.1351/pac199466020273>.
- Cressie, N., 1993. *Statistics for Spatial Data*. Wiley, New York.
- Dansgaard, W., 1964. Stable isotopes in precipitation. *Tellus* 16, 436–468.
- Darling, W.G., Bath, A.H., 1988. A stable isotope study of recharge processes in the English Chalk. *J. Hydrol.* 101, 31–46. [http://dx.doi.org/10.1016/0022-1694\(88\)90026-1](http://dx.doi.org/10.1016/0022-1694(88)90026-1).
- Darling, W.G., Bath, A.H., Talbot, J.C., 2003. The O and H stable isotopic composition of fresh waters in the British Isles. Surface waters and groundwater. *Hydrol. Earth Syst. Sci.* 7, 183–195. <http://dx.doi.org/10.5194/hess-7-183-2003>.
- Dawson, T.E., Ehleringer, J.R., 1991. Streamside trees that do not use stream water. *Nature* 350, 335–337.
- Dee, D.P., Uppala, S.M., Simmons, A.J., Berrisford, P., Poli, P., Kobayashi, S., Andrae, U., Balmaseda, M.A., Balsamo, G., Bauer, P., Bechtold, P., Beljaars, A.C.M., van de Berg, L., Bidlot, J., Bormann, N., Delsol, C., Dragani, R., Fuentes, M., Geer, A.J., Haiberg, L., Healy, S.B., Hersbach, H., Hölm, E.V., Isaksen, I., Källberg, P., Köhler, M., Matricardi, M., McNally, A.P., Monge-Sanz, B.M., Morcrette, J.J., Park, B.K., Peubey, C., de Rosnay, P., Tavolato, C., Thépaut, J.N., Vitart, F., 2011. The ERA-Interim reanalysis: configuration and performance of the data assimilation system. *Quart. J. Roy. Meteorol. Soc.* 137, 553–597. <http://dx.doi.org/10.1002/qj.828>.
- Deines, P., Hull, L.C., Stowe-Schuyler, S., 1990. Study of soil and groundwater movement using stable hydrogen and oxygen isotopes. In: Majumdar, S.K., Miller, E.W., Parizek, R.R. (Eds.), *Water Resources in Pennsylvania: Availability, Quantity and Management*. Pennsylvania Acad. Sci., Easton, pp. 121–140.
- DeWalle, D.R., Edwards, P.J., Swistock, B.R., Aravena, R., Drimmie, R.J., 1997. Seasonal isotope hydrology of three Appalachian forest catchments. *Hydrol. Process.* 11, 1895–1906.
- Earman, S., Campbell, A.R., Phillips, F.M., Newman, B.D., 2006. Isotopic exchange between snow and atmospheric water vapor: estimation of the snowmelt component of groundwater recharge in the southwestern United States. *J. Geophys. Res.* 111, D09302. <http://dx.doi.org/10.1029/2005JD006470>.
- Ehleringer, J.R., Cerling, T.E., West, J.B., Podlesak, D.W., Chesson, L.A., Bowen, G.J., 2008. Spatial considerations of stable isotope analyses in environmental forensics. In: Hester, R.E., Harrison, R.M. (Eds.), *Issues in Environmental Science and Technology*. Royal Society of Chemistry Publishing, Cambridge, pp. 36–53.
- Eichinger, L., Merkel, B., Nemeth, G., Salvamoser, J., Stichler, W., 1984. Seepage velocity determinations in unsaturated Quaternary gravel. In: *Recent Investigations in the Zones of Aeration*, Symposium Proceedings, Munich, pp. 303–313.
- Elliott, J.A., Efetha, A.A., 1999. Influence of tillage and cropping system on soil organic matter, structure and infiltration in a rolling landscape. *Can. J. Soil Sci.* 79, 457–463. <http://dx.doi.org/10.4141/CJSS2011-045>.
- Gehrels, J.C., Peeters, J.E., de Vries, J.J., Dekkers, M., 1998. The mechanism of soil water movement as inferred from O-18 stable isotope studies. *Hydrol. Sci. J. - J. Des Sci. Hydrol.* 43, 579–594. <http://dx.doi.org/10.1080/02626669809492154>.
- Genty, D., Labuhn, I., Hoffmann, G., Danis, P.A., Mestre, O., Bourges, F., Wainer, K., Massault, M., Van Exter, S., Régner, E., Orengo, Ph., Falourd, S., Minster, B., 2014. Rainfall and cave water isotopic relationships in two South-France sites. *Geochim. Cosmochim. Acta* 131, 323–343. <http://dx.doi.org/10.1016/j.gca.2014.01.043>.
- Gleeson, T., Novakowski, K., Kyser, T.K., 2009. Extremely rapid and localized recharge to a fractured rock aquifer. *J. Hydrol.* 376, 496–509. <http://dx.doi.org/10.1016/j.jhydrol.2009.07.056>.
- Gray, D.M., Toth, B., Zhao, L., Pomeroy, J.W., Granger, R.J., 2001. Estimating areal snowmelt infiltration into frozen soils. *Hydrol. Process.* 15, 3095–3111. <http://dx.doi.org/10.1002/hyp.320>.
- Grigelis, A. (editor-in-chief), 1978. *Geological Map of the Quaternary Deposits in the Soviet Baltic Republics*. Scale 1:500,000. Aerogeologija, Leningrad.
- Hansen, M.C., Potapov, P.V., Moore, R., Hancher, M., Turubanova, S.A., Tyukavina, A., Thau, D., Stehman, S.V., Goetz, S.J., Loveland, T.R., Kommareddy, A., Egorov, A., Chini, L., Justice, C.O., Townshend, J.R.G., 2013. High-resolution global maps of 21st-century forest cover change. *Science* 342, 850–853. <http://dx.doi.org/10.1126/science.1244693>.
- Hayashi, M., Farrow, C.R., 2014. Watershed-scale response of groundwater recharge to inter-annual and inter-decadal variability in precipitation (Alberta, Canada). *Hydrogeol. J.* 22, 1825–1839. <http://dx.doi.org/10.1007/s10040-014-1176-3>.
- Herczeg, A.L., Leaney, F.W.J., Stadler, M.F., Allan, G.L., Fifield, L.K., 1997. Chemical and isotopic indicators of point-source recharge to a karst aquifer, South Australia. *J. Hydrol.* 192, 271–299. [http://dx.doi.org/10.1016/S0022-1694\(96\)03100-9](http://dx.doi.org/10.1016/S0022-1694(96)03100-9).
- IAEA/WMO, 2015. *Global Network of Isotopes in Precipitation*. The GNIP Database Accessible at: <<http://www.iaea.org/water>> (last accessed on 1st May, 2015).
- Ingraham, N.L., Taylor, B.E., 1991. Light stable isotope systematics of large-scale hydrologic regimes in California and Nevada. *Water Resour. Res.* 27, 77–90.
- Jasechko, S., Birks, S.J., Gleeson, T., Wada, Y., Fawcett, P.J., Sharp, Z.D., McDonnell, J.J., Welker, J.M., 2014. The pronounced seasonality of global groundwater recharge. *Water Resour. Res.* 50, 8845–8867. <http://dx.doi.org/10.1002/2014WR015809>.
- van der Kamp, G., Hayashi, M., Gallén, D., 2003. Comparing the hydrology of grassed and cultivated catchments in the semi-arid Canadian prairies. *Hydrol. Process.* 17, 559–575. <http://dx.doi.org/10.1002/hyp.1157>.
- Kahmen, A., Sachse, D., Arndt, S.K., Tu, K.P., Farrington, H., Vitousek, P.M., Dawson, T.E., 2011. Cellulose delta O-18 is an index of leaf-to-air vapor pressure difference (VPD) in tropical plants. *Proc. Natl. Acad. Sci. USA* 108, 1981–1986. <http://dx.doi.org/10.1073/pnas.1018906108>.
- Kalvans, A., 2012. A list of the factors controlling groundwater composition in the Baltic Artesian Basin. In: Dēlina, A., Kalvāns, A., Saks, T., Bēthers, U., Virčavs, V. (Eds.), *Highlights of Groundwater Research in the Baltic Artesian Basin*. University of Latvia, Riga, pp. 91–106.
- Kane, D.L., 1980. Snowmelt infiltration into seasonally frozen soils. *Cold Reg. Sci. Technol.* 3, 153–161. [http://dx.doi.org/10.1016/0165-232X\(80\)90020-8](http://dx.doi.org/10.1016/0165-232X(80)90020-8).
- Kern, Z., Kohän, B., Leuenberger, M., 2014. Precipitation isoscape of high reliefs: interpolation scheme designed and tested for monthly resolved precipitation oxygen isotope records of an Alpine domain. *Atmos. Chem. Phys.* 14, 1897–1907. <http://dx.doi.org/10.5194/acp-14-1897-2014>.
- Kim, J.H., Jackson, R.B., 2012. A global analysis of groundwater recharge for vegetation, climate, and soils. *Vadose Zone J.* 11. <http://dx.doi.org/10.2136/vzj2011.0021RA>.
- Kink, H., 1997. Karst and springs. Water-bearing formation. In: Raukas, A., Teedumäe, A. (Eds.), *Geology and Mineral Resources of Estonia*. Estonian Academy Publishers, Tallinn, pp. 389–390.
- Klints, I., Dēlina, A., 2012. Groundwater abstraction in the Baltic Artesian Basin. In: Dēlina, A., Kalvāns, A., Saks, T., Bēthers, U., Virčavs, V. (Eds.), *Highlights of Groundwater Research in the Baltic Artesian Basin*. University of Latvia, Riga, pp. 106–123.
- Kohän, B., Szalai, J., 2014. Spatial analysis of groundwater level monitoring network in the Danube-Tisza Interfluvium using semivariograms. *Hung. Geogr. Bull.* 63 (4), 379–400. <http://dx.doi.org/10.15201/hungebull.63.4.2>.
- Kortelainen, N.M., Karhu, J.A., 2004. Regional and seasonal trends in the oxygen and hydrogen isotope ratios of Finnish groundwaters: a key for mean annual precipitation. *J. Hydrol.* 285, 143–157. <http://dx.doi.org/10.1016/j.jhydrol.2003.08.014>.
- Kottek, M., Grieser, J., Beck, C., Rudolf, B., Rubel, F., 2006. World Map of the Köppen-Geiger climate classification updated. *Meteorol. Z.* 15, 259–263. <http://dx.doi.org/10.1127/0941-2948/2006/0130>.
- Lachniet, M.S., Patterson, W.P., 2006. Use of correlation and multiple stepwise regression to evaluate the climatic controls on the stable isotope values of Panamanian surface waters. *J. Hydrol.* 324, 115–140. <http://dx.doi.org/10.1016/j.jhydrol.2005.09.018>.
- Levins, I., Levina, N., Gavena, I., 1998. Latvian groundwater resources. *Riga, State Geol Surv. Riga* 24 (in Latvian).
- Matheron, G., 1965. *Les Variables Régionalisées Et Leur Estimation (Regional Variables and Their Distribution)*. Masson et Cie, Paris, p. 305.
- Maule, C.P., Chanasyk, D.S., Muehlenbachs, K., 1994. Isotopic determination of snow-water contribution to soil water and groundwater. *J. Hydrol.* 155, 73–91. [http://dx.doi.org/10.1016/0022-1694\(94\)90159-7](http://dx.doi.org/10.1016/0022-1694(94)90159-7).
- Mazeika, J., Martma, T., Petrošius, R., Jakimavičiūtė-Maseliēnė, V., Skuratovič, Ž., 2013. Radiocarbon and other environmental isotopes in the groundwater of the sites for a planned new nuclear power plant in Ignalina. *Radiocarbon* 55, 951–962.
- Mokrik, R., 1997. *The Palaeohydrogeology of the Baltic Basin: Vendian & Cambrian*. Tartu University Press, Tartu, p. 138.
- Mokrik, R., Mazeika, J., 2002. Palaeohydrogeological reconstruction of groundwater recharge during Late Weichselian in the Baltic basin. *Geologia* 39, 49–57.

- Mokrik, R., 2003. The Paleohydrogeology of the Baltic Basin: Neoproterozoic & Phanerozoic. VUL, Vilnius, p. 333.
- Mokrik, R., Mažeika, J., Baublyte, A., Martma, T., 2009. The groundwater age in the Middle-Upper Devonian aquifer system, Lithuania. *Hydrogeol. J.* 17, 871–889. <http://dx.doi.org/10.1007/s10040-008-0403-1>.
- Mokrik, R., Juodkaziš, V., Štuopis, A., Mažeika, J., 2014. Isotope geochemistry and modelling of the multi-aquifer system in the eastern part of Lithuania. *Hydrogeol. J.* 22, 925–941. <http://dx.doi.org/10.1007/s10040-014-1120-6>.
- Mueller, M.H., Weingartner, R., Alewell, C., 2013. Importance of vegetation, topography and flow paths for water transit times of base flow in alpine headwater catchments. *Hydrol. Earth Syst. Sci.* 17, 1661–1679. <http://dx.doi.org/10.5194/hess-17-1661-2013>.
- Nikishin, A.M., Ziegler, P.A., Stephenson, R.A., Cloetingh, S.A.P.L., Furne, A.V., Fokin, P. A., Ershov, A.V., Bolotov, S.N., Korotaev, M.V., Alekseev, A.S., Gorbachev, V.I., Shipilov, E.V., Lankreijer, A., Bembinova, E.Yu., Shalimov, I.V., 1996. Late Precambrian to Triassic history of the East European Craton: dynamics of sedimentary basin evolution. *Tectonophysics* 268, 23–63. [http://dx.doi.org/10.1016/S0040-1951\(96\)00228-4](http://dx.doi.org/10.1016/S0040-1951(96)00228-4).
- O'Driscoll, M.A., DeWalle, D.R., McGuire, K.J., Gburek, W.J., 2005. Seasonal  $^{18}\text{O}$  variations and groundwater recharge for three landscape types in central Pennsylvania, USA. *J. Hydrol.* 303, 108–124. <http://dx.doi.org/10.1016/j.jhydrol.2004.08.020>.
- Oras, E., Lang, V., Rannamäe, E., Varul, L., Konsa, M., Limbo-Simovart, J., Vedru, G., Laneman, M., Malve, M., Price, T.D., 2016. Tracing prehistoric migration: isotope analysis of bronze and pre-roman iron age coastal burials in Estonia. *Estonian J. Archaeol.* 20, 3–32. <http://dx.doi.org/10.3176/arch.2016.1.01>.
- Pacheco, F.A.L., Van der Weijden, C.H., 2014. Modeling rock weathering in small watersheds. *J. Hydrol.* 513, 13–27. <http://dx.doi.org/10.1016/j.jhydrol.2014.03.036>.
- Pärn, J., Raidla, V., Vaikmäe, R., Martma, T., Ivask, J., Mokrik, R., Erg, K., 2016. The recharge of glacial meltwater and its influence on the geochemical evolution of groundwater in the Ordovician-Cambrian aquifer system, northern part of the Baltic Artesian Basin. *Appl. Geochem.* 72, 125–135. <http://dx.doi.org/10.1016/j.apgeochem.2016.07.007>.
- Perens, R., Savitskaja, L., Savva, V., Truu, M., Häelml, M., Jaštšuk, S., 2010. Estimation about Estonian oil shale deposits' groundwater reserves. *Geol. Surv. Estonia, Tallinn 131* (in Estonian).
- Podlesak, D.W., Torregrossa, A.M., Ehleringer, J.R., 2008. Turnover of oxygen and hydrogen isotopes in the body water,  $\text{CO}_2$ , hair, and enamel of a small mammal. *Geochim. Cosmochim. Acta* 72, 19–35. <http://dx.doi.org/10.1016/j.gca.2007.10.003>.
- Price, T.D., Frei, K.M., Tiesler, V., Gestsdottir, H., 2012. Isotopes and mobility: case studies with large samples. In: Kaiser, E., Burger, J., Wolfram, S. (Eds.), *Population Dynamics in Prehistory and Early History: New Approaches Using Stable Isotopes and Genetics*. Walter de Gruyter, Berlin, pp. 311–321.
- Punning, J.M., Toots, M., Vaikmäe, R., 1987. O-18 in Estonian natural-waters. *Isotopenpraxis* 23, 232–234. <http://dx.doi.org/10.1080/10256018708623797>.
- Pyrcz, M.J., Deutsch, C.V., 2014. *Geostatistical Reservoir Modeling*. Oxford University Press, New York.
- Raidla, V., Kirsimäe, K., Vaikmäe, R., Jõelet, A., Karro, E., Marandi, A., Savitskaja, L., 2009. Geochemical evolution of groundwater in the Cambrian-Vendian aquifer system of the Baltic Basin. *Chem. Geol.* 258, 219–231. <http://dx.doi.org/10.1016/j.chemgeo.2008.10.007>.
- Raidla, V., Kirsimäe, K., Vaikmäe, R., Kaup, E., Martma, T., 2012. Carbon isotope systematics of the Cambrian-Vendian aquifer system in the northern Baltic Basin: implications to the age and evolution of groundwater. *Appl. Geochem.* 27, 2042–2052. <http://dx.doi.org/10.1016/j.apgeochem.2012.06.005>.
- Raidla, V., Kirsimäe, K., Ivask, J., Kaup, E., Knöller, K., Marandi, A., Martma, T., Vaikmäe, R., 2014. Sulphur isotope composition of dissolved sulphate in the Cambrian-Vendian aquifer system in the northern part of the Baltic Artesian Basin. *Chem. Geol.* 383, 147–154. <http://dx.doi.org/10.1016/j.chemgeo.2014.06.011>.
- Rank, D., Volki, G., Maloszewski, D., Stichler, W., 1992. Flow dynamics in an alpine karst massif studied by means of environmental isotopes. In: *Isotope Techniques in Water Resources Development 1991*, IAEA Symposium 319, Vienna, pp. 327–343.
- Raukas, A., Kajak, K., 1997. Quaternary cover. In: Raukas, A., Teedumäe, A. (Eds.), *Geology and Mineral Resources of Estonia*. Estonian Academy Publishers, Tallinn, pp. 125–136.
- Remm, K., Jaagus, J., Briede, A., Rimkus, E., Kelviste, T., 2011. Interpolative mapping of mean precipitation in the Baltic countries by using landscape characteristics. *Estonian J. Earth Sci.* 60, 172–190. <http://dx.doi.org/10.3176/earth.2011.3.05>.
- Rozanski, K., 1985. Deuterium and oxygen-18 in European groundwaters – links to atmospheric circulation in the past. *Chem. Geol. (Isot. Geosci. Sect.)* 52, 349–363. [http://dx.doi.org/10.1016/0168-9622\(85\)90045-4](http://dx.doi.org/10.1016/0168-9622(85)90045-4).
- Satunas, J., Griģiene, A., Jusiene, A., Damusyte, A., Mazaika, J., 2009. Middle Weichselian palaeolacustrine basin in the Venta river valley and vicinity (northwest Lithuania), exemplified by the Purvial outcrop. *Quatern. Int.* 207, 14–25. <http://dx.doi.org/10.1016/j.quaint.2008.12.003>.
- Savitskaja, L., Viigand, A., Jaštšuk, S., 1995. Report of microcomponent and isotope composition research in Ordovician-Cambrian aquifer groundwater for estimating drinking water quality in North-Estonia. *Geol. Surv. Estonia, Tallinn, 54* (in Estonian).
- Savitskaja, L., Viigand, A., Jaštšuk, S., 1996a. Report of water quality in the Middle-Devonian –Silurian aquifer groundwater. *Geol. Surv. Estonia, Tallinn, 47* (in Estonian).
- Savitskaja, L., Viigand, A., Jaštšuk, S., 1996b. Report of water quality in the Upper-Devonian –Silurian aquifer groundwater. *Geol. Surv. Estonia, Tallinn, 42* (in Estonian).
- Savitskaja, L., Viigand, A., Jaštšuk, S., 1997. Report of microcomponent and isotope composition research in Silurian-Ordovician aquifer groundwater. *Geol. Surv. Estonia, Tallinn, 51* (in Estonian).
- Savitskaja, L., Viigand, A., Jaštšuk, S., 1998. Report of microcomponent and radionuclides research in Silurian-Ordovician aquifer groundwater. *Geol. Surv. Estonia, Tallinn, 31* (in Estonian).
- Savitski, L., 2005. The origin of out pumped water from mines and quarries. *Geol. Surv. Estonia, Tallinn, p. 29* (in Estonian).
- Saxton, K.E., McGuinness, J.L., 1982. Evapotranspiration. In: *Hydrologic Modeling of Small Watersheds*. In: Haan, C.T., Johnson, H.P., Brakensiek, D.L. (Eds.), *ASAE Monograph no. 5*. American Society of Agricultural Engineers, Michigan, USA, pp. 229–273.
- Sellers, W.D., 1972. *Physical Climatology*. University Chicago Press, Chicago, p. 272.
- Seyfried, M.S., Murdock, M.D., 1997. Use of air permeability to estimate infiltrability of frozen soil. *J. Hydrol.* 202, 95–107. [http://dx.doi.org/10.1016/S0022-1694\(97\)00061-9](http://dx.doi.org/10.1016/S0022-1694(97)00061-9).
- Skuratovič, Z., Mažeika, J., Petrošius, R., Martma, T., 2015. Investigations of the unsaturated zone at two radioactive waste disposal sites in Lithuania. *Isot. Environ. Health Stud.* 1–9. <http://dx.doi.org/10.1080/10256016.2015.1092968>.
- Song, X., Wang, S., Xiao, G., Wang, Z., Liu, X., Wang, P., 2009. A study of soil water movement combining soil water potential with stable isotopes at two sites of shallow groundwater areas in the North China Plain. *Hydrol. Process.* 23, 1376–1388. <http://dx.doi.org/10.1002/hyp.7267>.
- Taminskas, J., Marcinkevičius, V., 2002. Karst geoindicators of environmental change: the case of Lithuania. *Environ. Geol.* 42, 757–766. <http://dx.doi.org/10.1007/s00254-002-0553-8>.
- Telmer, K., Veizer, J., 2000. Isotopic constraints on the transpiration, evaporation, energy, and gross primary production budgets of a large boreal watershed: Ottawa River basin, Canada. *Global Biogeochem. Cycles* 14, 149–165. <http://dx.doi.org/10.1029/1999GB900078>.
- Terzer, S., Wassenaar, L.L., Araguás-Araguás, L.J., Aggarwal, P.K., 2013. Global isoscapes for  $\delta^{18}\text{O}$  and  $\delta^2\text{H}$  in precipitation: improved prediction using regionalized climatic regression models. *Hydrol. Earth Syst. Sci.* 17, 4713–4728. <http://dx.doi.org/10.5194/hess-17-4713-2013>.
- Tolstovs, J., Levina, N., Prilukova, T., 1986. Report on investigations of groundwater regime, balance and exogenic geological processes and the review of the State water cadaster (groundwater) of the Latvia SSR for years 1984–1986 (Summary report on years 1976–1985). Department of Geology of LSSR, Riga, p. 470 (in Russian).
- Tooming, H., Kadaja, J., 2006. *Handbook of Estonian Snow Cover*. Estonian Meteorology and Hydrology Institute, Estonian Research Institute of Agriculture, Saku-Tallinn, p. 504.
- Vaikmäe, R., Vallner, L., Loosli, H.H., Blaser, P.C., Juillard-Tardent, M., 2001. Palaeogroundwater of glacial origin in the Cambrian-Vendian aquifer of northern Estonia. In: Edmunds, W.M., Milne, C.J. (Eds.), *Palaeowaters of Coastal Europe: Evolution of Groundwater since the late Pleistocene*, vol. 189. Geological Society, London, pp. 17–27. <http://dx.doi.org/10.1144/GSL.SP.2001.189.01.03> (Special Publications).
- Vaitkus, G., 2004. CORINE Land Cover of Lithuania, 2000. Institute of Ecology of Vilnius University (in Lithuanian).
- Vallner, L., 1997. *Groundwater flow*. In: Raukas, A., Teedumäe, A. (Eds.), *Geology and Mineral Resources of Estonia*. Estonian Academy Publishers, Tallinn, pp. 159–162.
- Virbulis, J., Bethers, U., Saks, T., Sennikovs, J., Timuhins, A., 2013. Hydrogeological model of the Baltic Artesian Basin. *Hydrogeol. J.* 21, 845–862. <http://dx.doi.org/10.1007/s10040-013-0970-7>.
- Vitola, I., Virčavs, V., Abramenko, K., Lauva, D., Veinbergs, A., 2012. Precipitation and air temperature impact on seasonal variations of groundwater levels. *Environ. Clim. Technol.* 10, 25–33. <http://dx.doi.org/10.2478/v10145-012-0022-x>.
- Wassenaar, L.L., Van Wilgenburg, S.L., Larson, K., Hobson, K.A., 2009. A groundwater isotope ( $\delta\text{D}$ ,  $\delta^{18}\text{O}$ ) for Mexico. *J. Geochim. Explor.* 102, 123–136. <http://dx.doi.org/10.1016/j.gexplo.2009.01.001>.
- Welker, J.M., McClelland, S., Weaver, T.W., 1991. Soil water retention after natural and simulated rainfall on a temperate grassland. *Theoret. Appl. Climatol.* 44, 447–453. <http://dx.doi.org/10.1007/BF00868178>.
- Wenner, D.B., Ketchum, P.D., Down, J.F., 1991. Stable isotopic composition of waters in a small Piedmont watershed. In: Taylor, H.P. Jr., O'Neil, J.R., Kaplan, I.R. (Eds.), *Stable Isotope Geochemistry: A Tribute to Samuel Epstein*, The Geochemical Society, vol. 3, pp. 195–203 (Special Publication).
- Wershaw, R.L., Friedman, I., Heller, J.G., 1966. Hydrogen isotope fractionation of water passing through trees. In: Hobson, G.D., Speers, G.C. (Eds.), *Advances in Organic Geochemistry*. Pergamon Press, Oxford, pp. 55–67.
- West, A.C., February, E.C., Bowen, G.J., 2014. Spatial analysis of hydrogen and oxygen stable isotopes (“isoscapes”) in ground water and tap water across South Africa. *J. Geochim. Explor.* 145, 213–222. <http://dx.doi.org/10.1016/j.gexplo.2014.06.009>.
- Zuzevičius, A., Mažeika, J., Baltrūnas, V., 2007. A model of brackish groundwater formation in the Nemunas River valley, Lithuania. *Geologia* 60, 63–75.

**Paper II**

Pärn, Joonas; Raidla, Valle; Vaikmäe, Rein; Martma, Tõnu; Ivask, Jüri; Mokrik, Robert; Erg, Katrin (2016). The recharge of glacial meltwater and its influence on the geochemical evolution of groundwater in the Ordovician-Cambrian aquifer system, northern part of the Baltic Artesian Basin. *Applied Geochemistry*, 72, 125–135.





# The recharge of glacial meltwater and its influence on the geochemical evolution of groundwater in the Ordovician-Cambrian aquifer system, northern part of the Baltic Artesian Basin



Joonas Pärn<sup>a,\*</sup>, Valle Raidla<sup>a,b</sup>, Rein Vaikmäe<sup>a</sup>, Tõnu Martma<sup>a</sup>, Jüri Ivask<sup>a</sup>, Robert Mokrik<sup>c</sup>, Katrin Erg<sup>d</sup>

<sup>a</sup> Institute of Geology at Tallinn University of Technology, Ehitajate tee 5, 19086 Tallinn, Estonia

<sup>b</sup> Institute of Environmental Physics, University of Heidelberg, Neuenheimer Feld 229, Heidelberg, Germany

<sup>c</sup> Department of Hydrogeology and Engineering Geology, Vilnius University, Ciurlionio 21, 2009 Vilnius, Lithuania

<sup>d</sup> Geological Survey of Estonia, Kadaka tee 82, 12618 Tallinn, Estonia

## ARTICLE INFO

### Article history:

Received 22 June 2015

Received in revised form

18 July 2016

Accepted 19 July 2016

Available online 20 July 2016

### Keywords:

Palaeohydrogeology

Glacial meltwater

Mixing

Freshening

Ion exchange

## ABSTRACT

The geochemical evolution of groundwater in the Ordovician-Cambrian aquifer system in the northern part of the Baltic Artesian Basin (BAB) illustrates how continental glaciations have influenced groundwater systems in proglacial areas. The aquifer system contains water that has originated from various end-members: recent meteoric water, glacial meltwater and relict Na-Cl brine. The saline formation water that occupied the aquifer system prior to the glacial meltwater intrusion has been diluted by meltwaters of advancing-retreating ice sheets. The diversity in the origin of groundwater in the aquifer system is illustrated by a wide variety in  $\delta^{18}\text{O}$  values that range from  $-11\%$  to  $-22.5\%$ . These values are mostly depleted with respect to values found in modern precipitation in the area. The chemical and isotopic composition of groundwater has been influenced by mixing between waters originating from different end-members. In addition, the freshening of a previously saline water aquifer due to glacial meltwater intrusion has initiated various types of water-rock interaction (e.g. ion exchange, carbonate mineral dissolution).

© 2016 Elsevier Ltd. All rights reserved.

## 1. Introduction

Aquifers in sedimentary basins once covered by continental glaciers had sufficient transmissivity to discharge subglacial meltwater (Boulton et al., 1995; Piotrowski, 1997; Person et al., 2007; Lemieux et al., 2008; McIntosh et al., 2011). The recharge of glacial meltwater was able to modify groundwater flow patterns in these basins with water penetrating much deeper and faster under high hydraulic gradient induced by continental ice sheets compared to modern topographically driven recharge. The reorganisation of groundwater flow patterns also influenced the isotopic and chemical composition of the basinal fluids. Many studies have shown a direct influence of Quaternary glaciations on the formation of groundwater in proglacial sedimentary basins in North America and in Europe (e.g. Clayton et al., 1966; Siegel and

Mandle, 1984; Siegel, 1989, 1991; Stueber and Walter, 1991, 1994; Vaikmäe et al., 2001; Grasby et al., 2000; McIntosh et al., 2002; McIntosh and Walter, 2005, 2006; Ferguson et al., 2007; Raidla et al., 2009, 2012). Fluid pressure anomalies associated with the ice sheets have in most cases dissipated (except few cases such as described in Alberta Basin, Western Canada; e.g. Bekele et al., 2003) leaving the chemical and isotopic composition of groundwater as the main tool for studying the ice sheet-aquifer interactions during Pleistocene.

The influence of glacial meltwater recharge from the Scandinavian Ice Sheet on the proglacial sedimentary aquifers in the Baltic Artesian Basin (BAB) has been documented in Ediacaran and Cambrian sandstones (i.e. Cambrian-Vendian aquifer system) in its shallow northern part (e.g. Yezhova et al., 1996; Mokrik, 1997, 2003; Vaikmäe et al., 2001, 2008; Karro et al., 2004; Marandi, 2007; Raidla et al., 2009, 2012, 2014). Groundwater in the northern part of the Cambrian-Vendian aquifer system has the lightest isotopic composition recorded in Europe ( $\delta^{18}\text{O}$  values ranging from  $-18.5\%$  to  $-23\%$ ) (Vaikmäe et al., 2001) that is depleted with respect to

\* Corresponding author.

E-mail address: [joonas.parn@ttu.ee](mailto:joonas.parn@ttu.ee) (J. Pärn).

isotopic composition of the modern precipitation in the area (the annual weighted mean  $\delta^{18}\text{O}$  value of  $-10.4\%$ ; Punning et al., 1987).

In this paper we study the geochemical evolution of groundwater in the Ordovician-Cambrian (O-Cm) aquifer system. This aquifer system overlies the Cambrian-Vendian aquifer system in the northern part of the BAB. Specific aims are (1) to reconstruct the origin of groundwater in the aquifer system; (2) to reveal the sources of salinity in the studied waters and the main geochemical processes that control the groundwater chemistry; and (3) to assess the influence of glacial meltwater recharge on the geochemical evolution of groundwater in the aquifer system.

Understanding the processes influencing recharge, mixing and geochemical evolution of groundwater in O-Cm aquifer system is crucial for predicting the effects of groundwater abstraction on its composition and availability. The O-Cm aquifer system is an important source of public water supply in northern Estonia. In addition, the rocks associated with the aquifer strata contain several mineral resources that could have potential economic significance in the future. These include the shell detritus of phosphatic brachiopods in Lower Ordovician sandstones which form the biggest phosphorite deposit in Europe (Raudsep, 1997). It was mined for phosphatic fertilizer production from 1920s up to late 1980s. Furthermore, the Lower Ordovician organic-rich black shale known as graptolite argillite overlying the aquifer system contains high concentrations of trace metals and REE elements (e.g. U, Mo, V, Ni, Cd, Au, Sb, As, Pt) (Voolma et al., 2013; Hade and Soesoo, 2014). Any future plans for mining these mineral resources need to take into account the origin and renewability of groundwater in the O-Cm aquifer system.

## 2. Geology and hydrogeological setting

The O-Cm aquifer system is a confined water body in the northern part of the BAB. BAB is a Phanerozoic sedimentary basin that covers the territories of Estonia, Latvia, Lithuania and parts of Russia, Poland and Belarus (Fig. 1a) (Mokrik, 1997, 2003; Virbulis et al., 2013). Approximately half of the BAB is covered by the Baltic Sea. The thickness of the sedimentary cover reaches 5000 m in the south-western part of the basin, while the crystalline basement reaches to the surface at its northern and south-eastern parts. In the northern part of the BAB (Estonia and Latvia) the sedimentary cover contains rocks of Ediacaran to Devonian age which overlie the Paleoproterozoic crystalline basement (Fig. 1b). In the southern part of the basin in Lithuania and Poland the sedimentary succession is continued with sedimentary rocks of Mesozoic and Cenozoic age. General flow direction of deep groundwater in the BAB is directed from the south-western parts of the basin towards the periphery monoclines.

The O-Cm aquifer system is hosted by sand- and siltstones of Cambrian and Early Ordovician age which are located between the underlying Lower Cambrian claystones (i.e. Lükati-Lontova regional aquitard) and the overlying Lower Ordovician argillites, sandstones and carbonate rocks (Fig. 2). The sandstones in Cambrian and Lower Ordovician are mainly quartz arenites or subarkoses, with quartz content up to 90% (Raidla et al., 2006). The rocks forming the O-Cm aquifer system are distributed in most of the Estonian territory, except in the coastal region of northern Estonia and Mõniste-Lokno uplift area in southern Estonia (Fig. 2). The thickness of the aquifer system increases from 20 to 60 m in northern Estonia to ~120 m in Latvia (Juodkakis, 1980; Savitskaja et al., 1995; Perens and Vallner, 1997). The depth of the aquifer strata is 10–20 m from the ground surface in northern Estonia and increases to over 1000 m in Latvia. The lateral hydraulic conductivity of Cambrian and Lower Ordovician sandstones ranges from 1 to 3  $\text{m d}^{-1}$  (Perens and Vallner, 1997). Transmissivity ranges from 25 to 50  $\text{m}^2 \text{d}^{-1}$  in

northern Estonia and from 80 to 130  $\text{m}^2 \text{d}^{-1}$  in southern Estonia due to the increased thickness of the water-bearing rocks (Perens and Vallner, 1997).

The O-Cm aquifer system is confined by the overlying Silurian-Ordovician regional aquitard. The northern part of the aquitard consists of Lower Ordovician limestones, marls, siltstones, clays and argillites, extending ~100 km southward from the Estonia's northern coast (Fig. 2). The whole Silurian-Ordovician sedimentary sequence can be viewed as a regional aquitard at increasing depths as the number of fissures and cavities which are the main water conducting zones in carbonate rocks decreases with depth (Perens and Vallner, 1997). The transversal hydraulic conductivity of the Silurian-Ordovician regional aquitard ranges from  $10^{-7}$  to  $10^{-5} \text{m d}^{-1}$  (Perens and Vallner, 1997).

The O-Cm aquifer system is separated from the underlying Cambrian-Vendian aquifer system by the Lükati-Lontova regional aquitard which consists of siltstones and clays of the Lower Cambrian Lükati and Lontova Formations that have a transversal hydraulic conductivity of  $10^{-7} \text{m d}^{-1}$  (Perens and Vallner, 1997). In western Estonia the Lontova Formation is laterally replaced by siltstones and sandstones of the Voosi Formation (Fig. 2). The aquitard becomes sandier and thinner with its transversal hydraulic conductivity increasing to  $\geq 10^{-5} \text{m d}^{-1}$  (Perens and Vallner, 1997). In western Estonia and south-western Estonia, the Ediacaran

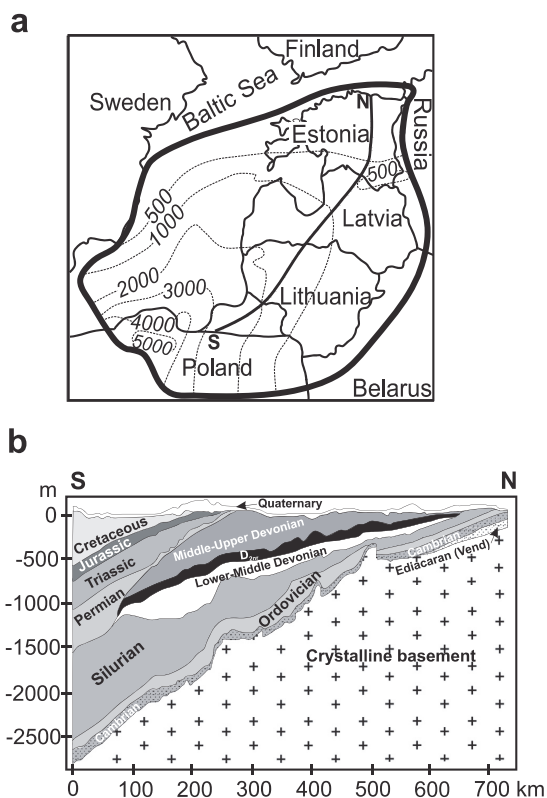


Fig. 1. (a) The location and boundaries of the Baltic Artesian Basin (BAB) together with contour lines marking the depth of the crystalline basement in meters b.s.l., (b) the geologic cross-section of the BAB along the line N-S on Fig. 1a.  $D_{2nr}$  – Narva regional aquitard, Q – Quaternary (modified from: Juodkakis, 1980; Virbulis et al., 2013).

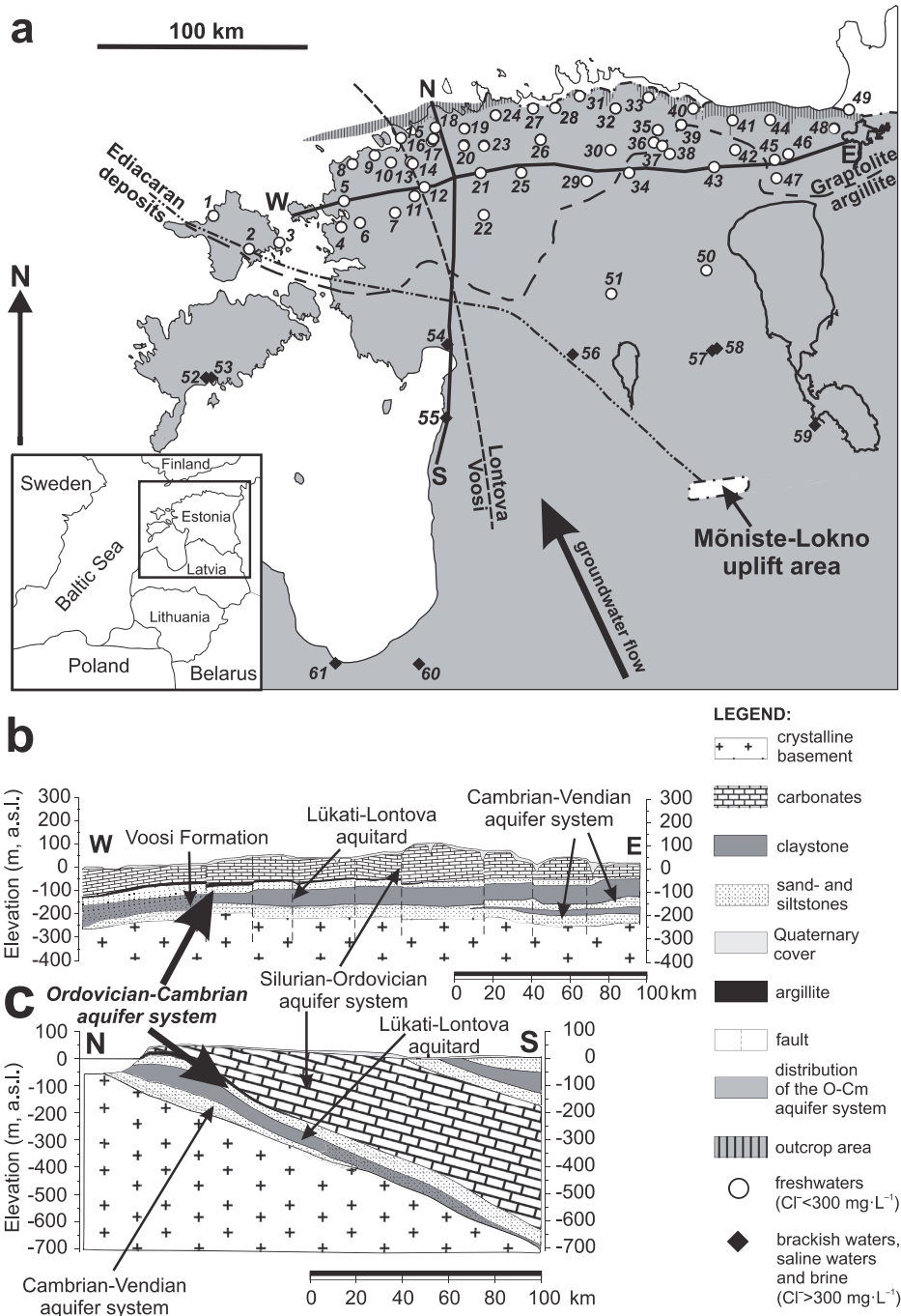


Fig. 2. (a) The distribution of the O-Cm aquifer system in the northern part of the Baltic Artesian Basin (BAB) and the locations of the sampled wells. Numbers indicate the position of the sampled wells in Table 1S; (b) the west-east cross-section of northern BAB; (c) the north-south cross-section of the northern BAB.

deposits underlying the Lükati-Lontova regional aquitard pinch out (Fig. 2). South and south-west from this line the water-bearing siliciclastic rocks consist only of Cambrian sand- and siltstones with interlayers of clay and the aquifer system is referred to as the Cambrian aquifer system (Perens and Vallner, 1997).

Previous studies have shown that the chemical composition of groundwater in the O-Cm aquifer system is diverse. In northern Estonia several chemical types of water such as Ca-Mg-HCO<sub>3</sub>, Mg-Ca-HCO<sub>3</sub> or Na-Mg-Ca-HCO<sub>3</sub>-Cl with the TDS concentrations of 200–500 mg L<sup>-1</sup> have been reported (Savitskaja et al., 1995; Perens et al., 2001). In southern Estonia and in the Western Estonian islands groundwater of Na-Cl-HCO<sub>3</sub> and Na-Cl types with TDS values > 2000 mg L<sup>-1</sup> has been found (Perens et al., 2001). The limited amount of previously published δ<sup>18</sup>O data from the O-Cm aquifer system indicates that in the northern part of the aquifer system groundwater with depleted isotopic composition with respect to modern precipitation can be found. The reported δ<sup>18</sup>O values range from -15‰ to -19‰ (Kivitt et al., 1993; Savitskaja et al., 1995; Vaikmäe et al., 2001; Raidla et al., 2009).

### 3. Material and methods

The study is based on 61 groundwater samples collected from wells screened in the O-Cm aquifer system in Estonia and Latvia. The majority of the samples have been collected by the Institute of Geology at Tallinn University of Technology from operational private, municipal water supply and observation wells in the period of 2012–2014. Eight samples were provided by the Geological Survey of Estonia (EGK) (EGK, 2014, 2015). The dataset has been complemented by results from earlier studies (Kivitt et al., 1993; Savitskaja et al., 1995; Babre et al., 2016) to improve the spatial coverage of the study area and to include wells that have been dismantled or are no longer in use. Only samples for which at least both the hydrochemical and δ<sup>18</sup>O data was available were considered. The parameters of the sampled wells together with the interpreted analytical data are given in Table 1S (Supporting Material). The locations of the sampled wells are given in Fig. 2.

The groundwater samples were collected into HDPE bottles from outside taps once electric conductivity values and dissolved O<sub>2</sub> levels had stabilised. The pH, temperature and electric conductivity were measured in the field using Hach HQ40d™ multi-parameter digital meter. HCO<sub>3</sub><sup>-</sup> concentrations were measured in the Laboratory of Estonian Geological Survey using the titration method (ISO 9963-1) within 48 h of the sample collection. Major and some minor ion concentrations were measured in the Institute of Geology at Tallinn University of Technology using DIONEX ICS-1100 ion chromatograph and in the Laboratory of Hydrogeochemistry in the Department of Hydrogeology and Engineering Geology of Vilnius University using DIONEX ICS-5000 ion chromatograph. The analytical precision for major and minor ionic components (Li<sup>+</sup>) was ±0.5–5.5% for measurements made in Tallinn and ±1–7.5% for measurements made in Vilnius, respectively, depending on the ions measured (Table 1S). The saturation indices of calcite and dolomite together with ionic strength, activities and stability diagrams for studied waters were calculated and drawn using the Geochemist Workbench 10.0<sup>®</sup> software and PHREEQC database (Parkhurst and Appelo, 1999). When the studied waters are referred to on the basis of salinity the classification by Stuyfzand (1989, 1993) is used: freshwater (Cl<sup>-</sup> concentrations < 300 mg L<sup>-1</sup>); brackish water (Cl<sup>-</sup> concentrations 300–10,000 mg L<sup>-1</sup>); saline water (Cl<sup>-</sup> concentrations > 10,000 mg L<sup>-1</sup>). The studied waters are referred to as brines when their Cl<sup>-</sup> concentrations exceed the average value of 19,400 mg L<sup>-1</sup> in modern seawater.

Stable isotope ratios of hydrogen and oxygen in water were analysed in the Laboratory of mass spectrometry at Institute of

Geology, Tallinn University of Technology. Isotope ratios are expressed in standard δ-notation relative to Vienna Standard Mean Ocean Water (V-SMOW). Prior to July 2006 the stable isotope ratios of oxygen were measured with Finnigan MAT Delta-E mass spectrometer using the conventional CO<sub>2</sub> equilibration technique (Epstein and Mayeda, 1953). For samples collected since the year 2010 both isotope ratios of hydrogen and oxygen were measured using the cavity ring-down laser spectroscopy (CRDS) and instrument Picarro L2120-i Isotopic Water Analyzer (Brand et al., 2009). Reproducibility of the stable isotope measurements was ±0.1‰ for δ<sup>18</sup>O and ±1‰ for δ<sup>2</sup>H. The δ<sup>18</sup>O and δ<sup>2</sup>H values for two samples collected in 2014 with high salinity (TDS > 3000 mg L<sup>-1</sup>) were measured in Department of Climate and Environmental Physics at University of Bern (Table 1S). The isotope ratios of hydrogen and oxygen were measured with Picarro L1102-i Isotopic Water Analyzer with the online method presented in Affolter et al. (2014). The reproducibility of the measurements was ±0.2‰ for δ<sup>18</sup>O and ±2‰ for δ<sup>2</sup>H.

### 4. Results and discussion

#### 4.1. Freshwaters in the northern part of the aquifer system

The data for the isotopic and major elemental composition of the sampled waters in the O-Cm aquifer system is presented in Table 1S (Supporting Material). The freshwaters in the northern part of the O-Cm aquifer system are characterized by wide variety in Cl<sup>-</sup> concentrations (from 0.12 to 3 mmol L<sup>-1</sup>) and in isotopic composition (δ<sup>18</sup>O values from -11.2‰ to -22.4‰) (Fig. 3a, b).

The freshwater in the O-Cm aquifer system is of meteoric origin as illustrated by the δ<sup>18</sup>O-δ<sup>2</sup>H co-variance that defines a line of δ<sup>2</sup>H = 7.87 · δ<sup>18</sup>O + 7.7 (r<sup>2</sup> = 0.99) close to global meteoric water line (GMWL) (Fig. 4).

The weighted annual mean δ<sup>18</sup>O value for modern precipitation in Estonia is -10.4‰ and the isotope composition of precipitation

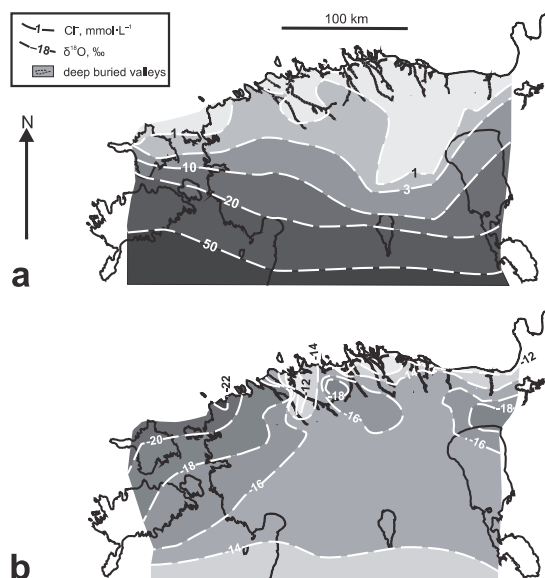


Fig. 3. Lateral distribution of (a) Cl<sup>-</sup> concentrations and (b) δ<sup>18</sup>O values in the O-Cm aquifer system.

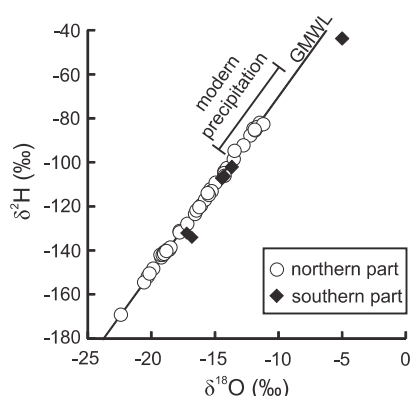


Fig. 4. The  $\delta^{18}\text{O}$  and  $\delta^2\text{H}$  isotopic composition of groundwater in the O-Cm aquifer system. The GMWL (Global Meteoric Water Line) defined by Craig (1961) is shown for reference.

has high intra-annual variability with  $\delta^{18}\text{O}$  values ranging from  $-13.8\text{‰}$  and  $-8.4\text{‰}$  in winter and summer months, respectively (Punning et al., 1987). In O-Cm aquifer system the  $\delta^{18}\text{O}$  values in the same range as the observed variation in modern precipitation (from  $-11.2$  to  $-13.8\text{‰}$ ) are found in freshwaters located in the northern Estonian coastal regions close to the outcrop area of the aquifer system (Fig. 2). Their lateral distribution coincides with the location of the deep buried valleys in northern Estonia that are filled with Quaternary sediments (Perens and Vallner, 1997) (Fig. 3b). These erosional valleys cut through the host rocks of the O-Cm aquifer system and expose the sequence to the recharge of recent meteoric water (Savitskaja et al., 1995).

South of the outcrop area, away from the areas where the deep buried valleys are distributed, the aquifer system is occupied by freshwaters with significantly depleted isotopic composition ( $\delta^{18}\text{O}$  and  $\delta^2\text{H}$  values from  $-14.3\text{‰}$  to  $-22.4\text{‰}$  and from  $-104\text{‰}$  to  $-169\text{‰}$ , respectively) with respect to modern precipitation (Figs. 3b and 4). This indicates that these waters have originated from recharge under colder climate conditions compared to the present. The periods with such conditions in the research area have been rare in Holocene and Late Glacial period. Their duration and magnitude has not been sufficient to produce precipitation with isotopic composition in the same range with these freshwaters. For example, Arppe and Karhu (2010) have suggested that the mean  $\delta^{18}\text{O}$  value of precipitation in Estonia during the Younger Dryas cold stage that represents the period with coldest climate conditions in the area during the last 12.5 ka, was only  $\sim -15.3\text{‰}$ . Furthermore, the five previously published radiocarbon activities from the O-Cm aquifer system for waters with  $\delta^{18}\text{O}$  values less than  $-14\text{‰}$  range from 2.5 to 4.5 pmC (Vaikmäe et al., 2001). Although Vaikmäe et al. (2001) did not calculate the  $^{14}\text{C}$  model ages based on this data, it is highly unlikely that the recharge of these waters took place during Holocene and Late Glacial period when the corresponding  $\delta^{18}\text{O}$  values are taken into account.

The most probable source for isotopically light water in O-Cm aquifer is glacial meltwater from ice sheets that covered the area in Pleistocene. The BAB area has been subject to multiple glaciations from at least Elsterian to Weichselian with the Scandinavian Ice Sheet extending southwards to northern Poland and northern Belarus in the LGM (ca 20–22 ka BP) (Kalm, 2006, 2013). The  $\delta^{18}\text{O}$  values from  $-19\text{‰}$  to  $-25\text{‰}$  have been reported for glacial meltwaters from Scandinavian Ice Sheet (Olausson, 1982; Pitkänen et al.,

1999) which fall in the same range with the most negative values found in freshwaters of the O-Cm aquifer system. Furthermore, Vaikmäe et al. (2001) and Raidla et al. (2009) have shown that the freshwaters with  $\delta^{18}\text{O}$  values less than  $-18\text{‰}$  in the underlying Cambrian-Vendian aquifer system originate from the subglacial meltwater recharge from the Scandinavian Ice Sheet.

The maximum thickness of the Scandinavian Ice Sheet during the Late Weichselian over the northern part of the BAB (i.e. Estonian and Latvian territory) reached  $\sim 2000$  m (Siebert and Dowdeswell, 2004). The evidence from previous studies in the areas affected by continental glaciations in North America suggest that increased hydraulic heads of the ice sheets evoked recharge of glacial meltwater to the proglacial sedimentary aquifers reversing the regional groundwater flow (e.g. Siegel, 1989; Stueber and Walter, 1991, 1994; Grasby et al., 2000; McIntosh et al., 2002; McIntosh and Walter, 2005, 2006; Ferguson et al., 2007; Person et al., 2007; McIntosh et al., 2011). Jöeleht (1998) has shown that molten conditions existed under the Scandinavian Ice Sheet in Estonian territory at least during the Late Weichselian glaciation making the recharge of subglacial meltwater to the proglacial aquifers of the BAB possible.

#### 4.2. Brackish waters, saline waters and brines in the southern part of aquifer system

About 400 km southward from the northern coastal areas of Estonia Na-Cl type brines are found in the O-Cm aquifer system with  $\text{Cl}^-$  concentrations and  $\delta^{18}\text{O}$  values of  $\sim 2000$  mmol  $\text{L}^{-1}$  and  $\sim -4.8\text{‰}$ , respectively (Table 15; Babre et al., 2016). The salinity of groundwater in the aquifer system decreases in northerly directions and brackish Na-Cl waters appear in southern Estonia (Figs. 2 and 3). The  $\delta^{18}\text{O}$  values also decrease from a mean value of  $-4.8\text{‰}$  in brines to minimum values of  $-17.6\text{‰}$  in brackish waters (Table 15). The relative residence times of different water types in the aquifer system can be disclosed using conservative chemical tracers (e.g. Rb, Cs, Sr, Li) whose concentrations increase with time (Edmunds and Smeadly, 2000).  $\text{Li}^+$  concentrations in O-Cm aquifer system rise with increasing  $\text{Cl}^-$  concentrations (Fig. 5a) and the  $\text{Li}^+$  concentrations in brackish waters exceed those found in freshwaters. This suggests that the brackish Na-Cl waters have relatively longer residence times compared to the freshwaters in the aquifer system. Thus, these brackish waters have probably evolved from the formation water that occupied the aquifer system prior to the glacial meltwater intrusion.

The  $\delta^{18}\text{O}$  and  $\delta^2\text{H}$  values in brackish water plot close to the GMWL while the brines in the central part of the BAB plot below the GMWL (Fig. 4). This indicates that these brines do not originate directly from meteoric recharge. The origin of chloride in saline waters and brines have been associated with various diagenetic processes in formation waters such as the dissolution of the late stage evaporates (e.g. halite), the entrapment and/or infiltration of evaporated seawater or membrane filtration (Hem, 1985; Kharaka and Hanor, 2007). There is no evidence for the occurrence of halite in the Lower Ordovician and Cambrian sedimentary rocks in the BAB. Pseudomorphs of halite crystals have only been reported from the Devonian sedimentary rocks in the central parts of the BAB (Kalvans, 2012). These rocks are separated from the host rocks of the O-Cm aquifer system by  $\sim 500$  m of Silurian and Ordovician deposits (Juodkazis, 1980). In the absence of a direct contact with evaporates the high chloride concentrations found in these waters suggest that they have most likely evolved from evaporated seawater. In many sedimentary basins in North America evidence of brines originating from remnant evaporated seawater has been found (e.g. Stueber and Walter, 1991; Wilson and Long, 1993; Lampen and Rostron, 2000). The heavy mean  $\delta^{18}\text{O}$  value of  $-4.6\text{‰}$  in Na-Cl brines is close to the value of  $0 \pm 2\text{‰}$  reported by

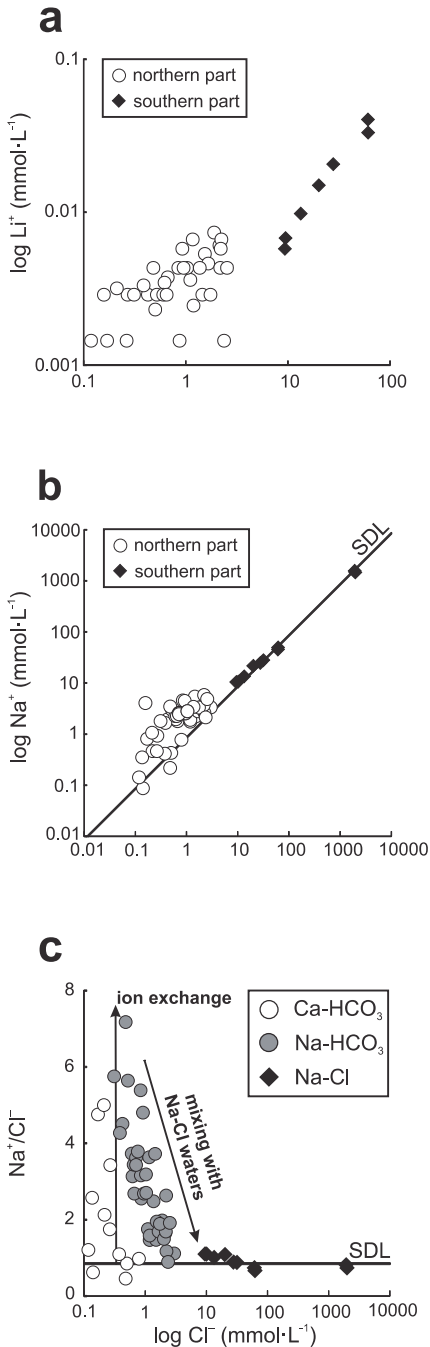


Fig. 5. (a)  $\text{Li}^+$  concentrations, (b)  $\text{Na}^+$  concentrations and (c)  $\text{Na}^+/\text{Cl}^-$  ratio versus  $\text{Cl}^-$  concentrations of groundwater in the O-Cm aquifer system. SDL (seawater dilution line) with a  $\text{Na}^+/\text{Cl}^-$  molar ratio of 0.85 is shown for reference.

Muehlenbachs (1998) for the ice-free Palaeozoic ocean water. The specific origin of these brines requires further studies but Mokrik (1997) has suggested that meteoric waters replaced the original connate seawater within the Cambrian sedimentary rocks during the Middle-Late Cambrian uplift of the BAB area and the seawater again intruded the sediments during a period from Ordovician to Devonian when the basin was considerably subsidised.

#### 4.3. Mixing

Variations in the oxygen isotope composition of different water types implies that mixing between waters originating from different end-members has occurred in the O-Cm aquifer system. Mixing processes that have been initiated by the co-existence of waters with different chemical and isotopic compositions have been reported from many groundwater systems around the world (e.g. Douglas et al., 2000; Pitkänen et al., 1999; Cartwright et al., 2012). These mixing processes can be disclosed using chloride concentrations and  $\delta^{18}\text{O}$  values that serve as conservative geochemical tracers which are not effected by water-rock interactions especially in low-temperature systems (Hem, 1985; Geyh, 2000). The three mixing end-members in the O-Cm aquifer system can be defined as follows:

1. Modern precipitation, with annual weighted mean  $\delta^{18}\text{O}$  value of  $-10.4\text{‰}$  (Punning et al., 1987) and low  $\text{Cl}^-$  concentration of  $0.06 \text{ mmol L}^{-1}$  (Treier et al., 2004);
2. Brine, with more positive isotopic composition compared to modern precipitation and high salinity. The end-member is represented by Na-Cl brines in Riga area, Latvia with a mean  $\delta^{18}\text{O}$  value of  $-4.8\text{‰}$  and  $\text{Cl}^-$  concentration of  $2000 \text{ mmol L}^{-1}$  (Babre et al., 2016);
3. The end-member representing glacial meltwater. The values characterizing this end-member have the largest uncertainty due to notable differences in both  $\delta^{18}\text{O}$  values and  $\text{Cl}^-$  concentrations that probably existed between different parts of the Scandinavian Ice Sheet. The  $\delta^{18}\text{O}$  values of the Pleistocene continental ice sheets have been estimated to have been  $-30\text{‰}$  and less (Dansgaard and Tauber, 1969). For glacial meltwaters from the Laurentide Ice Sheet in North America and from the Scandinavian Ice Sheet in northern Europe the  $\delta^{18}\text{O}$  values ranging from  $-17\text{‰}$  to  $-25\text{‰}$  (Remenda et al., 1994; Person et al., 2007) and from  $-19\text{‰}$  to  $-25\text{‰}$  (Olausson, 1982; Pitkänen et al., 1999) have been estimated, respectively. Groundwater in the Cambrian-Vendian aquifer system originating from isotopically light subglacial recharge of meltwater from the Scandinavian Ice Sheet is characterized by  $\delta^{18}\text{O}$  values from  $-18.5\text{‰}$  to  $-23\text{‰}$  (Vaikmäe et al., 2001; Raidla et al., 2009). The  $\text{Cl}^-$  concentrations found in the meltwaters of the modern continental ice sheets of Antarctica and Greenland range from  $\sim 0.01$  to  $1 \text{ mmol L}^{-1}$  (Brown, 2002; Yde et al., 2005). All things considered, the chosen end-member is characterized by the mean values of the expected variability in glacial meltwater with a  $\delta^{18}\text{O}$  value of  $-25\text{‰}$  and  $\text{Cl}^-$  concentration of  $0.1 \text{ mmol L}^{-1}$ .

The relationship between chloride and  $\delta^{18}\text{O}$  confirms a three-component mixing trend between waters originating from modern precipitation, glacial meltwater and brine end-members in the O-Cm aquifer system (Fig. 6). This trend is similar to that reported from the underlying Cambrian-Vendian aquifer system in the northern part of the BAB by Raidla et al. (2009) and to mixing relationships observed in groundwater from the Canadian Shield (e.g. Clark et al., 2000; Douglas et al., 2000; Stotler et al., 2012).

The differences in isotopic composition and in relative residence

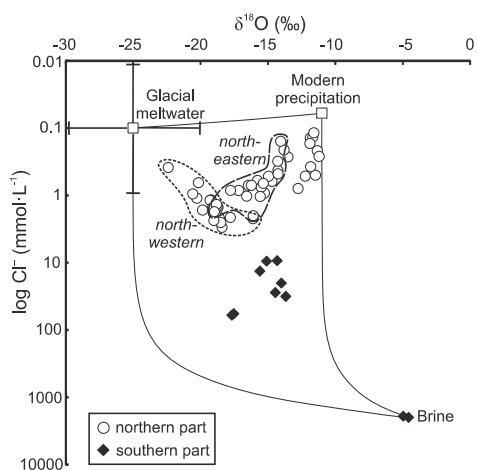


**Fig. 6.**  $\delta^{18}\text{O}$  values and  $\text{Cl}^-$  concentrations of groundwater in the O-Cm aquifer system and the end-members representing modern precipitation, glacial meltwater and brine. The definitions of the end-members are given in the text. The  $\delta^{18}\text{O}$  and  $\text{Cl}^-$  error bars shown for end-member representing glacial meltwater are based on the discussion in the text.

times of the O-Cm groundwater suggests that mixing between waters originating from different end-members has not been simultaneous. The mixing processes in the aquifer system have occurred in two separate stages. Firstly, the pre-glacial Na-Cl type formation waters were displaced by freshwaters originating from glacial meltwater recharge in the northern part of the aquifer system due to reversal of groundwater flow under high hydraulic gradient imposed by the Scandinavian Ice Sheet (Fig. 7). After the retreat of the ice sheet the recharge of meteoric waters occurred mainly through deep buried valley systems in northern and north-eastern parts of the aquifer system. These meteoric waters then mixed with freshwaters originating from glacial meltwater recharge. This process has been more pronounced in the north-eastern part of the aquifer system as the freshwaters with glacial origin from this part plot progressively closer to the modern precipitation end-member (Fig. 6). The isotopic composition of freshwaters in the aquifer system is characterized by less depleted values in the north-eastern part (Fig. 3b) with  $\delta^{18}\text{O}$  values ranging

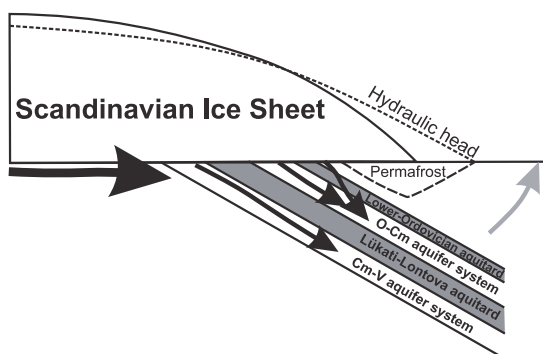


**Fig. 7.** A schematic section illustrating a possible mechanism for glacial meltwater recharge in the northern part of the BAB.

from  $-14.3\text{‰}$  to  $-19.0\text{‰}$ , whereas  $\delta^{18}\text{O}$  values in the north-western part vary from  $-15.3\text{‰}$  to  $-22.4\text{‰}$ . This can be related to the fact that the argillaceous rocks that form an important part of the overlying Lower Ordovician aquitard grow thinner towards the east and become intercalated with numerous quartzose silt beds (Voolma et al., 2013). Thus, the transversal conductivity of the overlying Lower-Ordovician aquitard is increased in easterly directions, which has made freshwaters in this part of the aquifer system more susceptible to recharge from the upper strata. Waters with  $\delta^{18}\text{O}$  values less than  $-18.0\text{‰}$  from the north-eastern part of the aquifer system plot on the same area in Fig. 6 as waters from north-western part of the aquifer system. This could mean that waters with  $\delta^{18}\text{O}$  values less than  $-18.0\text{‰}$  have been affected by similar hydrochemical evolution trends, while waters with  $\delta^{18}\text{O}$  values higher than  $-18.0\text{‰}$  have evolved through a slightly different evolutionary pathway.

#### 4.4. Dissolution of silicates and ion exchange

The  $\text{Na}^+$  and  $\text{Cl}^-$  relationships show that the brackish Na-Cl waters from the southern part of the aquifer system plot close to the seawater dilution line (SDL) with  $\text{Na}^+/\text{Cl}^-$  molar ratio of 0.85 (Fig. 5b). Freshwaters from the northern part of the aquifer system deviate from this relationship having  $\text{Na}^+/\text{Cl}^-$  values which exceed the marine values. This shows that these freshwaters have gained an excess amount of  $\text{Na}^+$  to that expected from mixing with Na-Cl waters.

The surplus of  $\text{Na}^+$  over the marine concentrations has been associated with the silicate mineral dissolution (e.g. albite) or ion exchange reactions (e.g. Toran and Saunders, 1999; Stuyfzand, 2008). Albite is present as an accessory mineral (<5 wt%) in the Cambrian and Lower-Ordovician sandstones (Raidla et al., 2006). However, the kinetics of albite dissolution connote long residence times (Appelo and Postma, 1999). Zhu (2005) has shown that in situ plagioclase dissolution rates in the low-temperature conditions (from  $15\text{ }^\circ\text{C}$  to  $35\text{ }^\circ\text{C}$ ) and in the pH range from 7.5 to 10 are very slow. It would take hundreds of thousands years for a clay coating only a few microns thick to develop. The pH and temperature in freshwaters from the O-Cm aquifer system ranges from 6.9 to 8.5 and from  $7.4\text{ }^\circ\text{C}$  to  $14\text{ }^\circ\text{C}$ , respectively (Table 15). Thus, in the temperature and pH range of groundwater in the O-Cm aquifer system the silicate mineral dissolution is extremely slow and can be considered almost negligible as a source of  $\text{Na}^+$  in freshwaters of the aquifer system.

An alternative explanation for the  $\text{Na}^+$  surplus in O-Cm freshwaters involves ion exchange reactions. Clay minerals, organic matter and oxides/hydroxides can have a certain exchange capacity for cations (and also for anions) due to a charge deficit which arises from substitutions of ions in the structure of the crystal (Appelo and Postma, 1999). This charge imbalance is compensated for by a surface accumulation of ions of opposite charge. The Cambrian and Lower Ordovician sandstones together with the over- and underlying formations contain various minerals with notable cation exchange capacity (Appelo and Postma, 1999) such as illite, illite-smectite, chlorite, glauconite and kaolinite (Kirsimäe and Jørgensen, 2000; Raidla et al., 2006; Voolma et al., 2013).

As shown previously, the O-Cm aquifer system was probably occupied by saline waters prior to glacial meltwater intrusion. The effect of the intrusion of fresh glacial meltwater into a saline water aquifer would have been similar to freshening observed in aquifers of modern coastal areas (e.g. Stuyfzand, 1993; Appelo, 1994; Appelo and Postma, 1999; Walraevens et al., 2001, 2007; Walraevens and Van Camp, 2005; Coetsiers and Walraevens, 2006; Vandenbohede and Lebbe, 2012). When freshwater flushes a salt water aquifer where ion exchangers have absorbed  $\text{Na}^+$ , the ion exchange

reactions are initiated as  $\text{Ca}^{2+}$ ,  $\text{Mg}^{2+}$  and  $\text{K}^+$  that are more strongly bound by the exchanger are taken up from water in return for  $\text{Na}^+$  (Appelo and Postma, 1999). As a consequence, Na-HCO<sub>3</sub> water type evolves. Freshening of aquifers due to recharge of glacial meltwater and the emergence of a related Na-HCO<sub>3</sub> water type has been reported from various sedimentary basins in North America (e.g. Siegel, 1989; McIntosh and Walter, 2006; Ferguson et al., 2007). The same phenomenon is evident in the O-Cm aquifer system. Here freshwaters with more negative isotopic composition ( $\delta^{18}\text{O}$  values  $< -14\text{‰}$ ) are of Na-HCO<sub>3</sub> water type while freshwaters with isotopic composition close to modern precipitation in the area are of Ca-HCO<sub>3</sub> water type.

The importance of freshening and related ion exchange processes on the geochemical evolution of freshwaters in the O-Cm aquifer system is illustrated by changes in the values of the  $\text{Na}^+/\text{Cl}^-$  ratio. Fig. 5c shows that in Ca-HCO<sub>3</sub> and Na-HCO<sub>3</sub> waters the values of  $\text{Na}^+/\text{Cl}^-$  ratio increase while the  $\text{Cl}^-$  concentrations remain stable. Walraevens and Van Camp (2005) have associated a similar pattern in the freshening Ledo-Paniselian aquifer in Flanders with cation exchange. The higher values for  $\text{Na}^+/\text{Cl}^-$  ratios coincide with lower  $\text{Cl}^-$  concentrations and are on average higher in the north-eastern part of the aquifer system, which can refer to the fact that cation exchange has had a more pronounced effect on waters in this part of the aquifer system. The subsequent decrease in  $\text{Na}^+/\text{Cl}^-$  values with increasing  $\text{Cl}^-$  concentrations towards values found in Na-Cl waters can attributed to mixing processes (Walraevens and Van Camp, 2005), which are in turn more pronounced in the north-western part of the aquifer system (see also Fig. 6). Similarly, Raidla et al. (2012) report that the locally occurring ion exchange has increased the  $\text{Na}^+/\text{Cl}^-$  ratio in freshwaters originating from glacial meltwater recharge in the underlying Cambrian-Vendian aquifer system.

Ideally the freshening of aquifers should be characterized by a sequence of water types from Na-HCO<sub>3</sub> to K-HCO<sub>3</sub>, Mg-HCO<sub>3</sub> and Ca-HCO<sub>3</sub>, respectively, which develop in time and along the flow-path as the cation exchange progresses (Chapelle and Knobel, 1983; Appelo, 1994; Appelo and Postma, 1999; Walraevens et al., 2007). This pattern of displacement chromatography may be obscured by flow conditions in aquifers (e.g. mixing of waters of different origin) with only a Na-HCO<sub>3</sub> water type emerging from ion exchange reactions (Appelo, 1994; Walraevens et al., 2007). This seems to be the case in O-Cm aquifer system. The observation that the modern recharge areas contain Ca-HCO<sub>3</sub> waters may indicate that the ion exchange capacity of the exchange sites in these areas has been exhausted.

#### 4.5. Carbonate mineral dissolution

The  $\text{Ca}^{2+}$  and  $\text{Mg}^{2+}$  activities suggest that Ca-HCO<sub>3</sub>, Na-HCO<sub>3</sub> and brackish Na-Cl waters are mainly in equilibrium or slightly saturated with respect to carbonate minerals present as carbonate cement in aquifer rocks ( $\text{SI}_{\text{calcite}}$  and  $\text{SI}_{\text{dolomite}} \sim -0.5$  to 0.5) (Fig. 8; Table 1S). This shows that these freshwaters are buffered by concurrent dissolution of carbonate minerals. Cambrian and Lower Ordovician sandstones are weakly cemented with authigenic carbonate minerals such as Fe-rich dolomite and calcite with average content of 3 wt% and 1 wt%, respectively (Raidla et al., 2006). Additionally, the intruding glacial meltwaters could have been in contact with the overlying Ordovician and Silurian carbonate rocks. Studies in North America have shown that carbonate rocks served as important pathways for transmission of glacial meltwater to the subsurface acting as subglacial drains (e.g. Grasby and Chen, 2005; McIntosh and Walter, 2006; McIntosh et al., 2011).

However, relationships between HCO<sub>3</sub><sup>-</sup>,  $\text{Ca}^{2+}$  and  $\text{Mg}^{2+}$  concentrations and pH values suggest that the influence of carbonate mineral dissolution on the geochemical evolution of freshwaters in O-Cm aquifer system has not been straightforward. The conversion of the dissolved CO<sub>2</sub> to HCO<sub>3</sub><sup>-</sup> should increase the pH values with progressing dissolution as H<sup>+</sup> is consumed. However, the situation in O-Cm freshwaters is reverse. Higher  $\text{Ca}^{2+}$  and HCO<sub>3</sub><sup>-</sup> concentrations coincide with lower pH values (Fig. 9).

This phenomenon can be related to recharge conditions for waters originating from glacial meltwater recharge. The initial dissolution of carbonate minerals would have depended on the concentration of CO<sub>2</sub> that was acquired by the recharging glacial meltwater. The high partial pressures of CO<sub>2</sub> in modern groundwater are mostly derived from the soil zone where bacterial oxidation of vegetation can raise the pCO<sub>2</sub> value from the modern atmospheric value of 10<sup>-3.5</sup> to 10<sup>-1</sup> (Clark and Fritz, 1997). Groundwater originating from glacial meltwater recharge would have carried less carbon dioxide than modern waters due to the fact that the pCO<sub>2</sub> in soils of proglacial areas or areas overlain by a continental ice sheet would have been very low. Raidla et al. (2012) have argued that the undersaturated glacial meltwater that recharged the underlying Cambrian-Vendian aquifer system was characterized by pCO<sub>2</sub> values of ~10<sup>-3.7</sup> which were concordant with the CO<sub>2</sub> concentrations of the atmosphere in the glacial period (Leuenberger et al., 1992). The pH value of waters evolving from such a low pCO<sub>2</sub> would have been  $>8$ , depending on whether the system was geochemically open or closed (Blaser et al., 2010). Thus, groundwater originating from glacial meltwater recharge would

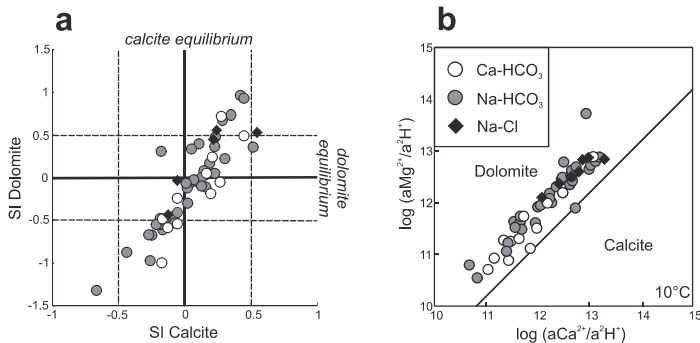


Fig. 8. (a) Saturation indices [ $\text{SI} = \log(\text{IAP}/K)$ ] for calcite and dolomite, calculated using PHREEQC database (Parkhurst and Appelo, 1999). (b) The  $\log(a\text{Ca}^{2+}/a^2\text{H}^+)$  versus  $\log(a\text{Mg}^{2+}/a^2\text{H}^+)$  stability diagram of groundwater in the O-Cm aquifer system at 10 °C. The measured groundwater temperatures range from 7.5 °C to 14 °C in the sampled waters (Table 1S).

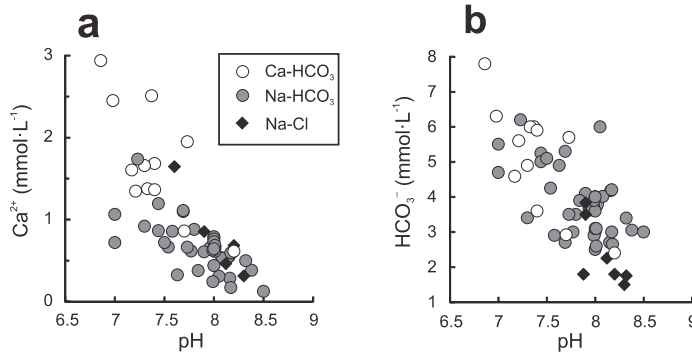


Fig. 9. Relationships between (a)  $\text{Ca}^{2+}$ , (b)  $\text{HCO}_3^-$  concentrations and pH in the O-Cm aquifer system.

have been less aggressive towards carbonate minerals compared to groundwater originating from recent meteoric water. This resulted in higher pH values and lesser amounts of dissolved  $\text{Ca}^{2+}$  and  $\text{HCO}_3^-$  in groundwater and is illustrated by the fact that  $\text{HCO}_3^-$  concentrations in Na- $\text{HCO}_3$  waters decrease with decreasing  $\delta^{18}\text{O}$  values (Fig. 10). Waters which are less affected by mixing with recent meteoric water and have more negative  $\delta^{18}\text{O}$  values are characterized by lower  $\text{HCO}_3^-$  concentrations. The Ca- $\text{HCO}_3$  waters originating from recent meteoric recharge do not display major variations in their isotopic composition with respect to  $\text{HCO}_3^-$  concentrations.

5. Conclusions

Groundwater in the O-Cm aquifer system represents a mixture of waters originating from three end-members: modern precipitation, glacial meltwater and relict Na-Cl brine. During the advances of continental ice sheets in Pleistocene the reversal of groundwater flow under high hydraulic gradient enabled the intrusion of glacial meltwaters into the aquifer system. That reversed the regional groundwater flow and replaced the Na-Cl type formation waters in its northern part. The intrusion of

glacial meltwaters initiated ion exchange reactions and the recharged waters acquired a Na- $\text{HCO}_3$  water type. Towards the deeper parts of the aquifer system these waters mixed with the Na-Cl waters. The second phase of mixing occurred as the meteoric waters recharged into the aquifer system through the deep buried valleys near its outcrop area. The water originating from recent meteoric recharge is represented by Ca- $\text{HCO}_3$  water type which has evolved mainly from carbonate mineral dissolution. The isotopic and chemical composition of groundwater indicates that the O-Cm aquifer system has been hydrodynamically more open in its northern and north-eastern parts and more closed in its north-western and southern parts. The presence of groundwater originating from glacial meltwater recharge in the aquifer system shows that the influence of Pleistocene glaciations on the geochemical evolution of groundwater has been greater compared to the influence of recharge conditions during Holocene.

These findings should be taken into account in future decisions concerning the management of this groundwater resource a large part of the aquifer system contains essentially non-renewable groundwater. A large scale withdrawal of groundwater from the aquifer system related to mining can cause non-reversible changes in the water quality. The study has shown that the Lower Ordovician organic-rich black shale known as graptolite argillite overlying the aquifer system may serve as an important local aquitard. It protects the aquifer system from recharge of recent meteoric water. The economic development of this resource (e.g. mining for trace and REE elements; potential production of shale gas) can increase the transversal conductivity of this aquitard. This in turn can lead to mixing between easily contaminable shallow groundwater and intact palaeogroundwater.

Acknowledgements

The activities of the present study were supported by Estonian Science Foundation Grant ETF8948 (R.V.). The paper is a contribution to the Estonian Research Council Project IUT19-22, PUTJD127 (V.R), IAEA CRP:F33019 (Contract No. 17850) and INQUA/UNESCO supported G@GPS Project. The manuscript was improved by the constructive comments by Prof. Kalle Kirsimäe and an anonymous reviewer. The authors would like to thank Dr. Stéphane Affolter, Dr. Roland Purtschert and Prof. Markus Leuenberger for  $\delta^{18}\text{O}$  and  $\delta^2\text{H}$  measurements from samples with high salinity in the Department of Climate and Environmental Physics at University of Bern and Mati Lelgus from the Geological Survey of Estonia for additional sample collection.

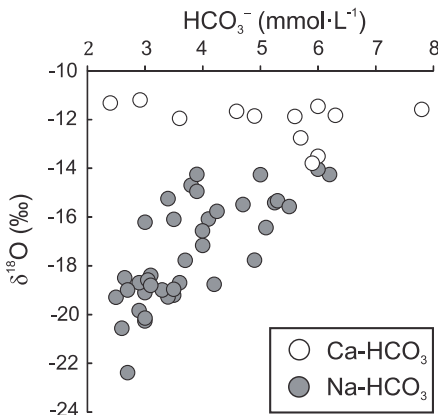


Fig. 10. Relationship between  $\text{HCO}_3^-$  concentrations and  $\delta^{18}\text{O}$  values in freshwaters of Ca- $\text{HCO}_3$  and Na- $\text{HCO}_3$  type in the O-Cm aquifer system.

## Appendix A. Supplementary data

Supplementary data related to this article can be found at <http://dx.doi.org/10.1016/j.apgeochem.2016.07.007>.

## References

- Affolter, S., Fleitmann, D., Leuenberger, M., 2014. New online method for water isotope analysis of speleothem fluid inclusions using laser absorption spectroscopy (WS-CRDS). *Clim. Past*, 10, 1291–1304.
- Appelo, C.A.J., 1994. Cation and proton exchange, pH variations, and carbonate reactions in a freshening aquifer. *Water Resour. Res.* 30, 2793–2805.
- Appelo, C.A.J., Postma, D., 1999. *Geochemistry, Groundwater and Pollution*. A.A. Balkema, Rotterdam.
- Appie, L., Karhu, J.A., 2010. Oxygen isotope values of precipitation and the thermal climate in Europe during the middle to late Weichselian ice age. *Quat. Sci. Rev.* 29, 1263–1275.
- Babre, A., Kalvāns, A., Popovs, K., Retiķe, I., Dēliņa, A., Vaikmāe, R., Martma, T., 2016. Pleistocene age paleo-groundwater inferred from water-stable isotope values in the central part of the Baltic Artesian Basin. *Isot. Environ. Health*. S. <http://dx.doi.org/10.1080/10256016.2016.1168411>.
- Bekele, E., Rostron, B., Person, M., 2003. Fluid pressure implications of erosion unloading, basin hydrodynamics and glaciation in the Alberta Basin, Western Canada. *J. Geochem. Explor* 78–79, 143–147.
- Blaser, P.C., Coetsiers, M., Aeschbach-Hertig, W., Kipfer, R., Van Camp, M., Loosli, H.H., Walraevens, K., 2010. A new groundwater radiocarbon correction approach accounting for palaeoclimate conditions during recharge and hydrochemical evolution: the Ledo-Paniselian Aquifer. *Belg. Appl. Geochem* 25, 437–455.
- Boulton, G.S., Caban, P., van Gijssel, K., 1995. Groundwater flow beneath ice sheets: Part I – large scale patterns. *Quat. Sci. Rev.* 14, 545–562.
- Brand, W.A., Geilmann, H., Crosson, E.R., Rella, C.W., 2009. Cavity ring-down spectroscopy versus high-temperature conversion isotope ratio mass spectrometry: a case study on  $\delta^2\text{H}$  and  $\delta^{18}\text{O}$  of pure water samples and alcohol/water mixtures. *Rapid Commun. Mass Sp.* 23, 1879–1884.
- Brown, G.H., 2002. Glacier meltwater hydrochemistry. *Appl. Geochem* 17, 855–883.
- Cartwright, I., Weaver, T.R., Condón, D.J., Keith Fifield, L., Tweed, S.O., Petrides, B., Swane, I., 2012. Constraining groundwater flow, residence times, inter-aquifer mixing, and aquifer properties using environmental isotopes in the southeast Murray Basin, Australia. *Appl. Geochem* 27, 1698–1709.
- Chapelle, F.H., Knobel, L.L., 1983. Aqueous geochemistry and the exchangeable cation composition of glauconite in the Aquia aquifer. *Md. Ground Water* 21, 343–352.
- Clark, I.D., Fritz, P., 1997. *Environmental Isotopes in Hydrogeology*. CRC Press, New York.
- Clark, I.D., Douglas, M., Raven, K., Bottomley, D., 2000. Recharge and preservation of Laurentide glacial melt water in the Canadian Shield. *Ground Water* 38, 735–742.
- Clayton, R.N., Friedman, I., Graf, D.L., Mayeda, T.K., Meents, W.F., Shimp, N.F., 1966. The origin of saline formation waters. I. Isotopic composition. *J. Geophys. Res.* 71, 3869–3882.
- Coetsiers, M., Walraevens, K., 2006. Chemical characterization of the neogene aquifer, Belgium. *Hydrogeol. J.* 14, 1556–1568.
- Craig, H., 1961. Isotopic variations in meteoric waters. *Science* 133, 1702–1703.
- Dansgaard, W., Tauber, H., 1969. Glacier oxygen-18 content and Pleistocene ocean temperatures. *Science* 166, 499–502.
- Douglas, M., Clark, I.D., Raven, K., Bottomley, D., 2000. Groundwater mixing dynamics at a Canadian Shield mine. *J. Hydrol.* 235, 88–103.
- Edmunds, W.M., Smedley, P.L., 2000. Residence time indicators in groundwater: the East Midlands Triassic sandstone aquifer. *Appl. Geochem* 15, 737–752.
- EGK, 2014. Annual Report of Groundwater Monitoring under National Environmental Monitoring Program for 2013. Geological Survey of Estonia, Tallinn (in Estonian).
- EGK, 2015. Annual Report of Groundwater Monitoring Program under National Environmental Monitoring Program for 2014, Part IV. Geological Survey of Estonia, Tallinn (in Estonian).
- Epstein, S., Mayeda, T., 1953. Variations of the  $\text{O}^{18}$  content of waters from natural sources. *Geochim. Cosmochim. Acta* 4, 213–224.
- Ferguson, G.A.G., Betcher, R.N., Grasby, S.E., 2007. Hydrogeology of the winnipeg formation in Manitoba, Canada. *Hydrogeol. J.* 15, 573–587.
- Geyh, M., 2000. Groundwater. Saturated and Unsaturated Zone. Technical Documents in Hydrology No. 39, vol. IV. UNESCO, Paris.
- Grasby, S.E., Chen, Z., 2005. Subglacial recharge into the Western Canada Sedimentary Basin: impact of Pleistocene glaciation on basin hydrodynamics. *Geol. Soc. Am. Bull.* 117, 500–514.
- Grasby, S.E., Osadetz, K., Betcher, R., Render, F., 2000. Reversal of the regional-scale flow system of the Williston Basin in response to Pleistocene glaciation. *Geology* 29, 635–638.
- Hade, S., Soesoo, A., 2014. Estonian graptolite argillites revisited: a future resource? *Oil Shale* 31, 4–18.
- Hem, J.D., 1985. Study and Interpretation of the Chemical Characteristics of Natural Water. U.S. Geological Survey, Water Supply Paper 2254. USGS Publishing Service Centre. <http://pubs.usgs.gov/wsp/wsp2254>.
- Jampen, H.T., Rostron, B.J., 2000. Hydrogeochemistry of pre-Mississippian brines, Williston basin, Canada—USA. *J. Geochem. Explor* 69–70, 29–35.
- Juodkazis, V.I. (Ed.), 1980. Hydrogeological Map of the Pre-quaternary Deposits of the Soviet Baltic Republics. Ministry of Geology of the USSR.
- Jõelett, A., 1998. Geothermal Studies of the Precambrian Basement and Phanerozoic Sedimentary Cover in Estonia and in Finland. PhD Thesis. Tartu University Press, Tartu.
- Kalm, V., 2006. Pleistocene chronostratigraphy in Estonia, southeastern sector of the Scandinavian glaciation. *Quat. Sci. Rev.* 25, 960–975.
- Kalm, V., 2013. Ice-flow pattern and extent of the last Scandinavian ice sheet southeast of the Baltic Sea. *Quat. Sci. Rev.* 44, 51–59.
- Kalvāns, A., 2012. A list of factors controlling groundwater composition in the Baltic Artesian Basin. In: Delina, A., Kalvāns, A., Saks, T., Beters, U., Vircaus, V. (Eds.), *Highlights of Groundwater Research in the Baltic Artesian Basin*. University of Latvia, pp. 91–105.
- Karro, E., Marandi, A., Vaikmāe, R., 2004. The origin of increased salinity in the Cambrian–Vendian aquifer system on the Kopli Peninsula, northern Estonia. *Hydrogeol. J.* 12, 424–435.
- Kharaka, Y.K., Hanor, J.S., 2007. Deep fluids in the continents: I. Sedimentary basins. In: Drever, J.I. (Ed.), *Surface and Ground Water, Weathering and Soils, Treatise on Geochemistry*, vol. 5. Elsevier, Oxford, pp. 1–48.
- Kirsimäe, K., Jørgensen, R., 2000. Mineralogical and Rb–Sr isotope studies of low-temperature diagenesis of Lower Cambrian clays of the Baltic paleobasin of Northern Estonia. *Clays Clay Min.* 48, 95–105.
- Kivit, A., Petersell, V., Tamm, J., Burova, L., Viigand, A., 1993. Report on Underground Resources in Estonia. Geological Survey of Estonia, Tallinn (in Estonian).
- Lemieux, J.M., Sudicky, E.A., Peltier, W.R., Tarasov, L., 2008. Dynamics of groundwater recharge and seepage over the Canadian landscape during Wisconsinian glaciation. *J. Geophys. Res.* 113, F01011. <http://dx.doi.org/10.1029/2007JF000838>.
- Leuenberger, M., Siegenthaler, U., Langway, C.C., 1992. Carbon isotope composition of  $\text{CO}_2$  during the last ice age from Antarctic ice core. *Nature* 357, 461–466.
- Marandi, A., 2007. Natural Chemical Composition of Groundwater as a Basis for Groundwater Management in the Cambrian–Vendian Aquifer System in Estonia. PhD Thesis. Tartu University Press, Tartu.
- McIntosh, J.C., Walter, L.M., 2005. Volumetrically significant recharge of Pleistocene glacial meltwaters into epiraticic basins: constraints imposed by solute mass balances. *Chem. Geol.* 222, 292–309.
- McIntosh, J.C., Walter, L.M., 2006. Paleowaters in Silurian–Devonian carbonate aquifers: geochemical evolution of groundwater in the Great Lakes region since the late Pleistocene. *Geochim. Cosmochim. Acta* 70, 2454–2479.
- McIntosh, J.C., Walter, L.M., Martini, A.M., 2002. Pleistocene recharge to mid-continent basins: effects on salinity structure and microbial gas generation. *Geochim. Cosmochim. Acta* 66, 1681–1700.
- McIntosh, J.C., Garven, G., Hanor, J.S., 2011. Impacts of Pleistocene glaciation on large-scale groundwater flow and salinity in the Michigan Basin. *Geofluids* 11, 18–33.
- Mokrik, R., 1997. The Palaeohydrogeology of the Baltic Basin. Vendian and Cambrian. Tartu University Press, Tartu.
- Mokrik, R., 2003. The Paleohydrogeology of the Baltic Basin. Neoproterozoic and Phanerozoic. Vilnius University Publishing House, Vilnius.
- Muehlenbachs, K., 1998. The oxygen isotopic composition of the oceans, sediments and the seafloor. *Chem. Geol.* 145, 263–273.
- Olausson, E., 1982. Stable isotopes. In: Olausson, E. (Ed.), *The Pleistocene/Holocene Boundary in South-western Sweden*. Sveriges geologiska undersökning 794E, Uppsala, pp. 82–92.
- Parkhurst, D.L., Appelo, C.A.J., 1999. User's guide to PHREEQC (version 2): a computer program for speciation, batch-reaction, one-dimensional transport, and inverse geochemical calculations. USGS Water Resour. Invest. Rep. 99–4259.
- Perens, R., Vallner, L., 1997. Water-bearing formation. In: Raukas, A., Teedumäe, A. (Eds.), *Geology and Mineral Resources of Estonia*. Estonian Academy Publishers, Tallinn, pp. 137–145.
- Perens, R., Savva, V., Leigus, M., Parm, T., 2001. The Hydrogeochemical Atlas of Estonia. Geological Survey of Estonia, Tallinn (in Estonian).
- Person, M., McIntosh, J.C., Remenda, V., Bense, V., 2007. Pleistocene hydrology of North America: the role of ice sheets in reorganizing groundwater systems. *Rev. Geophys.* 45 <http://dx.doi.org/10.1029/2006RG000206>.
- Piotrowski, J., 1997. Subglacial hydrology in north-western Germany during the last glaciations: groundwater flow, tunnel valleys and hydrological cycles. *Quat. Sci. Rev.* 16, 169–185.
- Pitkänen, P., Luukkonen, A., Ruotsalainen, P., Leino-Forsman, H., Vuorinen, U., 1999. Geochemical Modelling of Groundwater Evolution and Residence Time at the Olkiluoto Site. POSIVA, Posiva Oy, Helsinki, 98–10.
- Punning, J.M., Toots, M., Vaikmāe, R., 1987. Oxygen-18 in Estonian natural waters. *Isotopenpraxis* 23, 232–234.
- Raidla, V., Kirsimäe, K., Bitukova, L., Jõelett, A., Shogenova, A., Šliaupa, S., 2006. Lithology and diagenesis of the poorly consolidated Cambrian siliciclastic sediments in the northern Baltic Sedimentary Basin. *Geol. Q.* 50, 11–22.
- Raidla, V., Kirsimäe, K., Vaikmāe, R., Jõelett, A., Karro, E., Marandi, A., Savitskaja, L., 2009. Geochemical evolution of groundwater in the Cambrian–Vendian aquifer system of the Baltic basin. *Chem. Geol.* 258, 219–231.
- Raidla, V., Kirsimäe, K., Vaikmāe, R., Kaup, E., Martma, T., 2012. Carbon isotope systematics of the Cambrian–Vendian aquifer system in the northern Baltic Basin: implications to the age and evolution of groundwater. *Appl. Geochem* 27, 2042–2052.
- Raidla, V., Kirsimäe, K., Ivask, J., Kaup, E., Knöller, K., Marandi, A., Martma, T.,

- Vaikmäe, R., 2014. Sulphur isotope composition of dissolved sulphate in the Cambrian–Vendian aquifer system in the northern part of the Baltic Artesian Basin. *Chem. Geol.* 383, 147–154.
- Raudsep, R., 1997. Phosphorite. In: Raukas, A., Teedumäe, A. (Eds.), *Geology and Mineral Resources of Estonia*. Estonian Academy Publishers, Tallinn, pp. 331–336.
- Remenda, V.H., Cherry, J.A., Edwards, T.W.D., 1994. Isotopic composition of old ground water from Lake Agassiz: implications for late Pleistocene climate. *Science* 266, 1975–1978.
- Savitskaja, L., Viigand, A., Jashtshuk, S., 1995. Report of Microcomponent and Isotope Composition Research in Ordovician-cambrian Aquifer Groundwater for Estimating Drinking Water Quality in North-Estonia. Geological Survey of Estonia, Tallinn (in Estonian).
- Siegel, D.I., 1989. Geochemistry of the Cambrian-Ordovician aquifer system in the northern Midwest, United States. In: *Regional Aquifer-system Analysis—Northern Midwest Aquifer System*. US Geological Survey, pp. D1–D76.
- Siegel, D.I., 1991. Evidence for dilution of deep, confined ground water by vertical recharge of isotopically heavy Pleistocene water. *Geology* 19, 433–436.
- Siegel, D.I., Mandel, R.J., 1984. Isotopic evidence for glacial meltwater recharge to the Cambrian Ordovician aquifer, north-central United States. *Quat. Res.* 22, 328–335.
- Siegert, M.J., Dowdeswell, J.A., 2004. Numerical reconstructions of the Eurasian ice sheet and climate during the late Weichselian. *Quat. Sci. Rev.* 23, 1273–1283.
- Stotler, R.L., Frapce, S.K., Ruskeeniemi, T., Pitkanen, P., Blowes, D.W., 2012. The interglacial–glacial cycle and geochemical evolution of Canadian and Fennoscandian Shield groundwaters. *Geochim. Cosmochim. Acta* 76, 45–67.
- Stueber, A.M., Walter, L.M., 1991. Origin and chemical evolution of formation waters from Silurian–Devonian strata in the Illinois Basin, USA. *Geochim. Cosmochim. Acta* 55, 309–325.
- Stueber, A.M., Walter, L.M., 1994. Glacial recharge and paleohydrologic flow systems in the Illinois Basin: evidence from chemistry of Ordovician carbonate (Galena) formation waters. *Geol. Soc. Am. Bull.* 106, 1430–1439.
- Stuyfzand, P.J., 1989. A new hydrochemical classification of watertypes. *IAHS Publ.* 182, 89–98.
- Stuyfzand, P.J., 1993. *Hydrochemistry and Hydrology of the Coastal Dune Area of the Western Netherlands*. PhD thesis. Free University, Amsterdam.
- Stuyfzand, P.J., 2008. Base exchange indices as indicators of salinization or freshening of (coastal) aquifers. In: *Proc. 20th Salt Water Intrusion Meeting*, June 23–27 2008, Naples (FI) USA. Univ. Florida, pp. 262–265. IFAS Research.
- Toran, L.E., Saunders, J.A., 1999. Modeling alternative paths of chemical evolution of Na–HCO<sub>3</sub>-type groundwater near Oak Ridge, Tennessee, USA. *Hydrogeol. J.* 7, 355–364.
- Treier, K., Pajuste, K., Frey, J., 2004. Recent trends in chemical composition of bulk precipitation at Estonian monitoring stations 1994–2001. *Atmos. Environ.* 38, 7009–7019.
- Vaikmäe, R., Vällner, L., Loosli, H.H., Blaser, P.C., Juillard-Tardent, M., 2001. Palaeogroundwater of glacial origin in the Cambrian–Vendian aquifer of northern Estonia. In: Edmunds, W.M., Milne, C.J. (Eds.), *Palaeowaters of Coastal Europe: Evolution of Groundwater since the Late Pleistocene*, vol. 189. Geological Society, London, pp. 17–27. Special Publications.
- Vaikmäe, R., Kaup, E., Marand, A., Martma, T., Raidla, V., Vällner, L., 2008. The Cambrian–Vendian aquifer, Estonia. In: Edmunds, W.M., Shand, P. (Eds.), *The Natural Baseline Quality of Groundwater*. Blackwell Publishing, pp. 353–371.
- Vandenbohede, A., Lebbe, L., 2012. Groundwater chemistry patterns in the phreatic aquifer of the central Belgian coastal plain. *Appl. Geochem.* 27, 22–36.
- Virbulis, J., Beters, U., Saks, T., Sennikovs, J., Timuhins, A., 2013. Hydrogeological model of the Baltic Artesian Basin. *Hydrogeol. J.* 21, 845–862.
- Voolma, M., Soesoo, A., Hade, S., Hints, R., Kallaste, T., 2013. Geochemical heterogeneity of Estonian graptolite argillite. *Oil Shale* 30, 377–401.
- Walraevens, K., Van Camp, M., Lermytte, J., van der Kemp, W.J.M., Loosli, H.H., 2001. Pleistocene and Holocene groundwaters in the freshening Ledo-Paniselian aquifer in Flanders, Belgium. In: Edmunds, W.M., Milne, C.J. (Eds.), *Palaeowaters in Coastal Europe: Evolution of Groundwater since the Late Pleistocene*. Geological Society, London, pp. 49–70. Special Publications.
- Walraevens, K., Van Camp, M., 2005. Advances in understanding natural groundwater quality controls in coastal aquifers. In: *Groundwater and Saline Intrusion, Selected Papers from the 18th Salt Water Intrusion Meeting, Cartagena 2004, Spain*, pp. 449–463.
- Walraevens, K., Cardenal-Escarcena, J., Van Camp, M., 2007. Reaction transport modeling of a freshening aquifer (tertiary Ledo-Paniselian aquifer, Flanders-Belgium). *Appl. Geochem.* 22, 289–305.
- Wilson, T.P., Long, D.T., 1993. Geochemistry and isotope chemistry of Michigan Basin brines: Devonian formations. *Appl. Geochem.* 8, 81–100.
- Yde, J.C., Knudsen, N.T., Nielsen, O.B., 2005. Glacier hydrochemistry, solute provenance, and chemical denudation at a surge-type glacier in Kuannersuit Kuusuaq, Disko Island, West Greenland. *J. Hydrol.* 300, 172–187.
- Yezhova, M., Polyakov, V., Tkachenko, A., Savitski, L., Belkina, V., 1996. Palaeowaters of North Estonia and their influence on changes of resources and the quality of fresh groundwaters of large coastal water supplies. *Geologija* 19, 37–40.
- Zhu, C., 2005. In situ feldspar dissolution rates in an aquifer. *Geochim. Cosmochim. Acta* 69, 1435–1453.



### **Paper III**

Pärn, Joonas; Affolter, Stéphane; Ivask, Jüri; Johnson, Sean; Kirsimäe, Kalle; Leuenberger, Markus; Martma, Tõnu; Raidla, Valle; Schloemer, Stefan; Sepp, Holar; Vaikmäe, Rein; Walraevens, Kristine (2018). Redox zonation and organic matter oxidation in palaeogroundwater of glacial origin from the Baltic Artesian Basin. *Chemical Geology*, 488, 149–161.





ELSEVIER

Contents lists available at ScienceDirect

Chemical Geology

journal homepage: [www.elsevier.com/locate/chemgeo](http://www.elsevier.com/locate/chemgeo)

## Redox zonation and organic matter oxidation in palaeogroundwater of glacial origin from the Baltic Artesian Basin



Joonas Pärn<sup>a,b,\*</sup>, Stéphane Affolter<sup>c,d</sup>, Jüri Ivask<sup>a</sup>, Sean Johnson<sup>e,f</sup>, Kalle Kirsimäe<sup>g</sup>, Markus Leuenberger<sup>c</sup>, Tõnu Martma<sup>a</sup>, Valle Raidla<sup>a,b</sup>, Stefan Schloemer<sup>h</sup>, Holar Sepp<sup>g</sup>, Rein Vaikmäe<sup>a</sup>, Kristine Walraevens<sup>i</sup>

<sup>a</sup> Department of Geology, Tallinn University of Technology, Ehitajate tee 5, 19086 Tallinn, Estonia

<sup>b</sup> Department of Hydrogeology and Environmental Geology, Geological Survey of Estonia, Kreutzwaldi 5, 44314 Rakvere, Estonia

<sup>c</sup> Climate and Environmental Physics, Physics Institute, University of Bern, 3012 Bern, Switzerland

<sup>d</sup> International Foundation High Altitude Research Stations Jungfraujoch and Gornergrat, 3012 Bern, Switzerland

<sup>e</sup> iCRAG, School of Biological, Earth and Environmental Sciences, University College Cork, Ireland

<sup>f</sup> Institute for Marine and Antarctic Science, University of Tasmania, Hobart, Australia

<sup>g</sup> Department of Geology, University of Tartu, Ravila 14a, 50411 Tartu, Estonia

<sup>h</sup> Federal Institute for Geosciences and Natural Resources (BGR), 30655 Hanover, Germany

<sup>i</sup> Laboratory for Applied Geology and Hydrogeology, Ghent University, B-9000 Ghent, Belgium

### ARTICLE INFO

Editor: Michael E. Böttcher

#### Keywords:

Palaeohydrogeology

Redox zonation

Isotopic composition of sulphate

Bacterial sulphate reduction

### ABSTRACT

Ordovician-Cambrian aquifer system (O-Cm) in the northern part of the Baltic Artesian Basin (BAB), Estonia, is part of a unique groundwater reservoir where groundwater originating from glacial meltwater recharge from the Scandinavian Ice Sheet is preserved. The distribution of redox zones in the anoxic O-Cm aquifer system is unusual. Strongly reducing conditions are found near the modern recharge area characterized by low concentrations of sulphate ( $< 5 \text{ mg L}^{-1}$ ) and the presence of  $\text{CH}_4$  (up to 3.26 vol%). The concentrations of  $\text{SO}_4^{2-}$  increase and concentrations of  $\text{CH}_4$  decrease farther down the groundwater flow path. Sulphate in fresh glacial palaeogroundwater originates probably from pyrite oxidation while brackish waters have gained their sulphate through mixing with relict saline formation waters residing in the deeper parts of the aquifer system. Stable isotopic composition of sulphate, especially relations between  $\delta^{18}\text{O}_{\text{SO}_4}$ - $\delta^{18}\text{O}_{\text{water}}$  ( $\Delta^{18}\text{O}_{\text{SO}_4\text{-H}_2\text{O}}$  from +20.5 to +31.1‰) and  $\delta^{34}\text{S}_{\text{SO}_4}$ - $\delta^{34}\text{S}_{\text{H}_2\text{S}}$  ( $\Delta^{34}\text{S}_{\text{SO}_4\text{-H}_2\text{S}}$  value of +47.9‰) support a widespread occurrence of bacterial sulphate reduction in fresh glacial palaeogroundwater. We propose, that the observed unusual redox zonation is a manifestation of two different flow systems in the O-Cm aquifer system: 1) the topographically driven flow system which drives the infiltration of waters through the overlying carbonate formation in the modern recharge area; 2) the relict flow system farther down the groundwater flow path which developed as a response to large hydraulic gradients imposed by the Scandinavian Ice Sheet in Pleistocene. Thus, the strongly reducing conditions surrounding the modern recharge area may show the extent to which post-glacial recharge has influenced the aquifer system. O-Cm aquifer system is an example of an aquifer that has not reached a near-equilibrium state with respect to present day flow conditions and still exhibits hydrogeochemical patterns established under the influence of a continental ice sheet in Pleistocene.

### 1. Introduction

Although numerous occurrences of groundwater originating from glacial meltwater recharge are known in North America (e.g. Clayton et al., 1966; Siegel and Mandl, 1984; Grasby et al., 2000; McIntosh and Walter, 2006; Person et al., 2007), aquifer systems in the northern part of the Baltic Artesian Basin (BAB) are unique representing the largest known groundwater reservoir in Europe that contains groundwater

originating from glacial meltwaters of the ice sheets that covered Northern Europe in Pleistocene (Vaikmäe et al., 2001; Raidla et al., 2009, 2012; Pärn et al., 2016). These waters form a unique non-renewable groundwater resource and are characterized by the most depleted isotopic composition of groundwater found in Europe ( $\delta^{18}\text{O}$  values from -18 to -23‰; Vaikmäe et al., 2001; Raidla et al., 2009). The  $\delta^{18}\text{O}$  values in these waters are > 8‰ depleted with respect to annual weighted mean  $\delta^{18}\text{O}$  composition of modern precipitation

\* Corresponding author at: Department of Geology at Tallinn University of Technology, Ehitajate tee 5, 19086 Tallinn, Estonia.

E-mail address: [joonas.parn@ttu.ee](mailto:joonas.parn@ttu.ee) (J. Pärn).

<https://doi.org/10.1016/j.chemgeo.2018.04.027>

Received 13 October 2017; Received in revised form 16 April 2018; Accepted 22 April 2018

Available online 24 April 2018

0009-2541/© 2018 Elsevier B.V. All rights reserved.

(~ -10.3‰, IAEA/WMO, 2017). Since the termination of the Last Weichselian glaciation, topographically driven recharge of meteoric water has reorganized groundwater flow patterns in the BAB and the non-renewable glacial palaeogroundwater has been gradually displaced. In shallow aquifer systems, this process has run close to completion but in deeper aquifer systems of Ordovician-Cambrian and Cambrian-Vendian that are more isolated from modern hydrological cycle, large volumes of glacial palaeogroundwater are still preserved.

Previous studies have shown that glacial palaeogroundwater in the BAB has been influenced by mixing with modern meteoric water (Raidla et al., 2009; Pärn et al., 2016). However, the post-glacial time period after the end of the LGM has been in many cases too short for aquifers to adjust to a new equilibrium after the retreat of large Pleistocene ice sheets (e.g. Bense and Person, 2008; Rousseau-Guettin et al., 2013; Gerber et al., 2017). The extent to which modern hydrologic conditions have influenced glacial palaeogroundwater in the BAB can be assessed by the distribution of redox zones that have developed along the groundwater flow path.

In theory, the oxidative breakdown of organic matter in an aquifer proceeds along a groundwater flow path from aerobic respiration to denitrification, manganese reduction, iron reduction, sulphate reduction and methanogenesis. These subsequent pathways are manifested in depletion of the reactants (i.e.  $O_2(aq)$ ,  $NO_3^-$ ,  $SO_4^{2-}$ ) or in the accumulation of reaction products (i.e.  $Mn^{2+}$ ,  $Fe^{2+}$ ,  $CH_4$ ) in groundwater. The segregation of different terminal electron accepting processes between distinct zones along a groundwater flow path has been explained by the decreasing thermodynamic free energy yield from subsequent redox reactions (Bernier, 1981), the competitive exclusion of bacteria mediating these reactions (e.g. Chapelle and Lovley, 1992; Lovley and Chapelle, 1995) and by a partial-equilibrium model (Postma and Jakobsen, 1996). The latter model states that the initial fermentation of organic matter is rate limiting, while the subsequent processes using different terminal electron acceptors are much faster and approach chemical equilibrium. The spatial separation of the dominant terminal electron accepting processes along groundwater flow path may not be as strict as described earlier (e.g. Jakobsen and Postma, 1994, 1999; Park et al., 2006). Differences in both the stability and concentrations of reactants participating in redox reactions together with the hydrogeochemical conditions (e.g. type of iron-hydroxide, concentrations of sulphate, pH) influence which of the terminal electron accepting processes is thermodynamically favoured (Postma and Jakobsen, 1996). This can lead to simultaneous occurrence of several redox reactions (e.g. iron reduction and sulphate reduction, Simpkins and Parkin, 1993; Jakobsen and Postma, 1999; Park et al., 2006).

Several classifications have been proposed to differentiate between redox zones based on the concentrations of dissolved redox sensitive substances (e.g. Stuyfzand, 1993; Coetsiers and Walraevens, 2006). However, due to the possibility that various terminal electron accepting processes can proceed simultaneously in nature, other parameters may be necessary to determine which terminal electron acceptor is actually used for oxidation of organic matter. One of such parameters is the isotopic composition of dissolved sulphate ( $\delta^{34}S_{SO_4}$  and  $\delta^{18}O_{SO_4}$ ) which can help to differentiate between processes related to organic matter oxidation (i.e. bacterial sulphate reduction) and other chemical reactions (e.g. oxidation of reduced sulphur compounds). In a closed system with limited sulphate (re-)supply the  $\delta^{34}S_{SO_4}$  values of remaining  $SO_4^{2-}$  increase as sulphate is consumed because the lighter  $^{32}S$  isotope is preferentially selected in the enzymatic steps that lead to the production of hydrogen sulphide (Canfield, 2001). Both in natural environments and laboratory experiments enrichments of up to 72% in  $\delta^{34}S$  between residual sulphate and produced hydrogen sulphide have been observed (e.g. Wortmann et al., 2007; Canfield et al., 2010; Sim et al., 2011). On the other hand,  $\delta^{34}S$  values of sulphate produced by pyrite oxidation should lie close to  $\delta^{34}S$  values in parent minerals with reported values for sulphur isotope fractionation between sulphate and pyrite ranging from -2‰ to 0‰ (e.g. Balci et al., 2007; Pisapia et al.,

2007; Mazumdar et al., 2008; Heidel and Tichomirowa, 2010, 2011). Pyrite oxidation should only impart a small positive fractionation on the  $\delta^{18}O_{SO_4}$  value of the product sulphate in the range from +2.3 to +4.0‰ relative to ambient water (e.g. Van Stempvoort and Krouse, 1994; Balci et al., 2007; Mazumdar et al., 2008; Heidel and Tichomirowa, 2011). The oxygen isotope composition of residual sulphate during microbial sulphate reduction forms as a result of microbially mediated oxygen isotope exchange with ambient water (Mizutani and Rafer, 1973; Fritz et al., 1989). Isotopic exchange is supposed to occur through cell-internal sulfoxo-intermediates (e.g. sulphite) and sulphate-enzyme complexes (Brunner et al., 2005, 2012; Mangalo et al., 2007; Wortmann et al., 2007; Farquhar et al., 2008; Müller et al., 2013; Antler et al., 2013). This leads to a so-called “apparent oxygen equilibrium fractionation” (Turchyn et al., 2010) between the residual sulphate and water in order of +25 to +30‰ at temperatures between 25 °C and 5 °C, respectively, which is much larger than the  $\delta^{18}O_{SO_4}$  enrichment during pyrite oxidation (Fritz et al., 1989; Böttcher et al., 1998; Wortmann et al., 2007). The isotopic composition of the dissolved sulphate has also been used successfully in a number of case studies to identify the origin of waters in an aquifer and to study processes of inter-aquifer mixing (e.g. Fouillac et al., 1990; Dogramaci et al., 2001; Samborska and Halas, 2010; Labotka et al., 2016).

Previous studies have highlighted the important influence of redox reactions and organic matter oxidation on the hydrochemical evolution of glacial palaeogroundwater in the BAB (Raidla et al., 2012, 2014). However, these previous studies carried out in the Cambrian-Vendian aquifer system have been limited to wells situated near the northern margin of the BAB (Raidla et al., 2009) and due to their limited spatial distribution, the regional sequence of redox zones could not be studied. Ordovician-Cambrian (O-Cm) aquifer system offers more suitable conditions for studying the regional succession of redox zones in glacial palaeogroundwater as the wells that open the aquifer system cover the whole of the northern BAB. In this contribution, we study the influence of organic matter oxidation on the hydrochemical evolution of the O-Cm aquifer system using both hydrochemical and stable isotope data. More specifically, we aim to give an account of the distribution of redox zones in the aquifer system and the mechanisms that control it. We also aim to elucidate whether and to what extent the observed redox zonation in the aquifer system is related to the relict groundwater flow patterns established in Pleistocene and to what extent it responds to modern hydrologic conditions. The identification of mechanisms controlling redox zonation in the O-Cm aquifer system 1) enables to establish whether and to which extent the O-Cm aquifer system is in equilibrium with modern hydrologic conditions and 2) is required for the future interpretations of groundwater age in the aquifer system by means of  $^{14}C$  dating.

## 2. Geology and hydrogeological setting

O-Cm aquifer system is a confined water body in the northern part of the BAB hosted by sand- and siltstones of Cambrian and Early Ordovician age. The rocks forming the O-Cm aquifer system are distributed in most of the Estonian territory, except in a narrow coastal region of northern Estonia (Fig. 1). The thickness of the aquifer system increases from 20 to 60 m in northern Estonia to ~120 m in Latvia (Juodkakis (responsible editor, 1980; Savitskaja et al., 1995; Perens and Vallner, 1997). The depth of the aquifer system strata is 10–20 m below ground surface in northern Estonia and increases southward to over 1000 m in Latvia and Lithuania. O-Cm aquifer system merges with the underlying Cambrian-Vendian aquifer system in the south-western Estonia to form a single Cambrian aquifer system in the deeper parts of the BAB (Perens and Vallner, 1997).

Cambrian and Lower Ordovician sandstones forming the aquifer matrix are mainly quartz arenites or subarkoses, with quartz content up to 90% (Raidla et al., 2006). In addition, they contain accessory phosphorite (authigenic apatite) and are cemented with carbonate

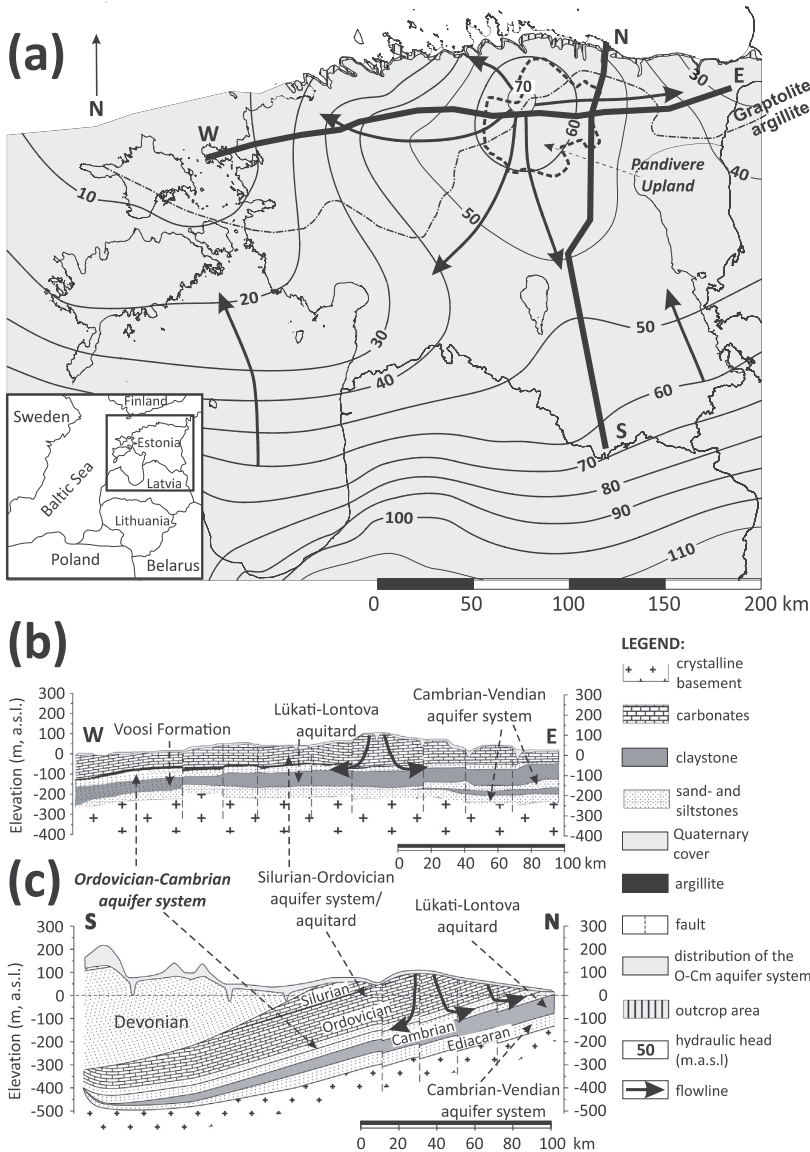


**Fig. 1.** (a) Location and distribution of the Ordovician-Cambrian (O-Cm) aquifer system in the northern part of the Baltic Artesian Basin (BAB) together with the distribution of pre-development freshwater heads (m.a.s.l.) and conceptual groundwater flow paths. Freshwater heads are calculated based on hydraulic head measurements given in Tšeban (1966) and Takcidi (1999). The distribution of Lower Ordovician black shale (graptolite argillite) and the outcrop area of the aquifer system together with the location of Pandivere Upland are shown for reference; (b) the west-east cross-section of northern BAB; (c) the north-south cross-section of the northern BAB.

minerals (mainly Fe-dolomite), whose abundance varies from 0 to 29 wt % with an average value of 3% (Raidla et al., 2006). The average content of pyrite and hematite is close to 1% or less (Raidla et al., 2006). Hematite is the most abundant Fe(III)-oxide in the aquifer matrix, but the occurrence of secondary goethite has also been reported (Mens and Pirrus, 1997; Raidla et al., 2006). Also, dispersed sedimentary organic matter of sapropelitic type can be found from the Cambrian sandstones in the underlying Lontova clays (total organic matter content of 0.8–2.6%; Raidla et al., 2006 and references therein). No sulphate-bearing evaporite minerals (i.e. anhydrite, gypsum) are present neither in the aquifer matrix nor in the overlying carbonate rocks of Ordovician and Silurian age. The lateral hydraulic conductivity of Cambrian and Lower Ordovician sandstones ranges from 1 to 3 m d<sup>-1</sup>

(from 1.2·10<sup>-5</sup> to 3.5·10<sup>-5</sup> m s<sup>-1</sup>; Perens and Vallner, 1997). Transmissivity ranges from 25 to 50 m<sup>2</sup> d<sup>-1</sup> (from 2.9·10<sup>-4</sup> to 5.8·10<sup>-4</sup> m<sup>2</sup> s<sup>-1</sup>) in northern Estonia and from 80 to 130 m<sup>2</sup> d<sup>-1</sup> (from 9.3·10<sup>-4</sup> to 1.5·10<sup>-3</sup> m<sup>2</sup> s<sup>-1</sup>) in southern Estonia due to the increased thickness of the water-bearing rocks (Savitskaja et al., 1995; Perens and Vallner, 1997).

The aquifer system is confined by the overlying Silurian-Ordovician regional aquitard. The northern part of this aquitard consists of Lower Ordovician limestones, marls, siltstones, clays and most importantly black shale (graptolite argillite), extending 100 km southward from Estonia's northern coast (Fig. 1). The overlying Lower Ordovician graptolite argillite is characterized by high abundance of pyrite (on average 2.4–6% of mineral phases) and is rich in sedimentary organic

matter (total organic content of 15–20%; Petersell, 1997). This organic matter is an immature low-sulphur, oil-prone Type II kerogen (Kosakowski et al., 2017). The whole Silurian-Ordovician sedimentary sequence can be viewed as a regional aquitard at increasing depths > 75 m (Perens and Vallner, 1997). The transversal hydraulic conductivity of the Silurian-Ordovician regional aquitard ranges from  $10^{-7}$  to  $10^{-5}$  m·d<sup>-1</sup> (from  $1.2 \cdot 10^{-12}$  to  $1.2 \cdot 10^{-10}$  m·s<sup>-1</sup>; Perens and Vallner, 1997). The Silurian-Ordovician regional aquitard contains various beds rich in organic matter, the most prominent of which is the Middle Ordovician oil shale (kukersite) in Kukruste Formation with the organic matter content of 10–60% (Bauert and Kattai, 1997). This organic matter in the Middle Ordovician oil shale is prevalently an immature Type I kerogen (Bauert and Kattai, 1997).

The O-Cm aquifer system is separated from the underlying Cambrian-Vendian aquifer system by the Lükati-Lontova regional aquitard which consists of siltstones and clays of the Lower Cambrian Lükati and Lontova Formations that have a transversal hydraulic conductivity of  $10^{-7}$  m·d<sup>-1</sup> ( $1.2 \cdot 10^{-12}$  m·s<sup>-1</sup>; Perens and Vallner, 1997). In western Estonia, this aquitard is laterally replaced by siltstones and sandstones of the Voosi Formation (Fig. 1b). The aquitard becomes sandier and thinner and its transversal hydraulic conductivity increases to  $\geq 10^{-5}$  m·d<sup>-1</sup> ( $\geq 1.2 \cdot 10^{-10}$  m·s<sup>-1</sup>; Perens and Vallner, 1997).

The thickness of the overlying carbonate formation is < 20 m near the outcrop area of the aquifer system (Fig. 1). In this area groundwater with chemical and isotopic composition similar to shallow aquifers recharged by modern precipitation can be found ( $\delta^{18}\text{O}$  values from -11.2 to -12.8‰; Pärn et al., 2016; Raidla et al., 2016). Modern recharge area of the aquifer system is situated in northern Estonia in the Pandivere Upland farther inland from the outcrop area. Pandivere Upland is characterized by heights ranging from 85 to 170 m.a.s.l (Fig. 1). In this area, the highest freshwater heads in the aquifer system can be found (50–70 m.a.s.l.; Fig. 1) that decrease radially in northern Estonia. Due to the increased thickness (> 100 m) of overlying carbonate rocks in the modern recharge area, the modern groundwater recharge is slow. This is exemplified by the fact that the isotopic composition of groundwater in the recharge area is significantly depleted ( $\delta^{18}\text{O}$  values from -14 to -17‰; Pärn et al., 2016) with respect to values found both in modern precipitation (about -10.3‰; IAEA/WMO, 2017) and in shallow aquifers (from -11.5 to -12.5‰; Raidla et al., 2016). This suggests that an important fraction of glacial palaeogroundwater is still present there. The fraction of glacial palaeogroundwater increases farther down the groundwater flow path with decreasing freshwater heads, which is manifested in the decrease of  $\delta^{18}\text{O}$  values down to ~-22‰ (Pärn et al., 2016). Both the modern groundwater in the vicinity of the outcrop area and glacial palaeogroundwater are fresh (TDS from 200 to 600 mg·L<sup>-1</sup>) and are characterized by Ca-HCO<sub>3</sub> and Na-HCO<sub>3</sub> water types, respectively (Pärn et al., 2016).

In deeper southern parts of the aquifer system the salinity of water gradually increases from brackish (TDS from 700 to 19,000 mg·L<sup>-1</sup>) to brine (TDS > 100 g·L<sup>-1</sup>) accompanied by an increase in freshwater heads (Raidla et al., 2009; Pärn et al., 2016; Babre et al., 2016; Gerber et al., 2017; Fig. 1). Together with the increasing salinity, the water type changes to Na-Cl. High freshwater heads in the southern parts of the aquifer system result from high salinity of groundwater (TDS up to ~150 g·L<sup>-1</sup>; Takicidi, 1999; Babre et al., 2016). The isotopic composition of these more saline waters also changes with increasing salinity. The  $\delta^{18}\text{O}$  values in brackish groundwater (from -13.7 to -17.3‰) are depleted with respect to  $\delta^{18}\text{O}$  values in saline groundwater (from -9 to -12.6‰) that are in turn depleted with respect to  $\delta^{18}\text{O}$  values in brine ( $\delta^{18}\text{O}$  values of about -4.5‰; Raidla et al., 2009; Pärn et al., 2016; Babre et al., 2016; Gerber et al., 2017). The origin of deep formation waters in the O-Cm and Cambrian aquifer systems have been related to relict seawater (Mokrik, 1997; Pärn et al., 2016; Gerber et al., 2017). Their composition, however, is influenced by mixing with freshwaters from the northern part of the BAB as manifested in changes in their

chemical and isotopic composition (Raidla et al., 2009; Pärn et al., 2016; Gerber et al., 2017).

### 3. Material and methods

To describe the redox zonation of the O-Cm aquifer system, a database containing published (Tšeban, 1966; Savitskaja et al., 1995; Pärn et al., 2016; EELIS, 2017; ESTEA, 2017) and previously unpublished report data from 134 wells was used (Table S1, supplementary material). The maps depicting the spatial distribution of redox sensitive dissolved substances (Fig. 2a-c) are compiled using residual kriging (cf. Hatvani et al., 2017). In addition to earlier hydrochemical data, 19 groundwater samples were collected from operational private, municipal water supply and observation wells screened in the O-Cm and Cambrian-Vendian aquifer systems in northern part of the BAB (Estonia) during two fieldwork campaigns in 2015 and 2016 for the analysis of hydrochemistry and stable isotopes ( $\delta^2\text{H}$ ,  $\delta^{18}\text{O}$ ,  $\delta^{13}\text{C}$ ,  $\delta^{34}\text{S}_{\text{SO}_4}$ ,  $\delta^{18}\text{O}_{\text{SO}_4}$ ; Table 1).

Water samples were collected into HDPE bottles once pH, electric conductivity values and dissolved O<sub>2</sub> levels had stabilized. The pH, temperature, electric conductivity and dissolved oxygen were measured in the field using a Hach HQ40d™ multi-parameter digital meter. HCO<sub>3</sub><sup>-</sup> and CO<sub>3</sub><sup>2-</sup> concentrations were measured in the Laboratory of Geological Survey of Estonia using the titration method (ISO 9963-1) within 48 h of the sample collection for samples collected in 2015. The analytical precision of these alkalinity measurements in laboratory was ± 3%. For samples collected in 2016 the alkalinity was measured in the field using a Millipore MColorstest™ titration kit. The precision of the alkalinity measurements in the field was ± 11 mg·L<sup>-1</sup>. Samples for hydrochemical analysis were filtered through a 0.45 µm filter and cation samples were acidified to pH ~2–3 using nitric acid. Major and minor ion concentrations were measured in the Department of Geology at Tallinn University of Technology using DIONEX ICS-1100 ion chromatograph. The analytical precision for major and minor ionic components was ± 0.5–2.6% and ± 1.3–4.3%, for cations and anions, respectively, depending on the ions measured (Table 1). Fe<sup>2+</sup> and Mn<sup>2+</sup> concentrations for samples collected in 2016 were determined in Laboratory for Applied Geology and Hydrogeology at Ghent University using atomic adsorption spectrometry (AAS) (Table S1). The analytical precision for both ions was ± 0.05 mg·L<sup>-1</sup>. The charge balance errors for all studied waters (i.e. together with the previously published data) remain below 10% and are below 5% for the majority of the samples. When the salinity of the studied waters is characterized in the text, the classification developed by Stuyfzand (1993) is used: freshwater (Cl<sup>-</sup> < 300 mg·L<sup>-1</sup>); brackish water (Cl<sup>-</sup> from 300 to 10,000 mg·L<sup>-1</sup>); saline water (Cl<sup>-</sup> from 10,000 to 19,400 mg·L<sup>-1</sup>) and brine (Cl<sup>-</sup> > 19,400 mg·L<sup>-1</sup>).

For samples with salinities below 1500 mg·L<sup>-1</sup>, stable isotope ratios of hydrogen ( $\delta^2\text{H}$ ) and oxygen ( $\delta^{18}\text{O}$ ) in water were analysed in the Laboratory of mass spectrometry at the Department of Geology, Tallinn University of Technology (Table 1). Isotope ratios are expressed in standard  $\delta$ -notation relative to Vienna Standard Mean Ocean Water (V-SMOW). Isotope ratios of hydrogen and oxygen were measured using the Picarro L2120-i Isotopic Water Analyzer (Brand et al., 2009). Analytical precision of the stable isotope measurements was ± 0.1‰ for  $\delta^{18}\text{O}$  and ± 1‰ for  $\delta^2\text{H}$ . The  $\delta^{18}\text{O}$  and  $\delta^2\text{H}$  values for five samples with high salinity (TDS > 1500 mg·L<sup>-1</sup>) were measured at the Department of Climate and Environmental Physics at the University of Bern (Table 1) with Picarro L2140-i Isotopic Water Analyzer using the online method presented in Affolter et al. (2014). This method allows to study saline water. The standard deviation between the replicates was better than ± 0.2‰ for  $\delta^{18}\text{O}$  and ± 0.6‰ for  $\delta^2\text{H}$ . Comparison between results published in this study that are measured in the laboratory at University of Bern with those measured previously from the same wells in the laboratory at Tallinn University of Technology (Pärn et al., 2016), shows that the results are similar within the analytical

**Table 1**  
Well parameters together with isotopic and chemical composition of studied groundwater from the Ordovician-Cambrian aquifer system.

Well ID	Location	Northing	Easting	Date	Filter depth	pH	EC	Temp.	$\delta^{18}\text{O}_{\text{water}}$	$\delta^2\text{H}_{\text{water}}$	$\delta^{13}\text{C}$	$\delta^{34}\text{S}_{\text{SO}_4}$	$\delta^{34}\text{S}_{\text{CDT}}$	$\delta^{18}\text{O}_{\text{SO}_4}$	$\Delta^{18}\text{O}_{\text{SO}_4+\text{H}_2\text{O}}$
			m		$\mu\text{S cm}^{-1}$		$^\circ\text{C}$		‰, V-SMOW	‰, V-SMOW	‰, V-PDB	‰, V-CDT	‰, V-SMOW		
13305	Kõrgessaare	58.97974	22.46643	13.09.2016	103–130	8.2	467	9.0	-20.6	-155.3	-7.0	13.8	-0.2	13.8	20.5
13361	Nõmme	58.83252	22.75914	13.09.2016	166–192	8.5	690	10.2	-18.3	-137.5	-10.1	19.6	3.8	19.6	22.1
13359	Käina	58.83339	22.78367	13.07.2015	170–200	8.5	669	9.8	-18.8	-140.6	-9.9	17.3		17.3	25.0
12422	Heltermaa	58.86444	23.04552	13.09.2016	144–172	8.3	667	10.4	-18.3	-138.1	-11.3	24.6	6.7	24.6	28.1
8104	Nõva	59.22150	23.67792	13.09.2016	70–85	8.2	377	8.5	-22.4	-169.5	-10.9	24.1	5.7	24.1	28.7
1551	Riisipere	59.10972	24.31833	28.09.2015	128–170	7.7	597	8.1	-17.9	-134.0	-10.5	57.2	10.8	57.2	28.8
15346	Karjaküla	59.33707	24.39515	16.11.2015	52–68	7.6	433	8.6	-19.4	-143.5	-9.7	32.4	9.4	32.4	27.9
1562	Lehtmetsa	59.32499	25.33760	07.09.2015	78–110	7.8	561	8.1	-19.0	-141.5	-7.1	50.8	8.9	50.8	27.0
51513	Viru-Nigüla	59.44414	26.69387	26.10.2015	33–50	7.1	691	7.5	-14.4	-104.9	-15.5	4.6	12.6	4.6	27.0
4002	Phlsee	59.25016	27.04895	15.09.2015	84–104	7.7	584	7.9	-16.5	-122.2	-9.8	9.3	8.7	9.3	25.1
5968	Estonia mine	59.19706	27.39929	31.08.2015	106–125	7.9	556	8.6	-17.7	-132.6	-8.8	28.6	7.0	28.6	24.6
3171	Varesmetsa	59.11426	27.39988	11.16–139	8.1	584	584	8.8	-18.9	-140.8	-10.1	15.7	4.6	15.7	23.4
10836	Kuressaare <sup>a</sup>	58.25367	22.46910	14.07.2015	475–502	7.9	6570	9.7	-17.3	-132.5	-22.2	22.2		22.2	23.5
4471	Pärnu	58.36016	24.58390	23.09.2015	401–456	7.9	3260	11.8	-14.2	-104.3	-9.3	52.5	9.3	52.5	23.4
8021	Häädemeeste <sup>b</sup>	58.07578	24.50345	23.09.2015	560–590	7.6	8910	12.6	-13.5	-101.7	-10.1	45.8	16.4	45.8	29.9
1224	Tartu	58.35111	26.77292	18.06.2015	342–397	8.4	1310	11.7	-14.3	-106.2	-10.5	34.2	11.9	34.2	26.2
3949	Värska no. 4 <sup>b</sup>	57.98817	27.62799	16.06.2015	528–545	8.3	9670	8.3	-15.0	-112.0	-13.2	26.6	15.7	26.6	30.7
3950	Värska no. 5	57.98599	27.62574	16.06.2015	470–500	8.1	3440	12.0	-14.7	-108.5	-10.8	20.1	16.4	20.1	31.1
4613	Värska no. 6 <sup>b</sup>	57.98621	27.62583	16.06.2015	575–595	7.5	28,100	12.4	-12.6	-93.4		30.2		30.2	27.6

Well ID	Ca <sup>2+</sup>	Mg <sup>2+</sup>	K <sup>+</sup>	Na <sup>+</sup>	Alkalinity	Cl <sup>-</sup>	SO <sub>4</sub> <sup>2-</sup>	Li <sup>+</sup>	Ba <sup>2+</sup>	Str <sup>2+</sup>	NH <sub>4</sub> <sup>+</sup>	F <sup>-</sup>	NO <sub>3</sub> <sup>-</sup>
	mg L <sup>-1</sup>												
13305	23.0	9.9	6.5	59.0	131.0	46.0	36.0	< 0.15	0.1	0.65	< 1.4	1.4	< 1.8
13361	9.2	3.1	4.5	14.0	142.0	11.0	31.0	< 0.15	< 0.05	0.35	< 1.4	2.1	< 1.8
13359	11.0	4.2	4.6	13.0	182.9	85.0	35.0	< 0.15	0.2	0.18	< 1.4	2.3	< 1.8
12422	16.0	5.8	4.8	11.0	142.0	11.0	32.0	< 0.15	< 0.05	0.34	< 1.4	1.7	< 1.8
8104	23.0	11.0	6.7	39.0	164.0	21.0	31.0	< 0.15	0.1	0.51	< 1.4	1.5	< 1.8
1551	28.0	11.0	7.9	82.0	231.9	80.0	13.0	< 0.15	0.4	0.46	< 1.4	1.5	< 1.8
15346	27.0	13.0	7.4	42.0	186.1	42.0	13.0	< 0.15	0.1	0.34	< 1.4	1.1	< 1.8
1562	26.5	12.9	8.9	73.0	216.6	81.0	9.0	< 0.15	0.2	0.42	< 1.4	1.2	< 1.8
51513	68.9	23.9	15.0	44.0	390.5	18.0	60.0	< 0.15	< 0.05	0.48	< 1.4	0.28	< 1.8
4002	30.5	23.9	9.1	67.0	341.7	28.0	20.0	< 0.15	0.1	0.49	< 1.4	0.33	< 1.8
5968	13.3	10.3	5.4	10.0	292.8	29.0	7.7	< 0.15	0.4	0.24	< 1.4	0.6	< 1.8
3171	9.8	4.9	4.1	12.0	237.8	51.5	11.0	< 0.15	0.5	0.13	< 1.4	0.57	< 1.8
10836	26.0	63.0	19.0	1000	109.8	2300	8.4	0.25	4.9	3.6	< 1.4	2.7	< 1.8
4471	64.9	24.5	14.0	600	259.3	1100	56.0	0.14	0.6	1.4	< 1.4	4.2	< 1.8
8021	192	82.7	31.0	1600	219.6	3500	88.0	0.26	0.5	3.9	< 1.4	3.4	< 1.8
1224	19.0	8.8	6.7	24.0	128.0	35.0	11.6	< 0.15	0.9	0.27	< 1.4	0.82	< 1.8
18.6	332	137.3	6.2	241	170.8	3300	280	0.04	< 0.05	0.2	0.004	0.84	< 1.8
3949	300	110	48.0	1700	170.8	3300	15.0	0.18	7.2	4.1	< 1.4	< 0.18	< 1.8
3950	90.0	30.0	13.0	560	146.4	1100	15.0	< 0.15	1.8	1.3	< 1.4	0.53	< 1.8
4613	1000	400	90.0	5100	85.4	11,000	19.0	0.71	36	1.9	2	0.90	12

Blank spaces indicate no data measured.  
 Analytical precision for major and minor ionic components measured in Department of Geology at Tallinn University of Technology: Cl<sup>-</sup> ± 2.8%; SO<sub>4</sub><sup>2-</sup> ± 4.3%; F<sup>-</sup> ± 1.3%; NO<sub>3</sub><sup>-</sup> ± 3.4%; K<sup>+</sup> ± 0.5%; Na<sup>+</sup> ± 1.0%; Mg<sup>2+</sup> ± 1.2%; Ca<sup>2+</sup> ± 0.5%; Li<sup>+</sup> ± 0.8%; Ba<sup>2+</sup> ± 0.4%; Str<sup>2+</sup> ± 0.2%; NH<sub>4</sub><sup>+</sup> ± 2.6%.  
<sup>a</sup>  $\delta^{18}\text{O}$  and  $\delta^2\text{H}$  values measured in the Department of Climate and Environmental Physics at University of Bern.  
<sup>b</sup> All data except the  $\delta^{13}\text{C}$  value published in Pärn et al. (2016).

precision reported by the two laboratories. The carbon isotope composition of DIC ( $\delta^{13}\text{C}_{\text{DIC}}$ ) was determined using a Thermo Fisher Scientific Delta V Advantage mass spectrometer at the Department of Geology, Tallinn University of Technology from DIC precipitated as  $\text{BaCO}_3$  in the field using  $\text{BaCl}_2 \cdot 2\text{H}_2\text{O}$  and  $\text{NaOH}$  (Clark and Fritz, 1997; Table 1). The results are expressed in ‰ deviation relative to Vienna Pee Dee Belemnite (V-PDB). Reproducibility of  $\delta^{13}\text{C}$  of the internal laboratory standards was better than  $\pm 0.1$ . Due to a risk that the alkaline solution used to precipitate  $\text{BaCO}_3$  could be contaminated with atmospheric  $\text{CO}_2$ , care was taken to minimize the contact time with the atmosphere during sample collection. Also, duplicate and triplicate samples were collected to assess the extent of possible contamination on different samples. The reproducibility of  $\delta^{13}\text{C}_{\text{DIC}}$  from these duplicate and triplicate samples was better than  $\pm 0.4\text{‰}$  which is close to typical analytical precision of  $\delta^{13}\text{C}$  measurements ( $\pm 0.3\text{‰}$ ).

The amount of water collected for sulphate isotope analyses ranged from 5 to 25 L, depending on the concentration of dissolved sulphate known from previous studies. The samples were stabilized in the field by adding chloroform to stop bacterial activity. Waters in which the presence of  $\text{H}_2\text{S}$  was suspected were stabilized in the field by precipitating the sulphides using Cd-acetate. All samples were kept under cold (4 °C) and dark conditions before further treatment. The samples were then pre-filtrated through a 0.7  $\mu\text{m}$  filter and acidified to pH  $\sim 3$  for the removal of dissolved carbonate species. The dissolved sulphate was precipitated using  $\text{BaCl}_2 \cdot 2\text{H}_2\text{O}$ . The precipitated  $\text{BaSO}_4$  was collected onto 0.45  $\mu\text{m}$  nitrocellulose membranes (Millipore), washed with distilled water to remove residual  $\text{BaCl}_2$  and dried at 100 °C for 24 h. The results of sulphur and oxygen isotope composition of dissolved sulphate are reported in delta notation ( $\delta^{34}\text{S}_{\text{SO}_4}$ ,  $\delta^{18}\text{O}_{\text{SO}_4}$ ) as part per thousand (‰) deviation relative to the Vienna Cañon Diablo Troilite (V-CDT) standard (Table 1). The  $\delta^{34}\text{S}_{\text{SO}_4}$  and  $\delta^{18}\text{O}_{\text{SO}_4}$  were measured using a Thermo Scientific Delta V Plus with Flash HT Plus mass spectrometer in the Department of Geology at University of Tartu. The values were calibrated using an internal  $\text{BaSO}_4$  standard for drift correction and four international reference standards (standards for O isotopes NBS 127 and NBS 19; standards for S isotopes NBS 127 and IAEA-SO-6) to calibrate the instrument. The long-term analytical precision is better than  $\pm 1\text{‰}$  for sulphate oxygen isotope ratios and better than  $\pm 0.8\text{‰}$  for sulphate sulphur isotope ratios. All symbols shown in figures for stable isotopic data have a larger size with respect to given analytical precision, except where indicated.

Methane concentration and stable isotope data of  $\text{CH}_4$  and  $\text{CO}_2$  from six samples in the O-Cm aquifer system were collected during a separate

fieldwork campaign in 2016 (Table 2). Both the gas composition of the samples and stable isotope composition of  $\text{CH}_4$  and  $\text{CO}_2$  were determined at BGR (Federal Institute for Geosciences and Natural Resources) using a CF-IRMS (Trace GC coupled to a MAT 253). The precision of  $\delta^{13}\text{C}_{\text{CH}_4}$  and  $\delta^{13}\text{C}_{\text{CO}_2}$  was  $\pm 0.3\text{‰}$ , while the precision of  $\delta^2\text{H}_{\text{CH}_4}$  measurements was  $\pm 3\text{‰}$ . Precision of absolute  $\text{CH}_4$  concentration measurements depends on concentration, but is in general better than  $\pm 10\%$ . The concentration of  $\text{CH}_4$  have been measured as percentage of volume (vol%) in a freely dissolving gas.

Isotopic measurements of rock matrix were conducted at the University of Tasmania, Hobart. Weight % C and S was ascertained using an Eltra CS-2000 elemental analyzer, following the same procedure as in Johnson et al. (2017), and Durand et al. (2017). This was used to ensure adequate concentrations of these elements before isotopic analysis. Samples were then analysed at the Central Science Laboratory, University of Tasmania. The  $\delta^{13}\text{C}_{\text{carb}}$  component was derived by treating the powders with phosphoric acid (100%  $\text{H}_3\text{PO}_4$ , 50 °C, 24 h). The evolved  $\text{CO}_2$  was then purified by means of subsequent cold traps, and then analysed using a dual inlet VG Optima. The analytical precision was less than  $\pm 0.05\text{‰}$ . Analytical precision based on full duplicate analyses and internal and international standards was better than  $\pm 0.3\text{‰}$ . However, some samples yielded little  $\text{CO}_2$  and could not be analysed. The  $\delta^{13}\text{C}_{\text{org}}$  component was derived using the same method as outlined for  $\text{C}_{\text{org}}\text{‰}$ , in order to evolve inorganic carbon species and then analysed using an Isoprime 100 PyroCube also at the Central Science Laboratory, University of Tasmania. In-situ pyrite analyses was conducted via laser combustion at the Scottish Universities Environmental Research Centre, East Kilbride (Wagner et al., 2002). Analytical precision for both techniques based on full duplicate analyses and internal and international standards (including combustion) was better than  $\pm 0.3\text{‰}$ .

#### 4. Results

Groundwater in the O-Cm aquifer system is anoxic as both  $\text{O}_2$  and  $\text{NO}_3^-$  concentrations are below detection limit ( $< 0.2\text{ mg}\cdot\text{L}^{-1}$  and  $< 1.8\text{ mg}\cdot\text{L}^{-1}$ , respectively; Table 1, Table S1). In a few cases  $\text{NO}_3^-$  concentrations were higher reaching up to  $9.7\text{ mg}\cdot\text{L}^{-1}$  but these elevated concentrations occur randomly without a clear spatial pattern. As values above the detection limit of  $\text{NO}_3^-$  are anomalies in multiple measurements from the same wells where all other measurements have  $\text{NO}_3^-$  below detection limit (Table S1), we consider these to be measurement errors and have omitted them from further interpretation.

**Table 2**

Methane concentrations (vol%) together with isotopic composition of  $\text{CH}_4$  and  $\text{CO}_2$  in the gas phase of groundwater in the Ordovician-Cambrian aquifer system.

Well ID	Location	Sampling date	Northing	Easting	$\text{CH}_4$ vol%	$\delta^{13}\text{C}_{\text{CH}_4}$	$\delta^{13}\text{C}_{\text{CO}_2}$	$\delta^2\text{H}_{\text{CH}_4}$	Reference
						‰, V-PDB	‰, V-PDB	‰, V-SMOW	
	Tudu, no. 900		59.17715	26.85716	1.17				Voitov et al., 1982
	Well no. 653		59.20667	24.01365	2.66				Voitov et al., 1982
	Saue		59.32568	24.55935	0.02				Pihlak et al., 2003
	Jöelähtme		59.44739	25.12183	0.06				Pihlak et al., 2003
	Aruküla		59.36507	25.08074	0.03				Pihlak et al., 2003
	Lehtse		59.24968	25.82657	1.54				Pihlak et al., 2003
	Uhtna		59.39384	26.56661	0.02				Pihlak et al., 2003
	Vaivara		59.37188	27.76206	1.75				Pihlak et al., 2003
	Tapa		59.25448	25.98554	3.26				Pihlak et al., 2003
	Keila		59.32450	24.37713	0.25				Pihlak et al., 2003
	Saku		59.30511	24.66130	0.002				Pihlak et al., 2003
	Pärnu		58.40756	24.50105	0.59				Pihlak et al., 2003
5968	Estonia mine	05.09.2016	59.17715	26.85716	0.03	−32.4	−24.3		This study
3171	Varesmetsa	06.09.2016	59.20667	24.01365	0.02	−36.0	−24.6		This study
1551	Riisipere	07.09.2016	59.32568	24.55935	0.40	−79.3	−24.3	−242	This study
13305	Kõrgessaare	13.09.2016	59.44739	25.12183	0.06	−64.7	−24.4		This study
10836	Kuussaare	12.09.2016	59.36507	25.08074	3.74	−95.8	−26.1	−442	This study
8021	Häädemeeste	16.09.2016	59.24968	25.82657	0.04	−30.8	−23.9	−210	This study

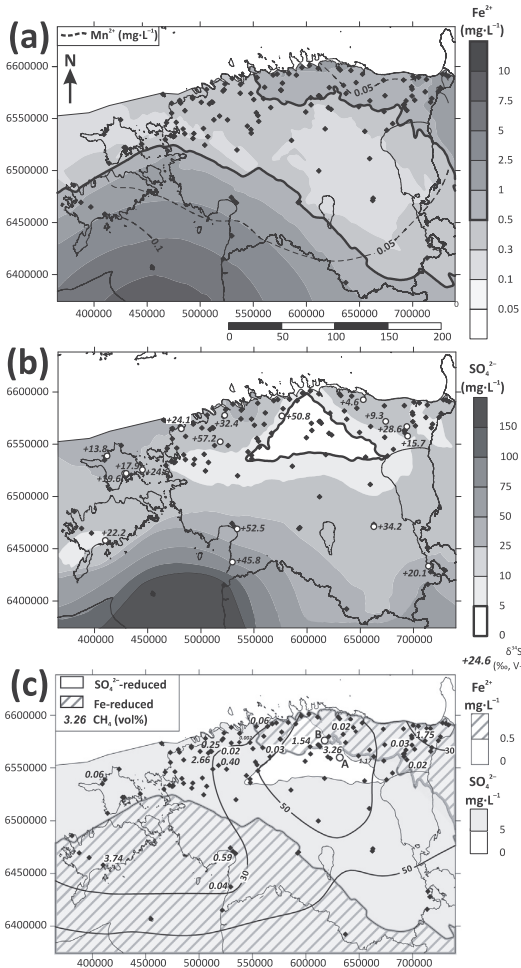


**Fig. 2.** Lateral distribution of (a)  $Mn^{2+}/Fe^{2+}$  and (b)  $SO_4^{2-}$  in the Ordovician-Cambrian aquifer system. Isolines denote the average concentrations from the time-series available from sampling points in  $mg\cdot L^{-1}$  (Table S1). White circles denote samples for which  $SO_4^{2-}$  stable isotope data is available (Table 1) while black diamonds denote samples whose hydrochemical data is used to compile the map (Table S1). The numbers in (b) indicate  $\delta^{34}S_{SO_4}$  values in ‰, V-CDT; (c) lateral distribution of Fe-reduced zone ( $Fe^{2+} < 0.5\ mg\cdot L^{-1}$ ) and  $SO_4^{2-}$ -reduced zone ( $SO_4^{2-} < 5\ mg\cdot L^{-1}$ ) in the O-Cm aquifer system. Solid lines indicate the freshwater head in m.a.s.l. Numbers near sampling points denote  $CH_4$  concentrations in % of total gas volume (Table 2). White circles denote the locations of Raeküla site (A) and Tõrma site (B) discussed in Section 5.4 and Fig. 6.

Concentrations of  $Mn^{2+}$  range from  $< 0.02$  to  $0.13\ mg\cdot L^{-1}$  (Table S1). These concentrations are in most cases much lower than for other redox sensitive dissolved substances (i.e.  $Fe^{2+}$  and  $SO_4^{2-}$ ) and thus have minor influence on the oxidation of organic matter in the aquifer system. Higher concentrations of  $Mn^{2+}$  coincide with high concentrations of  $Fe^{2+}$  (Fig. 2a).  $Fe^{2+}$  concentrations range from  $< 0.05$  to  $10.8\ mg\cdot L^{-1}$  (Table S1). The elevated  $Fe^{2+}$  concentrations ( $> 0.5\ mg\cdot L^{-1}$ ) are observed near the outcrop area of the aquifer bearing rocks and in brackish waters in deeper parts of the aquifer system (Fig. 2a). Dissolved  $SO_4^{2-}$  concentrations in the O-Cm aquifer

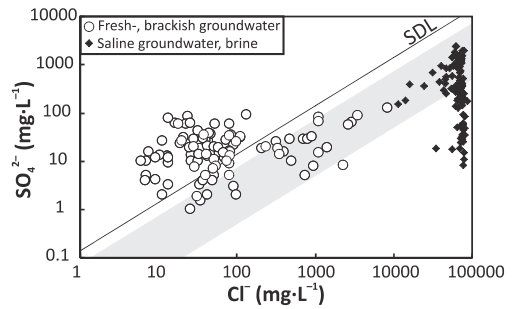


**Fig. 3.** Relations between  $SO_4^{2-}$  and  $Cl^-$  in the fresh and brackish groundwater in Ordovician-Cambrian aquifer system together with saline groundwater and brine in Cambrian aquifer system (Table S1). Hydrochemical data of saline groundwater and brine in Latvia is from Takcidi (1999). Seawater dilution line (SDL) represents the  $SO_4^{2-}/Cl^-$  ratio of modern seawater with the value of 0.14. The light grey area denotes the estimated range of values for Early Phanerozoic seawater (Cambrian-Devonian) composition based on  $SO_4^{2-}$  concentration ranges of 1–15 mM ( $\sim 100$ – $1400\ mg\cdot L^{-1}$ ) found in fluid-inclusions (Horita et al., 2002; Lowenstein et al., 2003; Brennan et al., 2004) and estimated by modelling (Algeo et al., 2015).

system range from values below detection limit to  $152\ mg\cdot L^{-1}$  (Fig. 2b; Table S1).  $SO_4^{2-}$  concentrations in fresh groundwater range from values below detection limit to  $73\ mg\cdot L^{-1}$  with the median value of  $10\ mg\cdot L^{-1}$  and in brackish groundwater the concentrations vary from 5 to  $152\ mg\cdot L^{-1}$  with a median value of  $28\ mg\cdot L^{-1}$  (Table S1). Much higher  $SO_4^{2-}$  concentrations are found in the saline groundwater and brine in the deeper Cambrian aquifer system (Fig. 3) with sulphate concentrations up to  $\sim 2800\ mg\cdot L^{-1}$  (Takcidi, 1999).

$SO_4^{2-}$  in fresh and brackish groundwater of the O-Cm aquifer system also differs in  $\delta^{34}S_{SO_4}$  and  $\delta^{18}O_{SO_4}$  values.  $\delta^{34}S_{SO_4}$  values in fresh groundwaters have a wide range from  $+4.6$  to  $+57.2\ ‰$  with the median value of  $+22\ ‰$  (Table 1). The  $\delta^{34}S_{SO_4}$  values in brackish and saline groundwater from the O-Cm and Cambrian-Vendian aquifer systems vary from  $+20.1$  to  $+52.5\ ‰$  with the median value of  $+30\ ‰$ . The  $\delta^{18}O_{SO_4}$  values in fresh groundwater range from  $-0.2$  to  $+12.6\ ‰$  and are strongly enriched with respect to  $\delta^{18}O$  values in ambient water ( $\Delta^{18}O_{SO_4-H_2O}$  from  $+20.5$  to  $+31.1\ ‰$ ; Table 1). Brackish and saline groundwater has  $\delta^{18}O_{SO_4}$  values from  $+9.3$  to  $+16.4\ ‰$  and is characterized by  $\Delta^{18}O_{SO_4-H_2O}$  values of about  $+30\ ‰$ .

Estimates of  $CH_4$  concentrations in the aquifer system range from 0.002 to 3.74% of total gas volume (Voitov et al., 1982; Pihlak et al., 2003; Table 2). Higher  $CH_4$  concentrations are found in areas with low  $SO_4^{2-}$  concentrations in the vicinity of the modern recharge area and also in the deeper southern parts of the aquifer system. In other parts of the aquifer system the share of  $CH_4$  in freely dissolved gas is lower, but  $CH_4$  is common in small detectable amounts all over the aquifer system. Differences in  $CH_4$  concentration coincide with differences in isotopic composition of  $CH_4$ .  $\delta^{13}C_{CH_4}$  and  $\delta^2H_{CH_4}$  values measured from the aquifer system range from  $-30.8$  to  $-95.8\ ‰$  and from  $-210$  to  $-442\ ‰$ , respectively, with lighter values characteristic to areas with lower  $SO_4^{2-}$  and higher  $CH_4$  concentrations (Table 2). At the same time, the  $\delta^{13}C$  values of co-existing  $CO_2$  have a very narrow range from  $-23.9$  to  $-26.1\ ‰$  (Table 2).

## 5. Discussion

### 5.1. Delineation of redox zones in the aquifer system

In terms of concentration,  $Fe^{2+}$  and  $SO_4^{2-}$  are the most important redox sensitive dissolved substances in the aquifer system. In previous studies characteristic threshold values for  $Fe^{2+}$  and  $SO_4^{2-}$  have been

interpreted as boundaries between Fe-reducing/Fe-reduced and  $\text{SO}_4^{2-}$ -reducing/ $\text{SO}_4^{2-}$ -reduced conditions (cf. Coetsiers and Walraevens, 2006). In our case these specific threshold values can be chosen to be  $0.5 \text{ mg}\cdot\text{L}^{-1}$  and  $5 \text{ mg}\cdot\text{L}^{-1}$  for  $\text{Fe}^{2+}$  and  $\text{SO}_4^{2-}$ , respectively, based on spatial distribution of those ions (Fig. 2a–c). Given these threshold values, an overlap between Fe-reducing and  $\text{SO}_4^{2-}$ -reducing conditions in various parts of the aquifer system is observed (Fig. 2c). Therefore, for refining the distribution of redox zones in the aquifer system the relative distributions of  $\text{Fe}^{2+}$ ,  $\text{SO}_4^{2-}$  and  $\text{CH}_4$  need to be elaborated in a broader hydrogeological and hydrochemical context.

In shallow parts of the aquifer system near the outcrop area, the occurrence of high  $\text{Fe}^{2+}$  ( $> 0.5 \text{ mg}\cdot\text{L}^{-1}$ ) concentrations and high  $\text{SO}_4^{2-}$  concentrations ( $> 5 \text{ mg}\cdot\text{L}^{-1}$ ) refer to a Fe-reduced zone and an ongoing  $\text{SO}_4^{2-}$  reduction (Fig. 2c). The same pattern of  $\text{Fe}^{2+}$  and  $\text{SO}_4^{2-}$  distribution in the deeper parts of the aquifer system (Fig. 2c) can be related to the dissolution of iron-bearing carbonate minerals (e.g. ankerite, siderite). Although the data of  $\text{CH}_4$  concentration in these deep parts of the aquifer system is scarce, methane is detected from brackish waters in the area (0.04–3.74 vol%; Fig. 2c). This finding together with the increased  $\text{Fe}^{2+}$  concentrations suggest that methanogenic conditions may be reached in the deeper parts of the aquifer system.

Where elevated  $\text{Fe}^{2+}$  concentrations ( $> 0.5 \text{ mg}\cdot\text{L}^{-1}$ ) are accompanied by low  $\text{SO}_4^{2-}$  concentrations ( $< 5 \text{ mg}\cdot\text{L}^{-1}$ ) both the Fe reduction and  $\text{SO}_4^{2-}$  reduction could have gone to completion. Alternatively, this situation can also develop by simultaneous occurrence of Fe- and  $\text{SO}_4^{2-}$  reduction (e.g. Simpkins and Parkin, 1993; Jakobsen and Postma, 1999; Park et al., 2006). Both hematite and goethite present in the aquifer matrix represent stable forms of Fe(III)-oxides and their presence makes sulphate reduction energetically more favourable in most environmental conditions (Postma and Jakobsen, 1996).

In the modern recharge area, low concentrations for both  $\text{SO}_4^{2-}$  ( $< 5 \text{ mg}\cdot\text{L}^{-1}$ ) and  $\text{Fe}^{2+}$  ( $< 0.5 \text{ mg}\cdot\text{L}^{-1}$ ) are observed together with the presence of  $\text{CH}_4$  suggesting that the sulphate reduction has run close to completion. This inference is supported by the fact that  $\text{Fe}^{2+}$  concentrations tend to decrease in a sulphate reducing zone due to precipitation of iron-sulphides, when  $\text{H}_2\text{S}$  produced during sulphate reduction reacts with ferrous iron. Such reaction has been shown to occur commonly in aquifers (e.g. Jakobsen and Postma, 1999; Hansen et al., 2001; Appelo and Postma, 2005; Park et al., 2006; Jakobsen and Cold, 2007). The sulphate concentrations increase ( $> 5 \text{ mg}\cdot\text{L}^{-1}$ ) and  $\text{CH}_4$  concentrations decrease farther down the groundwater flow path (Fig. 2b, c). This suggests that in these areas  $\text{SO}_4^{2-}$  reduction could be ongoing.

## 5.2. Origin of sulphate and the occurrence of sulphate reduction

Sulphate in the O-Cm aquifer system can originate from both mineral sources (e.g. oxidation of pyrite) and from mixing with saline waters with higher  $\text{SO}_4^{2-}$  concentrations. Raidla et al. (2012, 2014) have suggested that  $\text{SO}_4^{2-}$  in fresh glacial palaeogroundwater in the underlying Cambrian-Vendian aquifer system has originated from pyrite oxidation by oxygen dissolved in infiltrating glacial meltwaters. Given the fact that groundwater in the O-Cm aquifer system is of similar origin and  $\text{SO}_4$ -bearing minerals (e.g. gypsum, anhydrite) are absent in the aquifer matrix,  $\text{SO}_4^{2-}$  in the O-Cm aquifer system could also originate from pyrite oxidation similarly to the Cambrian-Vendian aquifer system. However, mixing between fresh groundwater and saline groundwater from deeper parts of the aquifer system has been shown to be an important process in the hydrochemical evolution of the aquifer system (Pärn et al., 2016). Thus, it is important to clarify, whether the  $\text{SO}_4^{2-}$  in fresh groundwater farther down the groundwater flow path originates from mixing or from pyrite oxidation and whether this initial sulphate pool has been later modified by bacterial sulphate reduction.

No chloride-bearing evaporite minerals (e.g. halite) are found in the aquifer matrix and there are no indications of modern day sea-water

intrusion into the aquifer system. Thus,  $\text{Cl}^-$  found in fresh- and brackish waters should be derived from mixing with deep formation waters. Under these environmental conditions  $\text{Cl}^-$  can be considered a conservative tracer and the relations between  $\text{Cl}^-$  and  $\text{SO}_4^{2-}$  can be used to identify the extent to which  $\text{SO}_4^{2-}$  in freshwaters has been derived from mixing with deep formation waters (Fig. 3).

Large variations in  $\text{SO}_4^{2-}$  concentration characterize the brine with  $\text{Cl}^- > 40,000 \text{ mg}\cdot\text{L}^{-1}$  in deep central parts of the BAB in Latvia (Talcidi, 1999) but no mixing with fresh groundwater is evident (Fig. 3). As chloride concentrations decrease to values below  $40,000 \text{ mg}\cdot\text{L}^{-1}$  in shallower parts of the BAB, a clearer covariance between  $\text{SO}_4^{2-}$  and  $\text{Cl}^-$  develops, suggesting a dilution of initial salinity. However, this concentration-dilution relationship between  $\text{Cl}^-$  and  $\text{SO}_4^{2-}$  does not follow the modern seawater dilution line (SDL;  $\text{SO}_4^{2-}/\text{Cl}^- = 0.14$ ) but is characterized by lower values of  $\text{SO}_4^{2-}/\text{Cl}^-$ , ranging from  $\sim 0.01$  to  $\sim 0.05$  (Fig. 3). Fluid-inclusion studies, as well as the isotopic composition of carbonate associated sulphate and evaporites have shown that lower  $\text{SO}_4^{2-}$  concentrations were characteristic for seawater in Early Phanerozoic (Cambrian-Devonian) (Horita et al., 2002; Lowenstein et al., 2003; Brennan et al., 2004; Halevy et al., 2012; Algeo et al., 2015). These lower concentrations of  $\text{SO}_4^{2-}$  lead to  $\text{SO}_4^{2-}/\text{Cl}^-$  relations similar to  $\text{SO}_4^{2-}/\text{Cl}^-$  values in the saline and brackish groundwater of the BAB (Fig. 3). In fresh groundwater ( $\text{Cl}^- < 350 \text{ mg}\cdot\text{L}^{-1}$ ) an increase in  $\text{SO}_4^{2-}/\text{Cl}^-$  ratio relative to that in brackish groundwater is evident indicating excess  $\text{SO}_4^{2-}$  gained with respect to mixing. Although mixing with saline waters appears to be the main source of  $\text{SO}_4^{2-}$  in brackish groundwater in the deeper parts of the aquifer system, another source of  $\text{SO}_4^{2-}$  is dominant in fresh groundwater in the shallow northern part of the aquifer system.

$\text{SO}_4^{2-}$  in fresh groundwater is characterized by lighter  $\delta^{34}\text{S}$  values (from  $+4.6$  to  $+57.2\text{‰}$ ; median value of  $+22\text{‰}$ ) compared to brackish and saline groundwater ( $\delta^{34}\text{S}$  values from  $+20.1$  to  $+52.5\text{‰}$ ; median value of  $+30\text{‰}$ ) suggesting a source with a lighter sulphur isotope composition relative to  $\text{SO}_4^{2-}$  in brackish waters. The  $\delta^{34}\text{S}$  values of pyrite from the Cambrian and Ordovician sandstones forming the aquifer matrix and those from overlying formations are indeed somewhat depleted with respect to  $\delta^{34}\text{S}_{\text{SO}_4}$  values in brackish groundwater but show a wide variability (Fig. 4). The majority of the measured  $\delta^{34}\text{S}_{\text{SO}_4}$  values in freshwaters fall in the same range as  $\delta^{34}\text{S}_{\text{pyrite}}$  values in the aquifer matrix and only a few are clearly enriched with respect to pyrite (Fig. 4). This suggests that the origin of  $\text{SO}_4^{2-}$  in these waters from pyrite oxidation is plausible.

However, multiple lines of evidence show that at least some of this initial  $\text{SO}_4^{2-}$  in fresh groundwater originating from pyrite oxidation has been further modified by sulphate reduction. Firstly, freshwaters with low  $\text{SO}_4^{2-}$  concentrations are characterized by heaviest  $\delta^{34}\text{S}_{\text{SO}_4}$  composition. Secondly, their enrichment in  $^{34}\text{S}_{\text{SO}_4}$  with respect to  $\delta^{34}\text{S}$  values in pyrite is much larger than expected from simple pyrite oxidation.  $\delta^{34}\text{S}_{\text{SO}_4}$  values in some freshwaters are  $> 20\text{‰}$  higher than the highest  $\delta^{34}\text{S}_{\text{pyrite}}$  values reported from the aquifer matrix (Fig. 4). Such large fractionation can be achieved during sulphate reduction. Thirdly, the spatial distribution of  $\delta^{34}\text{S}_{\text{SO}_4}$  values shows that  $^{34}\text{S}$ -enriched values are generally characteristic to samples lying closer to the  $\text{SO}_4^{2-}$  reduced zone (Fig. 2b, c). Fourthly, there is field evidence of ongoing sulphate reduction in the north-western part of the aquifer system. The characteristic odour of  $\text{H}_2\text{S}$  was detected from wells in that area and the isotopic composition of  $\delta^{34}\text{S}_{\text{H}_2\text{S}}$  was determined from one of the wells ( $-23.5\text{‰}$ ; Well no. 8104, Table 1). The comparison between  $\delta^{34}\text{S}_{\text{SO}_4}$  and  $\delta^{34}\text{S}_{\text{H}_2\text{S}}$  yielded a  $\Delta^{34}\text{S}_{\text{SO}_4\text{-H}_2\text{S}}$  value of  $+47.9$ , which lies in the range typical for sulphate reduction (Canfield, 2001).

Finally, strong evidence supporting the occurrence of sulphate reduction in the aquifer system is provided by the oxygen isotope composition of  $\text{SO}_4^{2-}$ . As pyrite oxidation should only impart a small positive fractionation on the  $\delta^{18}\text{O}_{\text{SO}_4}$  value of the product sulphate relative to ambient water (e.g. Van Stempvoort and Krouse, 1994; Balci et al., 2007), the  $\delta^{18}\text{O}_{\text{SO}_4}$  values in dissolved sulphate of O-Cm

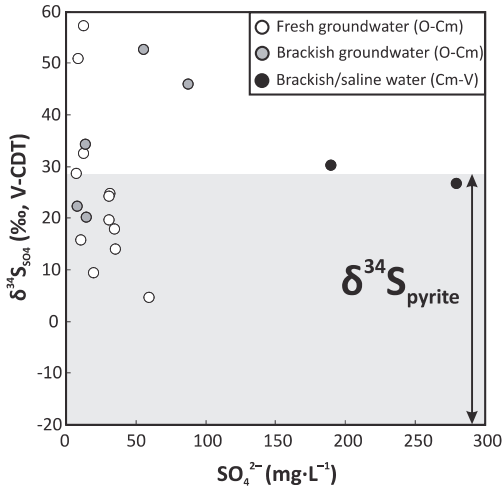


**Fig. 4.** Relation between  $\text{SO}_4^{2-}$  concentration and  $\delta^{34}\text{S}_{\text{SO}_4}$  values in the Ordovician-Cambrian (O-Cm) aquifer system and brackish/saline groundwater from the Cambrian-Vendian (Cm-V) aquifer system. The grey shaded area depicts the observed range of  $\delta^{34}\text{S}$  values in pyrite from Cambrian and Lower-Ordovician rocks (from  $-14.6$  to  $+28.8\text{‰}$ , Petersell et al., 1987, 1991; Johnson et al., 2016, in prep; Table S2, Supplementary material).

groundwater should have a light isotopic composition similar to the studied waters originating from glacial meltwater recharge (e.g.  $\delta^{18}\text{O}_{\text{water}}$  values from  $-14.4$  to  $-22.4\text{‰}$ ; Table 1). However, observed  $\delta^{18}\text{O}_{\text{SO}_4}$  values in fresh groundwater are much higher, ranging from  $-0.2$  to  $+12.6\text{‰}$  ( $\Delta^{18}\text{O}_{\text{SO}_4\text{-H}_2\text{O}}$  from  $+20.5$  to  $+31.1\text{‰}$ ; Table 1). Thus, they record a larger enrichment with respect to  $\delta^{18}\text{O}$  values in ambient water than expected from simple oxidation. The  $\Delta^{18}\text{O}_{\text{SO}_4\text{-H}_2\text{O}}$  values found in fresh groundwater from the O-Cm are consistent with large fractionation observed during bacterial sulphate reduction (Fritz et al., 1989; Böttcher et al., 1998; Wortmann et al., 2007). Furthermore,  $\delta^{18}\text{O}_{\text{SO}_4}$  and  $\delta^{18}\text{O}_{\text{water}}$  values in the O-Cm aquifer system show a coupled variation which is also an important characteristic of bacterial sulphate reduction (Fig. 5a; Fritz et al., 1989; Turchyn et al., 2010;

Antler et al., 2013). All in all, the relations between  $\delta^{18}\text{O}_{\text{SO}_4}$  and  $\delta^{18}\text{O}_{\text{water}}$  support the hypothesis that the initial pool of  $\text{SO}_4^{2-}$  in fresh groundwater of the O-Cm aquifer system has been reworked by sulphate reduction. This seems to be the case for all studied freshwaters irrespective of their  $\delta^{34}\text{S}_{\text{SO}_4}$  values and  $\text{SO}_4^{2-}$  concentrations. Thus, it can be concluded that areas farther away from the modern recharge area of the aquifer system with  $\text{SO}_4^{2-}$  concentrations  $> 5 \text{ mg L}^{-1}$  belong to the  $\text{SO}_4^{2-}$ -reducing zone.

High values of  $\Delta^{18}\text{O}_{\text{SO}_4\text{-H}_2\text{O}}$  (about  $+30\text{‰}$ ) together with the high values of  $\delta^{34}\text{S}_{\text{SO}_4}$  in saline and brackish groundwater in the deeper parts of the aquifer system also suggest that the original  $\text{SO}_4^{2-}$  in these waters has been reworked by sulphate reduction. However, the observed  $\Delta^{18}\text{O}_{\text{SO}_4\text{-H}_2\text{O}}$  values are also very close to  $\epsilon^{18}\text{O}_{(\text{SO}_4\text{-H}_2\text{O})}$  for abiotic oxygen isotope exchange in the temperature range of  $0$  to  $15^\circ\text{C}$  according to Zeebe (2010) (Fig. 5b). It has been shown that the oxygen isotope composition of sulphate is very stable in circum-neutral pH and temperatures below  $50^\circ\text{C}$  (Chiba and Sakai, 1985; Van Stempvoort and Krouse, 1994; Krouse and Mayer, 2000). However, some authors have argued that abiotic oxygen isotope equilibrium can be attained in a matter of  $10^4$  to  $10^5$  years (e.g. Halas et al., 1993; Boschetti, 2013 and the references therein). Compared to fresh glacial palaeogroundwater with an approximate age of  $\sim 20 \text{ ka}$  (Raidla et al., 2012), brackish and saline groundwater in the O-Cm and Cambrian-Vendian aquifer systems is much older. Gerber et al. (2017) have shown that  $^{81}\text{Kr}$  activities of these waters suggest ages of  $\sim 500 \text{ ka}$ . Thus, there remains a possibility that high  $\delta^{18}\text{O}_{\text{SO}_4}$  values in saline and brackish groundwater in the deeper parts of the BAB are caused by an abiotic oxygen isotope exchange between sulphate and water and are not directly related to sulphate reduction.

5.3. Methanogenesis

Methane is present in most parts of the O-Cm aquifer system and is found both in  $\text{SO}_4^{2-}$  reduced zone and in the zone where  $\text{SO}_4^{2-}$  reduction is ongoing (Fig. 2c). Methane is stable in anoxic conditions and can be transported away from areas of production without showing any significant reaction (Jakobsen and Postma, 1999; Hansen et al., 2001; Appelo and Postma, 2005). Thus, the presence of small concentrations of  $\text{CH}_4$  cannot be taken as evidence for active methanogenesis in the area. However, higher  $\text{CH}_4$  concentrations in the modern recharge area where  $\text{SO}_4^{2-}$  reduced zone is established

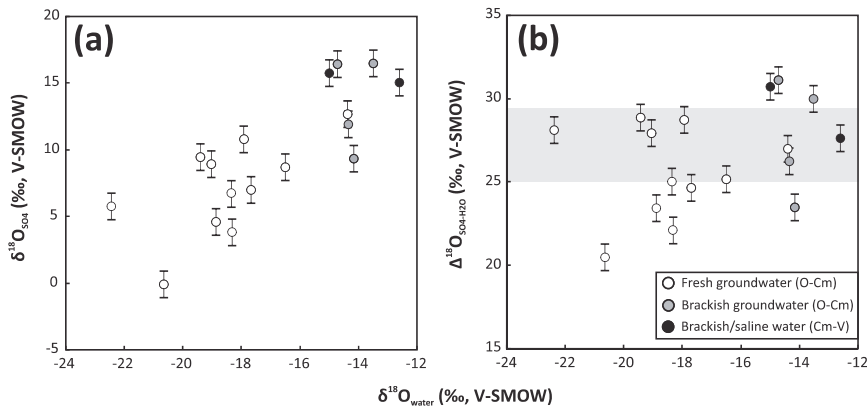


**Fig. 5.** Co-variance between  $\delta^{18}\text{O}_{\text{water}}$  and (a)  $\delta^{18}\text{O}_{\text{SO}_4}$ , (b)  $\Delta^{18}\text{O}_{\text{SO}_4\text{-H}_2\text{O}}$  values from fresh and brackish groundwater in the Ordovician-Cambrian (O-Cm) aquifer system and brackish/saline groundwater from the Cambrian-Vendian (Cm-V) aquifer system. Grey shaded area indicates  $\epsilon^{18}\text{O}_{(\text{SO}_4\text{-H}_2\text{O})}$  in the temperature range of  $0$ – $15^\circ\text{C}$ , calculated according to the relation provided by Zeebe (2010):  $\epsilon^{18}\text{O}_{(\text{SO}_4\text{-H}_2\text{O})} = 2.72 \cdot 10^6 \text{ T}^{-2} - 7.71$ . The temperature observed in sampled groundwater ranges from  $7.5$  to  $12.6^\circ\text{C}$  (Table 1).

suggest, that this part of the aquifer system has already evolved to methanogenic conditions (Table 2; Fig. 2c). Lower CH<sub>4</sub> concentrations farther down the groundwater flow path where SO<sub>4</sub><sup>2-</sup> concentrations are higher may rather be related to transport processes than to active CH<sub>4</sub> production. Increasing CH<sub>4</sub> concentrations together with increasing Fe<sup>2+</sup> concentrations in the deeper parts of the aquifer system suggest that methanogenic conditions have also developed in the deeper parts of the BAB. The available stable isotopic data of CH<sub>4</sub> support this explanation. δ<sup>13</sup>C<sub>CH4</sub> values measured from the aquifer system range from -30.8 to -95.8‰, and the difference in δ<sup>13</sup>C values between CH<sub>4</sub> and co-existing CO<sub>2</sub> ranges from 11 to 70‰ (Table 2). Methane exhibiting δ<sup>13</sup>C values lower than -60‰ can be attributed to a bacterial origin (methanogenesis; Whiticar, 1999). Comparison with the δ<sup>13</sup>C of co-existing carbon dioxide clearly indicates carbonate reduction as the main methanogenic pathway. This is substantiated by the relationship between δ<sup>2</sup>H of methane and the ambient water. Most of these samples are located near the SO<sub>4</sub>-reduced zone and in deeper parts of the basin. Methane with a heavier isotopic composition is mostly found farther down the groundwater flow path in the SO<sub>4</sub>-reducing zone and may represent methane transported from more reducing conditions that has been subsequently oxidized.

5.4. Development of the redox zonation

According to modern groundwater flow patterns (Fig. 1) and the distribution of redox zones (Sections 5.1–5.3; Fig. 2c), the conditions in the modern recharge area more strongly reducing than in areas farther down the groundwater flow path. This unusual distribution of redox zones seems to suggest that the observed redox zonation has not developed solely as a response to modern topographically driven flow conditions. As the isotopic composition of freshwater clearly points to

its glacial origin, it can be suspected that the observed redox zonation follows groundwater flow patterns established in Pleistocene. Indeed, the configuration of glacial land-forms and end-moraines in the study area indicates that the advance of Scandinavian Ice Sheet to its maximum extent in LGM occurred predominantly from the north-western direction (Kalm et al., 2011). Thus, the sequence of redox zones in the aquifer system could follow the advance of the ice sheet which occurred from north-west to the south-east. When interpreted this way, the higher Fe<sup>2+</sup> and SO<sub>4</sub><sup>2-</sup> concentrations farther down the groundwater flow path in the north-western part of the aquifer system and more reduced conditions in the central and southern parts of the aquifer system follow the expected sequence of redox zones along a flow path (Fig. 2a–c).

However, the isotopic and chemical composition of groundwater suggests that glacial palaeogroundwater in the vicinity of modern recharge area and the outcrop area of the aquifer system is influenced by mixing with a more recent meteoric end-member (Pärn et al., 2016). The development of strongly reducing conditions surrounding the modern recharge area is thus probably related to post-glacial hydrologic conditions. In the modern recharge area, the aquifer is overlain by a thick (> 100 m) formation of Silurian and Ordovician carbonates containing various beds rich in organic matter (Section 2). Infiltrating waters can become progressively more reduced during the vertical movement through the Silurian and Ordovician carbonates as the higher free energy electron acceptors are consumed (NO<sub>3</sub><sup>-</sup>, Fe<sup>3+</sup>). When these electron acceptors become unavailable, SO<sub>4</sub><sup>2-</sup> is left for bacteria to be utilized for oxidation of organic matter. This conceptual model is supported by changes in water chemistry with depth observed in wells opened in the overlying Silurian-Ordovician aquifer system in the modern recharge area (Fig. 6; Table 3). Although the vertical resolution of the constructed cross-sections is not high, a clear pattern is

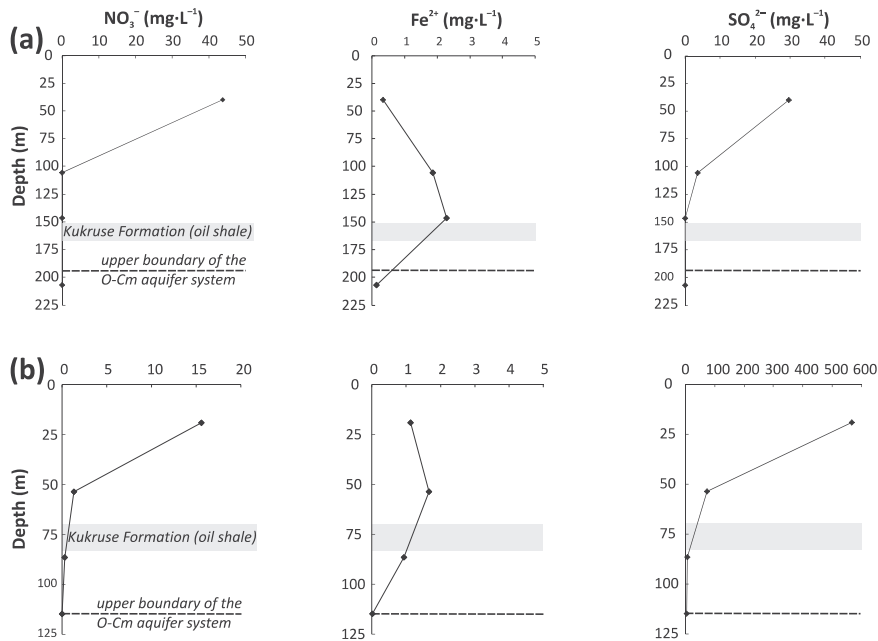


Fig. 6. Changes in the concentration with depth of NO<sub>3</sub><sup>-</sup>, Fe<sup>2+</sup> and SO<sub>4</sub><sup>2-</sup> from the Silurian-Ordovician aquifer system at two sites in the modern recharge area of the Ordovician-Cambrian (O-Cm) aquifer system – Raeküla (a) and Tõrma (b). The location of the sites is shown in Fig. 2c. The depicted concentrations represent averages of samples collected in various years (Table 3). For Raeküla site the sample representing the O-Cm aquifer system is well no. 3508 (Table 3, S1) located in close proximity (~8 km) to the Raeküla well-group. The positions of the Kukruse Formation containing kukersite beds with high content (10–60%) of organic matter and the upper boundary of the O-Cm aquifer system in the studied sites are shown for reference.

**Table 3**

Well parameters, number of measurements (n) and average concentrations of  $\text{NO}_3^-$ ,  $\text{Fe}^{2+}$  and  $\text{SO}_4^{2-}$  in two well fields in Raeküla/Tamsalu and Tõrma opened in the Silurian-Ordovician aquifer system at modern recharge area.

Well ID	Location	Northing	Easting	Filter depth	Filter mid-point	Aquifer	Sampling years	n ( $\text{SO}_4^{2-}$ , $\text{NO}_3^-$ )	n ( $\text{Fe}^{2+}$ )	$\text{SO}_4^{2-}$	$\text{Fe}^{2+}$	$\text{NO}_3^-$	Reference
				m	m								
3598	Raeküla	59.16630	26.33152	20–60	40	O3prg	2003–2006	4	4	29.7	0.3	43.6	EELIS, 2017
3599		59.16631	26.33147	91–120	105.5	O3nb-rk	2003–2013	9	9	3.6	1.9	< 0.4	EELIS, 2017
7295		59.16727	26.33089	125–168	146.5	O2kl-kk	2003–2006	4	4	< 3.3	2.3	< 0.4	EELIS, 2017
3508	Tamsalu	59.16561	26.10880	195–219	207	O-Cm	2014–2016	3	1	< 4.5	0.13	< 1.8	Table S1
3675	Tõrma	59.31481	26.32394	6.9–31.5	19.2	O3nb-O2rk	1981–2013	42	34	567.2	1.1	15.6	EELIS, 2017
3677		59.31483	26.32403	31.3–76	53.7	O2kl-kk	1981–2013	42	33	73.8	1.7	1.3	EELIS, 2017
3676		59.31482	26.32396	72.3–101	86.7	O2ls-O1kn	1981–2013	42	27	7.5	0.9	0.3	EELIS, 2017
19098		59.31468	26.32455	101–129	115	O-Cm	1981–1987	12	1	5.0	< 0.06	< 0.4	EELIS, 2017

visible. With increasing depth,  $\text{NO}_3^-$  present in shallow wells is consumed, followed by an increase in  $\text{Fe}^{2+}$ , indicating Fe-reduction and  $\text{SO}_4^{2-}$  depletion, which indicates  $\text{SO}_4^{2-}$ -reduction. A decrease in  $\text{Fe}^{2+}$  concentrations near the upper boundary of the O-Cm aquifer system could be explained by the formation of Fe-sulphides that precipitate from the solution in the presence of  $\text{H}_2\text{S}$ . Thus, recharging groundwater has the potential to evolve to low  $\text{SO}_4^{2-}$  concentrations and consequently the dissolved sulphate can become enriched in  $^{34}\text{S}$ . This is also in agreement with the occurrence of  $\text{CH}_4$  in the modern recharge area as all higher free energy electron acceptors have already been consumed during the vertical infiltration of groundwater into the aquifer system.

The areas farther down the groundwater flow path are less influenced by post-glacial groundwater recharge. The observed pattern of  $\text{SO}_4^{2-}$  distribution in those areas may be rather related to the oxidation of pyrite by oxygen carried by glacial meltwaters that has been subsequently reduced (Fig. 2b, c). An increase in  $\text{SO}_4^{2-}$  in the deeper southern parts of the aquifer system is related to mixing with saline waters from deeper parts of the aquifer system. The ongoing  $\text{SO}_4^{2-}$ -reduction in those areas is probably sustained by the oxidation of sedimentary organic matter present mainly in confining beds overlying the O-Cm aquifer system as the content of organic matter in the aquifer matrix is low (Section 2). McMahon and Chapelle (1991) have proposed that large pools of organic carbon in confining beds can support microbial activity in adjacent aquifers. The confining units serve as zones for the fermentation of organic matter and produced fermentation products (e.g. hydrogen, acetate) diffuse out of the confining layers to promote the organic matter oxidation in more permeable units (e.g. Chapelle and Bradley, 1996; Krumholz et al., 1997). Kerogen in the aquifer matrix of O-Cm and in adjacent aquitards is over 450 Ma old and is expected to have low reactivity. Still, it has been shown that refractory macromolecular kerogen can be utilized by bacteria (e.g. Petsch et al., 2005; Meslé et al., 2013, 2015), even more so when no other electron donors are available. Because graptolite argillite forming the overlying aquitard for the aquifer system in its northern part also contains significant amounts of pyrite, one can expect an accompanying transport of  $\text{SO}_4^{2-}$  together with the fermentation products into the aquifer system. It has been shown that diffusive transport of  $\text{SO}_4^{2-}$  from confining beds can influence organic matter oxidation via sulphate reduction in aquifers (Chapelle and McMahon, 1991). Elevated  $\text{SO}_4^{2-}$  concentrations are observed in the north-western part of the aquifer system (Fig. 2b). Here the thickness of the overlying graptolite argillite is the largest reaching up to ~8 m (Hade and Soesoo, 2014). Thus, in areas farther down the groundwater flow path,  $\text{SO}_4^{2-}$  reduction could be sustained by the diffusive transport of both the fermentation products of organic matter as well as  $\text{SO}_4^{2-}$  from the adjacent aquitards into the aquifer system.

### 5.5. Transient state of the O-Cm aquifer system

According to the interpretation provided above, the extent of a  $\text{SO}_4^{2-}$ -reduced zone near the modern recharge area could represent the extent to which the post-glacial topographically driven recharge has influenced the O-Cm aquifer system. Vallner (1997) has suggested that under modern hydraulic gradient, the actual groundwater velocities in the Cambrian sandstones are  $\sim 0.005 \text{ m d}^{-1}$  ( $\sim 5.8 \cdot 10^{-8} \text{ m s}^{-1}$ ), meaning that during the last 10,000 years the groundwater could have travelled only 30–40 km along the groundwater flow path. This estimate agrees with the extent of the  $\text{SO}_4^{2-}$ -reduced zone in the vicinity of the modern recharge area (Fig. 2b, c).

Previous studies in the Cambrian-Vendian aquifer system have shown that an important portion of DIC in glacial palaeogroundwater is derived from oxidation of organic matter ( $\delta^{13}\text{C}$  from  $-11.5$  to  $-22\%$ , Raidla et al., 2012, 2014). However,  $\delta^{13}\text{C}_{\text{DIC}}$  values of glacial palaeogroundwater in the O-Cm aquifer system (from  $-7.0$  to  $-15.5\%$ ; Table 1) are enriched in  $^{13}\text{C}$  with respect to values found in organic matter from adjacent aquifers and the aquifer matrix ( $\delta^{13}\text{C}_{\text{org}}$  from  $-20$  to  $-32\%$ ; Bityukova et al., 2000; Mastalerz et al., 2003; Kosakowski et al., 2017; Johnson et al., 2017, *in prep*; Table S2). Despite the occurrence of various reduction reactions that can oxidize organic matter in the O-Cm aquifer system, its influence on the overall hydrochemical evolution of groundwater is not as dominant as in the underlying Cambrian-Vendian aquifer system. If we suppose that the light  $\delta^{13}\text{C}_{\text{DIC}}$  was characteristic to pristine glacial palaeogroundwater in the BAB, the  $\delta^{13}\text{C}_{\text{DIC}}$  values enriched with respect to organic matter in the O-Cm aquifer system suggest that this glacial palaeogroundwater has been subject to significant hydrochemical changes after its infiltration. Thus, the influence of modern flow conditions is more pronounced here relative to deeper reservoirs containing glacial palaeogroundwater such as the Cambrian-Vendian aquifer system.

The above discussion suggests that the time elapsed since the termination of Late Weichselian glaciation has been too short for the O-Cm aquifer system to reach an equilibrium with post-glacial flow conditions. Gerber et al. (2017) have estimate that a time of ~50 ka is needed for the deep Cambrian aquifer system to reach a new steady state with respect to post-glacial hydraulic conditions after the large hydraulic perturbations caused by transgressions of ice sheets in Pleistocene. Similarly, Bense and Person (2008) show that the aquifers influenced by glaciations in sedimentary basins of North America have probably never reached a steady state during the advance and retreat cycles of ice sheets in Pleistocene. The proposed redox zonation in the O-Cm aquifer system in the BAB presents important field evidence supporting those findings. As an aquifer system containing glacial palaeogroundwater, it is still in a transient state after the ice sheet retreated > 10 ka ago.

## 6. Conclusions

The redox zonation in the O-Cm aquifer system containing palaeo-groundwater originating from glacial meltwater intrusion in Pleistocene shows more strongly reducing conditions in the vicinity of modern recharge area compared to areas farther down the groundwater flow path. We suggest that this unusual distribution of redox zones is a manifestation of two different flow systems in the aquifer system: 1) topographically driven flow system in post-glacial period which results in recharge of modern meteoric water through the overlying carbonate formation near the outcrop area and in the modern recharge area, and 2) flow system established in Pleistocene where the recharge of glacial meltwaters occurred at the northern/north-western margin of the aquifer system under a high hydraulic gradient imposed by the advancing Scandinavian ice sheet. The  $\text{SO}_4^{2-}$ -reduced conditions coupled to the presence of  $\text{CH}_4$  in the modern recharge area point to a rather weak connection between the O-Cm aquifer system and the overlying shallow aquifers, and its spatial distribution could mark the extent to which modern hydrologic conditions have influenced the aquifer system. Despite the potential shortcomings of the explanation provided above, the O-Cm aquifer system represents an important example of an aquifer system which has not reached a near-equilibrium state with respect to present day flow conditions and still exhibits hydrogeochemical patterns established in Pleistocene.

Supplementary data to this article can be found online at <https://doi.org/10.1016/j.chemgeo.2018.04.027>.

## Acknowledgements

The activities of the present study were supported by the Estonian Research Council Project IUT19-22 (R.V.), PUTJD127 (V.R.) and Archimedes Foundation (16-3.5/948) Kristjan Jaak Scholarship (J.P.). The paper is a contribution to the INQUA/UNESCO supported G@GPS Project. The authors would like to thank Zoltán Kern from the Research Centre for Astronomy and Earth Sciences, Budapest and Balázs Kohán from Eötvös Loránd University for their help in preparing the spatial distribution maps for  $\text{Fe}^{2+}$  and  $\text{SO}_4^{2-}$  presented in the study. Authors would also like to thank Konrads Popovs from University of Latvia, Riga for helping with data concerning Cambrian aquifer system in Latvia. Last but not least, we would like to thank Jill Van Reybrouck for Mn- and Fe-measurements carried out in Ghent University and Reeli Pärn for linguistic improvements. The manuscript was substantially improved by constructive comments by Ian Cartwright and Francis H. Chapelle.

## References

Affolter, S., Fleitmann, D., Leuenberger, M., 2014. New online method for water isotope analysis of speleothem fluid inclusions using laser absorption spectroscopy (WS-CRDS). *Clim. Past* 10, 1291–1304.

Algeo, T.J., Luo, G.M., Song, H.Y., Lyons, T.W., Canfield, D.E., 2015. Reconstruction of secular variation in seawater sulfate concentrations. *Biogeosciences* 12, 2131–2151.

Antler, G., Turchyn, A.V., Rennie, V., Herut, B., Sivan, O., 2013. Coupled sulfur and oxygen isotope insight into bacterial sulfate reduction in the natural environment. *Geochim. Cosmochim. Acta* 118, 98–117.

Appelo, C.A.J., Postma, D., 2005. *Geochemistry, Groundwater and Pollution*, 2nd Edn. Balkema, Leiden, The Netherlands.

Babre, A., Kalviāns, A., Popovs, K., Retiķe, I., Dēliņa, A., Vaikmāe, R., Martma, T., 2016. Pleistocene age paleo-groundwater inferred from water-stable isotope values in the central part of the Baltic Artesian Basin. *Isot. Environ. Health Stud.* <http://dx.doi.org/10.1080/10256016.2016.1168411>.

Balci, N., Shanks, W., Bernhard, M., Mandernack, K., 2007. Oxygen and sulfur isotope systematics of sulfate produced by bacterial and abiotic oxidation of pyrite. *Geochim. Cosmochim. Acta* 71, 3796–3811.

Bauert, H., Kattai, V., 1997. Kukersite oil shale. In: *Raukas, A., Teedumäe, A. (Eds.), Geology and Mineral Resources of Estonia*. Estonian Academy Publishers, Tallinn, pp. 313–327.

Bense, V.F., Person, M.A., 2008. Transient hydrodynamics within intercratonic sedimentary basins during glacial cycles. *J. Geophys. Res.* 113, F04005. <http://dx.doi.org/10.1029/2007JF000969>.

Berner, R.A., 1981. A new geochemical classification of sedimentary environments. *J. Sediment. Petrol.* 51, 359–365.

Bitiyukova, L., Bitiyukov, M., Shogenova, A., Rasteniene, V., Šliaupa, S., Zabele, A., Lashkova, L., Eihmanis, E., Kirsimäe, K., Jöeleht, A., Huegens, E., 2000. Organic Matter Distribution and Variations of Isotopic Composition of Organic Carbon in Cambrian Siliciclastic Rocks in Baltic Region. *Sediment* 2000, 20–23 June, 2000, Leoben, Austria. *Mitteilungen der Gesellschaft der Geologie und Bergbauausstudenten in Österreich. Sediment* 2000. Kurzfassungen/Abstracts, pp. 27–28.

Boschetti, T., 2013. Oxygen isotope equilibrium in sulfate–water systems: a revision of geothermometric applications in low-enthalpy systems. *J. Geochim. Explor.* 124, 92–100.

Böttcher, M.E., Brumsack, H.J., de Lange, G.J., 1998. Sulfate reduction and related stable isotope ( $^{34}\text{S}$ ,  $^{18}\text{O}$ ) variations in interstitial waters from the eastern Mediterranean. In: Robertson, A.H.F. (Ed.), *Proceedings of the Ocean Drilling Program, Scientific Results*. 160. pp. 365–373.

Brand, W.A., Geilmann, H., Crosson, E.R., Rella, C.W., 2009. Cavity ring-down spectroscopy versus high-temperature conversion isotope ratio mass spectrometry; a case study on  $\delta^2\text{H}$  and  $\delta^{18}\text{O}$  of pure water samples and alcohol/water mixtures. *Rapid Commun. Mass Spectrom.* 23, 1879–1884.

Brennan, S.T., Lowenstein, T.K., Horita, J., 2004. Seawater chemistry and the advent of biocalcification. *Geology* 32, 473–476.

Brunner, B., Bernasconi, S.M., Kleikemper, J., Schroth, M.H., 2005. A model for oxygen and sulfur isotope fractionation in sulfate during bacterial sulfate reduction processes. *Geochim. Cosmochim. Acta* 69, 4773–4785.

Brunner, B., Einsiedl, F., Arnold, G.L., Müller, I., Templar, S., Bernasconi, S.M., 2012. The reversibility of dissimilatory sulphate reduction and the cell-internal multi-step reduction of sulphate to sulphide: insights from the oxygen isotope composition of sulphate. *Isot. Environ. Health Stud.* 48, 33–54.

Canfield, D.E., 2001. Biogeochemistry of sulfur isotopes. In: Valley, J.W., Cole, D.R. (Eds.), *Stable Isotope Geochemistry, Reviews in Mineralogy*. Vol. 43. Mineralogical Society of America, pp. 607–636.

Canfield, D.E., Farquhar, J., Zerkle, A.L., 2010. High isotope fractionations during sulfate reduction in a low-sulfate euxinic ocean analog. *Geology* 38, 415–418.

Chapelle, F.H., Bradley, P.M., 1996. Microbial acetogenesis as a source of organic acids in ancient Atlantic Coastal Plain sediments. *Geology* 24, 925–928.

Chapelle, F.H., Lovley, D.R., 1992. Competitive exclusion of sulfate reducing bacteria: a mechanism for producing discrete zones of high-iron groundwater. *Groundwater* 30, 29–36.

Chapelle, F.H., McMahon, P.B., 1991. Geochemistry of dissolved inorganic carbon in Coastal Plain aquifer. 1. Sulfate from confining beds as an oxidant in microbial  $\text{CO}_2$  production. *J. Hydrol.* 127, 85–108.

Chiba, H., Sakai, H., 1985. Oxygen isotope exchange rate between dissolved sulfate and water at hydrothermal temperatures. *Geochim. Cosmochim. Acta* 49, 993–1000.

Clark, I.D., Fritz, P., 1997. *Environmental Isotopes in Hydrogeology*. CRC Press, New York.

Clayton, R.N., Friedman, I., Graf, D.L., Mayeda, T.K., Meents, W.F., Shimp, N.F., 1966. The origin of saline formation waters. 1. Isotopic composition. *J. Geophys. Res.* 71, 3869–3882.

Coetsiers, M., Walraevens, K., 2006. Chemical characterization of the Neogene Aquifer, Belgium. *Hydrogeol. J.* 14, 1556–1568.

Dogramaci, S.S., Herczeg, A.L., Schiff, S.L., Bone, Y., 2001. Controls on  $\delta^{34}\text{S}$  and  $\delta^{18}\text{O}$  of dissolved sulfate in aquifers of the Murray Basin, Australia and their use as indicators of flow processes. *Appl. Geochem.* 16, 475–488.

Durand, A., Chase, Z., Noble, T.L., Bostock, H., Jaccard, S.L., Kitchener, P., Townsend, A.T., Jansen, N., Kinsley, L., Jacobsen, G., Johnson, S.C., Neil, H., 2017. Export production in the New-Zealand region since the Last Glacial Maximum. *Earth Planet. Sci. Lett.* 469, 110–122.

EELIS, 2017. Estonian Environmental Agency - Estonian Nature Information System. VEKA database. <http://loodus.keskkonnainfo.ee/WebEelis/veka.aspx?type=artikkel&id=757660072>, Accessed date: 11 March 2017.

ESTEA, 2017. Estonian Environment Agency - Groundwater monitoring. [http://seire.keskkonnainfo.ee/index.php?option=com\\_content&view=article&id=640&Itemid](http://seire.keskkonnainfo.ee/index.php?option=com_content&view=article&id=640&Itemid), Accessed date: 27 March 2017.

Farquhar, J., Canfield, D.E., Masterson, A., Bao, H., Johnston, D., 2008. Sulfur and oxygen isotope study of sulfate reduction in experiments with natural populations from Fællestrand, Denmark. *Geochim. Cosmochim. Acta* 72, 2805–2821.

Fouillac, C., Fouillac, A.M., Criaud, A., 1990. Sulphur and oxygen isotopes of dissolved sulphur species in formation waters from the Dogger geothermal aquifer, Paris Basin, France. *Appl. Geochem.* 5, 415–427.

Fritz, P., Basharmal, G.M., Drimmie, R.J., Ibsen, J., Qureshi, R.M., 1989. Oxygen isotope exchange between sulphate and water during bacterial reduction of sulphate. *Chem. Geol. Isot. Geosci.* 79, 99–105.

Gerber, C., Vaikmāe, R., Aeschbach, W., Babre, A., Jiang, W., Leuenberger, M., Lu, Z.T., Mokrik, R., Müller, P., Purtscher, R., Raidla, V., Saks, T., Waber, H.N., Weissbach, T., Zappala, J.C., 2017. Using  $^{81}\text{Kr}$  and noble gases to characterize and date groundwater and brines in the Baltic Artesian Basin on the one-million-year timescale. *Geochim. Cosmochim. Acta* 205, 187–210.

Grasby, S.E., Osadetz, K., Betcher, R., Render, F., 2000. Reversal of the regional-scale flow system of the Williston Basin in response to Pleistocene glaciation. *Geology* 29, 635–638.

Hade, S., Soesoo, A., 2014. Estonian graptolite argillites revisited: a future resource? *Oil Shale* 31, 4–18.

Halas, S., Trembacowski, A., Soltky, W., Valenzziak, J., 1993. Sulphur and oxygen in natural waters: (2) deep-waters from horizons below Baltic Sea floor. *Isotopenpraxis* 28, 229–235.

Haley, I., Peters, S.E., Fischer, W.W., 2012. Sulfate burial constraints on the Phanerozoic sulfur cycle. *Science* 337, 331–334.

Hansen, I.K., Jakobsen, R., Postma, D., 2001. Methanogenesis in a shallow sandy aquifer, Romo, Denmark. *Geochim. Cosmochim. Acta* 65, 2925–2935.

Hatvani, I.G., Leuenberger, M., Kohán, B., Kern, Z., 2017. Geostatistical analysis and isoscape of ice core derived waterstable isotope records in an Antarctic macro region. *Polar Sci.* 13, 23–32.

- Heidel, C., Tichomirowa, M., 2010. The role of dissolved molecular oxygen in abiotic pyrite oxidation under acid pH conditions – experiments with  $^{18}\text{O}$ -enriched molecular oxygen. *Appl. Geochem.* 25, 1664–1675.
- Heidel, C., Tichomirowa, M., 2011. The isotopic composition of sulfate from anaerobic and low oxygen pyrite oxidation experiments with ferric iron – new insights into oxidation mechanisms. *Chem. Geol.* 281, 305–316.
- Horita, J., Zimmermann, H., Holland, H.D., 2002. Chemical evolution of seawater during the Phanerozoic: implications from the record of marine evaporites. *Geochim. Cosmochim. Acta* 66, 3733–3756.
- IAEA/WMO, 2017. *Global network of isotopes in precipitation. The GNIP Database*. Accessible at: <http://www.iaea.org/water/>, Accessed date: 25 May 2017.
- Jakobsen, R., Cold, L., 2007. Geochemistry at the sulfate reduction–methanogenesis transition zone in an anoxic aquifer—a partial equilibrium interpretation using 2D reactive transport modeling. *Geochim. Cosmochim. Acta* 71, 1949–1966.
- Jakobsen, R., Postma, D., 1994. In situ rate of sulfate reduction in an aquifer (Rømo, Denmark) and implications for the reactivity of organic matter. *Geology* 22, 1103–1106.
- Jakobsen, R., Postma, D., 1999. Redox zoning, rates of sulfate reduction and interactions with Fe-reduction and methanogenesis in a shallow sandy aquifer, Rømo, Denmark. *Geochim. Cosmochim. Acta* 63, 137–151.
- Johnson, S.C., McGoldrick, P.J., Systra, Y., Meffre, S., Large, R.R., Raub, T.D., Boyce, A.J., Lyons, T.W., 2016. Trace Metals and Isotopes in Estonian Black Shales: Cambro-Ordovician Shallow Water Anoxia on the Baltica Shelf? Goldschmidt, Yokohama, Japan. 1372.
- Johnson, S.C., Large, R.R., Coveney, R.M., Kelley, K.D., Slack, J.F., Steadman, J.A., Gregory, D.D., Sack, P.J., Meffre, S., 2017. Secular distribution of highly metalliferous black shales corresponds with peaks in past atmosphere oxygenation. *Mineral. Deposita* 52, 791–798.
- Juodkazis, V.I. (Ed.), 1980. *Hydrogeological Map of the Pre-Quaternary Deposits of the Soviet Baltic Republics*. Ministry of Geology of the USSR.
- Kalm, V., Raukas, A., Rattas, M., Lasberg, K., 2011. Pleistocene glaciations in Estonia. In: Ehlers, J., Gibbard, P.L., Hughes, P.D. (Eds.), *Quaternary Glaciations - Extent and Chronology - a Closer Look*. Elsevier, Amsterdam, pp. 95–104.
- Kosakowski, P., Kotarba, M.J., Piestrzyński, A., Shogenova, A., Wieclaw, D., 2017. Petroleum source rock evaluation of the Alum and Dictionema Shales (Upper Cambrian–Lower Ordovician) in the Baltic Basin and Podlasie Depression (eastern Poland). *Int. J. Earth Sci.* 106, 743–761.
- Krouse, H.R., Mayer, B., 2000. Sulphur and oxygen isotopes in sulphate. In: Cook, P., Herczeg, A.L. (Eds.), *Environmental Tracers in Subsurface Hydrology*. Kluwer Academic Publisher, pp. 195–231.
- Krumholz, L.R., McKinley, J.P., Ulrich, G.A., Sufita, J.M., 1997. Confined subsurface microbial communities in Cretaceous carbonate. *Nature* 386, 64–66.
- Labotka, M.D., Panno, S.V., Locke, R.A., 2016. A sulfate conundrum: dissolved sulfates of deep-saline brines and carbonate-associated sulfates. *Geochim. Cosmochim. Acta* 190, 53–71.
- Lovley, D.R., Chapelle, F.H., 1995. Deep subsurface microbial processes. *Rev. Geophys.* 33, 365–381.
- Lowenstein, T.K., Hardie, L.A., Timofeeff, M.N., Demico, R.V., 2003. Secular variation in seawater chemistry and the origin of calcium chloride basinal brines. *Geology* 31, 857–860.
- Mangalo, M., Meckenstock, R.U., Stichler, W., Einsiedl, F., 2007. Stable isotope fractionation during bacterial sulfate reduction is controlled by reoxidation of intermediates. *Geochim. Cosmochim. Acta* 71, 4161–4171.
- Mastalerz, M., Schimmelmann, A., Hower, J.C., Lis, G., Hatch, J., Jacobson, S.R., 2003. Chemical and isotopic properties of kukersites from Iowa and Estonia. *Org. Geochem.* 34, 1419–1427.
- Mazumdar, A., Goldberg, T., Strauss, H., 2008. Abiotic oxidation of pyrite by Fe(III) in acidic media and its implications for sulfur isotope measurements of lattice-bound sulfate in sediments. *Chem. Geol.* 253, 30–37.
- McIntosh, J.C., Walter, L.M., 2006. Paleowaters in Silurian–Devonian carbonate aquifers: geochemical evolution of groundwater in the Great Lakes region since the late Pleistocene. *Geochim. Cosmochim. Acta* 70, 2454–2479.
- McMahon, P.B., Chapelle, F.H., 1991. Microbial production of organic acids in aquifer sediments and its role in aquifer geochemistry. *Nature* 349, 233–235.
- Mens, K., Pirrus, E., 1997. Cambrian. In: Raukas, A., Teedumäe, A. (Eds.), *Geology and Mineral Resources of Estonia*. Estonian Academy Publishers, Tallinn, pp. 39–48.
- Meslé, M., Periot, C., Dromart, G., Oger, P., 2013. Biostimulation to identify microbial communities involved in methane generation in shallow, kerogen-rich shales. *J. Appl. Microbiol.* 114, 55–70.
- Meslé, M., Dromart, G., Haeseler, F., Oger, P., 2015. Classes of organic molecules targeted by a methanogenic microbial consortium grown on sedimentary rocks of various maturities. *Front. Microbiol.* 6, 589. <http://dx.doi.org/10.3389/fmicb.2015.00589>.
- Mizutani, Y., Rafta, A.T., 1973. Isotopic behaviour of sulphate oxygen in the bacterial reduction of sulphate. *Geochim. J.* 6, 183–191.
- Mokrik, R., 1997. *The Palaeohydrogeology of the Baltic Basin. Vendian and Cambrian*. Tartu University Press, Tartu.
- Müller, I.A., Brunner, B., Breuer, C., Coleman, M., Bach, W., 2013. The oxygen isotope equilibrium fractionation between sulfite species and water. *Geochim. Cosmochim. Acta* 120, 562–581.
- Park, J., Sanford, R.A., Bethke, C.M., 2006. Geochemical and microbiological zonation of the Middendorf aquifer, South Carolina. *Chem. Geol.* 230, 88–104.
- Pärn, J., Raidla, V., Vaikmäe, R., Martma, T., Ivask, J., Mokrik, R., Erg, K., 2016. The recharge of glacial meltwater and its influence on the geochemical evolution of groundwater in the Ordovician–Cambrian aquifer system, northern part of the Baltic Artesian Basin. *Appl. Geochem.* 72, 125–135.
- Perens, R., Vallner, L., 1997. Water-bearing formation. In: Raukas, A., Teedumäe, A. (Eds.), *Geology and Mineral Resources of Estonia*. Estonian Academy Publishers, Tallinn, pp. 137–145.
- Person, M., McIntosh, J.C., Remenda, V., Bense, V., 2007. Pleistocene hydrology of North America: the role of ice sheets in reorganizing groundwater systems. *Rev. Geophys.* 45. <http://dx.doi.org/10.1029/2006RG000206>.
- Petersell, V., 1997. *Dictionema argillite*. In: Raukas, A., Teedumäe, A. (Eds.), *Geology and Mineral Resources of Estonia*. Estonian Academy Publishers, Tallinn, pp. 313–326.
- Petersell, V.H., Zhukov, F.I., Loog, A.R., Fomin, Y.A., 1987. Origin of Tremadoc kerogen-bearing siltstones and argillites of North Estonia. *Oil Shale* 4 (1), 8–13 (in Russian).
- Petersell, V., Kivisilla, J., Pukkonen, E., Pöldvere, A., Täht, K., 1991. Evaluation of Ore Events and Mineralization Points in Estonian Bedrock and Crystalline Basement. Geological Survey of Estonia, Tallinn (in Russian).
- Petsch, S.T., Edwards, K.J., Eglinton, T.I., 2005. Microbial transformations of organic matter in black shales and implications for global biogeochemical cycles. *Palaeogeogr. Palaeoclimatol. Palaeoecol.* 219, 157–170.
- Pihlak, A.T., Matvienko, N., Bogdanov, R., 2003. Natural gases in Estonian wells. *Ekologicheskaya khimiya* 12, 141–159 (in Russian).
- Pisapia, C., Chaussidon, M., Mustin, C., Humbert, B., 2007. O and S isotopic composition of dissolved and attached oxidation products of pyrite by *Acidithiobacillus ferrooxidans*: comparison with abiotic oxidations. *Geochim. Cosmochim. Acta* 71, 2474–2490.
- Postma, D., Jakobsen, R., 1996. Redox zonation: equilibrium constraints on the Fe(III)/SO<sub>4</sub>-reduction interface. *Geochim. Cosmochim. Acta* 60, 3169–3175.
- Raidla, V., Kirsimäe, K., Bityukova, L., Jõelet, A., Shogenova, A., Šliaupa, S., 2006. Lithology and diagenesis of the poorly consolidated Cambrian siliclastic sediments in the northern Baltic Sedimentary Basin. *Mar. Geol. Quat. Geol.* 50, 11–22.
- Raidla, V., Kirsimäe, K., Vaikmäe, R., Jõelet, A., Karro, E., Marandi, A., Savitskaja, L., 2009. Geochemical evolution of groundwater in the Cambrian–Vendian aquifer system of the Baltic Basin. *Chem. Geol.* 258, 219–231.
- Raidla, V., Kirsimäe, K., Vaikmäe, R., Kaup, E., Martma, T., 2012. Carbon isotope systematics of the Cambrian–Vendian aquifer system in the northern Baltic Basin: implications to the age and evolution of groundwater. *Appl. Geochem.* 27, 2042–2052.
- Raidla, V., Kirsimäe, K., Ivask, J., Kaup, E., Knöller, K., Marandi, A., Martma, T., Vaikmäe, R., 2014. Sulphur isotope composition of dissolved sulphate in the Cambrian–Vendian aquifer system in the northern part of the Baltic Artesian Basin. *Chem. Geol.* 383, 147–154.
- Raidla, V., Kern, Z., Pärn, J., Babre, A., Erg, K., Ivask, J., Kalvāns, A., Kohān, B., Leigus, M., Martma, T., Mokrik, R., Popovs, K., Vaikmäe, R., 2016. A  $\delta^{18}\text{O}$  isotope for the shallow groundwater in the Baltic Artesian Basin. *J. Hydrol.* 542, 254–267.
- Rousseau-Gueutin, P., Love, A.J., Vasseur, G., Robinson, N.I., Simmons, C.T., de Marsily, G., 2013. Time to reach near steady state in large aquifers. *Water Resour. Res.* 49, 6893–6908.
- Samborska, K., Halas, S., 2010.  $^{34}\text{S}$  and  $^{18}\text{O}$  in dissolved sulfate as tracers of hydro-geochemical evolution of the Triassic carbonate aquifer exposed to intense groundwater exploitation (Olkusz-Zawiercie region, southern Poland). *Appl. Geochem.* 25, 1397–1414.
- Savitskaja, L., Viigand, A., Jashtshuk, S., 1995. Report of Microcomponent and Isotope Composition Research in Ordovician–Cambrian Aquifer Groundwater for Estimating Drinking Water Quality in North-Estonia. Geological Survey of Estonia, Tallinn (in Estonian).
- Siegel, D.I., Mandle, R.J., 1984. Isotopic evidence for glacial meltwater recharge to the Cambrian Ordovician aquifer, north-central United States. *Quat. Res.* 22, 328–335.
- Sim, M.S., Bosak, T., Ono, S., 2011. Large sulfur isotope fractionation does not require disproportionation. *Science* 333, 74–77.
- Simpkins, W.W., Parkin, T.B., 1993. Hydrogeology and redox geochemistry of CH<sub>4</sub> in a late Wisconsinan till and loess sequence in central Iowa. *Water Resour. Res.* 29, 3643–3657.
- Stuyfzand, P.J., 1993. *Hydrochemistry and Hydrology of the Coastal Dune Area of the Western Netherlands*. PhD thesis. Free University, Amsterdam.
- Takdici, E., 1999. *Datu bāzes "Urbumi" dokumentācija* [Documentation of the Database "Boreholes"]. Valsts ģeoloģijas dienests, Rīga (in Latvian).
- Tsebani, E., 1966. *Hydrogeology of the USSR XXX (Estonian SSR)*. Moscow. (in Russian).
- Turchyn, A.V., Brüchert, V., Lyons, T.W., Engel, G.S., Balci, N., Schrag, D.P., Brunner, B., 2010. Kinetic oxygen isotope effects during dissimilatory sulfate reduction: a combined theoretical and experimental approach. *Geochim. Cosmochim. Acta* 74, 2011–2024.
- Vaikmäe, R., Vallner, L., Loosli, H.H., Blaser, P.C., Juillard-Tardent, M., 2001. Palaeogroundwater of glacial origin in the Cambrian–Vendian aquifer of northern Estonia. In: Edmunds, W.M., Milne, C.J. (Eds.), *Paleowaters of Coastal Europe: Evolution of Groundwater Since the late Pleistocene*. Vol. 189. Special Publications, Geological Society, London, pp. 17–27.
- Vallner, L., 1997. *Groundwater Flow*. In: Raukas, A., Teedumäe, A. (Eds.), *Geology and Mineral Resources of Estonia*. Estonian Academy Publishers, Tallinn, pp. 137–152.
- Van Stempvoort, D.R., Krouse, H.R., 1994. Controls of  $\delta^{18}\text{O}$  in sulfate—review of experimental data and application to specific environments. In: Alpers, C.N., Blowes, D.W. (Eds.), *Environmental Geochemistry of Sulfide Oxidation*. ACS Symposium Series. American Chemical Society, Washington DC, pp. 446–480.
- Voitov, G., Karpov, I., Tibar, K., Sozinova, T., 1982. The Natural Anomalies in Methane's Carbon Isotope Composition in Estonia. 264. *Doklady Akademii Nauk USSR*, pp. 1217–1221 (in Russian).
- Wagner, T., Boyce, A.J., Fallick, A.E., 2002. Laser combustion analysis of  $\delta^{34}\text{S}$  of sulfosal minerals: determination of the fractionation systematics and some crystal-chemical considerations. *Geochim. Cosmochim. Acta* 66, 2855–2863.
- Whiticar, M.J., 1999. Carbon and hydrogen isotope systematics of bacterial formation and oxidation of methane. *Chem. Geol.* 161, 291–314.
- Wortmann, U.G., Chernyavsky, B., Bernasconi, S.M., Brunner, B., Böttcher, M.E., Swart, P.K., 2007. Oxygen isotope biogeochemistry of pore water sulfate in the deep biosphere: dominance of isotope exchange reactions with ambient water during microbial sulfate reduction (ODP Site 1130). *Geochim. Cosmochim. Acta* 71, 4221–4232.
- Zeebe, R.E., 2010. A new value for the stable oxygen isotope fractionation between dissolved sulfate ion and water. *Geochim. Cosmochim. Acta* 74, 818–828.



**Paper IV**

Pärn, Joonas; Walraevens, Kristine; van Camp, Marc; Raidla, Valle; Aeschbach, Werner; Friedrich, Ronny; Ivask, Jüri; Kaup, Enn; Martma, Tõnu; Mažeika, Jonas; Mokrik, Robert; Weissbach, Therese; Vaikmäe, Rein. Dating of glacial palaeogroundwater in the Ordovician-Cambrian aquifer system, northern part of Baltic Artesian Basin. *Manuscript*.

**Paper V**

Raidla, Valle; Pärn, Joonas; Czuppon, György; Ivask, Jüri; Marandi, Andres; Schloemer, Stefan; Sepp, Holar; Vaikmäe, Rein; Kirsimäe, Kalle. Origin and formation of methane in groundwater of glacial origin from the Cambrian-Vendian aquifer system in Estonia. *Manuscript*.

# Curriculum vitae

## Personal data

Name: Joonas Pärn  
Date of birth: 22.07.1989  
Place of birth: Tallinn  
Citizenship: Estonian

## Contact data

E-mail: [joonas.parn@ttu.ee](mailto:joonas.parn@ttu.ee)

## Education

2016–2017 PhD exchange student at Laboratory for Applied Geology and Hydrogeology, Ghent University, Belgium (supervisor Prof. Kristine Walraevens), Archimedes Foundation Kristjan Jaak Scholarship  
2014–2018 Tallinn University of Technology, Department of Geology, PhD  
2012–2014 Tallinn University of Technology, Department of Geology, MSc  
2008–2011 University of Tartu, Department of Geography, BSc  
2005–2008 Collegium Educationis Revaliae (Old Town Educational College), Tallinn, High School

## Language competence

English: Fluent  
German: Basic  
Estonian: Mother tongue

## Professional employment

2018–... Geological Survey of Estonia, hydrogeologist (1,00)  
2017–... Tallinn University of Technology, School of Science, Department of Geology, junior researcher (0,10)  
2014–2016 Tallinn University of Technology, School of Science, Department of Geology, junior researcher (1,00)

## **Elulookirjeldus**

### **Isikuandmed**

Nimi: Joonas Pärn  
Sünniaeg: 22.07.1989  
Sünnikoht: Tallinn  
Kodakondsus: Eesti

### **Kontaktandmed**

E-post: joonas.parn@ttu.ee

### **Hariduskäik**

2016–2017 SA Archimedese Kristjan Jaagu stipendiumi stipendiaat Genti ülikooli rakendusgeoloogia ja hüdrogeoloogia laboratooriumis Belgias (juhendaja Prof. Kristine Walraevens)

2014–2018 Tallinna Tehnikaülikool, Geoloogia Instituut, PhD

2012–2014 Tallinna Tehnikaülikool, Geoloogia Instituut, MSc

2008–2011 Tartu Ülikool, Geograafia osakond, BSc

2005–2008 Tallinna Vanalinna Hariduskollegium, Keskaridus

### **Keelteoskus**

Inglise keel: Kõrgtase

Saksa keel: Algtase

Eesti keel: Emakeel

### **Teenistuskäik**

2018–... Eesti Geoloogiateenistus, hüdrogeoloog (1,00)

2017–... Tallinna Tehnikaülikool, Geoloogia instituut, nooremteadur (0,10)

2014–2016 Tallinna Tehnikaülikool, TTÜ Geoloogia Instituut, nooremteadur (1,00)